Empirical Study of Heavy Vehicle Operating Speeds on Mountainous Downgrades in the Western Cape, South Africa

By

Jandré Oncke

Thesis presented in fulfilment of the requirements for the degree of
Master of Engineering in the Faculty of Engineering at Stellenbosch University

Supervisor: Prof. Christo J. Bester

Department of Civil Engineering

March 2016

Declaration

By submitting this thesis electronically, I declare that the entirety of the work contained therein is my own original work, that I am the authorship owner thereof (unless to the extent explicitly otherwise stated) and that I have not previously in its entirety or in part submitted it for obtaining any qualification.

Date: ……..

Abstract

Heavy vehicles play a major role in the economic well-being of a country through its significant role in moving freight. Therefore any adverse effect to the road freight, from being stuck in traffic to being involved in a fatal accident, will have negative impacts on the economy and on the safety of the persons involved. Therefore it is paramount to understand how and to what extent factors such as road geometrics, vehicle characteristics and weather conditions affect the safety of heavy vehicles. There are several countermeasures addressing the issue, with the most common approach being to supply drivers with better information. This is done through the use of a grade severity rating system (GSRS) or weight specific signs (WSS) that direct heavy vehicle drivers to adopt a slower and more suited speed for the relevant downgrade. However, there are no such countermeasure or system deployed in South Africa, and simply adapting the current GSRS and WSS might not suffice, since most of these models are outdated and does not account for newer technology or regulations. Thus, this research paper aimed to gain a better understanding of how the select geometric and vehicle characteristics influence the operating speed of heavy vehicles on downgrades, and ultimately to formulate a mathematical equation that can be used to estimate the operating speed of heavy vehicles on downgrades. The equations can be used to design WSS for South African mountain passes.

The variables that have been identified as important in this study include, operating speed, gross vehicle mass, gradient, downgrade length, curve radius, superelevation and stopping distance. The operating speed is taken as the dependent variable and measure of safety, since it is the most common relatable variable among the diverse and complex nature of heavy vehicle operating systems. In order to collect data of the select variables, the critical section for each mountain pass was identified. This was done by following descending heavy vehicles and determining the relevant speed profiles. This was done multiple times for each pass, so that a combination graph could be obtained, which was analysed to identify the critical section. Data for the variables were collected using various devices and means. The operating speed and number of axles were collected by video recordings, and gradient, downgrade length and curved radius were collected with instruments such as a GPS and theodolite. The mass of the heavy vehicles were obtained from the weighbridges situated along routes of the relevant mountain passes.

Analysing the data were primarily done through regressing the data, with the calculated operating speed through the critical sections as the dependent variable. Three regressions were done, namely a general regression, regression with a change in horizontal alignment and a regression with a compulsory stop at the base of the downgrade. Equations were found for heavy vehicle speeds on steep downgrades in general and on downgrades that subject operating speed to small curve radii. A logical exercise was also done, in which it was attempted to determine driver familiarity with the select downgrades. It was found that only half of all the observed heavy vehicle drivers exhibited familiarity with the given pass. Based on the finding that more relevant information is needed by the drivers and the lack of a sufficient means of conveying information to heavy vehicle drivers, it is fitting that an improved alternate to the GS 505 signs be found. The two equations found in this study can be used to this end.

Opsomming

Swaarvoertuie speel 'n belangrike rol in die ekonomiese welstand van die land deur die beweging van goedere. Enige nadelige inwerking op swaarvoertuie, van in verkeer vassit tot ongelukke, sal ŉ negatiewe impak op die ekonomie en die veiligheid van die betrokke persone hê. Daarom is dit belangrik om te verstaan hoe en tot watter mate faktore soos pad-geometrie, voertuigeienskappe en weerstoestande die veiligheid van swaarvoertuie beïnvloed. Daar is verskeie teenmaatreëls om die kwessie teen te werk, met die mees algemene benadering om beter inligting aan bestuurders te voorsien. Dit word gedoen deur middel van ŉ *grade severity rating system* (GSRS) of ‘n *weight specfic sign* (WSS), wat beter en meer direkte inligting aan swaarvoertuig bestuurders gee, sodat ŉ meer geskikte spoed gehandhaaf kan word. Daar is egter geen soortgelyke stelsel in Suid-Afrika nie, en net die aanpassing van die huidige “GSRS” en” WSS” sal nie voldoende wees nie, aangesien die meeste van hierdie modelle verouderd is en nie rekening hou met nuwe tegnologie of regulasies nie. Hierdie studie is daarop gemik om 'n beter begrip van hoe en tot watter mate die geometriese- en voertuigeienskappe die spoed van swaarvoertuie op afdraandes beïnvloed. Die studie sal dan verder gevat word om 'n wiskundige vergelyking te formuleer, wat gebruik kan word om die spoed van swaarvoertuie op afdraandes te bepaal. Die vergelykings kan gebruik word om “WSS” te ontwerp vir Suid-Afrikaanse bergpasse.

Die veranderlikes wat geïdentifiseer is as belangrik in hierdie studie sluit in: spoed, voertuigmassa, gradiënt, lengte van die afdraande, draairadius, verkanting en stop afstand. Die spoed word geneem as die afhanklike veranderlike en as die maatstaaf van veiligheid, want dit is die algemene veranderlike tussen swaarvoertuie ongeag van die voertuig se dryfstelsel. Om die data te bekom wat benodig word vir die studie, moet die kritiese punte van elke bergpas eers bepaal word. Dit is gedoen deur swaarvoertuie te agtervolg terwyl hulle teen die bergpas daal, waarna die relevante spoedprofiel bepaal is. Dit is meer as een keer gedoen vir elke bergpas, sodat 'n gekombineerde grafiek van die spoedprofiele saamgestel kon word, wat dan ontleed is om die kritiese punt te identifiseer. Data vir die veranderlikes is ingesamel met behulp van verskeie toestelle. Die spoed en aantal asse is verkry deur video-opnames; die helling, afdraande lengte en draai radiusse is ingesamel deur middel van ŉ GPS-toestel en ŉ teodoliet. Die massa van die swaarvoertuie is verkry uit die weegbrûe langs roetes van die betrokke bergpasse.

Ontleding van die data is hoofsaaklik gedoen deur regressie, met die swaarvoertuig spoed deur die kritiese punte, as die afhanklike veranderlike. Drie regressies is gedoen, naamlik 'n algemene regressie, ŉ regressie met 'n verandering in horisontale belyning en 'n regressie met 'n verpligte stop aan die voet die bergpas. Twee vergelykings is geformuleer om swaarvoertuig spoed op afdraandes te bepaal. Die eerste vergelyking is vir bergpasse in die algemeen en die tweede vergelyking maak voorsiening vir die kritieke draai radius. ŉ Logiese oefening is ook gedoen, waarin bestuurder bekendheid rakend die afdraandes bespreek word. Daar is gevind dat slegs die helfte van al die waargeneemde swaarvoertuigbestuurders vertroudheid met die verskeie bergpasse getoon het. Gebaseer op dié bevinding, word dit voorgestel dat beter en direkte inligting aan swaarvoertuig bestuurder oorgedra word, veral op bergpasse. Die twee vergelykings wat geformuleer is in hierdie studie, kan gebruik word vir die doel.

Contents

List of Figures

List of Tables

List of Acronyms and Symbols

ABS	Antilock Braking System
API	Application Programming Interface
°C	Degree Celsius
CSIR	Council for Scientific and Industrial Research
.csv	Comma Separated Values
F	Fahrenheit
FPS	Frames per second
GDP	Gross Domestic Product
GNSS	Global Network Satellite System
GPS	Global Positioning System
GSRS	Grade Severity Rating System
GVM	Gross Vehicle Mass
kg	Kilogram
km	Kilometre
.kml	Keyhole Mark-up Language
Lbs	Pounds
LED	Light Emitting Diode
mm	millimetre
MSL	Mean Sea Level
MUTCD	Manual on Uniform Traffic Control Devices
NCHRP	National Cooperative Highway Research Program
RTMC	Road Traffic Management Corporation
SANRAL	South African National Roads Agency Limited
SARTSM	South African Road Traffic Signs Manual
SBAS	Satellite Based Augmentation System
TEU	Twenty-foot Equivalent Unit (Shipping container measure)
USBPR	United States Bureau of Public Roads
VBA	Visual Basic for Applications
WSS	Weight Specific Sign

Glossary

Gross Domestic Product	The broadest quantitative measure of a nation's total economic activity. More specifically, GDP represents the monetary value of all goods and services produced within a nation's geographic borders over a specified period of time.
Logistical Cost	Logistics is defined as the management process for the movement of goods across country or across the globe. The cost of moving these goods includes transport, management and storage.
Accessibility	The closeness of a suitable transport mode.
Mobility	The ability of moving goods and services, and the level of ease with which it is done.
Hairpin	A curve in a road with a very acute inner angle, making it necessary for an oncoming vehicle to turn almost 180° along the road.
Cant	A cross-sectional slope or tilt of the road, more commonly referred to as superelevation.
Geodesy	The branch of mathematics dealing with the shape and area of the earth or large portions of it.
Escarpment	A long, steep slope, especially one at the edge of a plateau or separating areas of land at different levels.
Syntaxis	A convergence of mountain ranges, or geological folds, towards a single point.
Total Station	This is an electronic theodolite integrated with an electronic distance meter to read slope distances from the instrument to a particular point.
GSRS	The system developed to rate the severity of downgrades, based on various vehicular and geometric characteristics.

1 Introduction

1.1 Freight Transport: A South African Perspective

In 2011 South Africa celebrated 150 years of rail transport, with the first railway constructed in 1851 in Durban. The subsequent years saw the rail network expanding across South Africa, growing in both market share and as chosen mode of freight movement due to favourable regulations. This trend declined in the 1970s as other governments passed acts on transport deregulation. Studies conducted by the government found that the protected rail industry and stringent road freight regulations could have a detrimental effect on the South African economy. In 1988 the Transport Deregulation Act (Act 80 of 1988) was passed, which saw an end to the economic regulation of the freight industry (Cronin, 2011:1).

The deregulation lead to the manifestation of a road-orientated private sector within the freight industry. This created a competitive market between road and rail which ultimately lead to a shift in the market share (Cronin, 2011:1). In 1985 road freight had a market share of 33 percent, with rail accounting for the remaining 67 percent. However, the latest State of Logistics Survey found that rail had decreased in market share to 30.5 percent, with road now accounting for 69.5 percent (CSIR, 2013:88).

This shift in market share also increases the effect that road freight has on the economy, with logistical costs (i.e. transport, storage and management costs) accounting for 12.5 percent of South Africa's annual GDP (CSIR, 2013:88). It is of economic importance to ensure that South Africa's primary means of freight transport is managed as efficiently and safely as possible. Therefore it is important to understand what factors influence the effective operation of this sector, and to what extent each factor affects freight movement.

1.2 Problem Statement

One factor that lies in the engineering field is the interaction of heavy vehicles with the road environment. These road operations are affected by the following four sets of characteristics, namely heavy vehicle and load characteristics, geometric characteristics, driver behaviour, and weather conditions. An adverse combination of all four characteristics on a given heavy vehicle has the potential to cause an incident such as a runaway or rollover, possibly resulting in a fatal accident. Therefore, reducing incidents and the severity thereof can be seen as the primary motivation to improve the safety of heavy vehicle operations.

A scenario where all four characteristics are active at the same time occurs when a laden heavy vehicle driven by a tired or inexperienced driver traverses mountainous terrain under unfavourable conditions. Vehicle characteristics are influenced by the braking and retardation capability of the heavy vehicle as well as the laden state of the heavy vehicle. Mountainous terrain introduces severe gradients over lengthy stretches that markedly affect heavy vehicle speeds. This, coupled with considerable length of grade and small curve radii along the route, creates very strenuous operating conditions. Driver behaviour is influenced by the amount of information available to the driver before or upon entry to the mountainous stretch, with little to no information being unfavourable. Unfavourable weather conditions include extreme temperatures, which increase the ambient operating temperature and can subsequently lead to the earlier onset of brake failure or fade. Also, extremely wet road

conditions can lead to lower skid resistance, as a result of a lowered kinetic coefficient of friction between the tyres and road surface.

In an attempt to improve safety on downgrades, the American government developed a grade severity rating system (GSRS) in the late 1960s that would convey mass specific speed information to the drivers. The system is primarily based on the gradient, length of gradient and mass, with brake temperatures as the measure of the onset of brake failure. Based on these factors, a specific speed for the corresponding mass is calculated, which under strenuous conditions should allow for a safe descend nearly every time. Since the introduction of this system, it has seldom been updated to account for more rigid regulations and improved technology encountered in modern heavy vehicles. This implies that the current GSRS is outdated, since it had been developed primarily on drum brake systems, which were the norm during the development of this system. However, the US government requires that all modern heavy vehicles be fitted with air disc brakes, which have improved braking capacity and safety over drum brakes, to keep up with the latest braking regulations (Bendix Spicer Foundation Brake LLC, 2011).

Therefore the GSRS as currently implemented may be obsolete and too conservative for the new standards. Furthermore, the introduction of the air-disc brake would require a new grade severity rating system or an adaptation to be developed. However, since there are still drum-brake heavy vehicles in use today, a newly developed GSRS based on newer technologies and regulations might not be suitable for older heavy vehicles. Thus, under-conservative speed limits may be set for older heavy vehicles that do not have the same capabilities of the newer heavy vehicles.

In South Africa there is no grade severity rating system or weight-specific speed sign in place on severe downgrades. Instead, the general practice is to have a GS505 sign ("select low-range" sign) or having a sub-plate stating the length of grade. Thus, the problem exists that the heavy-vehicle drivers have little information available ahead of severe downgrades and that simply implementing the current American GSRS might result in over-conservative speed limits to be set.

1.3 Research Objectives

Road Transport is South Africa's primary mode of freight transportation. Thus understanding the challenges that are faced by road freight is of importance, for both the freight industry and the economic stability of industry in general. This research project aim to explore one such challenge, namely the interaction between mountainous downgrades and heavy vehicle operating speeds. The research objectives are:

- To compare the measured 85^{th} percentile speed of heavy vehicle with the posted speed limit;
- To determine to what extent selected geometric and vehicular factors influence operating speed;
- To determine the speed profiles through the critical sections

Based on these objectives, the aim is to achieve a clear understanding of the interaction of heavy vehicle operating speeds and mountainous downgrades.

1.4 Research Definitions

For the purpose of this research project, important concepts and terms are fully defined as to provide a clear understanding of what is meant. The concepts and terms, discussed below, are illustrated in Figure 1.

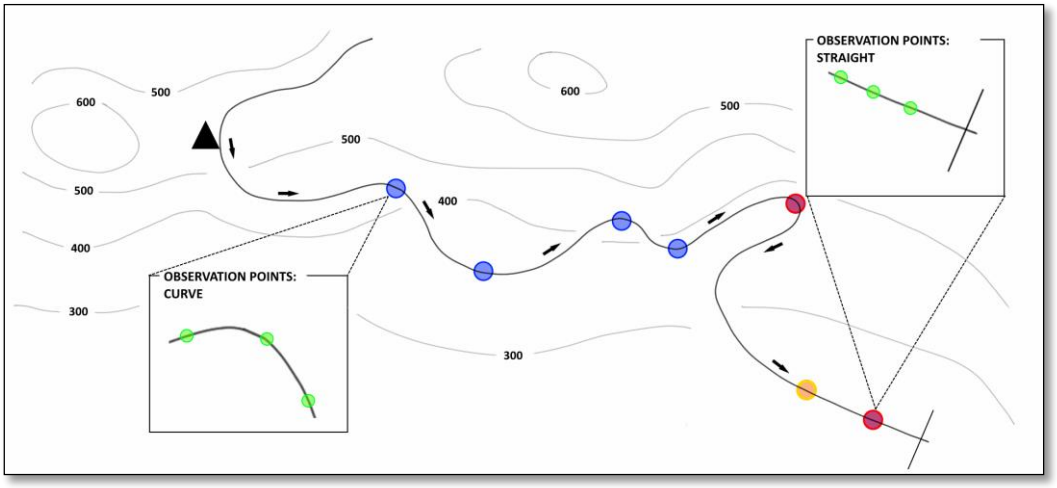

FIGURE 1: ILLUSTRATION OF THE RESEARCH DEFINITIONS
(**Black Triangle:** Summit of pass; **Black Arrows:** Direction of travel; **Blue Dots:** Speeds subject to curve radius; **Yellow Dot:** Speed subject to stopping; **Red Dots:** Critical sections; **Green Dots:** Observation points – entry, apex and exit in the direction of travel)

Mountainous downgrade

A mountainous downgrade is a descending slope that is situated within a mountain pass. Therefore traversing a downgrade entails travelling down the mountain, from the summit towards the base. A mountainous downgrade is depicted in Figure 1 by thick black arrows.

Speed subject to curve radius

This concept refers to speeds that have been decreased as to allow the vehicle to navigate safely around a curve. The location where this will be encountered is illustrated by the blue dots in Figure 1.

Speed subject to stopping distance

This concept refers to speeds that are increasing as the vehicle descends along a straight section of road, before it is deemed necessary to apply the brakes and bring the vehicle to a compulsory stop (e.g. stopping at red traffic lights). The location where this will be encountered is illustrated by the yellow dot in Figure 1.

Critical section

The critical section of a downgrade is the section that causes the most significant change in speed. For speeds subject to curve radius, this is the curve that has the lowest speed through the curve. As for speeds subject to stopping distance, however, this is the point along the straight where the highest speed is recorded. The locations of the critical sections are illustrated by the red dots in Figure 1.

Entry, apex and exit

These terms refer to the three observation points per each critical section. Entry is the first observation point, taken at the start of a curve or at a set distance before the critical point on a straight. The apex is the observation point at the centre of a curve or the critical section on a straight. Lastly, the exit observation point is taken at the end of a curve or at a set distance after the critical point on a straight. Refer to Figure 1 for a depiction of the observation points, illustrated by the green dots.

1.5 Chapter Overview and Layout

Chapter 2: Literature Review

This chapter reviews background information, concepts and definitions, and surveys existing research on factors that influence heavy vehicle operating speeds on downgrades. The structure of this chapter follows a top-down order, starting with a broad overview of the relationship between the global economy and freight transport. The subsequent sections then focus on heavy vehicle accidents on South Africa downgrades, heavy vehicle braking mechanics, GSRS, vehicular speed, and design guidelines and calculation models.

Chapter 3: Research Design

This chapter contains the research design that is relevant to the type of this study that will be conducted. The first section describes the type of study with the type of data required, after which the research objective is discussed. The research variables are then discussed along with the possible means of how to collect the data needed for each of the variables. Lastly the research plan is outlined, which explains how the research will be conducted.

Chapter 4: Research Methodology

The stepwise methods data collection, processing and analyses are described in this chapter. The first section describes and motivates the equipment that has been identified and used throughout this research project. The relevant methods for how this equipment has been used to collect, process and analyse the data are then described. The last section gives an account of the methodology and methods used for the data collection and the analysis.

Chapter 5: Survey Locations

This chapter identifies the relevant mountain passes. The first section discusses the geography of South Africa, introducing the reader to the geographical challenges faced by road freight. In the second section a literature-based systematic approach is used to identify the mountain passes that are used for the study. The last section identifies the critical locations, as outlined in the methodology, of each mountain pass.

Chapter 6: Collected and Processed data

This chapter provides the data that have been collected, along with their necessary processing in preparation for use in the analysis. The structure of this chapter is, first, a discussion of the collected data, and then an account of the subsequent processing of each variable individually. At the end of the chapter there is a summary that provides a condensed overview of the collected data and the processed results.

Chapter 7: Analysis and Results

The structure of this chapter is such that the research question is addressed in a systematic way. Firstly, the collected data will be presented and discussed to allow for preliminary deductions. This is followed by an analysis of the data, as outlined in the methodology. Lastly the results are compiled and interpreted.

Chapter 8: Conclusions and Recommendations

This chapter discusses the results that have been obtained in Chapter 7. Recommendations will then be made as to how the results can be used in real-world applications. Proposals for improvement to the research design and methodology are provided, along with possible topics for future research.

2 Literature Review

This chapter gives a brief overview of the interaction between freight movement and the global and local economic well-being of a country and topics relevant to this project, to allow better insight into and understanding of the research challenges faced.

2.1 Brief Overview: Road Freight and Economic Well-being

Highway transportation of freight has a strong impact on the development of the national economy (Li, 2009:284). This relationship is acknowledged by the South African Department of Transport (2013: 228), stating: *Transport is the heartbeat of economic growth and social development.*

Research done in China found that there is a numerical relationship between the gross domestic product (GDP) of a country and the annual turnover generated from the freight industry. Li (2009) found that for every one unit that the GDP increased, the freight industry's turnover had increased by 5.07. This relationship can be divided into a direct and indirect effect that transportation has on the economy. A direct impact is such that it affects the logistical costs (e.g. positive effect is when goods transportation can be done at low cost due to effective management). Indirect effects primarily result from transportation infrastructure that needs upgrading (i.e. construction) and maintenance, which creates job opportunities in the transportation services sector and construction industry (Li, 2009:284). Therefore the smooth and efficient movement of freight is paramount, since it is linked to the overall economic efficiency of a country, through created employment opportunities and impact on the affordability of consumer goods (Sarvi & Kuwahara, 2008:580).

Inland freight is transported in mainly two modes, by road and rail. The main driving factors in choosing the preferred mode of inland freight moving is accessibility (i.e. the closeness of a suitable transport mode) and mobility (i.e. intensity with which users make use of the transport mode) (Bester, 2013). Road freight has more favourable accessibility and flexibility over rail transport and as a result transportation by road is growing rapidly on a global scale. Road freight has an estimated market share of 80 percent for distances ranging up to a 100 kilometres (km) (Sarvi & Kuwahara, 2008:580). Road freight in Malaysia is involved in each step of the transportation cycle, from origin to manufacturing to consumers, since it is the cheapest mode of inland freight transportation. As a result, road freight in Malaysia is the most frequently used mode for both containerized and bulk cargo. As a result of Malaysia's preference for road freight, it was found that in 2008 freight transportation contributed 11.3 percent to the total GDP (Mat Daud, Endut & Jaafar, 2012:115).

South Africa transported 1.74 billion tonne of freight during 2013, of which 1.53 billion tonne was transported via road. The majority of the freight was localized (i.e. over distances of less than 200 km) with only 245 million tonne being transported over distances greater than 200 km, accounting for 16 percent of the annual road freight. However, this figure chances significantly if the distance is accounted for. This figure then represents 153 billion tonne-kilometre transported over great distances, which accounts for 50 percent of the annual road tonne-kilometres in 2013 (CSIR, 2013:88). Road freight in South Africa has 70 percent market share based on annual tonne-kilometres. With this significant market share, it was found that the logistical costs of road freight contributes 12.5 percent to the total annual GDP (CSIR, 2013:88).

2.2 Recent Accidents on Mountain Passes

The following section focuses on accidents that occurred on South African mountain passes in recent years, where heavy vehicles were involved and at least one severe injury or fatality recorded, whether it is a single vehicle accident or a collision between a heavy vehicle and other vehicles.

Sir Lowry's Pass

Early morning on 11 September 2012 a heavy vehicle experienced apparent brake failure and crashed into a smaller passenger vehicle at the intersection of the N2 and Sir Lowry's Pass Road. The heavy vehicle drove over the pick-up, dragging it underneath for approximately 100 metres before coming to a halt. The driver of the pick-up had sustained severe injuries and was declared dead on the scene. As for the heavy vehicle driver, he had only minor injuries. The heavy vehicle had overturned and came to a halt on its side, and the pick-up was torn into three pieces, giving an indication of the severity of the forces that were involved in this accident. Since this incident, no report has been publicly released and the outcome of this case is still unknown (Jackson, 2012).

During the morning hours of Saturday 29 November 2014 a heavy vehicle collided with six stationary passenger vehicles waiting at the intersection of the N2 and Sir Lowry's Pass Road. The cause of the accident is attributed to brake failure. The intersection is on the Cape Town side of Sir Lowry's Pass, at the base of the pass. It is preceded by a long continuous downgrade with a long straight section leading up to the intersection (Gordon, 2014:1).

As early as 2013 the letters addressed to both provincial and national transport departments had requested that an arrestor bed be installed ahead of the intersection on the downgrade leading up to the intersection. The Western Cape government had developed a plan to install an arrestor bed, but this plan was waylaid in October 2014 in a meeting between SANRAL and the provincial government. The apparent reason was that SANRAL wanted to investigate another possible location for the arrestor bed. The meetings regarding the arrestor bed are still continuing. In the meantime, improvements have been made to the intersection that detect fast traveling vehicles approaching the intersection and will extend the green phase for the vehicle on the N2, possibly allowing the runaway vehicle to safely cross the intersection and come to a gradual halt further on (Gordon, 2014:1).

Huguenot Tunnel and DuToitskloof Pass

During the past eight years there have been no recorded fatalities related to heavy vehicle incidents on the downgrade between the Paarl-side entrance of the tunnel and the toll plaza. This being said, Tuncor (managing corporation of the tunnel) experience an average of one runaway incident a month, but the arrestor bed helps with these incidents (Eksteen, 2014). The arrestor bed is well maintained with a complete and up-to-date service history for the arrestor bed.

Mr Eksteen (2014) said that two runaway incidents stood out from the rest. The first was a heavy vehicle that lost braking capacity and used the emergency toll gate to steer clear of the toll plaza and came to a gradual halt a few hundred metres further away. The second was a heavy vehicle that missed the arrestor bed off-ramp and crashed into a toll booth, but luckily there were no fatalities.

As for the alternative route via the mountain pass, there had only been three or four heavy vehicle accidents in the past eight years. In none of these were any fatalities reported. The pass downgrade stretches about 11 km with winding curves and a couple of straights (Eksteen, 2014).

Vanrhyns Pass

On Tuesday afternoon on 30 May 2000 a heavy vehicle transporting employees overturned on Vanrhyns Pass, resulting in 17 fatalities. The vehicle was descending the pass while underway from Nieuwoudtville towards Vanrhynsdorp. According to the survivors, the vehicle left the roadway and overturned in a shallow ditch, crashing into the mountainside. The investigators stated that it is still unclear as to why the truck veered off the road and that weather conditions had been dry and warm (George & Van Zilla, 2000).

Katbakkies Pass

Two occupants died when their heavy vehicle overturned on Katbakkies Pass on 20 August 2013. The driver stated that the brakes had failed and he subsequently lost control of the vehicle as it veered off the road. The pass is situated between the Koue Bokkeveld and Ceres. Among the injured were 18 other occupants of the vehicle. They were descending the pass while underway from Johannesburg to Lamberts Bay (Koyana & Hartley, 2013).

Hex River Pass

In the wet early morning hours of 5 May 2010 a bus underway from the Eastern Cape to Cape Town plunged down an embankment, resulting in 28 deaths. Upon further investigation it was found that the bus had been declared unroadworthy in the Eastern Cape (Booi, 2010). This was not the only transgression, as it was later found that the bus had also been overloaded. The bus was certified to carry 64 passengers, but it was found that 78 passengers were on board at the time of the accident. Two and a half years later the driver was convicted on 23 counts of culpable homicide under a plea agreement (Samodien, 2012).

On Friday 15 March 2013 a bus underway from Secunda to Cape Town veered off the road in the Hex River Pass, causing 22 fatalities. The pass is situated between the Western Cape towns of De Doorns and Touws River. According to the police spokesperson, brake failure was the cause of this accident (eNCA, 2013). However, this pass is equipped with an arrestor bed and during an investigation of the arrestor bed it was found that the bus did use it, but it just ran clear across the arrestor. The driver subsequently tried to navigate the bus through the second last curve of the pass, but was unable to do so. As a result of the high speed the bus left the roadway and crashed into the embankment. This accident resulted in 22 deaths, 8 passengers left in a critical condition, 14 serious injuries and 44 minor injuries (SAPA, 2013).

Franschhoek Pass

On Saturday 7 March 2015 a 32-seater bus overturned on the Villiersdorp side downgrade of the mountain pass. The bus driver allegedly swerved to avoid hitting two cyclists on the road, but didn't regain control quickly enough in the curve, causing the bus to roll over. This resulted in 3 fatalities and 26 seriously injured passengers (Sesant, 2015). As for the two cyclists, both were airlifted to hospital in a critical condition (eNCA, 2015). It is not clear exactly how the accident happened, but accusations have been made that the cyclists allegedly "cut the corner" (Sesant, 2015).

Piekenierskloof Pass

On Thursday 15 November 2007 a heavy vehicle driver was killed when his vehicle overturned on the pass. This was a single-vehicle accident and no one else was involved. The cause of the accident is still unknown (SAPA, 2007).

2.3 Heavy Vehicle Accidents

Accidents involving heavy vehicles exhibit a higher ratio of fatalities per fatal accident than accidents where no heavy vehicles were involved. This is attributed to the increased magnitude of the impact forces involved, because of the size and mass of the heavy vehicle involved. Heavy vehicles with a mass greater than 11,800 kg (i.e. 26,000 lbs) were involved in 7.1 percent of all recorded accidents in America, during 1987. These accidents, however, accounted for 10.4 percent of all road fatalities during 1987 (Brian & Bowman). This statistic still holds true as is evident from recent studies. In 2004 heavy vehicles accounted for 12 percent of all traffic fatalities in America, while a study in India found that heavy vehicles accounted for 32 percent of all road fatalities during 2009 (Mahanty & Subramanian).

The probability of heavy vehicle accidents on downgrades is greater than the probability of accidents occurring on level terrain. The reason is that severe downgrades generate potential energy that must be absorbed by the brakes to maintain a safe descending speed (Brian & Bowman). This energy is absorbed in the form of heat and if the brake temperature rises too high, brake fade will set in, reducing the braking efficiency and ultimately result in a runaway condition, as stated in Section 2.3.3. The American Trucking Association conducted a study on 497 heavy vehicle accidents and found that 40 percent of the fatalities occurred on severe downgrades (Brian & Bowman). A similar study was conducted by Kharrazi (2004), who found that 19.4 percent of all heavy vehicle accidents occurred at downgrades greater than 2 percent. However, if the cause of the accident is taken as heavy vehicle loss of control, then downgrades of greater than two percent account for 34.4 percent of heavy vehicle accidents.

2.3.1 Loss of Control Accidents

Kharrazi and Thomson (2004) define loss of control accidents as resulting from yaw instability (i.e. deviation from the driver's intended path) and rollovers. Their study found that 19 percent of accidents involving heavy vehicles were attributed to loss of control. Further breakdown of this percentage revealed that 30.8 percent had yaw instability, 54.6 percent rolled over and 14.6 percent experienced a combination of both (Kharrazi & Thomson, 2004).

A further distinction is made based on the critical manoeuvre and the accident type. Critical manoeuvres are defined as the manoeuvre that leads to the loss of control and are categorized as follows: negotiating a curve, turn at intersection, avoidance manoeuvre, lane change, road edge recovery, heavy braking on straight road, lane change in a curve, and going fast on a low friction road (Kharrazi & Thomson, 2004). The study revealed that the most common critical manoeuvre was failure to negotiate a curve, accounting for 59.4 percent of loss of control accidents; this was followed by avoidance manoeuvres and road edge recovery accounting for 11.1 percent and 10.9 percent respectively (Kharrazi & Thomson, 2004).

Accident types defined by Kharrazi and Thomson (2004) include: single-vehicle accident, head-on collisions, rear-end collisions, sideswipe and collision with pedestrians or animals. The most common accident type was found to be single-vehicle accidents, accounting for 84.3 percent of all heavy vehicle loss of control accidents.

2.3.2 Heavy Vehicle Runaways

A runaway vehicle is defined as a vehicle that no longer has the means to reduce its speed or bring it to a safe stop, primarily as a result of brake failure or brake fade (Carrier & Pachuta, 1981). With no ability to control the operating speed of the vehicle, it risks running off the road, rolling over because of excessive speed through a curve, or colliding with slower moving vehicles (Scott, Fay et al., 2003). Runaway conditions are primality attributed to brake fade or failure; however, Scott et al. (2003) state that the causes of runaways are more complex and can be best described by the combined factors of brake heating, brake system design, brake pad material composition, maintenance and brake adjustment. Poor brake adjustment is often the primary cause of runaway conditions, especially on foundation brake systems, since the rotor (i.e. drum) expands during braking. If the pushrods are poorly adjusted, the expansion of the rotor might be greater than the pushrod travel, resulting in insufficient braking force to be exerted on the rotor (Carrier & Pachuta, 1981). Therefore, heavy vehicle drivers have to manage the rate at which the brakes generate heat through maintaining a safe operating speed with regard to the vehicle mass (Carrier & Pachuta, 1981).

Data collected during 1979 in the state of Pennsylvania listed brake failure as a contributing cause of the accident for 2.27 percent of all vehicle-related accidents (i.e. both passenger and heavy vehicles), which resulted in 66 fatal accidents (Carrier & Pachuta, 1981). Further analysis of the data found that vehicle failure is the contributing cause for 8.8 percent of all semi-trailer heavy vehicle accidents, accounting for 22.7 percent of the related fatalities (Carrier & Pachuta, 1981).

In 1987 the American Trucking Association found that of the 497 heavy vehicle accidents, 16 percent were classed as runaways in the presence of a downgrade (Brian & Bowman). For the same year a total of 2,450 runaways were recorded across America, with an estimated annual cost of over 37 million US dollars. An analysis of the runaways revealed that 73 percent of the runaways were heavy vehicles heavier than 27,200 kg (i.e. 60,000 lbs), with 51 percent of these heavy vehicle drivers stating that brake failure was the cause of the accident (Brian & Bowman, 1987).

From the above statistics it is evident that downgrades are a significant contributing factor in heavy vehicle runaways and as a result various studies have been conducted on heavy vehicle runaways on downgrades. A study conducted by Carrier and Pachuta identified 18 sites in the state of Pennsylvania that have a high potential for heavy vehicle runaways. The identification was based on the accident records for the preceding three years for the 18 downgrades, over which a total of 63 heavy vehicle runaways were recorded. A comparative analysis revealed that runaways were more frequent on downgrades of greater than 5 percent and longer than 800 m (Carrier & Pachuta, 1981). In addition to this analysis, Carrier and Pachuta were on site for the four most recent runaways immediately after the accident occurred. All four of the drivers were interviewed, which enabled Carrier and Pachuta to conceptualize a typical runaway scenario: “Crested hill at low speed in reduced gear, but unfamiliar with the hill and didn’t know exactly which gear to be in … was under control most of way down the hill, but lost control when I rounded a curve and saw traffic at virtual standstill … pulled onto shoulder, sounded horn …

proceeded on shoulder to point where traffic stacked up … smashed into several waves of standing autos" (Carrier & Pachuta, 1981). In addition to the interviews conducted, the drum brakes were also examined within 10 minutes after the accidents. It was found that for all four accidents, half of the drums were cool to the touch. This suggested that the common cause of the accidents was poorly adjusted brakes, which significantly reduced the braking efficiency (Carrier & Pachuta, 1981).

Another study was conducted by Scott, simulating extreme operating and downgrade conditions. During the braking tests, it was evident that the brakes continuously faded as a result of frequent use, and that an increased brake pressure was applied to maintain a constant braking force. The analyses of the brake shoes revealed that the shoes exhibited growth (i.e. thickening) as a result of overheating. Examination of the brake drums revealed that small cracks had formed as a result of the high thermal stresses caused by the excessive and frequent braking (Scott, Fay et al., 2003).

2.3.3 Countermeasures

The following solutions for heavy vehicle safety have been proposed, pertaining to loss of control accidents and runaways in particular. It should be noted that some of the proposed solutions can be implemented to increase heavy vehicle safety in general.

- Introduce policies that standardise disc brakes and antilock braking systems (ABS) on heavy vehicles. Kharrazi (2004) found that none of the heavy vehicles, in the relevant study, lost control under heavy braking. As for disc brakes, they are safer in general since the rotor expands towards the stator and decreases the severe effects and outcomes of poorly adjusted brakes (Bendix, 2011).
- Educate drivers on proper gear selection and correct use of engine brakes and retarders as a means to control operating speed on downgrades (Scott, Fay et al., 2003).
- Improve signage on severe downgrades and construct escape ramps (Carrier & Pachuta, 1981). Interviews conducted with heavy vehicle drivers yielded four easy ways to implement solutions regarding signage: uniform signage with grade and length information, "Traffic may be stopped" signage, signs with alternating flashing lights ahead of severe problem areas, lane and speed restrictions with sufficient headways for heavy vehicles. Carrier and Pachuta found that drivers preferred the GSRS signage, discussed below.

2.4 Braking Systems and Mechanics

Brake systems are often described by the brake mechanism that is used on the vehicle, either drum brakes or disc brakes. Drum brakes have the rotor (i.e. drum) fitted over the stator (i.e. brake pads), whereas for the disc brake the stator (i.e. brake calibre and pads) fits over the rotor (i.e. disc). The brake driver forces the stator into contact with the rotor when the brakes are applied. For drum brakes this is done by rotating an 's'-shape cam and for the disc brake by a piston within the stator. Therefore the primary difference between braking systems is the type of brake mechanism implemented on each axle end.

Thus, to gain a better understanding of the braking system as a whole, the following sections focus on the braking system and function, friction materials, brake fade, braking strategies and braking regulations.

2.4.1 Braking System and Function

The brake system of a vehicle can consist of various subsystems and a multitude of different components, depending on the vehicle and the braking requirements (Mahanty & Subramanian, 2009). Heavy vehicles use pneumatics (i.e. compressed air) to operate their braking systems, unlike smaller vehicles that make use of hydraulic fluids. The reason for this difference is that brake fluid can safely operate up to 260 degrees Celsius (°C), after which it starts to boil and deteriorate. Therefore, in more strenuous operating conditions such as mountainous descents, heavy-vehicle braking can exceed the boiling point of brake fluid, which will result in inefficient braking capability and possibly a runaway incident (Emery, 2003).

The conventional air-brake system used in commercial vehicles can be divided into two main systems, namely the supply (i.e. pneumatic components) and control (i.e. mechanical components) systems (Mahanty & Subramanian, 2009).

The Supply System

The supply system is comprised of all the pneumatic components to allow generation of compressed air and safe operation thereof (Mahanty & Subramanian, 2009:130). This includes the compressor, oil separators, dryers, storage reservoirs, brake lines, treadle and relay valves, and braking chambers for each axle. The supply system is also divided into two circuits, namely the primary and secondary circuits. The primary circuit supplies compressed air to the rearward axle chambers and the secondary circuit supplies compressed air to the forward axle chambers. This is done to ensure that the heavy vehicle retains some means of controlling and reducing speed if any one of the two circuits fails (Mahanty & Subramanian, 2009).

The Control System

The control system is mechanical by nature, since it controls the physical interaction between the rotor and stator. This system is divisible into two subsystems, namely the parking circuit and driver control, each of which is used for a specific purpose. The parking circuit engages the braking system when the heavy vehicle is stationary to prevent rolling and accidental runaways. The parking circuit is split into front and rear circuits, ensuring that the heavy vehicle can remain stationary in the case of one circuit failing (Wikipedia, 2015). Driver control entails the physical operation of the brake pedal to reduce operating speed. This subsystem includes the brake pedal and brake mechanism on each axle end. The brake mechanism includes the push rod, slack adjuster, brake stator and brake rotor (Mahanty & Subramanian, 2009:130).

On modern braking systems, part of the control system is replaced with an electronic control. The advantage of this is that the brake rate and subsequent brake temperatures are controlled and managed more precisely. However, the driver does not receive physical feedback through the pedal any longer; therefore an active overheating detection circuit is included in the control system that relays the necessary feedback to the driver (Artus, Cocquempot et al. 2005).

Brake System Functioning

The main function of the brake system is to decelerate the vehicle in a safe and stable manner, whether to control operating speed or come to a complete stop. In applying the brakes, the brake pedal meters out compressed air from the supply reservoirs to the brake chambers on each axle or axle group (i.e. tandem or triple axle) (Mahanty & Subramanian, 2009). The air subsequently forces the pushrod forward, which actuates the brake driver, forcing

the rotor and stator into contact. The interaction between the stator and rotor converts the vehicle's kinetic energy into heat, through friction, slowing down the vehicle. Generated heat is then stored in the rotor, after which it dissipates to the atmosphere (Jacko, Spurgeon et al., 1968).

2.4.2 Friction Materials and Characteristics

Automotive vehicles control and reduce the vehicular speed though forcing the brake shoes on each axle end into contact with the rotor, resulting in frictional forces being generated that reduce the speed as needed. Friction materials for automotive brakes are complex composites that consist of three primary components, namely an organic resin binder, asbestos fibre as a reinforcing agent and modifiers that maintain friction level and wear rate (Jacko, Spurgeon, Rusnak & Catalano, 1968).

All of the materials that comprise the composite brake pads exhibit temperature-dependent wear as a result of the composition. Brake lining wear tends to be independent up until a certain threshold temperature, after which wear occurs at an exponential rate. During braking, the composite friction materials that comprise the brake pads are exposed to transient temperatures across the friction interface between the rotor and stator. If these transient temperatures exceed the threshold, the friction materials at the interface exhibit an increased rate of wear (Barber & Tuten, 1986).

The temperature build-up in the brake pads is a result of kinetic energy being converted at the sliding interface between the rotor and stator, which is subsequently absorbed by the brake pads and rotors, and dissipated to the atmosphere over time. When the rate of heat generation exceeds the rate of dissipation, the temperature rise at the sliding interface and between the rotor and stator, which may reach and exceed the threshold temperature of the friction materials (Jacko, Spurgeon, Rusnak & Catalano, 1968). Research done by Barber and Tuten (1986) found that regular braking of drum brakes can result in temperatures as high as 221°C. The study also concluded that the binder material exhibited constant wear up to temperatures of 232°C, after which pyrolysis sets in and the wear then increases exponentially. However, the binder used in this study was asbestos based, which is currently replaced with other compositions because of the health risks associated with the use of asbestos in the binder (Barber & Tuten, 1986).

The critical temperature threshold is taken as the material with the lowest thermal stability in the composition. The general decomposition temperatures for the three materials are found to be 287°C to 315°C for the modifier, 398°C to 427°C for the resin binder and 650°C to 677°C for the fibrous reinforcing agent (Jacko, Spurgeon, Rusnak & Catalano, 1968).

2.4.3 Brake Fade and Failure

Temperature is a critical variable when describing the state of brake pads and this temperature is closely related to the braking efficiency. The braking friction coefficient is the ratio between the effective braking force and the desired braking force. Fade temperature is defined as that temperature at which the friction coefficient has decreased to about 90 percent of its maximum value (Jacko, Spurgeon et al. 1968). Therefore a lack of braking efficiency can occur at high temperatures as the effective braking force decreases with an increase in temperature. When this phenomenon occurs, it is known as brake fade (Artus, Cocquempot et al. 2005).

Fade can occur in one of two ways. Firstly, gas can form from the decomposing and oxidizing materials at the sliding interface between the rotor and the stator, which exerts a force on the linings or pad by expanding and pushing it away from the rotor. The other one is a bit less common, but fade can also occur with the formation of a liquid phase or a low friction solid phase at the sliding interface (Jacko, Spurgeon et al. 1968). Variations in the brake pad composition can cause the onset of brake fade to occur at different temperatures. Low asbestos content (below 20%) results in early fade, occurring at around 21 to 204°C. Jacko et al (1968) found that an asbestos content of between 20 and 40% resulted in a fade threshold of 315°C with a high rate of wear. A good brake material composition was found to have an asbestos content of 50 percent or more, resin binder of 5 percent or more, and modifier of 5 percent or more. This results in a brake lining that has a fade threshold of 315°C with low wear and a sufficient friction coefficient of 0.3 (Jacko, Spurgeon et al. 1968).

Overly high temperatures can lead to several significant problems, since the brake pad's performance is temperature dependent and prone to fading at high temperatures. At high temperatures thermal stresses may develop and permanently deform the brake components. This build-up of heat may subsequently also heat any system fluids used in in brake system, causing it to vaporize, reducing the braking efficiency (Emery 2003).

A study conducted by Artus et al. (2005) approached the thermal estimation by stating that the disc can have a maximum energetic level, also defined as the capacity. During braking two main things happen: energy is absorbed and dissipated. Therefore the energetic level at any time during braking can be defined as the difference between the absorbed and dissipated energy. Energy absorbed by the disc is generally defined as the braking force at the road/tyre interface and the vehicular speed (Artus, Cocquempot et al. 2005).

The dissipated energy is the loss or cooling of the brake and is defined as the sum of the convected, radiated and conduction heat. 90 percent of heat is dissipated through heat convection, which is difficult to define and this complicates collecting data in the field. The testing of this equation also could not be done on severe downgrades of several kilometres or between gradients ranging from 3 percent to 10 percent for the safety of the people involved directly and indirectly in the study. Therefore, it is uncertain if this will hold for mountain passes or mountainous roads (Artus, Cocquempot et al. 2005).

As previously mentioned, during braking the kinetic energy is converted into thermal energy through friction between the brake pad and rotors faces. A study was conducted on temperature distribution on pad shapes. Two types of pads were used: flat surface pads and hatched pads. The testing rig that was set up measured the temperature distribution across the pad face at three points, namely the edge, the middle and the inner section. The test was done at 20, 30 and 40 km/h. The experiment revealed that hatched pads generally operate cooler than flat surface pads under the safe braking conditions. Therefore, hatched pads offer greater protection against brake fade (Albatlan, 2013).

2.4.4 Braking Strategies (Fancher Study)

Fancher (1992) conducted a study on the effectiveness on different braking strategies on downgrades. The experiment set out to determine what the temperature difference is between the braking strategies, rate at which martensite form and likelihood of drum cracking, and how the slack adjusters perform. This study was done on a downgrade, spanning 7.24 km with a varying gradient to obtain noticeable differences in brake temperatures. The testing vehicles consisted of two heavy vehicles, a 3-axle rigid body and a 5-axle semitrailer. The brake system

that was used for the experiment was a s-cam drum brake. The 3-axle test vehicle had a mass of 21,060 kg and the preliminary runs down the mountain yielded a safe descending speed for the pass to be 56 km/h. The 5-axle test vehicle had a mass of 36,300 kg. This vehicle was safely descending at 40km/h, but this was later changed to 32km/h, since the bulk temperatures of some brake drums reached temperatures higher than 530 °C.

Two braking strategies were identified and the control drivers were experienced test drivers. The first strategy is to keep the speed constant over the whole length of the downgrade while applying light pressure to the brakes and, secondly, they were to brake in snubs of 5 km/h. The drivers were to bring down the speed to the control speed when it reached 5 km/h above the control speed. The strategies were termed dragging and snubbing respectively.

The result for the 3-axle heavy vehicle revealed that snubbing was marginally better or running cooler than dragging or continuous braking. The average temperatures recorded during the runs were 205°C for dragging and 187°C for snubbing. Therefore, snubbing resulted in an 18°C cooler brake system. As for the five axle heavy vehicle the following had been found: for both dragging and snubbing the temperatures ranged from 232°C to about 260°C for all brakes adjusted on a pneumatically balanced braking system. So there is also no significant difference between the two braking strategies.

However it had been observed that if the five axle system is misadjusted and imbalanced, the temperatures can reach the 426°C to 538°C range for dragging with the snubbing limiting the range from about 343°C to 426°C. Therefore, if the brakes are poorly adjusted, snubbing is the better option (Fancher & Flick, 1992).

2.5 Grade Severity Rating System

As stated previously, the probability of heavy vehicle accidents occurring on downgrades is greater than the probability of accidents on level terrain. The gradient induces a potential energy that needs to be absorbed by the brakes to maintain a safe descending speed, but this can lead to brake fade and failure (Brian & Bowman, 1987).

There are many research projects that focused on the causes of heavy vehicle accidents on downgrades and the possible countermeasures available. However, there is lack of accurate information regarding the effectiveness of the various countermeasures in different situations. This hampers design and safety engineers in trying to minimize the adverse effects of downgrades on heavy vehicles and to choose the appropriate countermeasures for various situations (Abbott, 1982). Certain states in America have decided that more information should be conveyed to the drivers, despite their not knowing what countermeasures are best or more suited to the given downgrades. The countermeasures include informational signs (containing gradient, length of downgrade, gear selection and downgrade configuration), summit brake inspection areas and escape ramps (Abbott, 1982).

One such method to improve the road safety of heavy vehicles is to convey better quality information to the drivers. This method is intended to describe: length and gradient, recommended gear, nature and severity of downgrade, physical features, information on arrestor beds and truck turnarounds, and alternative routes (Brian & Bowman, 1987). In the light of providing drivers with better quality information, the United States Bureau of Public Roads (USBPR, 1961) developed a severity system that would assign a category to a given downgrade based on the gradient and the length of the downgrade. These categories were:

- Greater than 3 percent and longer than 16 km;
- Greater than 6 percent and longer than 1.6 km;
- Greater than 10 percent and longer than 320 m;

The original severity system has been extended multiple times. The first extension of the system occurred in the early 1960s to include more categories and introduce a rating system ranging from one (least severe) to ten (most severe), effectively introducing the grade severity rating system (Brian & Bowman). In 1975 new concepts were introduced such as the effect of downgrade length on brake fade and stopping distance as a measure of available braking capacity. This model was based on the work-energy theorem. The limitation of this model is that there is a lack of knowledge about the effects of non-brake forces (Abbott, 1982). The current GSRS determines brake temperatures based on downgrade length, gradient, mass, speed. This information is then used in determining a downgrades severity rating, which is then conveyed to drivers via road signs.

An alternative means of conveying downgrade information to drivers is through a weight-specific sign (WSS) (Abbott, 1982). In developing a WSS the main consideration is the number of weight ranges that should be used. With more ranges, more individual weight-specific speeds can be indicated. However, when this information is conveyed to the drivers, it may be confusing because of the amount of information given at once. Abbott (1982) stated that research had found that combining grade severity ratings and weight-specific signs is often confusing and contradictory, since each method recommends its own distinct definition of what is safe (Abbott, 1982). Further research found that WSS allows drivers to select the appropriate gear to maintain the recommended weight-specific speed, whereas the severity rating is difficult to quantify and translate to an appropriate gear selection. Therefore, Abbott concluded that a WSS is more effective in relaying the necessary information to drivers.

2.6 Vehicular Speed

Kay-Fitz (2002) states that when working with vehicular speed, attention should be given to the various terminology for speed. The most commonly used terms are design speed, operating speed and posted speed. The National Cooperative Highway Research Program (NCHRP) defines design speed as the selected speed which is used to determine the various geometric design features of the road. Operating speed, sometimes revered to as running speed, is the actual maximum speed at which a typical vehicle category or overall traffic can operate safely. The operating speed can be decreased or limited to a set speed, depending on the surrounding conditions, which is referred to as the posted speed limit.

According to the South African Geometric Design Guide for Rural Roads THR17 (CSIR, 1981), a distinction should be made between five types of speed, namely desired speed, design speed, operating speed, running speed and posted speed. The definitions are as follows (CSIR, 1981):

- Desired speed is the speed at which the driver wants to travel;
- Design speed is the selected speed as a safe basis to establish geometric design elements;
- Operating speed is the observed speed under free-flow conditions;
- Running speed is the average speed over any given distance;
- Posted speed is the set limitation to operating speed, so as to ensure safe traffic operations.

The selected design speed should be logical and in harmony with the topography and the functional classification of the road (CSIR, 2013). The topography is especially important when determining the design speed for rural roads, since the topography can introduce severe changes in road alignment. Therefore, the typical design speeds used for rural roads with regards to topography are as follows (CSIR, 1981):

- Flat terrain – design speed 90 to 120 km/h;
- Rolling Terrain – design speed of 80 to 100 km/h;
- Mountainous Terrain – design speed of 60 to 80 km/h.

Speed has a strong relationship with geometric features. Kay-Fitz (2002) states that the horizontal alignment for a set design speed is influenced directly by both the curve radius and superelevation, whereas for the vertical alignment the design speed is affected by both the gradient and vertical curves (i.e. crests and sags). Furthermore, the only horizontal geometrical property that directly influences the operating speed is curve radius. Additionally, gradient is the primary vertical alignment property that influences operating speed.

2.6.1 Studies on Operating Speed

The Council for Scientific and Industrial Research (CSIR) conducted a study from the mid-1970s to the mid-1980s found that traffic accident fatality rates decrease with a decrease in the speed limit (RTMC, 1985). An initial fatality rate of 0.59 decreased to 0.44 fatal accidents per million vehicle-kilometres travelled, when the speed limit was reduced from 120 km/h to 80km/h. During this time an estimated 12,500 lives were saved as a result of 140,000 fewer accidents (RTMC, 1985). A similar study was conducted in Europe during 1990, in which it was found that a three-kilometre per hour (3 km/h) reduction in speed avoided 120,000 to 140,000 accidents, possibly saving 5,500 lives (RTMC, 1985).

Bornes and Vaa (2011) conducted a study in Norway to determine how heavy vehicle operating speed varies among vehicle categories with changes in the weather and gradients and the effect on traffic flow. The study was conducted on the section of road between Andalsnes and Oppland county borders. The reason for choosing this section was motivated by the inclusion of a mountain pass on the route. During the data-collection phase three primary sets of data were collected, namely traffic-flow data, weather conditions and friction measurements. Bornes and Vaa (2011) found that there is a considerable difference in speed between passenger vehicles and heavy vehicles in the presence of mountainous gradients. Furthermore, it was found that heavy vehicles recorded speeds of 27 – 29 km/h slower than that of passenger vehicles, whereas on flat terrain the difference was only 4 km/h. Lastly, the study found that weather conditions had an influence on the traffic flow, but varied significantly with the type and intensity of conditions.

2.6.2 Operating Speed versus Posted Speed Limit

The posted speed limit is often referred to as the 85^{th} percentile speed, since this percentile is used to set the speed limit for a given road. The 85^{th} percentile is the speed at or below which 85 percent of all vehicles are observed to travel under free-flow conditions (Metro Count, 2011).

A study conducted by Kay-Fitz (2002) determined how the operating speeds of selected rural roads relate to the relevant posted speed limits. Table 1 summarizes the posted speed limit, the percentage of drivers that travelled

at speeds equal to or below the posted speed limit, and what percentage of the driver population is accounted for at speeds 5 and 10 mi/h greater that the posted speed limit.

It had been found that the posted speed limit for most of the rural roads, do not adhere to the generally accepted 85th percentile guideline, as only one posted speed limit was greater than the 85th percentile speed. One speed limit was acceptably near the 85th percentile speed, with the remaining three being significantly lower and is considered over-conservative (Kay-Fritz, 2002).

TABLE 1: 85TH PERCENTILE VERSUS POSTED SPEED LIMIT

Posted Speed Limit [mi/h]	At Speed Limit [%]	At 5 mi/h greater [%]	At 10 mi/h greater [%]
50	81	99	100
55	61	85	96
60	91	95	98
65	59	89	98
70	64	91	98

Setting a posted speed limit can be done by following the guidelines for speed limits outlined by the Manual on Uniform Traffic Control Devices (MUTCD), which states that when a speed limit is to be posted it should be the 85th percentile speed of the free-flow traffic rounded up to the nearest 10km/h. Other methods of setting the posted speed limit, other than using the 85th percentile, include roadway geometry (e.g. shoulder conditions, gradient and alignment), accident history and political pressure (MUTCD, 2009).

Kay-Fitz (2002) determined in a different study that the actual 85th percentile speed typically exceed the posted speed limits, with the limits being more representative of the 50th percentile. The study found that between 37 and 64 percent of the free-flow vehicles for rural roads travel at or below the posted speed limit. Half the sites had speed differences ranging between 6.44 to 12.88 km/h below the 85th percentile. At only ten percent of the surveyed sites did the posted speed limit reflect a rounding up to the nearest 5 km/h, as proposed in the MUTCD. This study revealed that most surveyed agencies use the 85th percentile speed as the basis for their speed limits; therefore there should be a strong relationship between the 85th percentile and posted speed limits. However, the opposite was found, with the posted speed almost always being set below the 85th percentile operating speed by as much as 12.88 to 19.31 km/h.

2.7 Calculation Models, Design Guidelines and Standards

This section focuses on the calculation models, design guidelines and standards pertaining to the collection and analyses of the relevant research variables. The section is structured to group together models and equations of similar field of science. Thus, the main focus groups are road geometrics, heavy vehicle characteristics, geometry, geodesy and applied statistics.

2.7.1 Road Geometrics

Road geometrics and characteristics that are relevant to the research project include the curve radius, gradient and superelevation, since they directly influence the operating speed, as discussed in Section 2.6. The variables are subsequently discussed along with the possible means of calculating it.

Gradient

The gradient of a road is defined as the rate of rise between two points and is calculated as the ratio of the change in altitude to the change in horizontal distance (Stewart, 2007). Figure 2 provides an illustration of a road gradient.

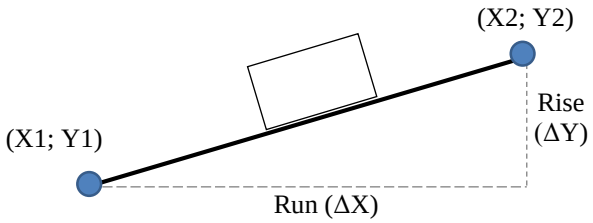

FIGURE 2: ILLUSTRATION OF ROAD GRADIENT

From the above figure the equation for determining the gradient m (m/m) is as follows (Stewart, 2007):

$$m = \frac{Y_2 - Y_1}{X_2 - X_1} = \frac{\Delta Y}{\Delta X} \quad (1)$$

Therefore, the gradient of a straight road can be determined by simply taking the changes in altitude and horizontal distance between two points and applying it directly to Equation (1). However, this is more difficult to determine on mountain passes, since the road is not straight (2D representation), but instead follows a complex set of alignment changes (3D representation). Therefore, the author suggested that the gradient be calculated using a simplified one-dimensional finite element approach, where the complex line is broken down into smaller straight line segments and averaged. Therefore Equation (1) becomes:

$$m = \frac{\sum_{i=1}^{n} \frac{\Delta Y_i}{\Delta X_i}}{\sum n} \quad (2)$$

The gradient of a road markedly affects the operating speed of heavy vehicles (TRH17, 1988). The reason for this is attributed to the vehicle's mass and the Earth's gravitational acceleration of the mass. Using Newton's second law and the direction of the mass (i.e. ascending or descending) the resultant force on the vehicle can be described. An ascending mass has a negative acceleration (i.e. opposite to gravity's direction), whereas a descending mass has a positive acceleration (i.e. same direction as gravity). Figure 3 provides a conceptual illustration.

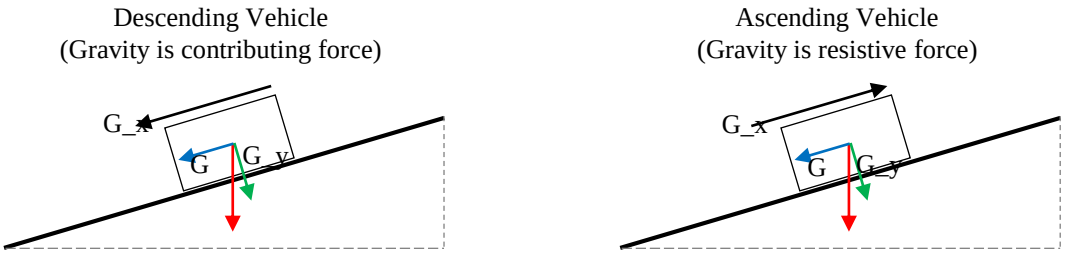

FIGURE 3: CONCEPTUAL ILLUSTRATION OF THE EFFECT OF GRADIENT ON A VEHICLE

Thus, an ascending heavy vehicle has to overcome deceleration (resistive force, $-G_x$) as a result of gravity, while a descending heavy vehicle has to control acceleration (contributing force, $+G_x$). According to the TRH17 (1988), road gradients range from 4% to a maximum of 10% for mountainous terrains. In South Africa a reduction in operating speed of 20 km/h constitutes intolerable conditions. Therefore, if gradients reduce the speed of heavy vehicles by 20 km/h or more, it may be necessary to provide auxiliary lanes for the slower moving vehicles.

Superelevation and Sideways Force Coefficient

A vehicle that is travelling along a flat circular path is forced outwards by a centrifugal force (CSIR, 1988:26). Therefore, if a vehicle is to safely navigate a horizontal curve at speed, the centrifugal force (i.e. outward force) needs to be counteracted. This is achieved through sideways friction between the tyres and the road, and is assisted by inclining the road towards the centre of the curve, inducing a centripetal force (i.e. inward force). This cross-sectional inclination is known as superelevation. The inward force depends on the component of the vehicle's weight on the incline and the side friction between the tyres and the road surface (Garber & Hoel, 2010:85). See Figure 4 for an illustration of superelevation.

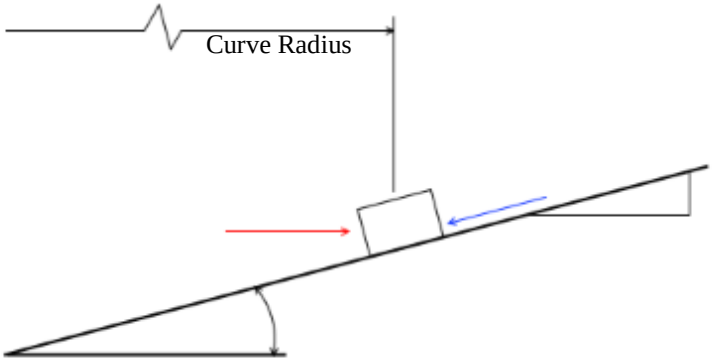

FIGURE 4: ILLUSTRATION OF SUPERELEVATION
(Red Arrow: Centrifugal Force pushing vehicle outwards; **Blue Arrow:** Centripetal force generated by the superelevation, pushing the vehicle inward)

According to TRH17 (1988), the maximum rate of superelevation (e) used in the design of South African rural roads is ten percent (CSIR, 1988:26). The side friction is developed between the tyre and the road surface, and is speed dependent. The maximum design sideways friction (f_{max}) factor is expressed by the following equation:

$$f_{max} = 0.19 - \frac{v}{1600} \tag{3}$$

Equation (3) determines the maximum design sideways friction factor for a given design speed v (m/s). Furthermore, this equation also represents a safety factor of approximately three (CSIR, 1988:26).

Curve Radius

The minimum radius is a limiting value for a given design speed (CSIR, 1988:21). At a given speed (v) the minimum radius is determined from the maximum rate of superelevation (e_{max}) and the maximum allowable side friction (f_{max}). The following equation, as stated by Papacostas and Prevedouros (2005:51), allows for the calculation of the minimum radius (R_{min}), in metres:

$$R_{min} = \frac{v^2}{g}(e_{max} + f_{max}) \quad (4)$$

Equation (4) can be also be used to obtain any design radius, through substituting the maximum values of the superelevation and friction factor with those of the design values (Papacostas & Prevedouros, 2005). This equation is also contained in the 17th Technical Recommendations for Highways (TRH17, 1988) manual. Table 2 is included in the TRH17 (1988), which specifies the minimum radius for given design speeds (CSIR, 1988:22):

TABLE 2: MINIMUM RADIUS FOR GIVEN DESIGN SPEED

Design Speed (km/h)	Radius (m)
50	80
60	110
70	160
80	210
90	270
100	350
110	430
120	530
130	640
140	760

The minimum radii listed in Table 2 have been obtained through assuming the maximum rate of superelevation and sideway friction factor. These radii should be used only under the most critical conditions (CSIR, 1988:21). Also

2.7.2 Heavy Vehicle Characteristics

The two main heavy vehicle variables for this research project are speed and mass, and the accurate collection of such data is very important. Obtaining the mass of vehicles is done by means of two methods, namely static weighing and dynamic weighing.

Heavy vehicle mass

The mass of a vehicle describes how much the relevant vehicle weighs, usually expressed in kilograms or tonnes. The weight is the force equivalent of the mass, as a result of the Earth's gravitational force acting on the mass. The load has two components, namely static and dynamic. The static load is equivalent to stationary weighed vehicles and one part component for moving-weighed vehicles. The gross vehicle mass (GVM) is the sum of all axle loads of a stationary vehicle. The two weighing methods are outlined below.

Static Weighing Method - this requires the vehicle to be stationary during weighing. This means that only a limited number of vehicles can be weighed for a given time interval, and on heavily trafficked roads the masses will only represent a sample of the actual masses to be obtained.

Dynamic Weighing Method - at sites such as multi-lane highways or where the terrain and traffic flow do not allow for the static weighing of all vehicles or for a representative sample to be obtained, in-motion or dynamic weighing is recommended. Weigh-in-motion accuracy depends on the speed at which the vehicle passes over

the devices. The slower the speed the more accurate the weight. Low-speed devices are generally classed as devices that weigh vehicles travelling at 15 km/h or slower. Furthermore, these devices require physical setup in the field and preferably on multi-lane roads so as not to affect the traffic flow adversely. It is also important to note that this means of data collection is very dependent on the mass measuring equipment accuracy, which in turn is dependent on the technology, that can often times be very expensive.

Heavy vehicle operating speed

To determine the operating speed of a vehicle, two parameters are needed, namely the distance travelled and the time taken to do so. Measuring the operating speed of vehicles in the field can be done with various devices. The devices and methods are described below.

Radar gun – this device sends out frequencies that reflect back off the observed vehicle and the time differential is used to calculate the speed of the vehicle at the given moment. Therefore this device measures the spot speed of a vehicle (Bushnell, 2012). This device does not require any physical setup, since it is a handheld device.

Piezo-electric strips – these devices are similar to those used in speed enforcement, which consists of two strips, at a set distance, that record the vehicle's time spent between the strips, which is subsequently used to calculate the speed of the vehicle. This device requires physical setup on and next to the road.

2.7.3 Geometry

Geometry is the field of mathematics concerned with the properties of points, lines and shapes and how these relate to each other. The two most commonly used branches of geometry are Euclidean and analytical. Euclidean geometry is based on a small set of axioms (i.e. starting points of reasoning) that are used to deduce geometrical theorems, with the most well-known being Pythagoras' Theorem. Analytical geometry is the study of geometry with a coordinate system. Equations (5) through (8) are basic plane geometric equations that are generally useful. See Figure 5 for an illustration.

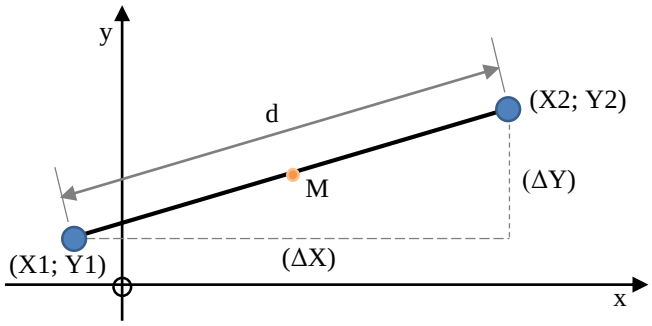

FIGURE 5: ILLUSTRATION OF GEOMETRICAL EQUATIONS

Linear equation – this equation gives the corresponding y value for a given x value based on the relevant gradient (m) and intercept (c) values. The line's direction can be changed by changing the sign of the gradient. Note that in doing so, the equations will have different y-intercept values.

$$Y = mX + c \tag{5}$$

Midpoint equation – this equation gives the corresponding mid-point coordinates between two points.

$$M\left(\frac{X_1 + X_2}{2}; \frac{Y_1 + Y_2}{2}\right) \tag{6}$$

Distance equation – this equation is based on Pythagoras' Theorem, which states that the sum of the areas of the right-angled sides of a triangle will result in the area of the hypotenuse. Therefore, taking the square root will result in the length of the hypotenuse being obtained.

$$d = \sqrt{(X_2 - X_1)^2 + (Y_2 - Y_1)^2} \tag{7}$$

Another equation that is useful for calculations with straight lines and angles is the cosine-area rule, also referred to as the cosine law of triangles. The equation is used to determine unknown angles and distances, given two known side lengths (i.e. a and b) with a known included angle (C). The equation is as follows:

$$c^2 = a^2 + b^2 - 2ab \times \cos(C) \tag{8}$$

2.7.4 Geodesy

Geodesy is a branch of applied mathematics that deals with the measurement and representation of the Earth in three-dimensional space. This is particularly important for global positioning systems (GPS), which rely on accurate measurements on the Earth's surface. Because of the ellipsoidal nature of the Earth, there are various equations that can be used to calculate the distance between coordinates (d_{coord}) on the Earth's surface, depending on the accuracy required. The three most commonly used equations are as follows:

(i) Spherical Laws of Cosine – Assumption that the earth is round, accurate for larger distances

$$d_{coord} = \mathrm{r} \times \arccos(\sin \emptyset_1 . \sin \emptyset_2 + \cos \emptyset_1 \cos \emptyset_2 cos\Delta\lambda) \tag{9}$$

(ii) Haversine Formula – more suited for small distances, also assume that earth is spherical

$$d_{coord} = r \times 2 \arcsin\left(\sqrt{\sin^2\left(\frac{\Delta\emptyset}{2}\right) + \cos \emptyset_1 \cos \emptyset_2 \sin^2\left(\frac{\Delta\lambda}{2}\right)}\right) \tag{10}$$

(iii) Vincenty's Formula – accurate for all distances, accounts for ellipsoids

$$d_{coord} = r \arctan\left(\frac{\sqrt{(\cos \emptyset_2 \sin \Delta\lambda)^2 + (\cos \emptyset_1 \sin \emptyset_2 - \sin \emptyset_1 \cos \emptyset_2 \cos \Delta\lambda)^2}}{\sin \emptyset_1 . \sin \emptyset_2 + \cos \emptyset_1 \cos \emptyset_2 cos\Delta\lambda}\right) \tag{11}$$

Note that the Earth's radius and flattening parameter are defined by the World Geodic System of 1984 (i.e. WGS84). Since the Earth is ellipsoidal, there are two defined radii (r). The major radius is 6,378,137 m at the equator and the minor radius is 6,356,752.3142 m. Note that Equations (9) through (11) denote the latitude as $\emptyset$ and longitude as λ.

2.7.5 Applied Statistics

It is general engineering practice to adopt a 95% confidence interval. This means that there is a 95% chance of the hypothesis testing true, or in other words, that the obtained value will fall within a certain set of values. Other confidence intervals include 90% and 50%.

In statistics a normal distribution model is used to visually represent the spread of the data; where the mean is the centre highest value of the normalised data, forming the point of inflection on the resultant normal distribution curve. Multiples of the standard deviation (i.e. number of standard deviations) is then applied on both sides of the mean creating an interval with a certain confidence percentage that a value will be in between the upper and lower limits. The multiples are known as a z-score value or just a z-value. The general z-score for a 95% confidence interval, distributed equally about the mean, is 1.96 ~ 2 and 90% is 1.64 (Montgomery & Runger, 2007).

Median – The median of a data set is the value that divides the data set into two equal halves. The data set must be sorted in an ascending order. If the data set consists of an even number of observations, the median is defined as the average of the nth and (n+1) values.

Mean – Also referred to as the arithmetic mean, the average is the numerical representative value of the sum of the observation values, divided by the number of observations.

Mode – The value that has the highest frequency in the data set. It is possible for a data set to have more than one mode, in which case the most relevant one is used.

Central Tendency – The tendency of data to cluster around a single value. The values usually used to express the central tendency are either the mean, median or mode. The value that is used as the representative value is dependent on the relationship among the values for the relevant data set.

Percentile – The set of values that divide the sample into 100 equal parts. The most commonly used percentiles to describe operating speeds are the 50^{th} percentile or the central tendency, and the 85^{th} percentile, often used as the recommended speed limit.

Standard Deviation – A measure of variability for a given data set.

Regression – The statistical method used to determine the relationship between a dependent variable and one or more independent variables. The approach here is a reverse stepwise regression, since all variables are included at the start, after which insignificant variables are removed from the study.

Correlation – The measure of interdependence among data. This can be used among multiple variables, but is often used with only two variables. Correlated data results in a correlation coefficient ranging from -1 to +1, with a value of zero indicating no correlation. The sign convention associated with the coefficient indicates the orientation of the correlated data.

Bin Ranges – Defines the size of the ranges for a given data, such as to accomplish a sufficient sorting of the data for further analyses. The general equation used is as follows:

$$\boldsymbol{Bin_{ranges}} = \frac{\boldsymbol{Maximum\ Difference}}{\boldsymbol{Number\ of\ Ranges}} \tag{12}$$

3 Research Design

This chapter focuses on the research design, with the main emphasis being placed on the research variables, and possible research equipment.

3.1 Research Type

This research project is empirical (quantitative) by design. The proposed research topic, as stated in Section 1.3, entails the detailed observation of heavy vehicles that are descending mountainous terrain. Observations are recorded along with other surveyed data obtained from the relevant mountain passes. The primary data is obtained directly from the field for specific use in this research project. The primary data that is readily obtained from the field is the observation point data (i.e. time and distance for the relevant observation point) for each passing heavy vehicle, gradient, length of gradient, curve radius and superelevation. Primary data that is not readily obtainable from the field is the operating speed of the heavy vehicles. The operating speed will be obtained through the post processing of the collected observation point data.

This research project also contains a secondary data set, which was collected offsite and by another party. The data referred to is the mass of the observed heavy vehicles. Since there is no simple means of determining the mass in field, the data that is required has to be sourced from third parties (i.e. weighbridges). The primary and secondary data are discussed in Section 3.3

Both primary and secondary data sets are quantitative by nature, since both constitute measurable values. Therefore the data analysis is prone to yield quantitative results, which will numerically indicate the significance of the research variables, pertaining to the operating speed. Subsequently, these significances will be used to a descriptive end to define and describe the degree to which the research variables influence the downgrade operating speeds of heavy vehicles.

However, the collected data will also be analysed to derive the speed profiles. Since the collected data are based on observations made at various control points, the analysed results will yield speed profiles. Based on these speed profiles, conclusions can be drawn regarding the driver's familiarity with the pass and the possible need for improved signage. These conclusions will then be used to explore the possible need for improved signs that convey more information to drivers.

3.2 Research Objective

As stated in the previous chapter, freight is important to a country's economy. Hence there is a need to optimize and efficiently manage the transportation of freight. Since South Africa's primary means of transporting freight is by road, it is important to understand what affects road freight and how.

Mountain passes have been identified as having significant effects on the time and cost of road freight. Time is mainly affected by the lower operating speeds maintained while traversing mountainous terrain. This decrease in speed is attributed to a combination of factors, such as the gradient, length of gradient and changes in road alignment. These factors all arise from the physical nature of the mountain pass; however, there is a human factor that also influences operating speed, namely driver familiarity which can be derived or discussed on the obtained

speed profiles. These factors also adversely affect fuel consumption, which is one of the primary expenditures of road freight (State of Logistics Survey, 2012). Other risks inherent in mountainous terrain, especially on downgrades, are the possibility of rollovers and runaway incidents.

It can therefore be inferred that mountainous terrain has a considerable effect on the efficiency of road freight. Therefore this research project aims to determine to what extent the above factors affect heavy vehicle operating speeds on mountainous downgrades. The need for improved signs, conveying more information to drivers, will also be explored.

3.3 Research Variables

The following section contains the variables that are considered in this research project. The primary focus of this section is to discuss the influence of the variables on heavy vehicle operating speeds. Note that the means of collection is discussed in Section 3.4.

3.3.1 Gradient

The gradient is included as a variable for two reasons. Firstly, a heavy vehicle travelling along a downgrade will accelerate at an increased rate, as an effect of the gradient, resulting in operating speeds to increase more rapidly. Secondly, this results in a more frequent use of the brakes to maintain a safe descending speed, which might induce brake fade as a result of the higher operating temperatures of the brakes.

For the purpose of this research project and to ensure that the gradient is representative of the whole mountainous downgrade, the gradient is to be determined over the whole length of the relevant downgrade. Furthermore, note that the sign convention of the gradient is taken as positive for the downgrade so as to simplify calculations. Collecting the required data can be done using the following means: GPS, surveying equipment, Google Earth and design documentation.

3.3.2 Length of Gradient

The length of the gradient is an important factor for descending vehicles. The reason is that the longer the length of the downgrade, the more the operating speed needs adjusting as to maintain a safe descending speed. Hence, lengthy downgrades can result in excessive brake use with an increased risk of brake fade, resulting in a possible runaway incident. Therefore, heavy vehicles tend to descend slower, gaining more control through the use of retarders, but sacrificing operating speed.

For the purpose of this research project, the length of the gradient is taken as the distance from the summit of the pass to the base of the pass (i.e. the length over which the gradient is determined). The reason for including the whole length and not just the length from the summit to the critical section is that the gradient affects the heavy vehicle's operating speed over the whole downgrade. The following methods have been identified as possible means for collecting the relevant data: GPS, measuring wheel, Google Earth and design documentation.

3.3.3 Curve Radius

Curve radius is the numerical description of the circle curve that tangentially connects two straight sections of road. This constitutes the physical manifestation of horizontal changes in road alignment, ranging from gradual curves to hairpins. Therefore the curve radius can serve as an indication of the severity of a given curve, with the smaller the radius the slower the operating speed. For heavy vehicles this is primarily a result of a high centre of

mass, which makes it more sensitive to rollovers if the operating speed is too fast. Thus drivers must maintain a slower and safer operating speed in the presence of small radius curves or hairpins.

In light of this research project, curve radius is of particular importance since mountainous terrain subjects heavy vehicles to significant changes in road alignment. The critical curve radius to be used in the analysis is the radius that affects the operating speed the most (i.e. results in the greatest reduction in operating speed). The following methods can be used in collecting the relevant data for the calculation of the curve radius, namely GPS, surveying equipment and design documentation.

3.3.4 Superelevation

Superelevation, also referred to as cant, is the difference in elevation between the two edges of the road. The outer edge is raised as to provide a banked curve, allowing for higher operating speeds around the curve. The increase in speed is attributed to the sideways friction generated between the vehicles tyres and the road surface. This friction allows the vehicle to stick to the road at higher cornering speeds.

Since this is an integral part of curves, in it that it affects operating speed, this is also included in this research project. The superelevation is measured only on mountain passes that have critical curves (i.e. subjecting operating speeds to curve radius). Furthermore, the superelevation will be taken near the apex, since the apex is a point of interest and the superelevation is fully developed here. Collecting the needed data can be done using the following means: GPS, surveying equipment and design documentation

3.3.5 Stopping Distance

The stopping distance is defined as the distance required by a given vehicle to come to a complete and safe stop. For heavy vehicles the stopping distance is much greater than for passenger vehicles, because of the increased mass and size of the heavy vehicle requiring more kinetic energy to be dissipated. This increased mass and size affect the approach operating speed and the distance at which the brakes are applied to ensure that the heavy vehicle can come to a complete and safe stop. This variable is included in the research, since some mountain passes or steep lengthy downgrades require a compulsory stop at the base of the pass. This combination of steep downgrade and compulsory stop creates a strenuous operating condition for the brakes, since they will be applied more frequently during the descent to ensure that a slower and safer operating speed is maintained. However, this increased usage of the brakes can lead to exceedingly high temperatures developing in the brakes, which might lead to brake fade and ultimately result in a runaway incident.

For the purpose of this project, the stopping distance will be obtained for mountain passes that have compulsory stops at the base, preceded by a continuous downgrade. This distance will be taken as the distance measured from the relevant apex observation point to the stopping point. This variable can be collected through the following methods: Google Earth, measuring wheel.

3.3.6 Vehicle Mass

The mass of a vehicle comprises of two components, namely the mass of the vehicle itself and the mass of its load. This combination is referred to as the gross vehicle mass (GVM). Mass directly influences the operating speed of a vehicle, since the heavier the vehicle the more force is required to accelerate or stop the mass. This is described by Newton's second and third laws. Therefore, laden heavy vehicles will transcend downgrades at

slower operating speeds, since the required braking force to control or stop the heavy vehicle increases as the speed increases as a result of the garnered forward momentum.

Due to the significant influence that mass has on operating speed, it is paramount that the mass of the observed heavy vehicles is obtained. The mass that is needed during analysis is the combined mass of the heavy vehicle and the freight, thus the gross vehicle mass (GVM). To associate the correct GVM with the relevant heavy vehicle, the registration number will be used. There are two identified means of obtaining the mass namely weigh-in-motion and weighbridges.

3.3.7 Number of Axles

The number of axles is a means of estimating the probable mass or of classifying heavy vehicles into groups. For the purpose of this research project the number of axles per heavy vehicle is recorded to serve as a means of sorting the observed heavy vehicles in axle classes. The number of axles that is relevant to this study is four and more, including the steering axle. The reason is that in the case of three-axle heavy vehicles, it is hard to distinguish between a rigid body three-axle heavy vehicle and a three-axle little box truck. Therefore, if four axles and more are used, all the configurations will be articulated heavy vehicles, with a tractor and trailer. Bowman and Brian (1987) stated that only five or more axles are of importance when it comes to operating speed studies, since the lower axles classes are in the transitional zone between passenger car and heavy vehicles. Many three-axle box trucks do not have E80 axles, thus are not classified as heavy vehicles. The following strategies can be used for collecting this variable: video recording, physical counting.

3.3.8 Operating Speed

Speed is defined as the time taken to travel a given distance, with the shorter the time for a set distance the faster the travelling speed. Operating speed can then be described as the general speed at which a vehicle travels along a given road. Heavy vehicle operating speeds are more susceptible to changes in road alignment, because of the size and mass of the heavy vehicle itself.

Speed is the dependent variable for this research project, which will be analysed to determine how the selected geometric and vehicle characteristics affect it. The operating speed is determined at the critical section (see Section 1.4) of each relevant mountain pass for each passing heavy vehicle.

3.3.9 Speed Profiles

The speed profiles are determined by analysing the relevant observation point operating speeds, and can be used to draw conclusions regarding the manner in which heavy vehicles pass through the relevant critical section. This data can further more be used to gain a possible understanding of how heavy vehicles drivers perceive the relevant critical section, based on the shape of the obtained speed profiles. Furthermore, the can be used as a motivational means, in the possible recommendation of improved speed signs.

3.4 Proposed Methods of Data Collection

This section focuses on the possible means that can be used to collect the research variables. For each method the advantages and disadvantages are discussed, as relevant to the research project.

3.4.1 GPS

For the purpose of this research project the use of a GPS has two advantages. Firstly, the data obtained is relevant to multiple research variables. Secondly, the device is very small in comparison to other equipment, and allows for easy operation within a moving vehicle, while maintaining a moderate to high degree of accuracy. The accuracy of the device is dependent on the device itself and on the topography of the terrain in which it is used.

Since the device will be used in mountainous terrain (i.e. mountain passes), the accuracy of the measurements may be affected. The reason is that the close proximity of the mountains interfere or affects the signal strength of the device's connection to the relevant satellites. The accuracy can be increased through the use of a larger antenna, either internal or external. Another disadvantage is that GPS data are often stored in raw proprietary formats (i.e. licensed software needed to use the data), which requires post processing of the data to get it in a usable and editable format.

Operating in a mountain pass has an additional disadvantage, namely fuel consumption, if readings are taken from within a moving vehicle and multiple iterations are done. This can be addressed by taking the measurements on foot. However, this introduces an unsafe working environment, since mountain passes have restricted or limited roadside clearance, which leads to operating in close proximity to the road.

3.4.2 Total Station

Total stations are sophisticated surveying instruments, used in the land surveying and construction industries. The reason for their popularity is that they have a high degree of accuracy, being capable of measuring distance to the nearest millimetre, along with both horizontal and vertical angles to any desired observation point. Furthermore, it uses a laser to measure distance, which allows it to measure distances spanning several kilometres. Lastly, it is a digital device capable of saving measured data in readily usable formats.

However, using a total station in mountainous terrain has some disadvantages. The first is that it requires physical setup, which can often not be done safely because of the restricted space on mountain passes. Secondly, measuring mountain passes with a total station may require multiple setups, as a result of the changes in road alignment limiting the sight distances within mountain passes. Lastly, another person is required to help take the measurements, since one person operates the total station and the other the staff. This can be circumvented, if the total station has the functionality to automatically track and record the staff. However, this creates another problem, since the researcher will then be away from the device, and it can be damaged (e.g. by baboons) or stolen.

3.4.3 Google Earth

Google Earth is a virtualized software-based model of the Earth. Apart from enabling users to view the Earth in three dimensions, the software also allows for user-defined features to be added to the model. These features include points, lines and polygons, which are constructed using the relevant user-defined coordinates. Features can also be analysed in a simple manner, for instance, the gradient of a line feature can be obtained through the built-in elevation viewer. Lastly, the software is open source and licensed as freeware, enabling users to extend the functionality of the software through simple programming.

The main drawback of this method is the questionable accuracy of any measurements made, since this model is merely a representation of the Earth. Errors in measurements originate from stitching errors in the image overlays, sometimes causing jagged edges to form and affecting the accuracy of a measurement near this error.

Thus rather than using this software for accurate measurements, it can be used as a comparative means to check that measurements are similar to what is expected. However, Google has stated that distances vary at most by 20 metres, which is negligible if the relative measured distance is several kilometres.

3.4.4 Design Documentation

This method uses the actual design documentation of the given mountain passes, often archived by road authorities or district engineers. Research variables obtained from this documentation will have a high level of accuracy, since they are the actual dimensions used to which the pass had been constructed.

The main drawback of this method is mountain passes in South Africa have been in existence for several decades, and as a result the actual design documents may no longer exist. If the design documentation is in existence, a further minor disadvantage might be encountered. Since the document is not readily available, a formal request has to be made pertaining to the reason for viewing of the relevant documentation. This can be a lengthy procedure, since both parties (i.e. applicant and third party) have to be in agreement of a suitable time and place. However, if the relevant documentation is available and permission has been granted, this method yields the actual values of the relevant variables.

3.4.5 Measuring Wheel

The stopping distance can be collected through the use of a measuring wheel. Therefore the exact measurement can be obtained that are accurate to within millimetres. The main advantage is simplicity, and there are no device disadvantages. The main disadvantage of using this means is that it requires the researcher to operate in close proximity to the roadway. This creates a dangerous working environment, further exacerbated since the measurements are to be taken in mountain passes that often have limited roadside clearance.

3.4.6 Weigh in Motion

Weigh-in-motion equipment consists mainly of two parts, namely the pressure plate and a data logger. The pressure plate is placed on the roadway in the given lane in which the observations are made, whereas the data logger is simply the means of recording the data. The accuracy of the equipment is dependent on the speed of the vehicle passing over the pressure plate. Since the general practice is to work to a confidence interval of 95%, the weighing speed should be limited to a maximum of 15 km/h (i.e. for slow weigh-in-motion devices). This reduction in operating speed in a single lane, as is often encountered on mountain passes, will disrupt traffic flow.

The advantage of implementing this technology is the immediate acquisition of the actual mass for any observed heavy vehicle. However, care should be taken as to where this equipment is set up. Since it affects operating speeds, placing it near the critical section or on the relevant downgrade might skew the collected speed data, as it might alarm drivers.

3.4.7 Weighbridges

Weighbridges are the most accurate means of obtaining the actual mass of a heavy vehicle. The reason is that weighbridges require any vehicle to be stationary during weighing, which eliminates the forward component of the kinetic force. Therefore only the normal force acts on the load cells, resulting in the true mass being obtained.

However, there are two drawbacks, namely accessibility and availability of the data. Since weighbridges are governed by third parties, access to the relevant data is not readily possible. Thus, access to the data needs to be applied for, which is often a lengthy process. Secondly, not all of the heavy vehicles on the road are weighed. Therefore, there is a chance that an observed heavy vehicle might not have a corresponding mass.

If access to the data is granted, a means is needed to link the observed heavy vehicle to its relevant mass data. This is achieved through using the observed heavy vehicles' registration numbers.

3.4.8 Physical Counting

This method entails physically counting the number of axles of the passing heavy vehicles. Afterwards, the count is recorded alongside the registration number to link it to the relevant speed and mass variables. The primary advantage of this method is its simplicity. However, this simplicity holds some disadvantages as well. Firstly, if the relevant registration number is not obtained, that axle count is useless. Secondly, the obtained counts and corresponding registration numbers have to be manually entered into the database, which is a time-consuming procedure.

3.4.9 Video Recording

Using cameras as the means for collecting heavy vehicle speeds, it must be done in conjunction with datum markers. These markers delineate the control area in which the speed will be determined. The cameras will account for the time component of the heavy vehicle's speed – in other words, the time it took to pass through the control area. The advantage of this method is that the video footage can be replayed multiple times to ensure that the exact time component is obtained. Furthermore, this footage can be used for the collection of other variables, such as the axle count and registration numbers. However, because of the topography of mountain passes, a single camera will not be sufficient to cover the whole critical section. Therefore, additional cameras will be required, which can be costly.

The main disadvantage of this method is the camera itself. The reason is that the recording quality and battery life are important to keep in mind. However, an increase in quality has a corresponding decrease in battery life. Thus a trade-off must be considered as to obtain the highest possible recording time with the minimal impact on the quality. Another disadvantage is that the cameras run the risk being damaged or stolen.

Lastly, the data have to be linked to the relevant heavy vehicle. The registration numbers will be used for this purpose. Therefore, the cameras should be able to capture high-quality footage that allows for the reading of registration numbers as well.

3.4.10 Piezoelectric Strips and Radar

These are instruments that use piezoelectric strips or forward scanning frequencies to determine speed. There is one predominant advantage for using this type of equipment, namely accuracy. Furthermore, the data are recorded to digital format, allowing for easy entry into the database. This method also doesn't require any post processing

of the collection data, since these devices measure the actual operating speed. There are, however, multiple disadvantages as well, the foremost being that the equipment is very expensive. Furthermore, these devices are intrusive in the environment, resulting in their being easily spotted. This in turn may result in skewed or inaccurate speeds being measured, since the drivers may reduce speed to avoid the possibility of a traffic infringement. The equipment is only used to cover one point.

3.5 Research Execution

This section describes the general approach of the research project to answer the research questions, and various influential factors have also been identified, as stated in Section 3.3. The observation design contains the general approach to the way the research question will be answered. This includes all the various stages of the project, from the identification of the relevant mountain passes, identification of the critical sections, collection of data and the analyses thereof.

The first stage is to identify the mountain passes that will be used during this project. This stage is based on various statistics, as contained in the literature review, and the physical properties of the road network. What is meant by the physical properties is the identification of the busiest corridors or roads and ascertaining whether these roads intersect or cross mountainous terrain. The results of these aspects are provided in Chapter 5, where the relevant mountain passes are identified.

After the identification of the mountain passes, the critical sections along the downgrades have to be identified. This is approached through use of a GPS device and following a small number of heavy vehicles as they are descending the relevant mountain pass. The processed GPS data will then be plotted to obtain the relevant speed profiles, which are then analysed to determine the points of interest (areas of significant changes in speed). The points of interest will then be plotted on an aerial map of the relevant mountain pass, and geometric features will be discussed to ascertain the possible cause of these changes in operating speed. Afterwards the critical section will be identified. The reason for identifying the critical section is that it is assumed that the greatest fluctuations in speed occur here and that the independent variables have the greatest effect here.

The third stage is the collection of the data, which is primarily done in the field. However, as stated in the literature review, the mass can be obtained in the field, but this often occurs at very low speeds and the equipment needed to conduct these weigh in motion is very expensive. Therefore, the mass of the heavy vehicles will be obtained from the relevant weighbridges in the surrounding areas. The various forms of data that will be collected in the field require the use of a range of different kinds of equipment. Lastly, the analysis of the data will be undertaken. The data will be analysed to determine the significance of the identified influential factors on the descending speeds of heavy vehicles in mountain passes.

3.6 Summary of Research Design

This research project sets out to determine to what extent various factors affect the operating speeds of heavy vehicles in mountain passes. The factors that are specified as having a significant influence on the operating speed form the research variables that are to be collected in field. Therefore, this study is empirical by design and will consist mainly of primary data (i.e. data collected in the field by the researcher). A possible secondary data set has been identified, namely the heavy vehicle mass. The reason is that it might prove to be too difficult to collect

the mass in the field, in which case third party (i.e. weighbridge) data will be used. Table 3 contains the identified research variables along with the possible means of collecting the relevant data:

TABLE 3: SUMMARY OF RESEARCH VARIABLES

Research Variable	Equipment	Advantage	Disadvantage
Gradient (Quantitative; Independent)	GPS	• Operated in moving vehicle • Collect data over whole downgrade • Can use data in other variables	• Accuracy may be affected by mountains • Data in raw format, requires post processing
	Survey equipment	• High degree of accuracy • Exact measurement	• Stationary setup • Limited roadside clearance, unsafe
	Google Earth	• Quick and easy • Exact plotting on virtual Earth	• Questionable accuracy
	Design documents	• True accuracy	• Third party, needs permission to view • Documents may not exist
Length of downgrade (Quantitative; Independent)	GPS	• Can be used in moving vehicle • High degree of accuracy	• Accuracy may be affected by mountains
	Measuring wheel	• Exact measurement • High degree of accuracy	• Close proximity operating to road • Can be influenced by surface roughness
	Google Earth	• Sufficient degree of accuracy • Quick and easy	
	Design documents	• High degree of accuracy	• Third party, needs permission to view • Documents may not exist
Curve radius (Quantitative; Independent)	GPS	• Can use in moving vehicle • Moderate accuracy obtained • Can be walked, higher accuracy	• Accuracy may be affected by mountains • If walked, safety risk • Data in raw format, requires post processing
	Survey equipment	• High degree of accuracy • Exact measurement	• Multiple setup to cover whole curve • Close proximity to roadway, unsafe
	Design documents	• True accuracy	• Third party, needs permission to view • Documents may not exist
Superelevation (Quantitative; Independent)	GPS	• Exact measurement • High degree of accuracy	• Close proximity to road, unsafe
	Survey equipment	• True accuracy	• Close proximity to road, unsafe • Requires two people
	Design documents	• True accuracy	• Third party, needs permission to view • Documents may not exist
Stopping Distance (Quantitative; Independent)	Measuring wheel	• High degree of accuracy • Exact measurement	• Close proximity to roadway, risk to safety.
	Google Earth	• Sufficient degree of accuracy • Quick and easy	
	Design documents	• High degree of accuracy	• Third party, needs permission to view • Documents may not exist

Mass (Quantitative; Independent)	Weigh in motion	• Can achieve high accuracy • Have actual mass of observed heavy vehicle	• Accuracy affect by crossing speed • Placement near critical section will skew observed speed
	Weighbridges	• High degree of accuracy	• Not all heavy vehicles are weighed • Requires permission to access the data
Number of Axles (Quantitative; Independent)	Physical counting	• Simple method	• Manual entry into database • Requires corresponding registration number
	Video recording	• Ability to replay video • Get exact count • Have corresponding registration number on video	• Trade-off between battery life and video quality • Risk of damage or theft of camera
Operating speed (Quantitative; Dependent)	GPS	• Can follow heavy vehicles • Moderate to high accuracy • Complete speed profile over downgrade	• High fuel consumption and expensive • Difficult to obtain registration number for correspondence
	Speed traps or radar	• High degree of accuracy • Speed data in digital format	• Intrusive to the environment, thus might skew speed data • Capture spot speed at a single point
	Video recording	• Replay ability • Can be used to collect other variables	• A camera only cover on observation point

The effect and extent of how the relevant variables influence the operating speed is then found by analysing the collected data of the research variables, as listed in Table 3. The effect is analysed through comparing the calculated 85th percentile speed with that of the posted speed limit. This show how heavy vehicle operating speeds are affected, regardless of the research variables. Secondly, the extent of the impact that the variables have on the operating speed will be analysed through using multivariable regression, with the operating speed as the dependent variable.

After the analyses, the need for improved road signs is explored and discussed on the basis of driver familiarity. This variable is not obtained in the field, since it is qualitative in nature. Therefore, speed profiles will be used to draw conclusions regarding the driver's degree of familiarity.

4 Research Methodology

4.1 Research Equipment and Software

The following equipment and software have been identified and used during the course of this research project, since it was believed that the use thereof would result in accurate data acquisition and processing in preparation for the analysis.

4.1.1 Physical Equipment

The physical equipment relates to all the devices that were used in the field for data collection. The equipment that has been used is described below.

GoPro Cameras + Equipment

Hero3 Black Edition cameras were used to capture the necessary footage. The reason for choosing these cameras was based on considerations of the quality of image that can be recorded versus the size of the device. A small device was thought to be better suited to the research, since the device is not easily seen from a passing vehicle. Therefore, a more accurate representation of the operating speed and the true driving behaviour will be obtained. Furthermore, the camera has a multitude of resolution options, which allows for clear image recording of moving vehicles. Coupled with an array of frames per second (FPS) options, the time accuracy of each vehicle can be controlled from 24FPS to 240FPS. Therefore an optimal overall setting can be achieved that allows for accurate high-quality recordings. This is particularly important, since this allows for the acquisition of the registration numbers and axle count directly from the recording.

Other GoPro equipment includes the various fittings that allow for the cameras to be placed anywhere with the minimum amount of effort. Therefore, these cameras can be fitted with ease in the field, resulting in brief setup times. Figure 6 illustrates the GoPro equipment, along with the accessories, used during this project.

FIGURE 6: GOPRO CAMERA AND EQUIPMENT USED
(**Top Left to Right:** GoPro Wi-Fi remote, GoPro Hero 3 camera, GoPro tripod mount; **Bottom Left to Right:** GoPro dual battery charger, Camera USB cable, Remote USB cable, Car 12v USB adapter; **Source:** www.gopro.com)

Minor disadvantages had to be circumvented, if accounted for. The foremost was the battery life, which can record one hour forty minutes at most on a high-quality setting. This was overcame with the use of the GoPro car adapter, which fully charges batteries in little over an hour. Another disadvantage was that the video quality, regardless of the settings, is poor in low light or over-exposure conditions, such as caused by shadows and headlights respectively. Therefore, it was necessary to record during well-lit conditions. The following figure illustrates this decrease in quality for different light exposure conditions.

FIGURE 7: ILLUSTRATION OF LIGHTING CONDITIONS AND QUALITY
(Left: Low ambient lighting; **Centre:** Headlight interference; **Right:** Good lighting**)**

Trimble Geo6000 GPS

This device was used, since it is a high-accuracy GPS that was readily available at the time of data collection. The degree of accuracy for this device is dependent on two factors, namely the antenna and the correction method used. Consisting of a larger than normal Global Network Satellite System (GNSS) receiver, real-time corrections using a Satellite Based Augmentation System (SBAS) result in accuracies of less than 750 mm. If greater real-time accuracies are required, an external GNSS receiver can be fitted to the device (Trimble, 2011).

The Geo 6000 is integrated with a SIM card slot, allowing the GPS access to a mobile network. Therefore, the accuracy can be further increased through post processing of the satellite data using the mobile network towers as geographic references. This increases the accuracy of a measured point to within a 100 mm (Trimble, 2011). Thus this device has a great accuracy, which is required for certain research variables such as the gradient and curve radius. See Figure 8 for an image of the GPS used in this project.

FIGURE 8: TRIMBLE GEO 6000 GPS SCHEMATIC
(**Source**: seilermapsupport.wordpress.com)

Other advantages of this GPS include a good battery life and large internal memory. Thus, there are no concerns surrounding the reliability of the device when used for extended periods in the field. Furthermore, the large display, as seen in Figure 8, allows

for easy navigation through the files and settings since it is touch enabled. It also boasts a built-in light sensor that adjusts the screens brightness according to the intensity of the ambient outside light.

Datum Markers

The purpose of this equipment was to delineate the control area of each observation point on the relevant video recordings. This is done through creating two transverse datum lines across the road between two pairs of datum markers.

The datum markers are essential in obtaining the speed of the observed heavy vehicles. The reason is that the longitudinal distance between the datum lines serves as the distance component of the speed variable, whereas the time component of the speed is taken do be the time travelled from the first datum line to the second datum line, for a relevant observation point. In order to ensure a high degree of accuracy, the datum line must be such as to indicate the exact moment when the heavy vehicle enters and exits the control area. There are two means of achieving this. Firstly, simplistic datum discs can be used that allow for the creation of a datum line on the footage, post-recording. Figure 9 illustrates the simplistic datum discs on the left.

FIGURE 9: DATUM MARKERS
(**Left:** Datum discs; **Right:** Laser Light-box and Laser module)

The datum discs have one main advantage, namely their simplicity. These markers are easy to construct and use in the field. However, there is one disadvantage to this system. Since the datum lines are created post-recording, it is essential that the video footage remain stable during the recording. The reason is that the datum line tends not to move accurately with the footage stutter and may result in inaccurate time measurements.

Secondly, a real-time alternative can be used to indicate the exact time the heavy vehicle crosses the datum lines. To achieve this, a laser light-box has been designed that flashes a bright light when the laser beam is broken. These flashes of light are then recorded on the video and can later be used to obtain the duration of the heavy vehicle within the control area. Figure 9 illustrates the laser light-box datum marker and its use in the field.

The laser light-boxes, depicted in Figure 9, are very accurate. The instant the laser beam is broken, the light switches on. This is achieved through using a red light filter, which filters the sun's white light, yet it allows the laser beam to pass through, acting as a switch. To ensure that the light flashes are seen by the camera, a sufficient FPS is required along with bright enough lights. Therefore an array of seven 10-millimetre LEDs (i.e. 7 x 10mm LEDs) is used. There is one major disadvantage to this alternative. It is a very sensitive system in the sense that wind gusts and vibrations from passing vehicles can trigger the light to flash. Therefore the only way to get around

this problem work around is to set up the device at a significant distance from the roadway, which is often not possible in mountain passes. See Appendix A for the circuit layout and explanation.

Bosch Measuring Wheel - GWM 40

This Bosch GWM40 measuring wheel was used, since it has a very high degree of accuracy. The accuracy of this wheel is to the nearest 50 mm, which is more than sufficient for measuring distances longer than ten metres. Another advantage of this device is the size of its wheel. Nearly 400 mm in diameter, this is one of the largest measuring wheels commercially available. This counteracts the disadvantage that measuring wheels usually have, which is sensitivity to rough surfaces. Surface roughness can greatly influence a measuring wheel's accuracy, since the interaction surface can cause slipping and skipping of the wheel. Therefore the bigger the wheel, the lesser the impact on the accuracy. Refer to Figure 10 for a depiction of the measuring wheel used.

FIGURE 10: BOSCH GWM40 MEASURING WHEEL
(**Source**: http://www.bosch-professional.com/)

Trimble MR5 Total Station

The total station is a sophisticated surveying apparatus, more commonly referred to as an electronic theodolite. This device is capable of measuring distances and angles relative to both the vertical and horizontal planes. Therefore, the total station can describe and measure any point in real space (i.e. three dimensions). Refer to Figure 11 for an illustration of the total station used.

FIGURE 11: TRIMBLE M3 DR5 TOTAL STATION
(**Left to Right:** Optical prism, Total station back and front, Carry case, tripod, prism staff)

Using the total station has many advantages, the foremost being the ease with which high-accuracy measurements can be taken. Distances are measured to a 1-millimetre accuracy, whereas angles are determined to the nearest decimal second (i.e. dd°mm'ss.s"). However, there are two disadvantages. The foremost is that this instrument requires physical setup on a tripod and on mountain passes there is often not enough space to set up and operate the device safely. Using the device requires two people – one operates the total station and the second person the staff and prism. See **Figure 11** for a depiction of the staff and prism. Furthermore, recording basic survey

measurements to file cannot be done, hence they have to be recorded on paper. This requires manual entry into the database, which can be time consuming, depending on the number of points measured.

4.1.2 Research Software

The software-based equipment was used primarily during the processing of the collected raw data and its subsequent analysis. The software that was used is described below.

Google Earth

Google Earth is a virtual globe and geographical information program. The geodetic system used by Google earth is the WGS84, as described in the literature review (Chapter 2). This software is provided by Google under an open source license, allowing easy and free access to image data of the Earth. Since this software is open source, it encourages users to create and add features through coding extensions or executable files for this program. The language used for coding is Keyhole Mark-up Language (.kml) and can be done in a simple scripting program such as Notepad. Google Earth comes with an assortment of included functions, such as placemarks, line and area features. These functions create features on the virtual globe, which can then be opened to view the corresponding characteristics such as coordinates, altitude, length and area. Figure 12 depicts the user interface of Google Earth.

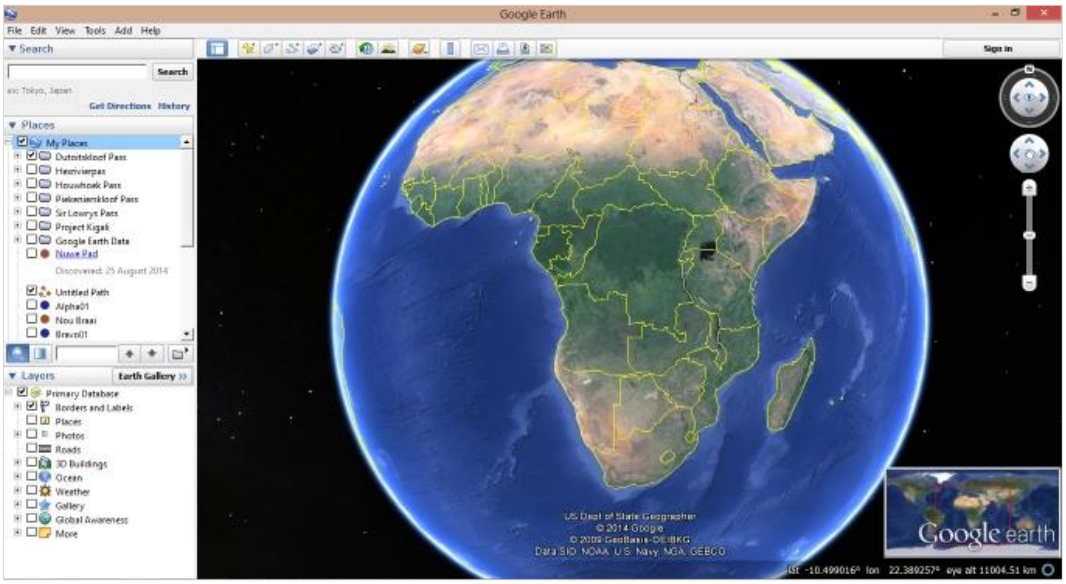

FIGURE 12: USER INTERFACE OF GOOGLE EARTH

This software is mainly used for basic data collection for comparative reasons, since the accuracy is relatively low. A study done in 2013 (Mohammed, Ghazi & Mustafa) found that the horizontal and vertical accuracies changes on a regular basis, as a result of regular updates released by Google. The horizontal accuracy was found to be ±1.8 m and the vertical as ±1.73 m. Therefore plotting individual points is fairly accurate, but the compounded error that could occur when creating a path (i.e. continuous line feature) can be significant. The decision for using Google Earth to a comparative means is supported by an official statement made by Google, which states that Google Earth makes no claims regarding the accuracy of the coordinates and should not be used for any navigational or other purpose requiring high levels of accuracy.

Therefore Google Earth is used for comparative purposes with the gradient and the curve radius. However, the downgrades length were obtained primarily through the use of Google Earth, since a 100 m accuracy is considered

sufficiently accurate enough for these lengths. As mentioned earlier, files can be coded for Google Earth. Therefore, this enables the user to plot specific and relevant data with ease, especially if there are multiple entries.

Kinovea

Kinovea is a video analysis program, published by its namesake company. This software is distributed under an open source license, with a non-profit agreement. Therefore, anyone is free to contribute and make use of this software (Kinovea, 2015). As a result, this program has an abundance of features, which allows Kinovea to have a high analytical functionality. Furthermore, Kinovea supports the most widely used multimedia formats for both standard (e.g. .avi) and high resolutions (e.g. .mp4). Since the GoPro cameras record high-quality footage in MPEG-4 (.mp4), the videos can readily be used with Kinovea.

The reason for using this software was to accurately establish the datum lines of the control area. This is achieved through overlaying an editable layer on the video footage, which then allows for shapes to be drawn on the video. Refer to Figure 13 for an illustration of how this was done.

FIGURE 13: KINOVEA USER INTERFACE AND DRAWING FEATURE

The major drawback of using this software is that it cannot analyse large high-quality video files. The reason is that the software is not capable of reading and displaying the high-resolution images fast enough, causing the video to stutter. However, this can be overcome through extracting a video clip from the original file, containing only the relevant recorded data.

VLC Media Player + Extensions

VLC Media Player is an open source program that can play a variety of different media formats. Furthermore extension can be programmed for this software using the scripting language lua. Therefore, this software is the ideal choice with which to view the recorded footage. The version of VLC that was used is the 2.0.8 Twoflower build. The reason for using this version is that it has all the features of the newer versions, but still recognizes the lua 5.1 application programming interface (API). This API is more user-friendly for programming and has more functionality available than the newer version of lua.

VLC has an abundance of features built into the standard program. These features will facilitate the playback and extraction of specific video clips as well as analysing them. The features include three-, ten- and twenty-second skipping, screen recording, split screen and image overlay. The skipping and screen recording features were appealing from a data extraction point of view, since they would make the playback easier and not as time consuming as playing the videos back in real time and they allow for easy video-scrolling back and forth. The screen recording feature enables the simple and fast recording of a specific section of video with the simple click of a button, and the files are automatically tagged with the time and date, as well as the original file name.

All the extensions have an open source license and are downloaded directly from the VideoLAN forum. One extension was identified for use in this project, namely Clipper.lua (refer to Appendix B). This extension extracts the decimal accurate time for any given frame in a video. The reason is that most open-source media players do not have a decimal accurate time display, but rather display only to the nearest second. However, this project requires the decimal accurate time, since the control area for most observation points is relatively small and can be travelled through within one to two seconds, which would result in an inaccurate operating speed being calculated.

Further functionality of the Clipper extension includes both time and frame skipping, thereby allowing the exact desired frame to be acquired. This can be used in conjunction with the image overlays created in Kinovea to obtain the exact time the heavy vehicle entered and exited the control area (i.e. crossing the datum lines). Refer to Figure 14 for an illustration of the VLC user interface and the clipper extension interface.

FIGURE 14: VLC USER INTERFACE AND CLIPPER EXTENSION

Microsoft Excel

Microsoft Excel is used to create and log data entries to the database. After all of the relevant data for each research variable have been collected, Excel is then used to create queries and analyse the data. Microsoft Office allows macros to be created for any of the Office programs. The scripting language is Visual Basic for Applications (VBA), which is done within the developer interface of each program. VBA is used to create specific macros that will help the sorting and extracting of the necessary data used in further analysis. Other functionalities include the ability to conduct statistical analyses with relative ease and the creation of descriptive graphs.

4.2 Method of Data Collection

This section focuses on the methods that are used for collecting the research variables. As stated in the previous section, some equipment was used for the collection of multiple variables. Therefore, the structure of this section is determined by the equipment used for the relevant data collection. It should be noted that the following methods were designed by the researcher.

4.2.1 Trimble GPS: Initial Speed and Road Geometry

The Trimble GPS was primarily used for collecting the initial speed data. This was done through following selected heavy vehicles as they descended the whole length of the relevant mountain pass. Therefore, this data inherently contains the relevant data required for other research variables such as the gradient, length of downgrade and curve radius. Collecting the data was done in six steps, as described below.

- Set up data log file for recording coordinates continuously
- Get behind heavy vehicle on upgrade
- Start logging at summit
- Follow heavy vehicle along downgrade
- Stop logging at base and repeat if necessary

The log file consists of multiple data entries that are continuously recorded, depending on the specified time interval. Each data entry that is logged consists of three values defining the instantaneous location of the GPS. These values are the longitude, latitude and altitude. The log file that is obtained is in a proprietary file format, which needs conversion before it can be used outside of the GPS. Converting the data files is done with the Pathfinder software, provided with the GPS. The output files subsequently obtained are of the format comma-separate-values (.csv), which is readily usable in Microsoft Excel.

4.2.2 GoPro Cameras: Heavy Vehicle Speed (Time) and Characteristics

As stated in Section 4.1.1, the GoPro cameras are used to capture the heavy vehicles as they pass through a critical section. Each critical section has three observation points (i.e. entry, apex and exit), each with its own camera. For the heavy vehicle's data to be considered in this study, it must be recorded by all three cameras. The reason is that a basic speed profile is desired for each heavy vehicle as it passes through the critical section. The data that are collected from the video footage include the time component of the speed, the number of axles and registration number. The process is as follows:

- Set up cameras and datum markers
- Switch on cameras and check settings
- Start recording
- Download video footage and clear memory card
- Repeat recording

The data contained within each video include the continuous time (i.e. video length) and visual imagery (i.e. picture). The recorded footage is in the format MPEG-4 part 14 (.mp4), which is a multimedia file format. This format does not require any conversion and is readily playable on any media player that is enabled to play this file format.

4.2.3 Bosch Measuring Wheel: Heavy Vehicle Speed (Distance)

The measuring wheel is used to collect the relevant longitudinal distances between the datum markers of each control area. This measurement accounts for the distance component in calculating the speed of heavy vehicles through the relevant control area. The data obtained will require manual entry into the database. The reason is that the measuring wheel is analogue, therefore the measurements have to be recorded on paper in the field.

4.2.4 Trimble Total Station: Superelevation

Obtaining the data required for calculation the superelevation is done with the total station. Only the mountain passes that subject speed to curve radius are surveyed. Caution should be exercised during this procedure, since the device is operated next to the road, with limited roadside clearance. The total station is set up so that full superelevation can be seen from one spot. With the set up complete, take the required measurements. The data collected for each point include the horizontal angle, vertical angle and distance prism. This data is then manually entered into the database, after which it is processed through using Euclidean geometry as discussed in Section 2.7.3.

4.2.5 Weighbridges: Heavy Vehicle Mass

Due to the intrusive nature of the weigh-in-motion equipment and its cost, it was decided to obtain the mass from the weighbridges. Therefore, the method used is as follows:

- Contact third party
- Supply information and proof of research
- Obtain data required

The data that is obtained, contains only the necessary information that is needed by the applicant. The reason is that some of the data is protected under the Protection of Personal Information Act of 2013. For this research project, the data required included the registration numbers, GVM, number of axles and the date of weigh.

4.2.6 Google Earth: Stopping Distance and Length of Downgrade

Google Earth is fairly accurate when it comes to distances. Therefore, it was used to obtain the relevant stopping distances and lengths of downgrade. The reason for using Google Earth instead of the other methods is that it allows the distance to be specified exactly and is the safest option of all. This method is outlined below.

- Create path feature
- Extract distance value
- Repeat

The data obtained are in metres and do not require any processing before being used in the analysis. The distances, however, are rounded off to the nearest ten metres upon entry into the database.

4.3 Method of Data Processing

Some of the collected data requires processing before it can be used in the analyses. Therefore, this section contains the methods applied to the data that does require processing to obtain the relevant variable that is used in the analyses. Unlike the previous section, the structure of this one is defined by the variable to be obtained as a result of the relevant processing.

4.3.1 Gradient

As stated previously, the gradient is defined as the ratio of vertical change divided by horizontal change. Processing the GPS data that have been collected by following heavy vehicles along the downgrade is done as follows.

- Import GPS data in spreadsheet
- Calculate horizontal change between consecutive coordinates
- Calculate vertical change between consecutive coordinates
- Calculate gradient, using Equation (1)
- Repeat for all mountain passes

The values that are obtained in the completion of the processing are the averaged gradient for each relevant mountain pass. These values are then entered into the database.

4.3.2 Initial Speed

The initial speed refers to the speed profiles that are obtained from the GPS data that were collected during the following of the heavy vehicles. This GPS data is the same data that is used to determine the gradient.

- Calculate true distance between consecutive coordinates, using Equation (7)
- Calculate speed between consecutive coordinates, with time component as the GPS logging interval time
- Repeat for all mountain passes

The interval speed between two consecutive points is obtained for all the points in the data set. Note that the interval speeds are not averaged, since this data is used in plotting the speed profiles in identifying the critical sections.

4.3.3 Curve Radius

The curve radius data were collected during the following of the heavy vehicles along the downgrade. Therefore, this GPS data is the same as that used in calculating the gradient, as stated in Section 3.3.1.

- Import relevant GPS data, from gradient data set
- Identify coordinates on curve radius
- Calculate gradient between consecutive coordinates, using Equation (1)
- Calculate midpoint coordinates and perpendicular ray(constructions line), using Equation (6)
- Calculate intersection distance between perpendicular rays, using Equations (5) and (8)

The data obtained for each mountain pass is averaged as to obtain the single representative curve radius for the given mountain pass and critical section. These radii are then added to the database.

4.3.4 Heavy Vehicle Speed

The variable is calculated by using the time and distance components of the heavy vehicle through the relevant control area. The time component is collected through recordings and the distance component through the relevant measurements taken in the field.

- Extract video clips of heavy vehicles passing through the control areas

- Create image overlays, to delineate control area on recordings
- Determine time component of speed
- Calculate operating speed for all heavy vehicles

Once all of the speeds have been calculated they are entered into the database.

4.3.5 Superelevation

The data required to calculate the superelevation is done with a total station. The data include the horizontal angle, vertical angle and sight distance from the total station to measured points.

- Convert angles to decimal degree notation
- Calculate horizontal and vertical component for each measured point
- Calculate horizontal and vertical change between transverse pair, using Equation (8)
- Calculate superelevation
- Repeat for all transvers pairs

The superelevation is then obtained by averaging the transverse pairs, after which it is entered into the database.

4.3.6 Heavy vehicle mass

The data pertaining to the mass of the heavy vehicles are obtained from the third party. Therefore, to simplify the analysis, the data are queried in order to obtain only the mass of the relevant heavy vehicles.

- Construct data set used to query mass data set
- Extract relevant heavy vehicle mass
- Calculate mass for each relevant heavy vehicle

4.4 Method of Data Analysis

Once all the necessary processing was completed and the final values of the research variables obtained, the analyses were conducted. The analyses were done in Microsoft Excel.

4.4.1 Critical Section Analysis

The data used for this analysis was the processed GPS data, as obtained through the method described in Chapter 4.3.1. This analysis entailed the identification of the critical section of each of the relevant research mountain passes. Identifying the critical sections was done through analysing the speed profiles of the heavy vehicle that were followed. The steps of analysis are outlined below.

- Eliminate fluctuations in speed, makes analysis easier
- Plot adjusted speed vs cumulative distance
- Identify points of interest, values are outside of the 95% confidence interval
- Combine individual speed profiles, overlay points of interest, resulting in areas of interest
- Identify critical sections
- Repeat for all mountain passes

The critical section of each mountain pass was then surveyed to obtain more data for the relevant mountain pass. The critical section analysis is conducted in Section 7.1.

4.4.2 Speed Analysis

This section focuses on the speed at which heavy vehicles descended the relevant downgrades, regardless of the independent research variables. The reason for this is to determine how the observed 85th percentile speed compares to the posted speed limits. This will provide insight into how the drivers perceive the mountain passes in general. The data used in this analysis was the speed data, as described in Section 4.3.4.

- Determine speed ranges
- Determine central tendency
- Calculate 85th percentile speed
- Determine speed profiles through critical sections

After the 85th percentile speed and relevant profiles have been obtained, the results are discussed and conclusions regarding driver familiarity and sign information relevance are drawn.

4.4.3 Multivariable Regression

This section determines the influence and significance of the research variables. This is done through a multivariable regression, with the speed as the dependent variable.

- Correlation mass with number of axles
- Perform multivariable regression for mountain passes in general
- Perform multivariable regression for speed subject to curve radius
- Perform multivariable regression for speed subject to stopping distance
- Repeat regression if necessary

With all of the regressions done, mathematical models were constructed using the variable coefficients obtained from the regression.

4.5 Assumptions and Limitations

The identification of limitations and the assumptions made for a research project is of great importance. The reason is that this identifies possible weaknesses in the research design. Limitations are weaknesses that can have a significant effect on the outcome of a project and are out of the researcher's control. To account for the limitations, they are addressed in a specific way as to reduce their impact on the project. Assumptions are made regarding weaknesses that are somewhat out of the researcher's control, but that still influence the outcome of the project. Since there is no simple means to test if an assumption is correct, the reason for assuming a weakness should be motivated clearly.

4.5.1 Assumptions

Assumption1: GPS Accuracy

The Trimble Geo 6000 GPS is truly as accurate as described. Since there is no easy way of testing it in the field, this assumption is motivated as follows. Firstly, Trimble is a well-known manufacturer of positing and surveying

equipment, hence their equipment specifications can be trusted. Secondly, the Geo 6000 has a relatively large GNSS receiver, which is descriptive of a higher degree of accuracy.

Assumption 2: Roadworthiness of Heavy Vehicles

Since it is near impossible to check and determine the condition of all observed heavy vehicles, it is assumed that all road-going heavy vehicles are roadworthy. This assumption is justified by the fact that the livelihood of the drivers and logistic companies depends on the heavy vehicles reaching their destinations safely and on time. Furthermore, regular maintenance is a preventative means of minimizing the chance of mechanical failure, which results in costly repairs.

4.5.2 Limitations

Limitation 1: Number of Heavy Vehicles Weighed

Note every heavy vehicle get weighed at the weighbridges. Therefore, some observed heavy vehicles will have no corresponding mass data. This can be accounted for by two means. Firstly, a correlation can be done between the mass and number of axles for the heavy vehicles that have both variables. If a strong correlation is found, the number of axles can be used instead of the mass. This means that all observed heavy vehicles can be included in the regression analysis. Secondly, the period of the mass data can be extended (e.g. one month's data versus six months' data). The increase in the amount of data available will result in more observed heavy vehicles having a corresponding mass.

Limitation 2: Weather Conditions

Weather conditions influence the operating speed of heavy vehicles. Wet roads and strong cross-winds lead to lower friction coefficients and lateral instability, respectively. Therefore, the observations were made on days of similar weather conditions as to minimize the uncontrollable variables.

4.6 Summary of Methods

As is evident from the preceding section, the physical equipment is primarily used for the collection of data. Due to the nature of some equipment, the data that is collected with it can be used to calculate the required data for multiple research variables. The Geo 6000 is used in this way, since the gradient, initial speed and curve radius can all be obtained from the same data set. Another piece of equipment used to this end is the GoPro camera. The time component of the speed, the registration number and the number of axles are obtainable from the video footage.

The research software is used for the processing of some of the collected data, such as the video footage and GPS coordinate data. The video footage is viewed using the VLC media player and the necessary data are extracted using extension programs. After the video footage has been processed, it is entered into an Excel database along with the GPS data for further processing.

With all of the data processed and entered into the database, the analyses can be carried out. Three analyses are conducted namely: critical section analysis, speed analysis and multivariable regression analysis. These analyses determine how and to what extent the research variables influence the downgrade operating speeds of heavy vehicles. Refer to Figure 15 for a flowchart of the research methodology.

The identified assumptions and limitations for this research project are as follows:

The research assumptions for this project are as follows:

- Assumption 1: That the chosen GPS is as accurate as indicated by the manufacturer;
- Assumption 2: All observed heavy vehicles are roadworthy.

The limitations are as follows:

- Limitation 1: Not every single heavy vehicle gets weighed at the weighbridges;
- Limitation 2: Weather conditions can adversely impact on operating speeds.

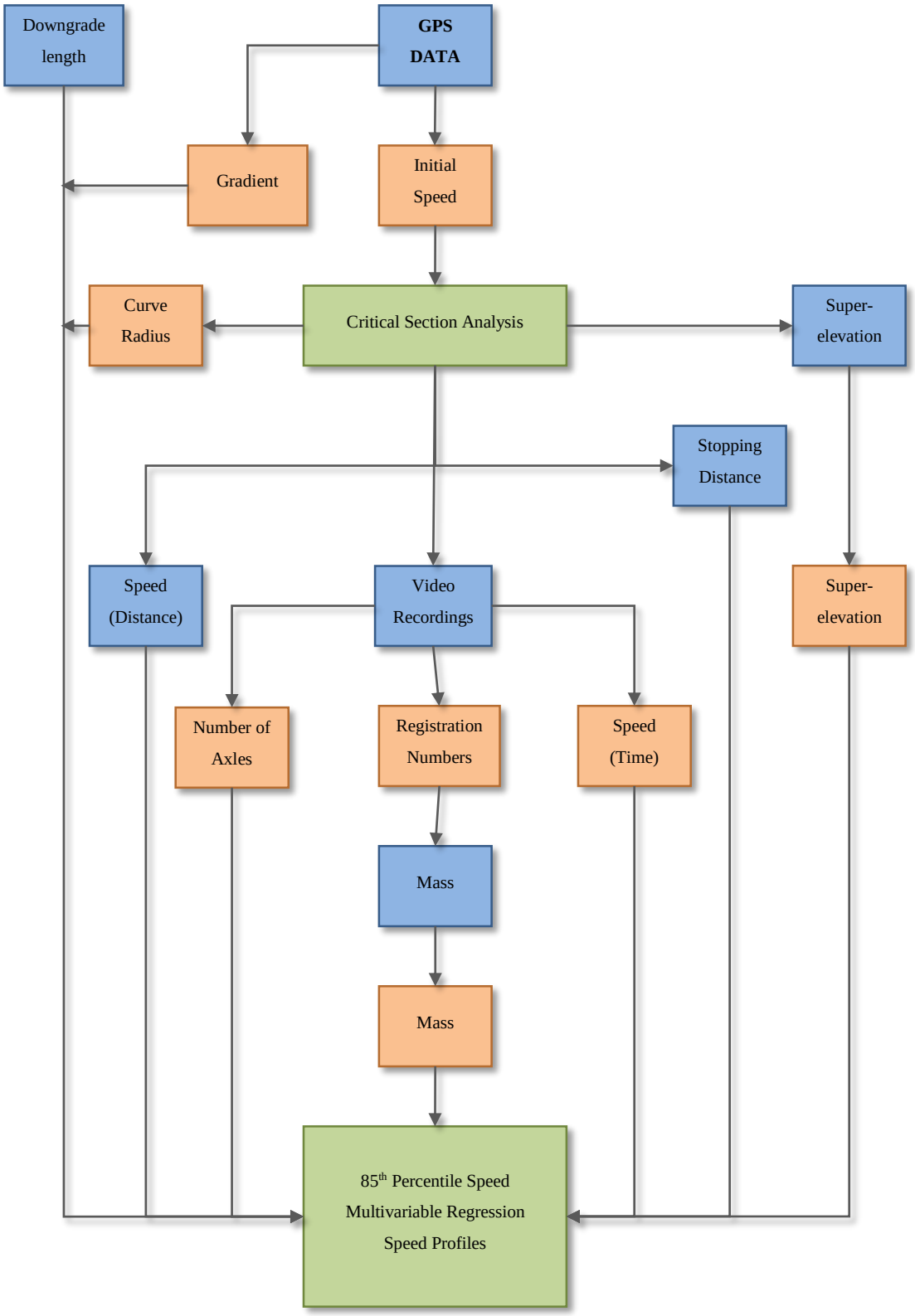

FIGURE 15: FLOWCHART OF DATA COLLECTION, PROCESSING AND ANALYSES
(Blue: Collected Data; **Orange:** Processed Data; **Green:** Analyses**)**

5 Survey Locations

This chapter focuses on the survey locations that were used for the study. The emphasis is on the selection of the mountain passes and the identification of the critical sections.

5.1 Geography of South Africa

South Africa has three primary geographical regions and 22 physiographic regions. The three primary regions are the Central Plateau, the Marginal Zone and the Great Escarpment (Briney, 2014). Figure 16 illustrates the location of the three primary geographical regions.

FIGURE 16: THE THREE PRIMARY GEOGRAPHIC REGIONS OF SOUTH AFRICA
(**Red:** Central Plateau; **Thick Black Line:** Great Escarpment; **Green:** Marginal Zone)

The Central Plateau, depicted in red in Figure 16, forms the southernmost part of the Great African Plateau. The surface of the plateau is largely flat and gradually slopes downward from the east. Altitudes range from approximately 3,000 m above sea level in the east to 900 m above sea level in the west (Reader's Digest Association South Africa, 1984:12). Twelve of South Africa's physiographic regions are situated within the Central Plateau and include the Upper Karoo, Highveld and Southern Kalahari.

The Great Escarpment, depicted by a thick black line in Figure 16, is a major geological formation that demarcates the Central Plateau and the Marginal Zone. This formation lies predominantly within South Africa's borders, but extends into the neighbouring countries of Mozambique, Namibia and Angola. The escarpment is not considered a physiographic region, but comprises a number of imposing mountain ranges such Kamiesberg, Roggeveld and Drakensberg (Reader's Digest Association South Africa, 1984:12).

The Marginal Zone, depicted in green in Figure 16, is situated between the Great Escarpment and the coast. Altitudes vary from sea level to approximately 2,300 m above sea level, with the width ranging between 60 km and 240 km. The Marginal Zone is divided into 10 physiographic regions, including the Coastal Belt and the Cape Fold Mountains (Reader's Digest Association South Africa, 1984:12).

The Cape Fold Mountains are mainly situated in the Western Cape and are comprised of mountain ranges which are divided into three structural regions. Regions are identified by the geological manner in which the mountain ranges occur (i.e. are the mountain ranges converging or forming branches). According to Mielke and de Wit (2009:521), the three regions are a syntaxis around Worcester, a northbound branch expanding towards Vanrhynsdorp and an eastward branch expanding to Port Elizabeth. Refer to Figure 17 for an illustration of the

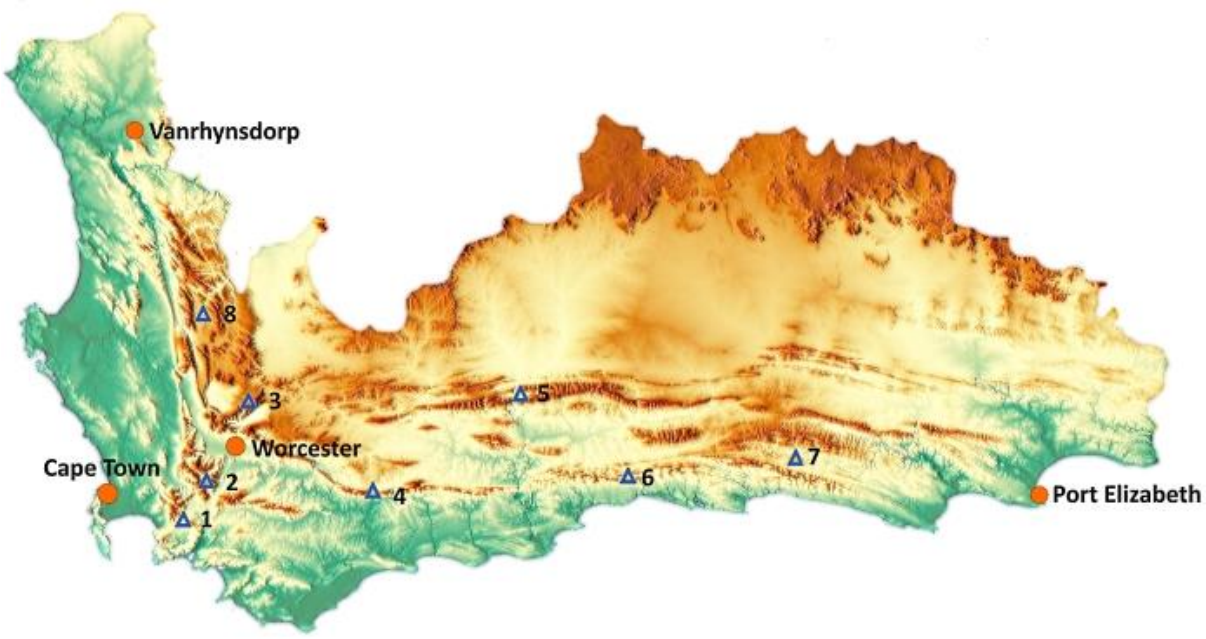

FIGURE 17: STRUCTURAL REGIONS AND MOUNTAIN RANGES OF THE WESTERN CAPE
(**Mountain Ranges: 1**-Hottentots Holland, **2**-Boland, **3**-Hex River, **4**- Langeberg, **5**-Swartberg, **6**-Outeniqua, **7**-Tsitsikamma, **8**-Cederberg; **Source:** www.maps-for-free.com)

three structural regions.

Each of the three structural regions have mountain ranges associated with it (refer to Figure 17). The syntaxis consists of the Hottentots Holland, Boland and Hex River Mountains. The eastward branch consists of the Langeberg, Swartberg, Outeniqua and Tsitsikamma Mountains. The Cederberg mountain range forms part of the northbound branch (Reader's Digest Association South Africa, 1984:12).

5.2 Mountain Passes Used in Research

The Western Cape has the greatest number of mountain passes in South Africa, with an estimated 154 mountain passes (Roberts, 2014). This can be attributed to the predominant presence of the Cape Fold Mountains within the Western Cape. The Cape Fold Mountains create a geological barrier between Cape Town and the rest of South Africa (refer to Figure 17). Therefore a great number of mountain passes are needed since South Africa's primary means of freight transport is along the road network. For this reason the research has been conducted on the Western Cape's mountain passes.

5.2.1 Mountain Pass Selection Criteria

The selection of the mountain passes are dependent on the degree of interaction or exposure between road freight and mountainous terrain. Therefore, the following freight haul distances were found in the literature and form the basis of the selection criteria:

- Sarvi (2008) stated that a short haul distance of a 100km exist around metropolitan areas.
- The latest State of Survey Logistics Report (2013) state an average haul distance of 186km.
- Conduct the study on freight corridors and routes with weighbridges, ensuring a high amount of observed heavy vehicles.

Therefore, the Western Cape Mountain passes that is used will be identified using the above listed criteria.

5.2.2 Selected Mountain Passes

Road freight accounts for approximately 80% of the market share for the transportation of freight over distances of 100 km or less (Sarvi, 2008). This percentage holds true for South Africa, as stated in the Department of Transport Vision report, since the South African freight industry moves 80% of all freight via road (CSIR, 2013), not only over distances of 100 km or less. Therefore, Sarvi's (2008) statement indicates that short-haul heavy vehicles travel primarily via road, it can be assumed that the short-haul distance in South Africa will be longer. As stated in the criteria, the average haul distance is 186 km. Thus, since Cape Town is a major import and export location for freight, it is taken as the central point from which freight is moved from or taken to in the Western Cape and beyond. Figure 18 shows both the 100 km and the 186 km haul distances, as originating from the Port of Cape Town.

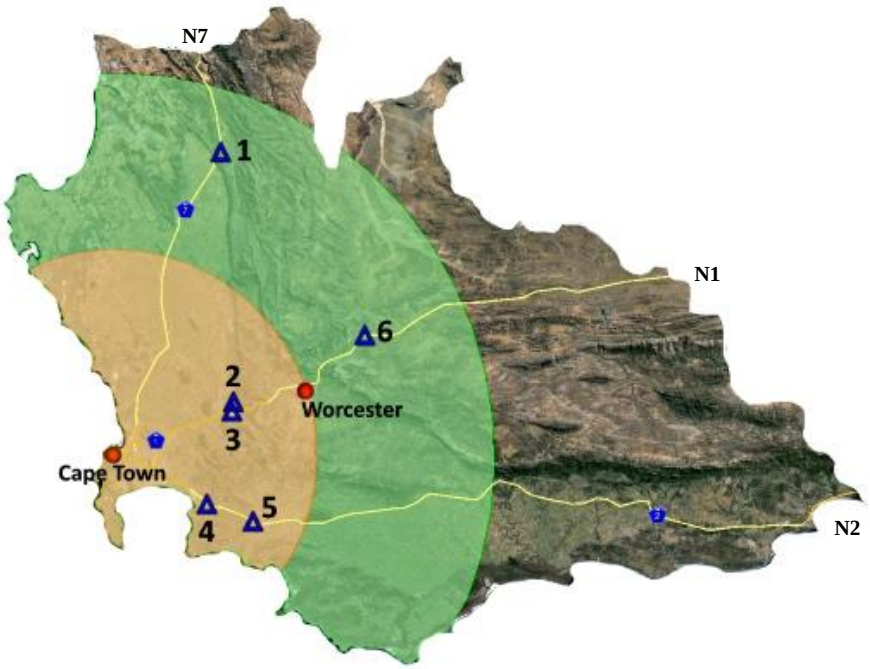

FIGURE 18: AVERAGE FREIGHT DISTANCE RADII AROUND THE PORT OF CAPE TOWN AND MOUNTAIN PASSES (**Orange Hue:** 100 km Haul Radius; **Green Hue:** 186 km Haul Radius; **N1:** Northeast bound yellow line; **N2:** Eastbound yellow line; **N7:** Northbound yellow line; **Mountain Passes: 1**-Piekenierskloof, **2**-Dutoitskloof, **3**-Huguenot Tunnel, **4**-Sir Lowry's, **5**-Houwhoek, **6**-Hex River)

As can be seen in Figure 18, there is a great deal of road freight movement through the Cape Fold Mountains. Three major freight corridors pass through the Cape Fold Mountains, namely the N1, N2 and N7. The N1 connects to Gauteng, the N2 extends along the south and east coast to Port Elizabeth and Durban, and the N7 is the primary route to Namibia. There are also multiple weighbridges situated along these corridors.

Major mountain passes that are situated within the two radii depicted in Figure 18 and along the freight corridors were chosen for this project. Refer to Figure 18 for an illustration of the locality of the chosen mountain passes. The mountain passes identified are Dutoitskloof Pass, Hex River Pass, Houwhoek Pass, Huguenot Tunnel, Piekenierskloof Pass and Sir Lowry's Pass.

5.3 Critical Sections

This section describes the critical sections that were identified for each mountain pass. The critical sections are identified in Section 7.1 and are summarized in Table 4 below.

TABLE 4: CRITICAL SECTIONS FOR THE RELEVANT MOUNTAIN PASSES

Mountain Pass	Critical Type	Speed Limit	Longitude	Latitude
N1 - Dutoitskloof (DTKP**)**	Curve	100 km/h	19.072382	-33.699693
N1 - Hex River (HRP**)**	Curve	60 km/h	19.756751	-33.403128
N1 - Huguenot Tunnel (HGNTT**)**	Straight	80 km/h	19.061542	-33.740754
N2 - Houwhoek (HHP**)**	Curve	80 km/h	19.175576	-34.220918
N2 - Sir Lowry's (SLP**)**	Straight	60 km/h	18.929444	-34.148227
N7 - Piekenierskloof (PKNKP**)**	Curve	100 km/h	18.986093	-32.611231

As can be seen from the Table 4, there are four mountain passes identified as influencing speed through curve radius and two that influence speeds through the presence of a straight. This allows the heavy vehicles to pick up speed before reducing it again to come to a complete stop. Figures 19 through to 24 depict the mountain passes and the respective critical sections that have been identified.

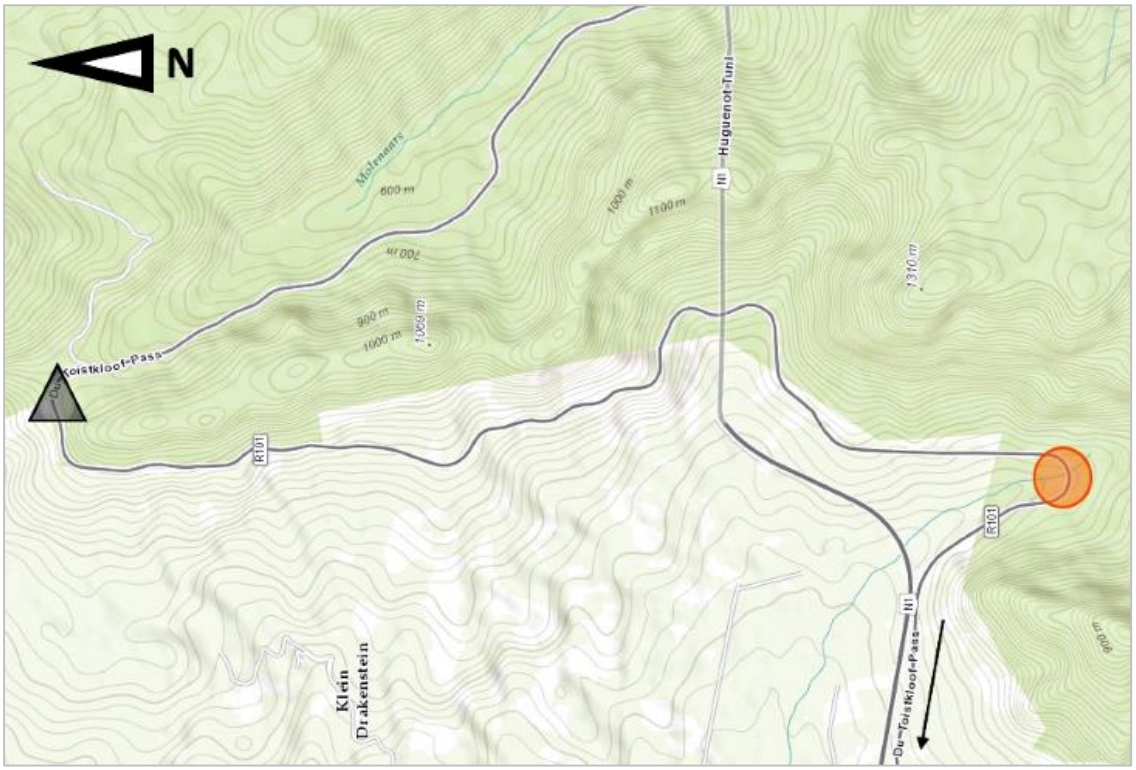

FIGURE 19: DUTOITSKLOOF PASS
(**Black Arrow:** Cape Town inbound; **Orange Dot:** Critical section direction Cape Town inbound**; Grey Triangle:** Pass summit)

FIGURE 20: HEX RIVER PASS
(**Black Arrow:** Cape Town inbound; **Orange Dot:** Critical section direction Cape Town inbound**; Grey Triangle:** Pass summit)

FIGURE 21: HOUWHOEK PASS
(**Black Arrow:** Cape Town inbound; **Orange Dot:** Critical section direction Cape Town outbound**; Grey Triangle:** Pass summit; **Yellow Hue:** Town of Botriver)

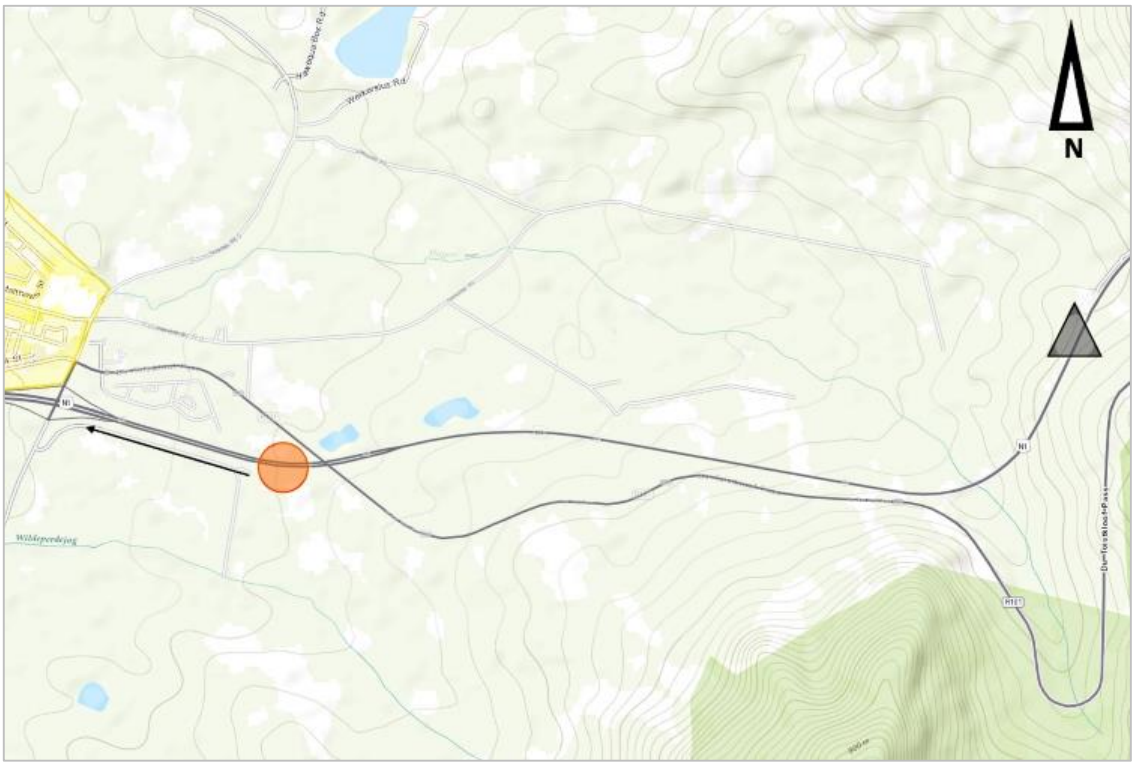

FIGURE 22: HUGUENOT TUNNEL (PAARL SIDE)
(**Black Arrow:** Cape Town inbound; **Orange Dot:** Critical section direction Cape Town inbound**; Grey Triangle:** Pass summit; **Yellow Hue:** Paarl)

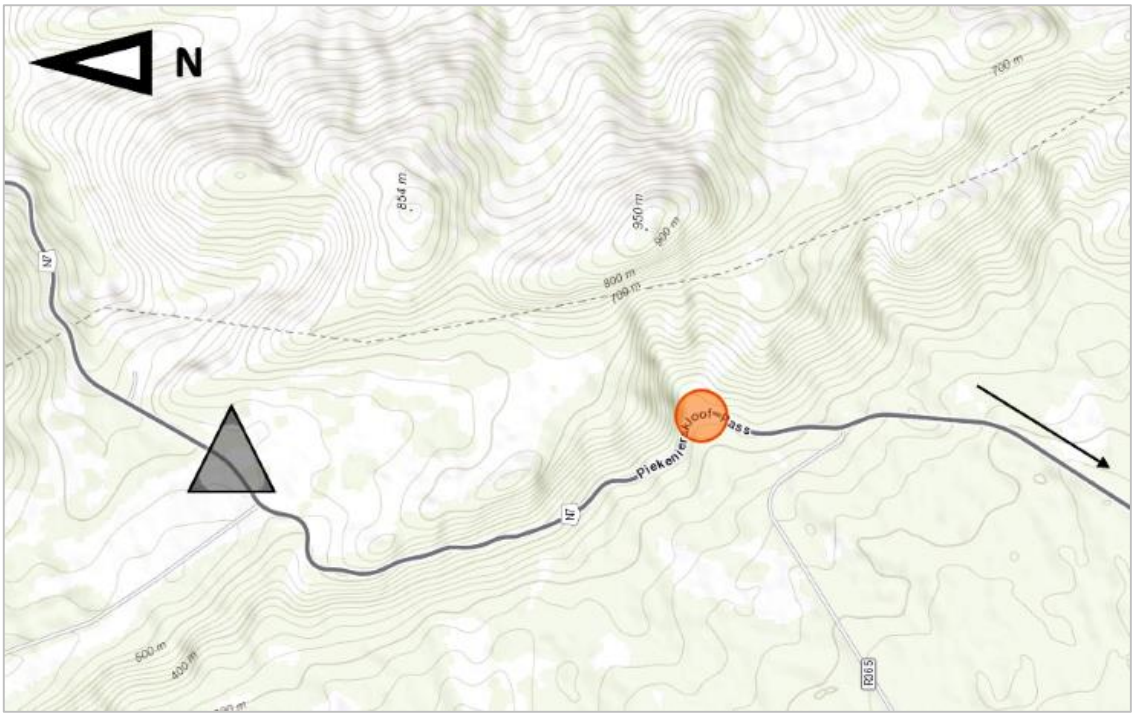

FIGURE 23: PIEKENIERSKLOOF PASS
(**Black Arrow:** Cape Town inbound; **Orange Dot:** Critical section direction Cape Town inbound**; Grey Triangle:** Pass summit)

FIGURE 24: SIR LOWRY'S PASS
(**Black Arrow:** Cape Town inbound; **Orange Dot:** Critical section direction Cape Town inbound**; Grey Triangle:** Pass summit)

6 Collected and Processed Data

This section focusses on the collected data and the relevant processing thereof in preparation for the analyses. It should be noted that all of the data were collected on days with similar weather conditions to eliminate some uncontrollable variables. The preferred weather conditions for this research project were wind-still days with temperatures in the range of 30 to 35°C. Furthermore, there had to be no overcast weather for the day, as this could influence the quality of the recorded video footage. The chapter discusses the collection and processing of the required data for each research variable individually.

6.1 Gradient

The initial GPS recordings (from followed heavy vehicles), which had been used in calculating the initial heavy vehicle speed profiles, were used to determine the gradients of the relevant mountain passes. This was possible, since the speed profile calculations included the calculation of the change in altitude (i.e. ΔY) and change in horizontal distance (i.e. ΔX) for each consecutive coordinate pair. However, small variations or spikes were found while processing the data in preparation for the gradient calculations. The spikes were a result of incorrectly logged GPS altitude values, yielding inaccurate gradients when used in the calculations. These spikes had no effect on the speed profiles, but did affect the gradients significantly. This is attributed to the way in which the gradients were calculated, making them more sensitive to small variations or spikes in the data.

Therefore, the required gradient data were collected again. In collecting the additional data, no heavy vehicles were followed and a constant speed was maintained by the research vehicle during data acquisition. This was done in an attempt to collect data that would result in deltas (i.e. ΔY and ΔX) of similar magnitude during calculation. Since similar deltas will easily identify any incorrect or significantly different value, any such value could then be dealt with accordingly. This included interpolation to smooth out small spikes or replacing larger spikes with the known delta magnitudes. The following figure illustrate the correction methods used:

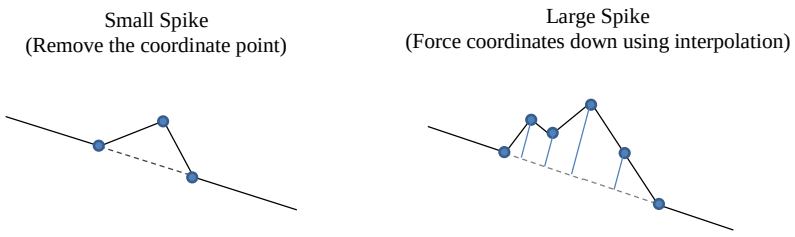

FIGURE 25: GPS DATA ERRORS AND MEANS OF CORRECTING THEM

The additional GPS data yielded far fewer spikes and variations, which were easily dealt with using the methods illustrated in Figure 27. The additional data included 5 GPS logging descents for each of the mountain passes subjected to curve radius (i.e. Du Toitskloof Pass, Hex River Pass, Houwhoek Pass and Piekenierskloof Pass) and 6 logging descents for the two mountain passes with compulsory stops at their base (i.e. Huguenot Tunnel and Sir Lowry's Pass).

The gradients for each individual descent was calculated in three different manners. This was done as to cross-check the results, with a favourable outcome having all three results of similar value or with small (i.e. 0.0x) variations amongst them. The three methods that were used are outlined below.

Simplified Finite Element Method (SFEM) – This method is based on the FEM analysis approach, but is only applied in a one-dimensional situation (i.e. line) that is modelled in real space. Therefore this method calculates each gradient between two consecutive coordinates and then averages them out.

Average Deltas (AD) – The horizontal and vertical deltas (i.e. run and rise) are averaged for each of the mountain passes, after which the gradient is calculated.

Average Gradient (AG) – The gradients are calculated for each horizontal and vertical delta pair, after which the obtained gradients are then averaged.

The results are shown in Table 5.

TABLE 5: GRADIENT RESULTS USING VARIOUS CALCULATION METHODS

Mountain Pass	**Gradient Results**			**Max. Diff.**
	AD [%]	AG[%]	SFEM[%]	
Dutoitskloof	5.69%	5.80%	5.85%	0.16%
Hex River	6.33%	6.31%	6.28%	0.05%
Houwhoek	6.42%	6.44%	6.46%	0.03%
Huguenot Tunnel	5.41%	5.49%	5.89%	0.48%
Piekenierskloof	5.66%	5.66%	5.63%	0.03%
Sir Lowry's	5.92%	5.98%	5.98%	0.07%

From Table 5 it can be seen that the maximum difference between the three results of each mountain pass is generally insignificant (i.e. less than 0.1%), except for Dutoitskloof Pass and Huguenot Tunnel, having maximum differences of 0.16% and 0.48% respectively. The exact reason as to what caused these significant differences is not clear, since all spikes in the data had been corrected. It may be that these difference might be a result of the spike corrections, but it is unclear as to why.

The gradients that are to be used in the analyses are calculated as the average for the three separate results for each mountain pass. As for the two mountain passes having a maximum difference greater than 0.1%, the relevant gradient (i.e. AD, AG or SFEM) causing the error will be excluded, since it was found that the remaining two gradient results are then within 0.1% of each other. Therefore, the average gradients to be used in the analyses are shown in Table 6.

TABLE 6: GRADIENT VALUES TO BE USED IN ANALYSES

Mountain Pass	**Dutoitskloof**	**Hex River**	**Houwhoek**	**Huguenot Tunnel**	**Piekenierskloof**	**Sir Lowry's**
Gradient	5.82%	6.31%	6.44%	5.45%	5.65%	5.96%

The compiled data for the gradient results and final gradients are contained in Appendix C.

6.2 Initial Speed from Heavy Vehicle Followings

The GPS data that were obtained by following the heavy vehicles are used to plot the speed profiles that will be analysed to determine the critical sections for the relevant mountain passes. Each following was done using the method as outlined in Section 4.2.1 and was post processed using the TerraSync software, which then saves the data to a comma-separated-value (.csv) file. Figure 26 illustrates the imported csv data into the database.

	A	B	C	D	E
1	DTKP - R012216A			Radians	
2	Latitude	Longitude	MSL	Latitude	Longitude
3	-33.69656079	19.0714276	810.1	-0.588115932	0.332859205
4	-33.69657646	19.07131546	810.9	-0.588116206	0.332857247
5	-33.6965985	19.07112861	809.3	-0.588116591	0.332853986
6	-33.69664003	19.07085925	808.9	-0.588117315	0.332849285
7	-33.69668044	19.07053855	808.8	-0.588118021	0.332843688
8	-33.69670191	19.07018947	807.3	-0.588118395	0.332837595
9	-33.69672084	19.06984595	805.1	-0.588118726	0.3328316
10	-33.69675938	19.06950571	803.8	-0.588119398	0.332825661

FIGURE 26: EXAMPLE OF THE GPS LOGGED DATA

As can be seen from Figure 28 the data set contains the longitude, latitude and altitude or mean sea level (MSL) of each recorded coordinate. Note that the altitude is given as the mean sea level (MSL), which is the average altitude in metres. The coordinates (i.e. latitude and longitude) are converted from decimal degrees, the standard logging format on the GPS, into radians for future use in the relevant formulas. After the conversion of the coordinates, the distance between each consecutive coordinate pair is calculated, as outlined in Section 4.3.2. The distance can be calculated using three different equations, as explained in the literature review. For the purpose of this project, all three equations (Equations (9) through (11)) were used to ensure a high level of accuracy and to serve as a check for possible errors, in applying the equations, or inconsistencies. Figure 27 illustrates the spreadsheet used for the calculation of the distance using each of the three methods.

F	G	H	I	J	K	L	M	N	O	P	Q
Spherical Laws of Cosine (SLC)				Haversine Formula (HF)				Spherical Vincenty Formula (SVF)			
Distance [m]	Delta_elev [m]	Spatial Distance [m]	Speed [m/s]	Distance [m]	Delta_elev [m]	Spatial Distance [m]	Speed [m/s]	Distance [m]	Delta_elev [m]	Spatial Distance [m]	Speed [m/s]
10.520285	0.748000	10.546843	5.273421	10.519703	0.748000	10.546263	5.273131	10.519703	0.748000	10.546263	5.273131
17.459087	1.543000	17.527138	8.763569	17.458895	1.543000	17.526946	8.763473	17.458895	1.543000	17.526946	8.763473
25.343314	0.372000	25.346044	12.673022	25.343535	0.372000	25.346265	12.673133	25.343535	0.372000	25.346265	12.673133
30.007255	0.093000	30.007399	15.003700	30.007191	0.093000	30.007335	15.003668	30.007191	0.093000	30.007335	15.003668
32.382584	1.512000	32.417864	16.208932	32.382479	1.512000	32.417759	16.208879	32.382479	1.512000	32.417759	16.208879
31.849669	2.199000	31.925491	15.962746	31.849611	2.199000	31.925433	15.962717	31.849611	2.199000	31.925433	15.962717
31.766932	1.333000	31.794887	15.897443	31.766914	1.333000	31.794869	15.897435	31.766914	1.333000	31.794869	15.897435
30.853868	0.483000	30.857648	15.428824	30.853925	0.483000	30.857705	15.428852	30.853925	0.483000	30.857705	15.428852
31.218603	0.777000	31.228270	15.614135	31.218534	0.777000	31.228202	15.614101	31.218534	0.777000	31.228202	15.614101
32.064291	0.831000	32.075058	16.037529	32.064219	0.831000	32.074986	16.037493	32.064219	0.831000	32.074986	16.037493
30.246135	0.248000	30.247152	15.123576	30.245884	0.248000	30.246901	15.123451	30.245884	0.248000	30.246901	15.123451
31.828721	7.215000	32.636233	16.318117	31.828639	7.215000	32.636153	16.318076	31.828639	7.215000	32.636153	16.318076

FIGURE 27: EXAMPLE OF SPREADSHEET WITH TRUE DISTANCE CALCULATIONS

The distance values, depicted Figure 28, have been calculated using Equations (9), (10) and (11). Note that this distance is the distance as measured on the surface of the Earth, whereas the real-space distance (i.e. distance

pertaining to all three dimensions) is required, thus not accounting for the rise in travelled distance. This was easily corrected by taking the difference in MSL as the vertical change in distance (ΔY) between two consecutive coordinates and applying equation (7) to calculate the actual real-space travelled distance. This distance constitutes one part of the required data needed to calculate the speed between two coordinate points. The other is the time component, which is taken as the time interval between concurrently logged coordinates. This value is consistent for each followed heavy vehicle, since it is a required criterion set ahead of logging the data. Calculating the speed is then simply done by dividing the distance travelled between two consecutive coordinates by the time taken to travel it (i.e. the time interval set on the GPS). Figure 28 illustrates the resultant calculated speeds,

R	S	T
Summary [km/h]		
SLC	HF	SVF
66.6	66.6	66.6
68.0	68.0	68.0
69.8	69.8	69.8
67.2	67.2	67.2
67.7	67.7	67.7
66.1	66.1	66.1
63.6	63.6	63.6
62.3	62.3	62.3
60.3	60.3	60.3

FIGURE 28: EXAMPLE OF CALCULATED SPEEDS

As can be seen in Figure 28 there are no differences in the obtained speed, regardless of the equation used in calculating the travelled distance.

6.3 Curve Radius

There are four mountain passes identified that influence the descending speed through the presence of curve radius. These four mountain passes are Dutoitskloof Pass, Houwhoek Pass, Hex River Pass and Piekenierskloof Pass. The curve radius data were collected together with the initial speed data. The initial speed data were collected by following descending heavy vehicles on each mountain pass. The curve radius that is relevant to this research study is situated within the identified critical sections, as determined in Section 7.1. Therefore the whole data log is not relevant in determining the curve radius, only the radius through the critical section. Hence the first step was to determine the entry and exit coordinates for each of the relevant mountain pass's critical section. This was done through plotting the data log files in Google Earth and visually identifying the start and exit coordinates. These coordinates were then used as the search parameters on the relevant data spreadsheets, after which the interlaying coordinates were extracted to a new spreadsheet. The resultant spreadsheet is provided as Appendix D. Table 7 contains the identified start and exit coordinates, along with the total number of interlaying coordinates extracted to the new spreadsheet.

TABLE 7: START AND END COORDINATES OF CRITICAL SECTION CURVES

Mountain Pass	Start Longitude	Start Latitude	End Longitude	End Latitude	Interlaying Coordinates
Dutoitskloof	19.0691	-33.7538	19.0660	-33.7540	49
Hex River	19.7569	-33.4054	19.7578	-33.4064	61
Houwhoek	19.1873	-34.2178	19.1899	-34.2190	51
Piekenierskloof	18.9547	-32.6517	18.9557	-32.6536	56

Now that the necessary data were obtained and extracted, the curve radius could be determined. This was done through the method described in Section 4.3.3. As stated, this problem was approached in terms of analytical geometry. Therefore, the laws of cosine and linear equations applied. These equations are Equation (8) and (5) respectively, as stated in Section 2.7.3. The next step was to obtain the intersecting length between the two consecutive distances, using Equation (5). See Figure 29 for an example of the spreadsheet that was used for determining the radius.

	A	B	C	D	E	F	G	H	I	J	K	L	M	N
1	DTKP - R012218A		Linear Calculations					Intersection		Radians				
2	Long	Lat	Gradient	Mid_Long	Mid_Lat	Perpendicular	Intercept	Long_2	Lat_2	Long	Lat	Long_2	Lat_2	Radius
3	19.069082	-33.753881	1.3005779	19.068995	-33.753994	-0.768888948	-19.092055							
4	19.068908	-33.754108	1.3005779	19.06882	-33.754221	-0.768888948	-19.092416	19.068062	-33.753638	0.3328152	-0.5891203	0.3328005	-0.5891121	106.13329
5	19.068733	-33.754334	0.6643735	19.068589	-33.75443	-1.505177395	-5.0528217	19.066914	-33.75191	0.3328122	-0.5891243	0.3327804	-0.589082	325.31245
6	19.068444	-33.754526	0.5077599	19.068284	-33.754608	-1.969434946	3.7991372	19.067805	-33.753664	0.3328071	-0.5891276	0.332796	-0.5891126	115.22395
7	19.068124	-33.754689	0.131504	19.067943	-33.754713	-7.604329677	111.24421	19.067631	-33.752344	0.3328015	-0.5891305	0.3327929	-0.5890895	252.49691
8	19.067761	-33.754737	-0.0199256	19.067583	-33.754733	50.18660087	-990.69194	19.067637	-33.75206	0.3327952	-0.5891313	0.332793	-0.5890846	281.59941
9	19.067406	-33.75473	-0.1508047	19.067238	-33.754704	6.631092553	-160.19132	19.067542	-33.752686	0.332789	-0.5891312	0.3327914	-0.5890955	215.30615
10	19.06707	-33.754679	-0.3277992	19.066907	-33.754625	3.050648117	-91.921048	19.067505	-33.752801	0.3327832	-0.5891303	0.3327907	-0.5890975	203.20563
11	19.066743	-33.754572	-0.5345425	19.066599	-33.754495	1.870758532	-69.423498	19.067288	-33.753207	0.3327774	-0.5891284	0.332787	-0.5891046	155.7414
12	19.066456	-33.754418	-0.8619329	19.066334	-33.754313	1.160183176	-55.874753	19.067387	-33.753092	0.3327724	-0.5891257	0.3327887	-0.5891026	173.66374
13	19.066212	-33.754209	-1.2937607	19.066111	-33.754078	0.77294047	-48.491047							
14	19.06601	-33.753947												
15													Average	203.18699
16													Radius	205

FIGURE 29: SCREENSHOT OF EXCEL SPREADSHEET USED IN CALCULATING THE RELEVANT CURVE RADIUS

The curve radius was obtained five times during the initial speed data collection. It should be noted that there was a large degree of variation for the intersecting radii; however, when the averages were taken, they adhered to the design specifications as stipulated in the TRH17. Table 8 shows the average radius and standard deviation along with the specified curve radius, which is based on the design speed of the downgrade. This variation is attributed to the fact that some of the segments recorded neared collinearity, resulting in a larger intersecting radius, since lines parallel to collinear lines never cross. Table 8 shows the average curve radius. For the expanded list of results refer to Appendix D.

TABLE 8: AVERAGE CURVE RADIUS FOR THE RELEVANT CRITICAL SECTIONS

Mountain Pass	Ave. Radius [m]	Std. Dev [m]	Speed [km/h]	f_{max} [-]	Superelevation [-]	TRH17 Rec.
Dutoitskloof	200	10	100	0.14	0.0996	350
Hex River	120	7.07	60	0.1525	0.1027	110
Houwhoek	200	10.37	80	0.14	0.1185	210
Piekenierskloof	160	20.49	80	0.14	0.1002	210

6.4 Superelevation

The data required for calculating the superelevation are as stated in Section 4.3.5. A Trimble total station, model M3-DR5, was used in collecting the relevant data. The data were collected near the apex of each critical section, since the maximum superelevation occurs here. The device was set up each time to obtain a full view of the apex. After the setup and levelling of the device were finished, the basic survey function of the total station was used to measure the relevant horizontal and vertical angles as well as the distance. The way in which the measurements were done was intended to measure the nearest point first and then proceed to the next point on the same side of the shoulder. Each point was taken on the road edge, directly next to an easily identifiable marker, such as a road sign. After five points had been collected on the one side, the five transverse points were collected. The transverse points are the points on the other side of the road for a relevant point. The road infrastructure ensured that the measurements taken were perpendicular across the road. The reason for measuring all points on the one side and then the corresponding points on the other side is for safety, since this procedure meant the road was crossed only twice. Figure 30 illustrates the manner in which the measurements were done.

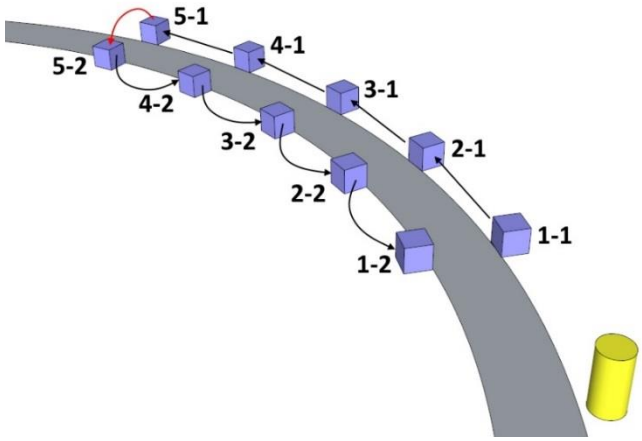

FIGURE 30: COLLECTING THE RELEVANT POINTS REQUIRED FOR CALCULATING THE SUPERELEVATION

For the complete set of data measured in the field, please refer to Appendix E. The data listed in Table 9 were processed to obtain the superelevation, as discussed in Section 4.3.5. Pythagoras' Theorem was used extensively in calculating the superelevation for measured points per mountain pass. The equations used in determining the superelevation were Equations (5) through to (8). Table 9 contains the superelevation for the four relevant mountain passes that were used in the analyses.

TABLE 9: SUPERELEVATION FOR THE RELEVANT CRITICAL SECTIONS

Mountain Pass	Ave. Horizontal Change [m]	Ave. Vertical Change [m]	Superelevation [-]
Dutoitskloof	6.629	0.660	0.0996
Hex River	7.391	0.759	0.1027
Houwhoek	7.414	0.878	0.1185
Piekenierskloof	10.722	1.074	0.1002

6.5 Length of Downgrade

Google Earth was used to obtain the downgrade length of each mountain pass, following the method outlined in Section 4.2.6. The path feature was used to draw a line following the centre line of the road from the summit to the base. In two instances the summit was replaced with a compulsory stop preceding the downgrade. The downgrades referred to are Hex River Pass and Huguenot Tunnel. Therefore the length of the downgrade was measured from the compulsory stop to the base and not the summit as for the other mountain passes. Once a path had been plotted in Google Earth, its properties was viewed and used to obtain the length of the downgrade. The results are shown in the Table 10.

TABLE 10: DOWNGRADE LENGTH OF EACH MOUNTAIN PASS

Mountain Pass	Length of Downgrade [km]
Dutoitskloof	13
Hex River	3.6
Houwhoek	2.7
Huguenot Tunnel	4.8
Piekenierskloof	4.5
Sir Lowry's	6.1

6.6 Stopping Distance

This data is needed in the analysis of the factors that influences the operating speed of heavy vehicles that have to come to a stop at the base of the downgrade. Two mountain passes were identified (refer to Section 5.2.2), namely Huguenot Tunnel and Sir Lowry's Pass. This is the distance over which the heavy vehicles have to decrease their speeds and come to a compulsory stop. At Huguenot Tunnel this is a tollgate and at Sir Lowry's Pass a signalised intersection. The exit observation point of the critical section was taken in both cases as the point where the posted speed limit is indicated prior to stopping. See Figure 31 and Figure 32 for an illustration of the stopping distances for these two downgrades.

FIGURE 31: STOPPING DISTANCE MEASUREMENT FOR HUGUENOT TUNNEL

FIGURE 32: STOPPING DISTANCE MEASUREMENT FOR SIR LOWRY'S PASS

The stopping distances were determined using Google Earths path function as discussed in Section 4.2.6. The reason for doing this is one of accessibility, since the toll plaza does not allow anyone to be on foot next to the road. Furthermore, the GPS could have been used in the car, but that would have required passing through the tollgate multiple times, which would have been costly. Therefore an alternative means had to be found, namely using Google Earth. In order to maintain consistency, this alternative was applied to Sir Lowry's Pass as well. The average distances for Sir Lowry's Pass and Huguenot Tunnel are 570 m and 650 m respectively.

6.7 Heavy Vehicle Speed

As discussed in Section 4.3.4, the speed of an object is the rate of change of the object's position. Given this definition, the two defining components of speed (i.e. distance and time) were collected for each observed heavy vehicle. These components were defined in the field through the position of the observations points. Since the observation points define the control area, the distance component had been obtained as the measured distance between the transverse lines of the control area. Furthermore, the control area also defines the time interval which the heavy vehicle took to pass from the first transverse line to the second. The difference defines the time component.

The time component was collected through the combined use of GoPro cameras and datum markers, as outlined in Section 4.3.4. After that the footage was processed using VLC media player and Kinovea software. As stated in Section 4.1.1, two datum markers were used throughout the research, namely light-boxes and datum discs. In some mountain passes it was found that the rolling vibration of descending heavy vehicles caused the light-boxes to flash too soon, resulting in inaccurate measurements. For these locations the light-boxes were substituted with the datum discs. Table 11 indicates the relevant critical sections and the datum marker used.

TABLE 11: CAMERA SETTINGS AND DATUM MARKERS USED PER MOUNTAIN PASS

Mountain Pass	Datum Marker	Video Recording
Dutoitskloof	Laser Light-Box	30 FPS 1080P Narrow View
Hex River	Laser Light-Box	30 FPS 1080P Narrow View
Houwhoek	Laser Light-Box + Datum Discs	30 FPS 1080P Narrow and Medium View
Huguenot Tunnel	Datum Discs	30 FPS 1080P Narrow View
Piekenierskloof	Laser Light-Box	30 FPS 1080P Narrow and Medium View
Sir Lowry's	Datum Discs	30 FPS 1080P Narrow and Medium View

After the collection of the video footage, the time component of the speed had to be obtained. This was accomplished through the combination of VLC media player and Kinovea analytical software. Firstly, the overlay images were obtained through clipping video segments in VLC using the recording function. This was done so as not to overload the resource buffer of the Kinovea software, as was encountered the first time a full-length recording was run. The video clips contained a single observation point with a heavy vehicle passing through it. The clips were no longer that 15 seconds in length. The clip was imported into Kinovea and pause-played. This means that the video was advanced forward frame by frame. This allowed for the transverse line to be created at the precise time the heavy vehicle broke the light-boxes laser beam. As for the datum discs, the line was drawn regardless of a heavy vehicle being in the frame or not, since the line could be drawn from the centre of each disc to the other, which represents the transverse line. See Figure 33 for an illustration for creating the transverse lines. This process was completed for all three observation points of each of the six mountain passes. These image overlays were then imported to the relevant video clips and using VLC's overlay feature, it was made transparent and overlaid on the recorded videos. It should be noted that the overlay image should have the same resolution as the video onto which it is placed.

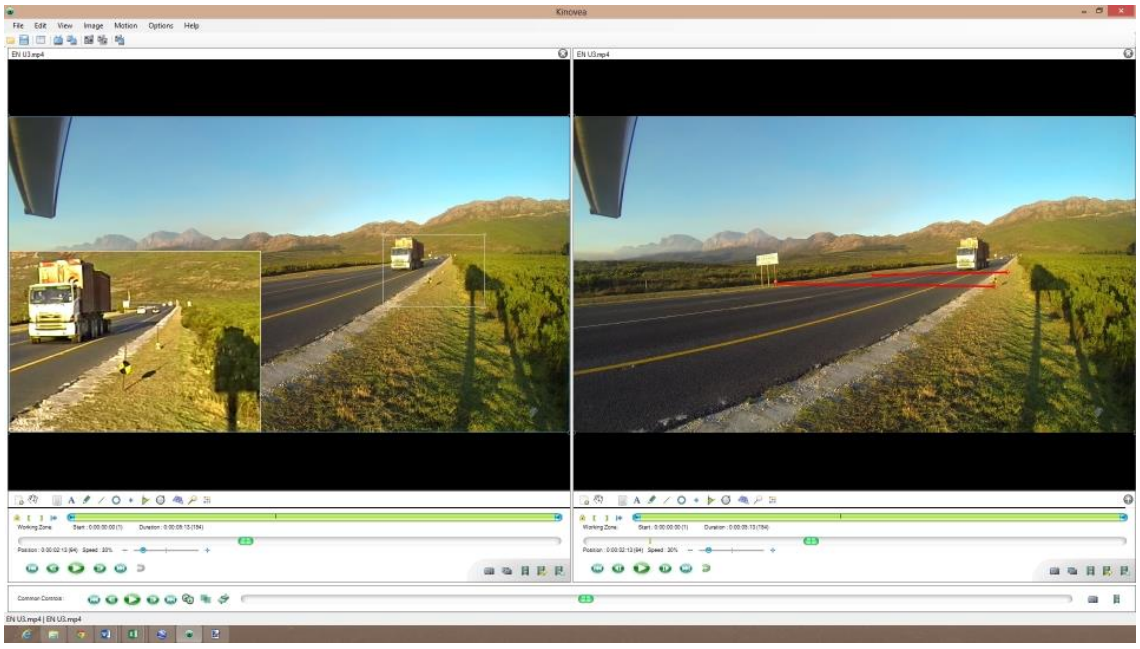

FIGURE 33: CREATING TRANSVERSE LINES USING KINOVEA

To extract the time data from the video easily, an extension was created for VLC, since there were in excess of 1,200 video clips. The extension was written in VLC's base language, lua. The interface was written in such a way that the user can extract the time from the data-structure at the immediate point of interest. This time was then logged in a comma-separated-value format (.csv). The clip name was logged first and followed by the crossing times of the entry and exit transverse lines. This was used in conjunction with a downloaded extension from the VLC forums, named Clipper. This extension allowed for the accurate forward and backward skipping of video frames. See Figure 34 for an illustration of the two extensions used. After all of the relevant times had been extracted to the logger user interface, the times were saved in a text file created by the logger extension. Note that the clips were also used to obtain the number of axles and registration number, as discussed in Sections 6.8 and 6.9 respectively.

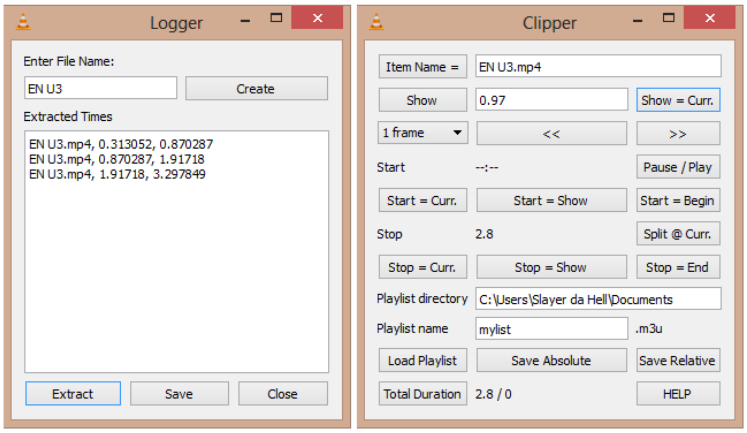

FIGURE 34: VLC EXTENSIONS USED FOR TIME LOGGING AND EXACT FRAME SKIPPING

The extensions illustrated in Figure 34 are, on the left, the time logging program which had been programmed for this project and, on the right, the clipper extension which was obtained from the VLC forum, as stated in Section 4.1.2. Both codes for the programs can be found in Appendix B. One particular problem of note is the stability of the recordings. This can be successfully achieved for the most part by setting the cameras sufficiently far from the road, so as to not be susceptible to wind gusts or rolling vibrations of passing vehicles. The other measures are as stated in the assumptions (Section 4.5.1), to do all recordings on wind-still days, which will help to improve the accuracy of the image overlays, which impose the control area on the video clip of the relevant observation point. See Figure 35 for an illustration of distortion as a result of wind.

In some instances the front wheels of the heavy vehicle could not be seen. The shadow of the heavy vehicle was then used to construct the transverse datum line, since it was assumed that the distance between the transverse lines was sufficiently close to one another to not be influenced by the suns position.

The distance component was collected through the use of a measuring wheel, as stated in Section 4.2.3. This distance was measured on the outside road marking (line) of the descending lane, between the first and second transverse lines of each observation for each mountain pass. The reason for measuring the outside line and not the centre line was a safety consideration, because of the nature of where the measurement was to be taken, on a road with limited sight distance. The difference in measuring on the road shoulder as opposed to the centreline is negligibly small. The distance measurements for the relevant mountain passes and observation points are set out in Table 12.

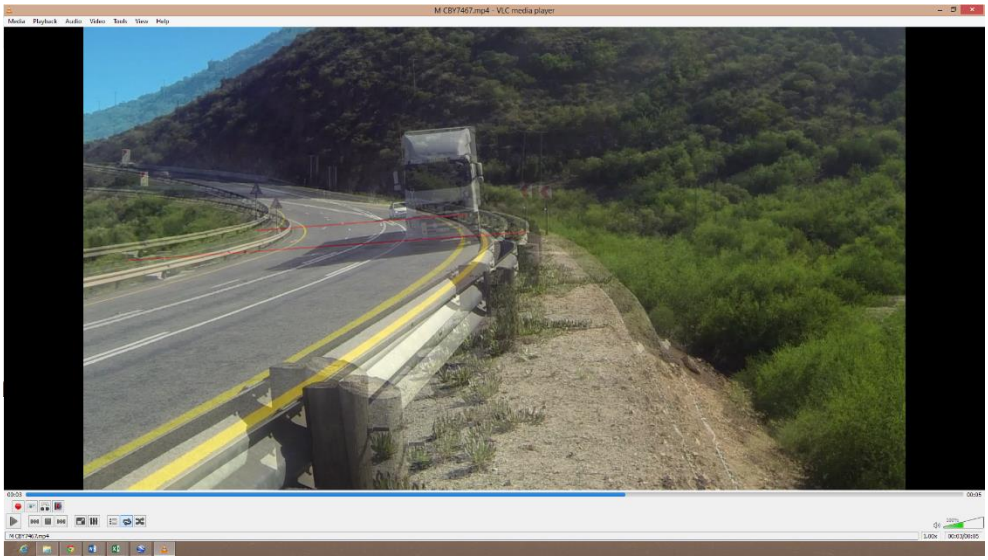

FIGURE 35: DISTORTION OF TRANSVERSE DATUM LINES DUE TO WIND

TABLE 12: MEASURED DISTANCES FOR THE OBSERVATION POINTS PER MOUNTAIN PASS

Mountain Pass	Entry	Apex	Exit
Dutoitskloof	25.1	23.6	25.4
Hex River	46.5	10	21.1
Houwhoek	63.4	24.5	26
Huguenot Tunnel	30.2	35.9	30.8
Piekenierskloof	25.5	25.2	57.6
Sir Lowry's	10.1	20	25.8

As can be seen from the above table, there are significant changes in the distance between the two transverse lines that delineate each control area. The reason for this discrepancy can be attributed to the placement of the road-side infrastructure, which was used in most passes as fixing points for the equipment.

6.8 Number of Axles

This was obtained visually from the extracted video clips. The number of axles included the steering axles. Only heavy vehicles with four or more axles were considered for this research project, since the heavy vehicle is then articulated and generally has E80 axles. Figure 36 represents how the axles were counted from the video clips. Table 13 indicates the number of heavy vehicles per axle class for each one of the six mountain passes.

TABLE 13: NUMBER OF HEAVY VEHICLES PER AXLE CLASS

Mountain Pass	4 -Axles	5 - Axles	6 - Axles	7 - Axles	More
Dutoitskloof	4	9	21	19	0
Hex River	4	6	14	36	0
Houwhoek	7	7	26	21	4
Huguenot Tunnel	5	8	38	61	0
Piekenierskloof	5	13	33	35	4
Sir Lowry's	4	1	24	12	0
Totals	29	44	156	184	8

FIGURE 36: OBTAINING THE NUMBER OF AXLES FROM THE VIDEO FOOTAGE

6.9 Heavy Vehicle Registration

The heavy vehicle registration numbers were obtained from the video clips that were created for determining the heavy vehicle operating speed. The high quality of the video recordings enabled the accurate reading of the registration number of the tractor. The settings that were used were a narrow field of view, and recording at 1080p resolution. This enabled a more distant focal point, allowing for clarity at a greater distance. Figure 37 illustrates the quality at which the registration numbers were obtained.

FIGURE 37: QUALITY OF THE VIDEO RECORDINGS

It should be noted that there were some instances when the registration number could not be read. It was found that the Western Cape registration numbers were the easiest to read, mainly because of their high contrast, black on white. The number plates of the Northern Cape and Limpopo were at times difficult to read, because of the

green text sometimes being influence by ambient light. Another reason for not being able to read the number plate was its placement on the vehicle. In some instances the number plates were obstructed by the bulbar or similar structure. Note none of the registration numbers are shown in this report and accompanying appendices. A total of 421 legible heavy vehicle registration numbers were obtained for the six mountain passes.

6.10 Heavy Vehicle Mass

Obtaining the mass of the heavy vehicles is a general challenge and often expensive in the field, but having to do this in a mountain pass is near impossible, because of the limited space available and the intrusive nature of the task. The weigh in motion significantly reduce the speeds of heavy vehicles, although they are still moving. Therefore an alternative means had been used, namely weighbridges. Only the weighbridges that were of relevance to the selected mountain passes were contacted. Figure 38 illustrates the locality of the relevant weighbridges and mountain passes.

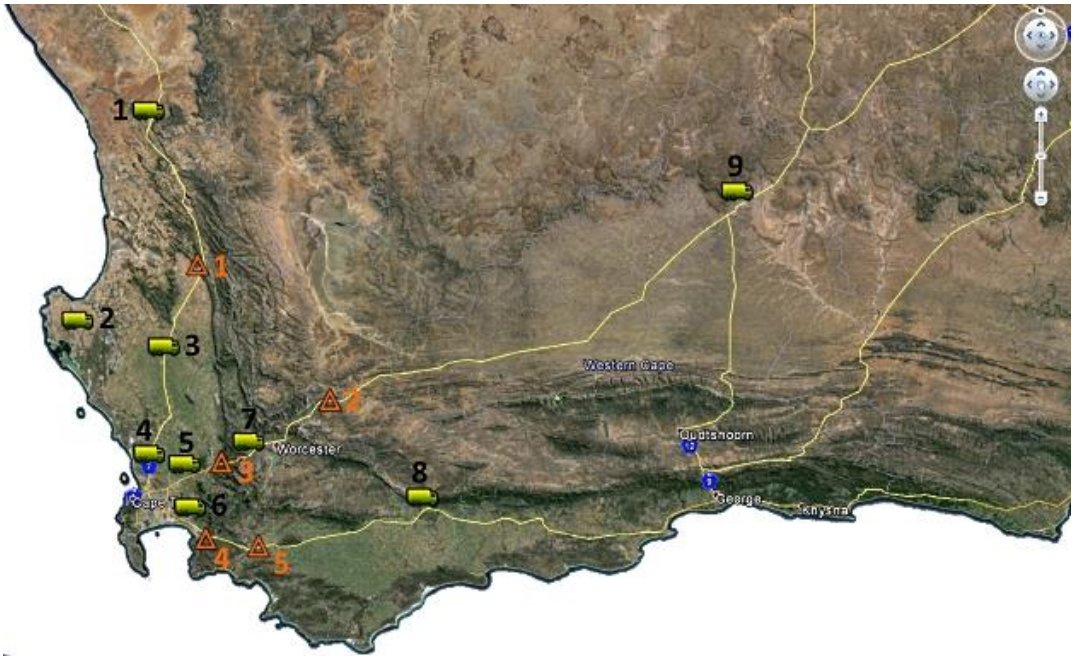

FIGURE 38: WESTERN CAPE WEIGHBRIDGES AND THEIR RELATION TO THE RELEVANT MOUNTAIN PASSES

The chosen weighbridges were primarily ahead of the pass in the direction of travel. For example, the Beaufort West weighbridge was used to obtain information on heavy vehicles travelling towards Cape Town, since the Hex River downgrade is in the inbound direction to Cape Town.

All of the contacted weighbridges indicated that their managing corporation had to be contacted. This was done in a timely manner, since it had been expected that a lengthy process might ensue. Obtaining the information had proven difficult, since a formal request had to be directed to the Western Cape Government, which agreed to release only selected information. The information that was provided included the registration number, number of axles and gross vehicle mass along with the weigh dates. All of the other information was protected under the Protection of Personal Information act.

Information covering a six-month period was provided, which contained more than 250,000 individual entries for the seven identified weighbridges. The following table contains the weighbridge, pass relevance, direction of travel and number of entries for the six-month period.

TABLE 14: PASS RELEVANCE AND WEIGHS PER SEMESTER

Weighbridge	Pass Relevance	Direction	Weighs per 6 Months
1 – Klawer	PKNKP	CPT IO	15040
2 – Vredenburg	-	CPT O	-
3 – Moorreesburg	PKNKP	CPT IO	14619
4 – Vissershok	-	CPT O	-
5 – Joostenberg Vlakte	HRP; DTKP; HGNTT	CPT IO	45476
6 – Somerset West	HHP	CPT O	18019
7 – Rawsonville	HRP; DTKP; HGNTT	CPT IO	58801
8 – Swellendam	HHP; SLP	CPT IO	40423
9 – Beaufort West	HRP; DTKP; HGNTT	CPT IO	83723

As can be seen from the number of heavy vehicles relevant to this study and the amount of weigh information entries, there is a lot of unnecessary information. In order to obtain only the relevant masses, a Visual Basic for Applications (VBA) macro was programmed in Excel. The purpose of this macro was to take the relevant list of heavy vehicles and search for all corresponding registration numbers in the mass data. Refer to Appendix B for the macro code. Nearly all of the heavy vehicle numbers which formed the query had multiple results within the mass data. Therefore, to obtain a single mass to represent a registration number, the average of all the weigh masses were taken. Figure 39 illustrates the query dataset and the averaged mass spreadsheet, respectively. For the complete extracted spreadsheet refer to Appendix F1. Of the 421 queried heavy vehicles across all six mountain passes, only 238 heavy vehicles had corresponding mass data for the past six months.

Query Data

ID	Make	Axels	Entry	Apex	Exit	Profile
DTKP_1	Volvo	6	54.7	61.9	68.2	Increasing
DTKP_10	Hino	7	55.8	64.9	57.1	Downward Parabola
DTKP_11	MAN	5	65.8	70.5	62.3	Skew Right Down
DTKP_12	Volvo	7	78.6	61.1	66.7	Skew Left Up
DTKP_13	Freightliner	6	62.3	67.7	61.7	Downward Parabola
DTKP_14	Mercedes	4	80.0	59.5	67.2	Skew Left Up
DTKP_15	Freightliner	6	54.3	62.4	65.7	Increasing
DTKP_16	MAN	5	36.8	47.3	44.7	Skew Left Down
DTKP_17	Freightliner	7	31.9	43.6	54.7	Increasing
DTKP_18	Mercedes	6	39.0	53.3	40.8	Downward Parabola
DTKP_19	Volvo	6	76.6	59.5	95.2	Skew Right Up
DTKP_2	Freightliner	6	47.8	49.9	44.5	Skew Right Down
DTKP_20	Volvo	7	54.8	44.8	52.7	Upward Parabola
DTKP_21	Freightliner	7	58.0	67.3	67.9	Increasing
DTKP_22	Iveco	7	69.9	58.2	57.9	Decreasing
DTKP_23	MAN	7	46.7	47.0	62.6	Increasing
DTKP_24	MAN	5	94.8	66.5	103.5	Skew Right Up
DTKP_25	MAN	6	55.4	63.1	59.2	Skew Left Down
DTKP_26	Mercedes	6	102.7	67.6	92.4	Skew Left Up
DTKP_27	Mercedes	5	60.9	43.0	50.0	Skew Left Up
DTKP_28	Kenworth	5	45.0	52.6	47.8	Skew Left Down
DTKP_29	Kenworth	5	81.4	47.1	57.5	Skew Left Up
DTKP_3	Freightliner	7	50.3	42.5	53.2	Skew Right Up
DTKP_30	Mercedes	6	41.6	45.3	62.9	Increasing
DTKP_31	International	7	54.0	57.8	36.4	Skew Right Down

Heavy Vehicle Summary

Truck ID	Axels	Ave Axels	Avg_Mass	StDev	Entry	Apex	Exit	Profile
DTKP_10	7	7	33040	3754.2	55.8	64.9	57.1	Downward Parabola
DTKP_13	6	6	37675	7859.2	62.3	67.7	61.7	Downward Parabola
DTKP_15	6	6	42858	1629.8	54.3	62.4	65.7	Increasing
DTKP_16	5	5	27945	6609.8	36.8	47.3	44.7	Skew Left Down
DTKP_18	6	6	39849	5712.6	39.0	53.3	40.8	Downward Parabola
DTKP_19	6	6	47657	775.7	76.6	59.5	95.2	Skew Right Up
DTKP_20	7	7	50706	4188.5	54.8	44.8	52.7	Upward Parabola
DTKP_21	7	7	51378	9644.1	58.0	67.3	67.9	Increasing
DTKP_22	7	7	45910	5490.0	69.9	58.2	57.9	Decreasing
DTKP_23	7	7	49244	9136.0	46.7	47.0	62.6	Increasing
DTKP_24	5	5	36524	1735.5	94.8	66.5	103.5	Skew Right Up
DTKP_25	6	6	45840	2032.5	55.4	63.1	59.2	Skew Left Down
DTKP_27	5	5	40928	650.7	60.9	43.0	50.0	Skew Left Up
DTKP_28	5	5	37350	490.0	45.0	52.6	47.8	Skew Left Down
DTKP_29	5	5	37350	490.0	81.4	47.1	57.5	Skew Left Up
DTKP_30	6	6	36037	13446.2	41.6	45.3	62.9	Increasing
DTKP_31	7	7	50287	11934.7	54.0	57.8	36.4	Skew Right Down

FIGURE 39: EXAMPLE OF QUERY DATA AND EXTRACTED DATA

6.11 Speed Profiles

These values were obtained by taking the three observation speeds and determining what shape they have. Table 15 indicates the identified profiles or shape.

TABLE 15: SPEED PROFILES AND DEFINITIONS

Profile	Illustration	Description
Increasing (linear positive)	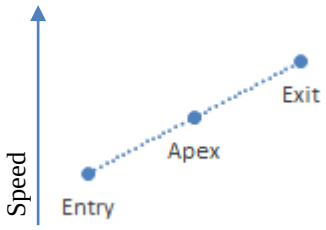	The entry speed is the slowest and the exit speed is the fastest of the three observation speeds. The heavy vehicle linearly increased speed throughout the curve.
Decreasing (Linear negative)		The entry speed is the fastest with the exit speed is the slowest of the three observation points. The heavy vehicle linearly decreased speed throughout the curve.
Skew left up (Positive skew left parabola)		The apex speed was the slowest of the three observed speeds, with the entry speed being the fastest. The heavy vehicle reduced speed towards the apex and increased upon exiting the curve.
Skew right up (Positive skew right parabola)	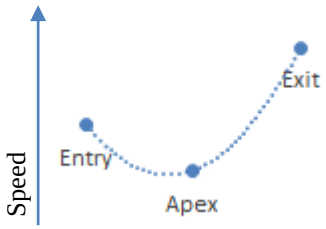	The apex speed was the slowest of the three observed speeds, with the exit speed being the fastest. The heavy vehicle reduced speed towards the apex and increased speed upon exiting the curve.
Skew left down (Negative skew left parabola)	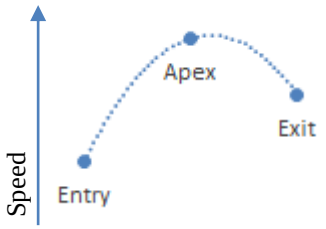	The apex speed was the fastest of the three observed speeds, with the entry speed being the slowest. The heavy vehicle increased speed towards the apex and slightly reduced speed towards the exit.
Skew right down (Negative skew right parabola)		The apex speed was the fastest of the three observed speeds, with the exit speed being the slowest. The heavy vehicle slightly increased speed towards the apex and reduced speed towards the exit.

Upward symmetric (Parabola positive)		The apex speed is slowest observed speed with the entry and exit speeds being equal.
Downward symmetric (Parabola negative)	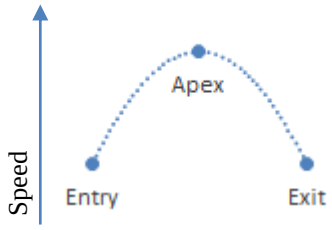	The apex speed is fastest observed speed with the entry and exit speeds being equal.

The speed profiles are primarily classified as linear, skew or symmetric. Linear profiles represent a gradual, linear change in speed between the three observation points. The parabolic profiles have entry and exit speeds that are very close in magnitude to each other, regardless of whether the apex speed is faster or slower than the entry and exit speeds. The skew profiles can be seen a specific type parabolic profile, since the main difference between the skew and parabolic profiles is based on the relation of the entry-apex and apex-exit speed pairs, with it being defined as parabolic if the speed pairs are similar in magnitude (i.e. of close value). Thus a skew profile is a parabolic curve, where there is a significant difference between the speed pairs. Figure 40 contains a screenshot of the Excel spreadsheet used for the speed profiles.

Dutoitskloof Pass		Entry Time [s]			Apex Time [s]			Exit Time [s]			Speed [km/h]			Shape
ID	Axels	T1	T2	ΔT	T1	T2	ΔT	T1	T2	ΔT	Entry	Apex	Exit	0.05
DTKP_1	6	2.67	4.32	**1.65**	2.93	4.30	**1.37**	2.71	4.05	**1.34**	54.7	61.9	68.2	Increasing
DTKP_2	6	4.04	5.93	**1.89**	4.08	5.79	**1.70**	3.12	5.18	**2.05**	47.8	49.9	44.5	Skew Right Down
DTKP_3	7	5.43	7.22	**1.80**	3.53	5.52	**2.00**	4.34	6.06	**1.72**	50.3	42.5	53.2	Skew Right Up
DTKP_4	5	4.90	6.35	**1.45**	3.75	5.32	**1.58**	3.44	4.44	**1.00**	62.3	53.9	91.4	Skew Right Up
DTKP_5	4	3.93	5.52	**1.60**	3.24	4.48	**1.24**	1.98	3.45	**1.47**	56.6	68.4	62.2	Skew Left Down
DTKP_6	7	5.28	6.97	**1.69**	2.26	3.50	**1.24**	1.65	3.09	**1.44**	53.5	68.6	63.5	Skew Left Down
DTKP_7	6	1.62	3.71	**2.08**	3.33	4.86	**1.53**	3.46	4.92	**1.46**	43.4	55.5	62.8	Increasing
DTKP_8	6	4.68	5.93	**1.26**	3.69	5.16	**1.47**	2.25	3.41	**1.15**	71.9	57.8	79.3	Skew Right Up

FIGURE 40: SPREADSHEET USED TO CLASS SPEED PROFILES

Note that the accompanying speeds and mass are provided in Appendix F2. The significance check was chosen as a 5 percent range; therefore if the entry and exit speeds have a difference of greater than five percent, it is classed as a skew profile.

6.12 Summary of Processed Data

The number of heavy vehicles included in the study was dependent on the number of heavy vehicles that have legible registration numbers. The reason is that the registration number serves as the linking median between an observed heavy vehicle's mass and its speed. This study observed 421 heavy vehicles over six mountain passes, subjecting speeds to two primarily influence factors, namely curve radius and stopping distance. The data are summarized in Table 16.

TABLE 16: SUMMARY OF POST PROCESSED DATA

Mountain Pass	Gradient	Length of Gradient	Curve Radius	Superelevation	Stopping distance
Appendix	C	-	D	E	-
Dutoitskloof	5.82	13.0	200	0.996	-
Hex River	6.31	3.6	120	0.1027	-
Houwhoek	6.44	2.7	200	0.1185	-
Piekenierskloof	5.65	4.5	160	0.1002	-
Huguenot Tunnel	5.45	4.8	-	-	650
Sir Lowry's	5.96	6.1	--	-	570

The initial speed followings, heavy vehicle speeds and masses are shown in, Appendices D and G respectively.

7 Analyses and Results

7.1 Critical Section Analysis

In this section the initial speed data are analysed and discussed to identify the critical sections of each mountain pass. The data being referred to were collected by following several heavy vehicles along the whole downgrade of each mountain pass. Refer to Section 6.2 for the relevant collected data and the subsequent processing thereof. The method for analysing the data was outlined in Section 4.4.1.

In general the goal of this analysis is to identify areas of interest, which will be used to determine the critical section of each mountain pass. The areas of interest are defined by overlapping points of interest, which were obtained from the individual speed profile of each heavy vehicle that was followed. Therefore, the first step was creating the relevant speed profiles. The processed speeds were plotted on the y-axis and the cumulative distance of the relevant points on the x-axis. An example of such a speed profile is shown in Figure 41.

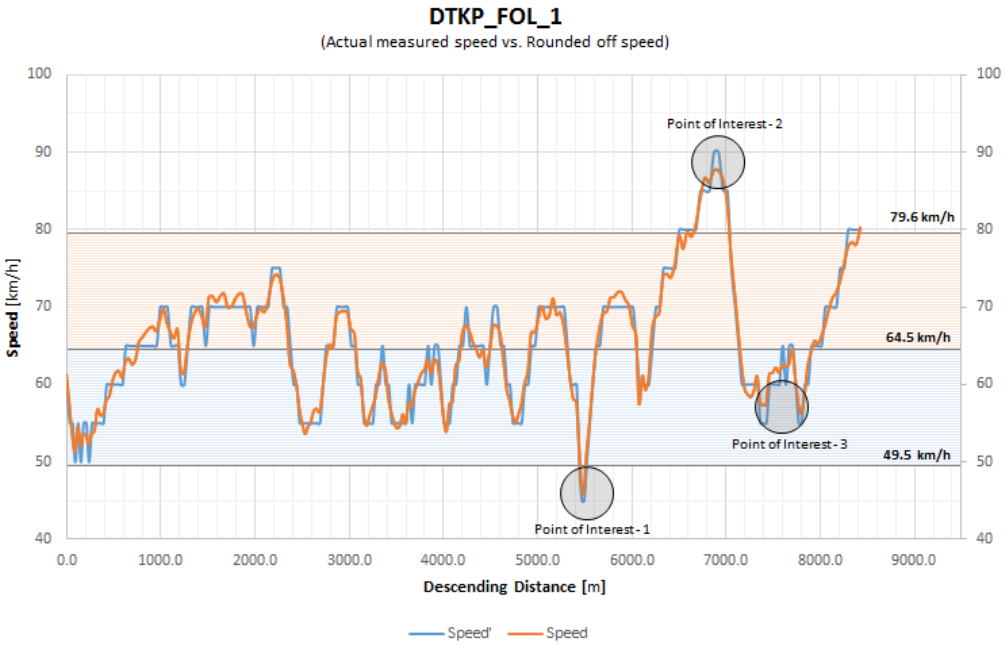

FIGURE 41: EXAMPLE OF THE INDIVIDUAL SPEED PROFILE FOR A FOLLOWED HEAVY VEHICLE (**Orange Hue:** upper 95% confidence limit; **Blue Hue:** lower 95% confidence limit)

Note that the graph in Figure 41 has two graph plots: a plot representing the actual speed (orange line) and an adjusted plot (blue line). The adjusted plot is a rounding off of the actual speed data to the nearest 5 km/h interval. The reason for rounding off the actual data is that there are a lot of fluctuations in the speed, which is the result of small variations in the following distance between the trailing vehicle and heavy vehicle that was followed. Therefore, to smooth the curve and eliminate most of the fluctuations in the speed profile, the actual speed data were rounded. As is evident in Figure 41, the adjusted speed profile (i.e. rounded-off speed) fits the actual speed profile to a high degree. Therefore, the adjusted speed profile is representative of the actual speed profile. Also note that a moving average can be used to achieve the same result.

Figure 411 also indicates the 95 percent confidence interval around the mean speed of the profile, resulting in an upper and lower limit. These limits are then used in identifying any points of interest, which are defined as an abnormally high or low observed speed (i.e. an outlier of the data set). Also seen in the above figure is a point of interest that is situated between the upper and lower limits. The reason for this is that by inspection of the speed profile, the researcher deemed that point as being of interest. Table 17 summarises the defining parameters of each followed heavy vehicles' speed profile

TABLE 17: SUMMARY OF INDIVIDUAL SPEED PROFILE PARAMETERS

Followed ID	Lower limit	Mean	Upper Limit	Points of interest
DTKP_FOL_1	49.5	64.5	79.6	3
DTKP_FOL_2	25.2	33.5	41.8	2
DTKP_FOL_3	25.5	56.4	87.4	2
DTKP_FOL_4	39.2	53.8	68.5	2
DTKP_FOL_5	49.9	63.8	77.6	2
HRP_FOL_1	6.2	19.3	32.5	1
HRP_FOL_2	33.9	49.7	65.5	2
HRP_FOL_3	14.2	21.4	28.6	1
HRP_FOL_4	16.5	22.6	28.6	2
HRP_FOL_5	44.2	62.4	80.8	2
HHP_FOL_1	44.3	53.1	62	2
HHP_FOL_2	52.9	57.2	62.6	1
HHP_FOL_3	68.6	73.9	79.1	3
HHP_FOL_4	63.4	72.9	82.3	1
HHP_FOL_5	52.2	64	75.6	2
HGNTT_FOL_1	55.5	74	92.6	2
HGNTT_FOL_2	33.7	40	46.1	3
HGNTT_FOL_3	52.6	67.9	83.2	2
HGNTT_FOL_4	56.7	77.7	98.6	3
HGNTT_FOL_5	55.9	60.8	65.7	0
HGNTT_FOL_6	70.1	75	79.9	2
PKNKP_FOL_1	22.2	32.8	43.3	1
PKNKP_FOL_2	13.1	60.3	107.4	1
PKNKP_FOL_3	51.9	78.8	105.8	0
PKNKP_FOL_4	57.5	72.3	87.2	1
PKNKP_FOL_5	28.6	34	39.3	2
SLP_FOL_1	29.5	46.5	63.5	2
SLP_FOL_2	16.1	22.3	28.5	1
SLP_FOL_3	41.3	67.3	93.3	1
SLP_FOL_4	55	68.3	81.5	1
SLP_FOL_5	41.2	50.4	59.6	2
SLP_FOL_6	6.5	28.7	50.9	1

Refer to Appendix G for all the individual speed profiles.

In order to gain a better insight into how the drivers perceive a given mountain pass, the individual speed profiles were combined into a summary graph for each relevant mountain pass. This allows for areas of interest to be identified; these are defined as the overlapping or grouping of points of interest. Overlaying the graphs required some additional work to line up the individual speed profiles on a single graph. This was done by identifying a common start and end GPS coordinate pair (i.e. start and end coordinate points), after which the relevant included speed and cumulative distance were plotted on the overlay graph.

Once all of the relevant summary graphs were plotted, they were analysed to identify the areas of interest. Firstly, the graph was discussed in general, addressing the number of followed heavy vehicles and the spread of the speed profiles. Furthermore, general trends (e.g. speed increases or decreases) were identified and briefly discussed. The following sections of this chapter analyse the initial speed profile summary graph of each mountain pass individually, in order to identify the critical sections.

7.1.1 Dutoitskloof Pass

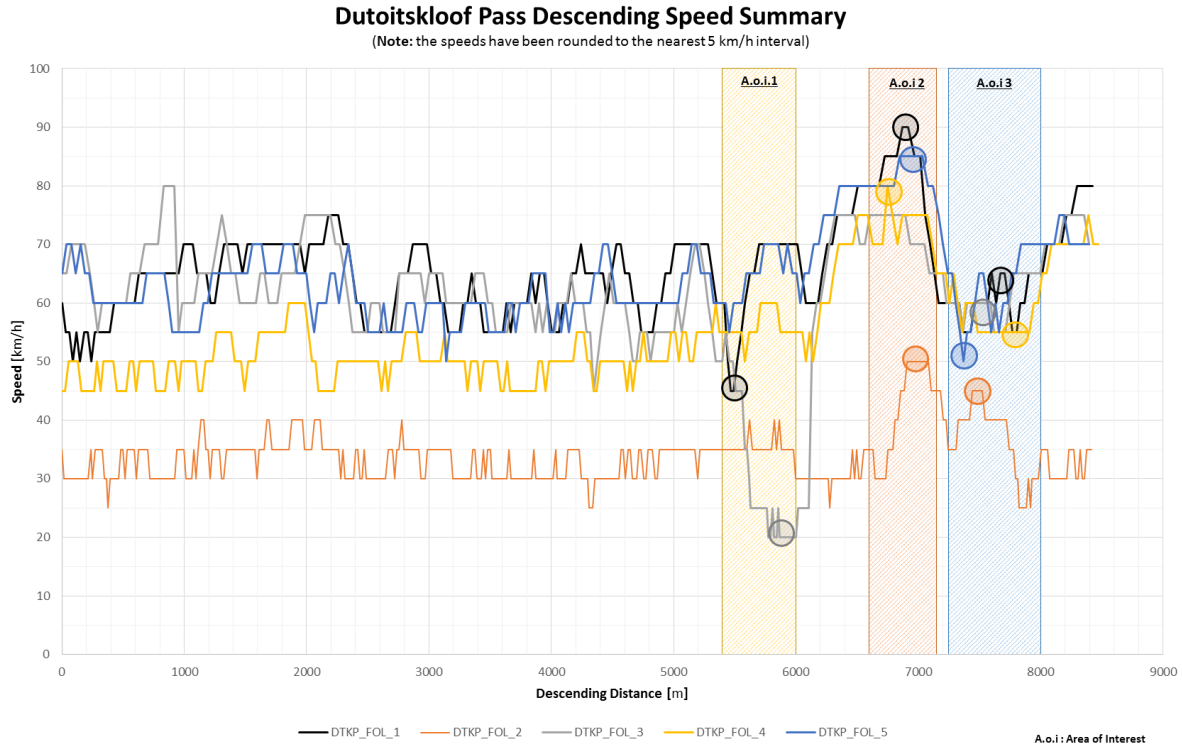

The following figure illustrates the combined speed profiles of the individual heavy vehicles that were followed on Dutoitskloof Pass.

FIGURE 42: INITIAL SPEED PROFILES SUMMARY - DUTOITSKLOOF PASS
(**Yellow Band:** Area of interest 1; **Orange Band:** Area of interest 2; **Blue Band:** Area of interest 3)

Five heavy vehicles were followed along the whole length of the downgrade, while logging the relevant GPS data. The processed data are shown in Figure 42, which combines the individual speed profiles of the followed heavy vehicles. As can be seen from the above figure, there is a good spread of speed data. This indicates that one slow descending (i.e. heavily laden) and four fast descending (i.e. empty or lightly loaded) heavy vehicles were followed. These followings resulted in the identification of 11 points of interest, which were grouped into three areas of interest. These points were plotted in Google Earth and shown in Figure 43.

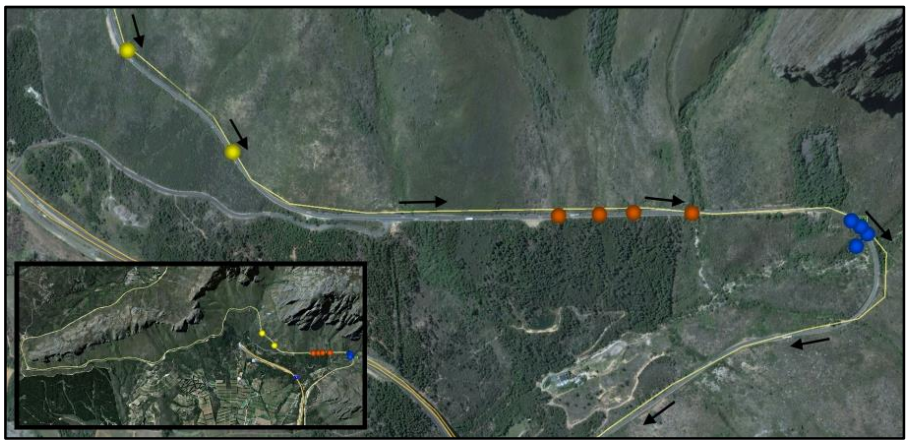

FIGURE 43: AREAS OF INTEREST ON DU TOITSKLOOF PASS
(**Yellow Markers:** Area of interest 1; **Orange Markers:** Area of interest 2; **Blue Markers:** Area of interest 3; **Black Arrows:** Downgrade and Cape Town inbound direction)

Area of Interest 1

This area is defined by two points of interest, indicated by a sudden decrease in speed. This decrease in speed is attributed to the fact the area allows for passenger vehicles to overtake the slower heavy vehicles. And it has been observed that some heavy vehicle drivers tend to reduce speed purposefully, allowing more passenger vehicles to pass.

Area of Interest 2

Consisting of four points of interest, this area is situated ahead of the 180-degree curve, which can be seen on the right-hand side of Figure 43. This area is defined by four points of interest that show a maximum achieved speed for four of the followed heavy vehicles. The reason for the four maximum descending speeds is attributed to the straight and steep downgrade within this area of interest, therefore, allowing heavy vehicles to increase the descending speed.

Area of Interest 3

Four of the five heavy vehicles decreased speed upon entering the curve and maintained a fairly constant speed through it. This gives rise to the idea that the drivers decreased their speed to navigate the curve safely. This is further supported by the fact that heavy vehicles increased speed as they exited the curve, indicating that a definite decrease in normal travelling speed is needed to traverse the curve safely.

This project aims to understand the effect of mountainous road geometry on heavy vehicle speeds. Therefore, the third area of interest is given top priority, since the descending speeds are significantly influenced by the presence of the curve (i.e. curve radius). Thus, the critical section of Dutoitskloof pass is identified as the third area of interest.

7.1.2 Hex River Pass

On Hex River Pass five heavy vehicles were followed along the downgrade, while logging the corresponding GPS data. The relevant speed profiles were obtained for each of the followed heavy vehicles and were combined as shown in Figure 44. It can be seen that three of the followed heavy vehicles descended at a slow rate of speed and one at a moderate rate. The fifth heavy vehicle (i.e. blue line on Figure 44) is observed as descending at speeds in

excess of the 60 km/h speed limit. However, its speed decreased to the recommended speed limit of 50 km/h upon entering the second area of interest (i.e. orange band on Figure 44).

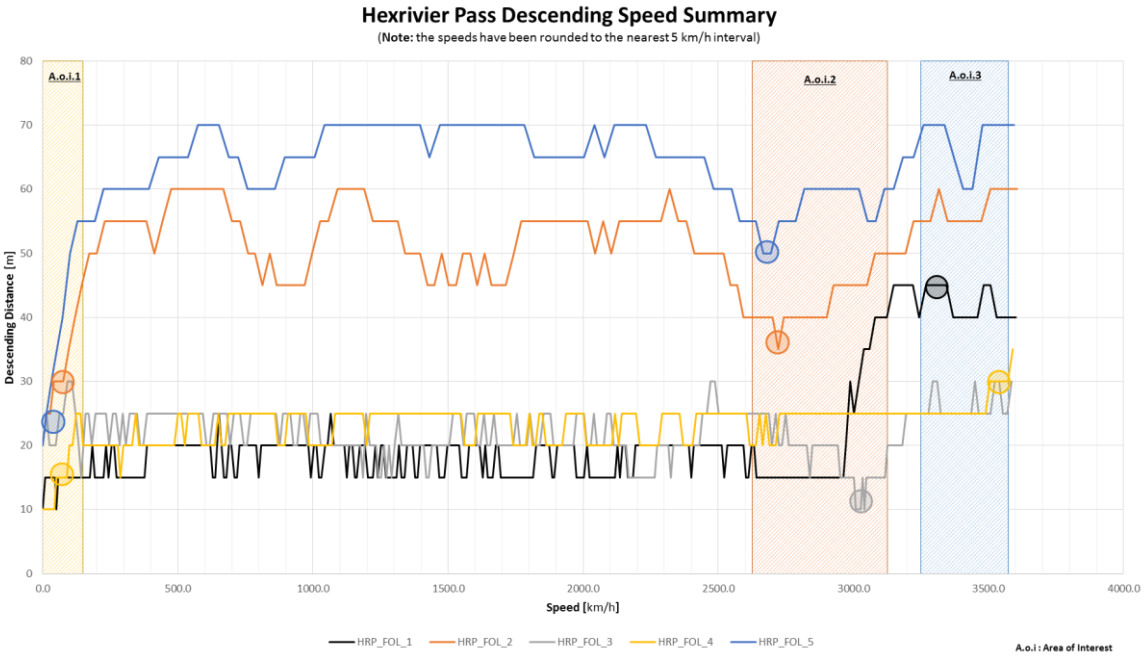

FIGURE 44: INITIAL SPEED PROFILE SUMMARY – HEX RIVER PASS
(**Yellow Band:** Area of interest 1; **Orange Band:** Area of interest 2; **Blue Band:** Area of interest 3)

Furthermore, it is seen that four of the five followed heavy vehicles increased operating speed upon exiting the second area of interest. Overlaying the individual speed profiles resulted in three areas of interest, containing eight points of interest. Figure 44 shows the locality of these points.

FIGURE 45: AREAS OF INTEREST ON HEX RIVER PASS
(**Yellow Markers:** Area of interest 1; **Orange Markers:** Area of interest 2; **Blue Markers:** Area of interest 3; **Black Arrows:** Downgrade and Cape Town inbound direction)

Area of Interest 1

This area consists of three points of interest that represent a very slow rate of speed. In two instances it is also observed that the speed increases rapidly over a short distance. The reason for this disturbance in speed (i.e. slow speed) is attributed to the compulsory stop that is situated ahead of the mountainous descent. It was also observed

that none of the followed heavy vehicles came to a complete stop, but only reduced speed. This can be attributed to the rural location of the mountain pass and the lack of traffic enforcement on the pass itself.

Area of Interest 2

In this area it was observed that three of the followed heavy vehicles reduced speed significantly. As indicated by the orange markers in Figure 45, this reduction in speed is attributed to a sharp s-shape curve that requires a slow entry speed as to navigate it safely. Note that one of the markers is relatively far from the entrance of the curve. The reason for this is that the relevant heavy vehicle (i.e. grey line on Figure 44) had an overall slower rate of descent, and therefore required a reduction in speed at a later point.

Area of Interest 3

This area has two points of interest that indicate an increase in speed. However, once the individual speed profiles were combined, it was found that all of the heavy vehicles in this area increased their operating speed. The reason is that this area is at the base of the mountain pass and is followed by a straight section of road with a good sight distance. Therefore, the drivers perceive it as being safe to increase their speed from this area onwards.

The critical section for this mountain pass was identified as the second area of interest (i.e. orange markers on Figure 45). This section is deemed the critical curve, since it is the first half of the s-curve and therefore is the limiting section. Thus the greatest reduction was speed is observed here to ensure a safe entry speed into the s-curve.

7.1.3 Houwhoek Pass

Figure 46 illustrates the overlain speed profiles of the individual heavy vehicle that were followed on Houwhoek Pass:

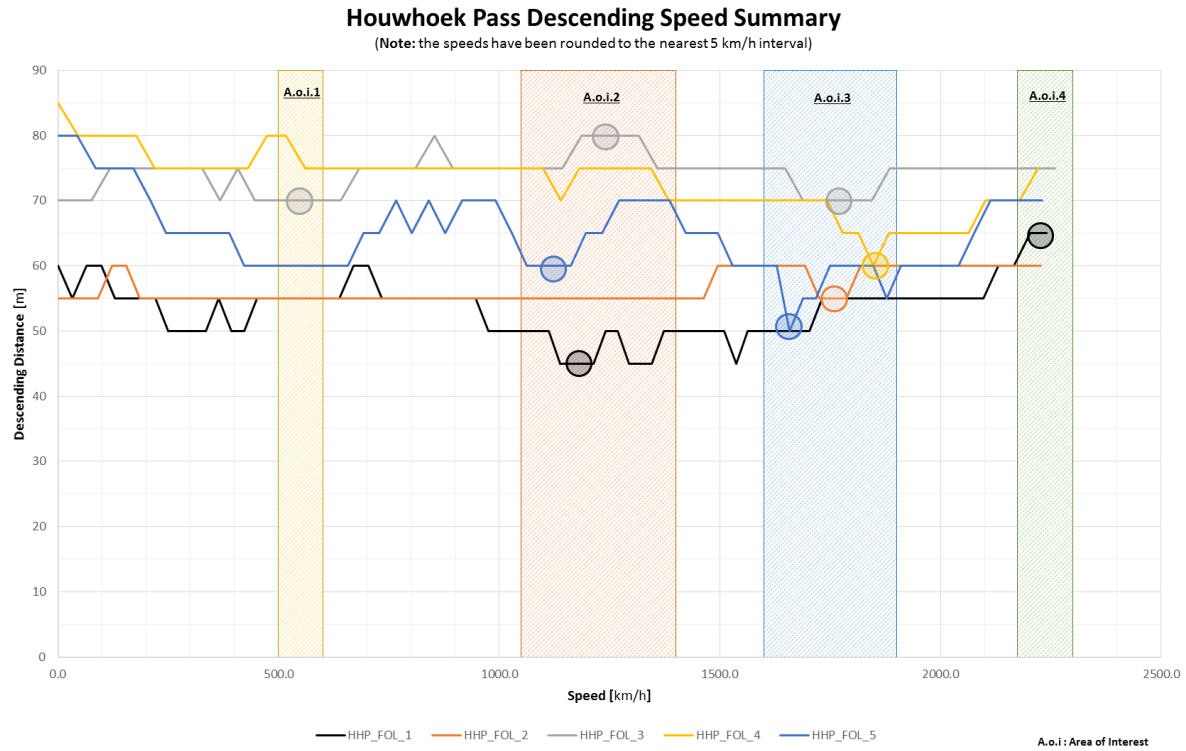

FIGURE 46: INITIAL SPEED PROFILE SUMMARY - HOUWHOEK PASS
(**Yellow Band:** Area of interest 1; **Orange Band:** Area of interest 2; **Blue Band:** Area of interest 3; **Green Band:** Area of interest 4)

The speed profiles of five heavy vehicles were obtained on Houwhoek Pass. The profiles were determined through the collection and processing of the relevant GPS data, as discussed in Section 4.2.1. The spread of the obtained speeds were considered to be fairly representative of how drivers perceive the pass. Since no slow travelling heavy vehicles were followed, this can be indicative that drivers perceive the pass safe to navigate at higher speeds. Furthermore, the speed profiles are relatively uneventful, since this pass has a short downgrade length of 2.7 kilometre and a posted speed limit of 80 km/h. The combining of individual speed profiles resulted in the identification of four areas of interest, defined by nine points of interest. Figure 47 depicts the location of the areas of interest on Houwhoek Pass.

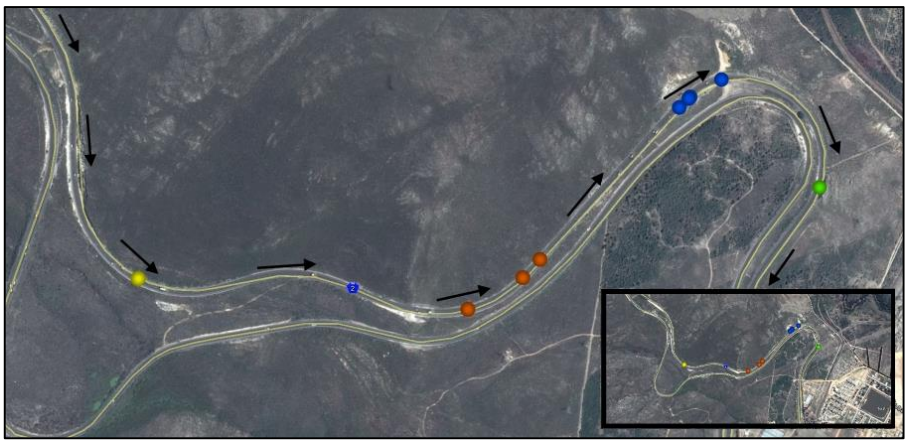

FIGURE 47: AREAS OF INTEREST ON HOUWHOEK PASS
(**Yellow Markers:** Area of interest 1; **Orange Markers:** Area of interest 2; **Blue Markers:** Area of interest 3; **Green Marker:** Area of interest 4; **Black Arrows:** Downgrade and Cape Town inbound direction)

Area of Interest 1

This area consists of a single point of interest that was found to be irrelevant, as can be seen in Figure 46. This point was identified since it is representative of where the third followed heavy vehicle (i.e. grey line on Figure 46) had its slowest observed speed. It should be noted that this point of interest is situated just after the summit of the mountain pass.

Area of Interest 2

In this area two of the three relevant points of interest indicate a decrease in speed, with the remaining point indicating an increase in speed. One of the two heavy vehicles that reduced speed kept it constant until the third area of interest. The other one increased speed again, indicating that it had reduced speed to navigate the curve safely. Following the curve in this area is a straight section of road that leads into the hairpin curve of area three (i.e. blue markers on Figure 47).

Area of Interest 3

Four of the five followed heavy vehicles recorded their slowest speeds in this area. The reason for this trend is that this area of interest is situated at the entrance of a sharp curve, as can be seen in Figure 47. Therefore, a reduction of speed is required to navigate the curve safely, keeping in mind that the approach to this section is a steep and straight downgrade. It is also observed from Figure 47 that all five of the followed heavy vehicles exited this area of interest at a near constant speed.

Area of Interest 4

This area is identified by a single point of interest that indicates an increase in speed. As can be seen from Figure 47, this is expected since this area is situated at the exit of the last curve of the pass. Even though only a single point of interest was identified in this area, two other followed heavy vehicles also exhibited an increase of speed in this area. From this area onwards there is a straight section of road with a long sight distance. Therefore heavy vehicles drivers feel that it is safe to increase their speed again.

The third area of interest (i.e. blue markers on Figure 47) is identified as the critical section. The reason is that the slowest speeds were observed at this section. Furthermore, the preceding section of road is a steep and straight downgrade that leads into this curve. Therefore, heavy vehicles may increase speed on the straight and have to immediately reduce it again to navigate the curve safely. This causes an increased strain on the braking system of the relevant heavy vehicles, as was observed on two different occasions.

7.1.4 Huguenot Tunnel

Figure 48 illustrates the combined speed profiles of the individual heavy vehicles that were followed on Huguenot Tunnel toll section.

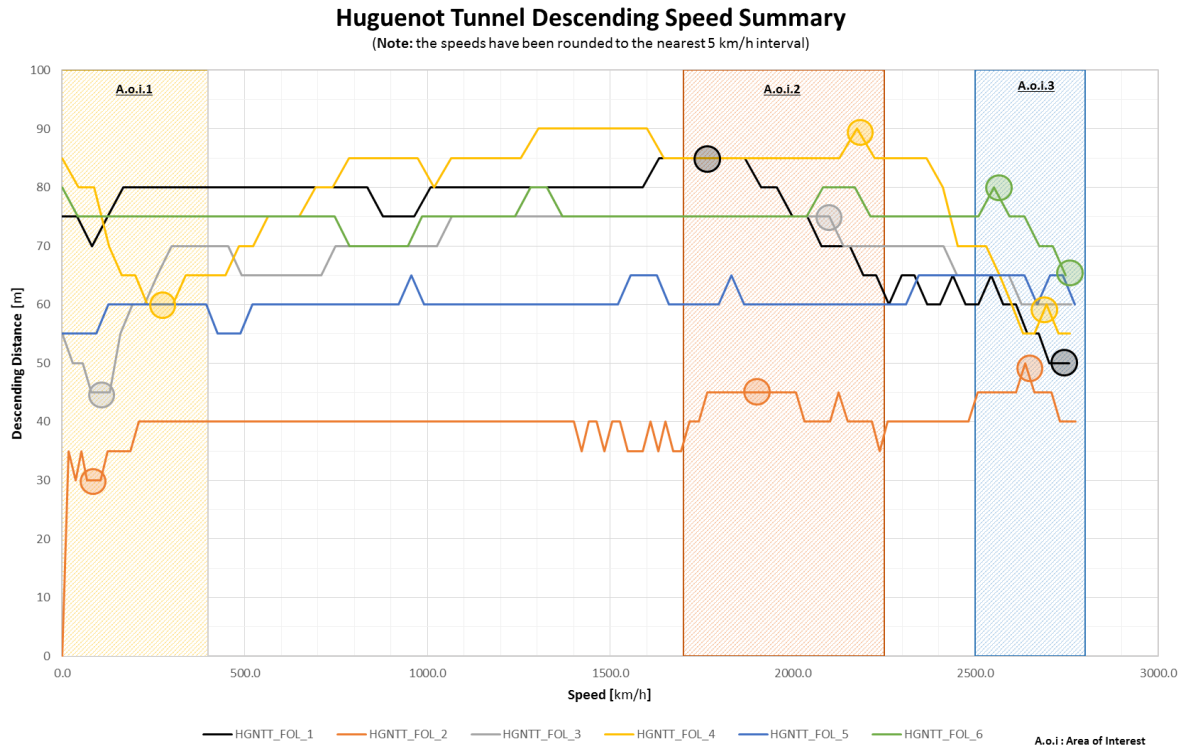

FIGURE 48: INITIAL SPEED PROFILE SUMMARY - HUGUENOT TUNNEL
(**Yellow Band:** Area of interest 1; **Orange Band:** Area of interest 2; **Blue Band:** Area of interest 3)

Six heavy vehicles were followed on the Paarl side of the Huguenot Tunnel, which is not a mountain pass by true definition. The reason for including this section of road is that it resembles a mountainous downgrade in the sense that it is both long and of sufficiently steep gradient. Figure 48 depicts a good spread of the combined descending speed profiles, since it includes a slow rate, a moderate rate and four fast rates of descent. The individual speed profiles resulted in a total of 12 points of interest, identifying three areas of interests. The locality of these areas is depicted in the Figure 49.

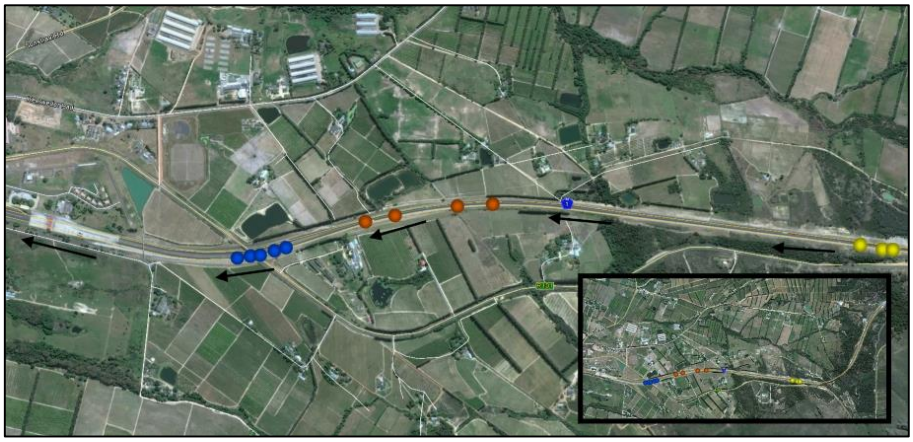

FIGURE 49: AREAS OF INTEREST ON PAARL SIDE OF HUGUENOT TUNNEL (**Yellow Markers:** Area of interest 1; **Orange Markers:** Area of interest 2; **Blue Markers:** Area of interest 3; **Black Arrows:** Downgrade and Cape Town inbound direction)

Area of Interest 1

Three of the six heavy vehicles showed a significant reduction in speed in this area. The reason is that the descending lane was blocked off due to construction just past the bridge, causing the heavy vehicle descending lane to merge with the adjacent lane. It was observed that the heavy vehicles found the merging difficult, since a safe gap is not always provided. Thus, as they were not able to change lanes ahead of time, the heavy vehicles reduced speed to wait for a gap in the traffic.

Area of Interest 2

This area consists of four points of interest, with three points indicating a reduction in speed. The reduction in speed is to allow for a safe approach towards the tollgates, since a compulsory stop is required of all vehicle as they pass through the gates.

Area of Interest 3

Five points of interest were combined to identify this area of interest. Five of the followed heavy vehicles reduced speed in this area, since the posted speed limit of 60 km/h is enforced with closed-circuit surveillance cameras. Therefore, it was found that all of the followed heavy vehicles reduced or maintained operating speeds at or below 60 km/h, as seen in Figure 48.

The critical section was identified as being between the second and third areas of interest (i.e. orange and blue markers on Figure 49). The reason is that heavy vehicles reach a maximum descending speed in this section, where speed must be reduced to zero if they are to stop safely. As for the inclusion of the third area, this section was used to see how well the drivers adhere to the 60 km/h approach speed to the toll plaza.

7.1.5 Piekenierskloof Pass

Five heavy vehicles were followed along the downgrade in the direction of Cape Town. The spread of the obtained speeds is good, since it includes two slow, one moderate and two fast rates of descent. The individual speed profiles are fairly uneventful, since the followed heavy vehicles maintained constant speeds. In total only five points were identified, with the third followed heavy vehicle (i.e. grey line in Figure 50) not having a single point of interest. Subsequently three areas of interest were identified that revealed an interesting trend in the speed profiles. As can be seen in Figure 50, all speeds are fairly constant from the summit (i.e. left side of the graph) to

the first area of interest, after which three of the five followed heavy vehicles increased their speed. Figure 50 depicts the location of the areas of interest on Piekenierskloof pass.

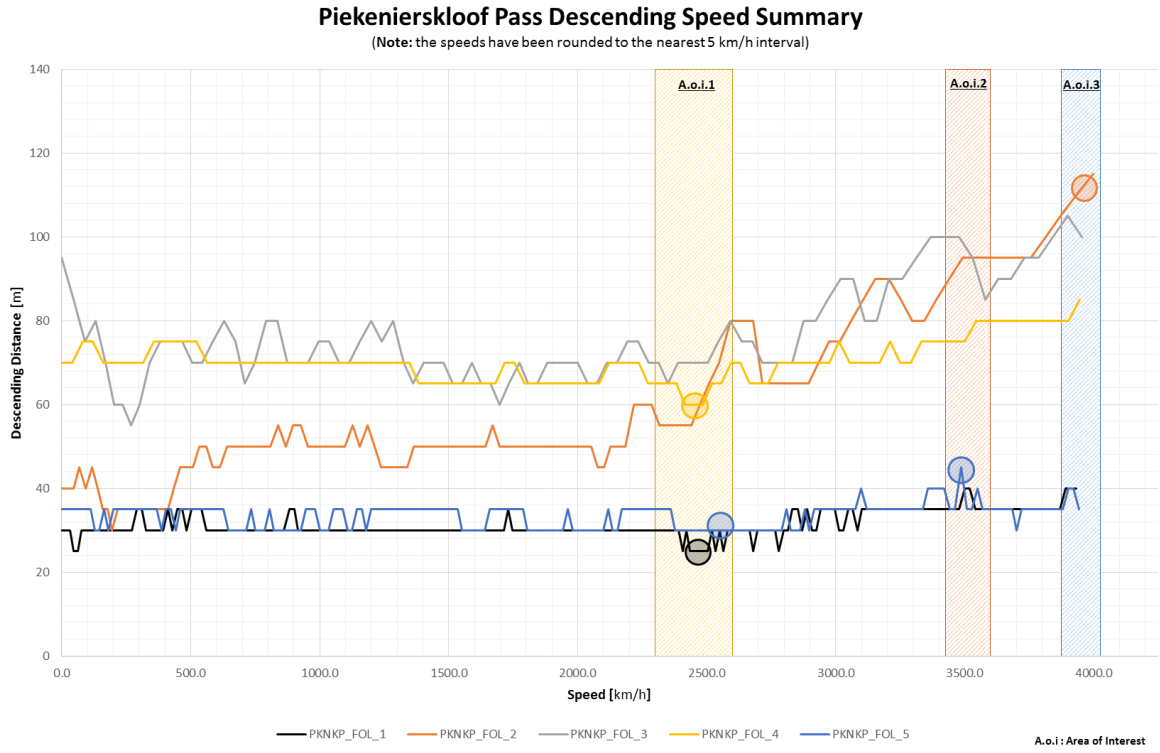

FIGURE 50: INITIAL SPEED PROFILE SUMMARY - PIEKENIERSKLOOF PASS
(**Yellow Band:** Area of interest 1; **Orange Band:** Area of interest 2; **Blue Band:** Area of interest 3)

FIGURE 51: AREAS OF INTEREST ON PIEKENIERSKLOOF PASS
(**Yellow Markers:** Area of interest 1; **Orange Markers:** Area of interest 2; **Blue Markers:** Area of interest 3; **Black Arrows:** Downgrade and Cape Town inbound direction)

Area of Interest 1

Three of the five heavy vehicles that were followed recorded their slowest speed along the downgrade in this vicinity – refer to yellow markers in Figure 51. As seen in Figure 51, this area is ahead of or on the approach leading into a relatively sharp curve. Therefore it is argued that the heavy vehicles reduced speed on the approach to safely navigate the curve.

Area of Interest 2

Referring to the orange marker in Figure 51, one heavy vehicle recorded a spike in its speed here. There is no apparent reason for this spike in speed and it is therefore attributed to an incorrectly logged GPS data point, as discussed in Section 6.1.

Area of Interest 3

This section of downgrade is just pass the turn-off towards Eendekuil, as seen in Figure 51. From this section onwards drivers tend to increase their operating speed. This is attributed to an increased sight distance of several kilometres, no severe changes in vertical alignment and no compulsory stop at the base of the mountain pass. This is evident on Figure 50, with three of the five heavy vehicles, recording speeds in excess of the posted speed limit of 80 km/h.

Therefore, the first area of interest was found to be of the greatest significance and identified as the critical section. The reason is that heavy vehicles decrease their travelling speed ahead of the curve, as seen in Figure 51, to safely navigate it. Furthermore, after this area of interest, it was found that heavy vehicles increase their speed because of a long sight distance and small changes in horizontal alignment.

7.1.6 Sir Lowry's Pass

Figure 52 illustrates the speed profiles of the individual heavy vehicle that were followed on Sir Lowry's Pass:

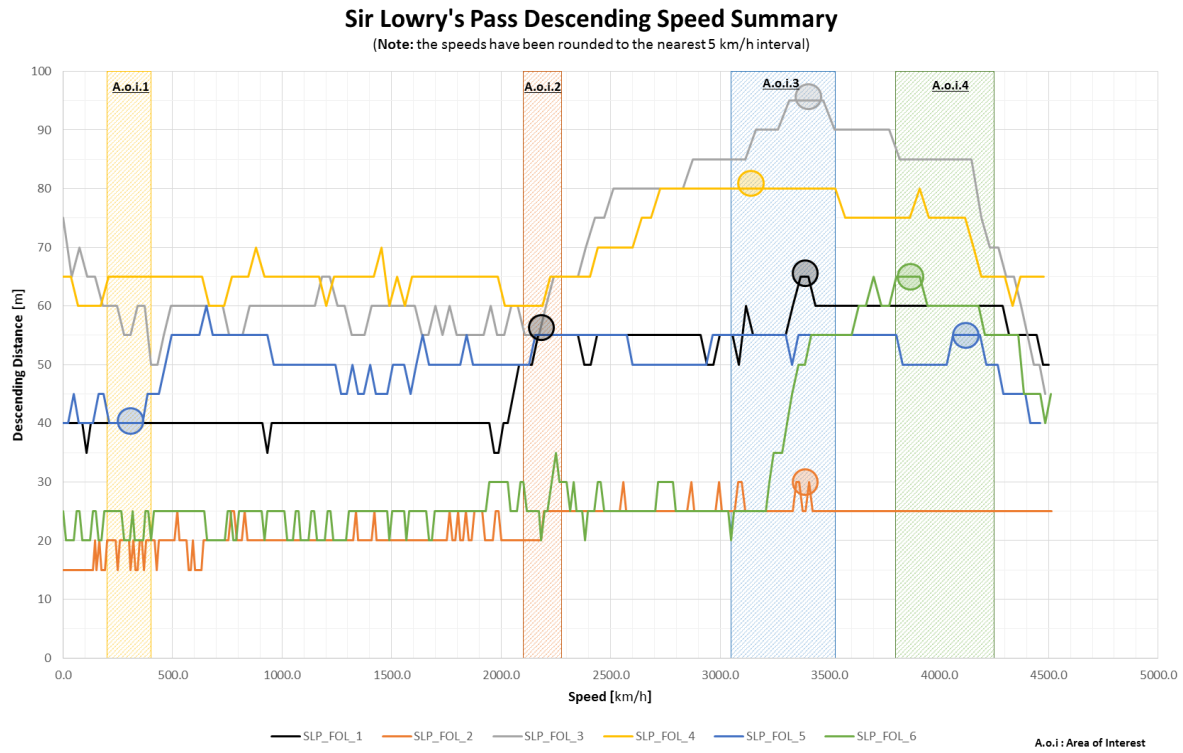

FIGURE 52: INITIAL SPEED PROFILE SUMMARY - SIR LOWRY'S PASS
(**Yellow Band:** Area of interest 1; **Orange Band:** Area of interest 2; **Blue Band:** Area of interest 3; **Green Band:** Area of interest 4)

Six heavy vehicles were followed along the Cape Town inbound downgrade of Sir Lowry's Pass. As in the case of the Huguenot Tunnel section, this pass has a compulsory stop at the foot of the pass in the form of a signalized intersection. The obtained speeds are considered very representative of the norm, since they include two slow,

two moderate and two fast heavy vehicle rates of descent. Figure 52 consist of eight points of interest and subsequently four areas of interest. As seen in Figure 52, heavy vehicle speeds tend to remain fairly constant between the first and second areas of interest. However, the general trend between the second and third areas show an increase in descending speed, followed by a decreasing trend after that. Figure 53 depicts the location of the areas of interest for the relevant mountain pass.

Area of Interest 1

This area is defined by a single point of interest, with the fifth followed heavy vehicle (i.e. blue line on Figure 52) having its slowest speed here, after which it increased speed. Thus it is argued that the driver felt he could increase his speed and still descend the pass in a safe manner, as indicated by his speed profile on Figure 52.

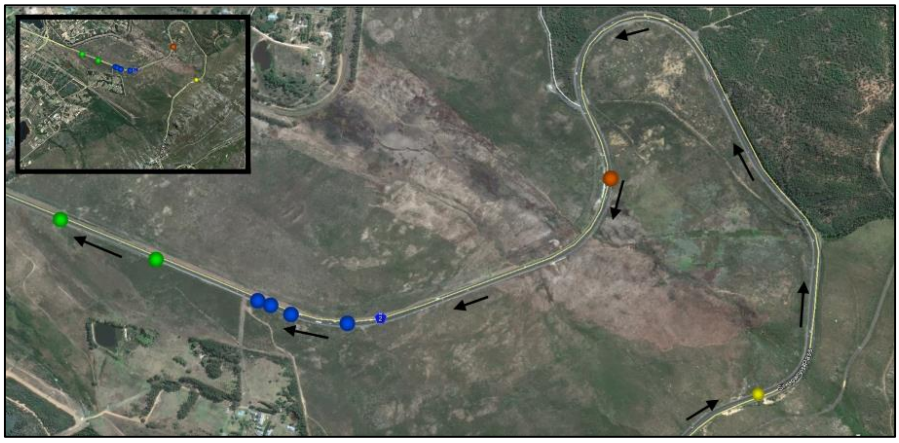

FIGURE 53: AREAS OF INTEREST ON SIR LOWRY'S PASS
(**Yellow Markers:** Area of interest 1; **Orange Markers:** Area of interest 2; **Blue Markers:** Area of interest 3; **Green Marker:** Area of interest 4; **Black Arrows:** Downgrade and Cape Town inbound direction)

Area of Interest 2

A single point of interest defines this area. The first followed heavy vehicle (i.e. black line on Figure 52) is seen as having a constant descending speed until this point and then an increase in speed. It was observed that subsequently the operating speed after this area was constant again. Therefore, it was found that the driver deemed it safe to increase speed, since this area has a long sight distance and the following curve is gradual in nature.

Area of Interest 3

Four of the followed heavy vehicles have a maximum speed within this area, of which two are in excess of the posted speed limit of 80 km/h. The reason for the increase in speed, on approach to this section, is that drivers have a long sight distance and there are no severe changes in horizontal alignment. The decrease in speed upon exiting this area is attributed to the signalised intersection at the end of the downgrade. This constitutes a compulsory stop if the traffic signal is red (i.e. red light for traffic on downgrade). Therefore, it is found that heavy vehicles start to reduce operating speed from this area to allow for a safe approach to the intersection.

Area of Interest 4

This area is defined by the two heavy vehicles not included in the third area of interest (i.e. blue and green lines on Figure 52). It was observed that in this section the relevant two heavy vehicles started reducing speed in their approach to the signalised traffic intersection.

The critical section of Sir Lowry's Pass was identified as the section between the third and fourth areas of interest. This decision was based on the observations made as to where the followed heavy vehicles start reducing speed so as to approach the intersection safely.

7.1.7 Summary of Critical Sections

The initial following data were used to plot the relevant speed versus distance for each heavy vehicle that was followed. The graphs were then smoothed by rounding off the speed values, resulting in a cleaner-looking graph. It was found that rounding to the nearest 5 km/h interval yielded a sufficiently smooth graph while maintaining a good representation of the actual data. Subsequently, the lower and upper 95 percent confidence interval values were calculated and plotted on the graph. This highlights any significant changes in operating speed, which were then marked as a points of interest for the given speed profiles. After all of the points of interest for all speed profiles were identified, the relevant profiles and points of interests were combined for each mountain pass. This led to areas of interests (i.e. convergence of multiple points of interests) being identified. These areas were then inspected to ascertain why the heavy vehicles reduced or increased operating speed. Based on the inspection, a critical section was identified that was to be used in this research project of the heavy vehicle observations. Table 18 summarizes the critical sections identified.

TABLE 18: SUMMARY OF IDENTIFIED CRITICAL SECTIONS

Mountain Pass	Area of Interest	Speed Influence	Reference Figure
Dutoitskloof Pass	3	Decrease, due to curve	Figure 43
Hex River Pass	2	Decrease, due to curve	Figure 45
Houwhoek Pass	3	Decrease, due to curve	Figure 47
Huguenot Tunnel	2 and 3	Increase, due to straight	Figure 49
Piekenierskloof Pass	1	Decrease, due to curve	Figure 51
Sir Lowry's Pass	3 and 4	Increase, due to straight	Figure 53

7.2 Observed Heavy Vehicle Speeds

This section focuses on the analyses of the observed heavy vehicle operating speeds which were recorded with the GoPro cameras, as discussed in Section 4.2.2. The analysis in Section 4.4.2 describes the method used to analyse the speed and obtain descriptive results. Therefore this section is structured as follows: calculation of the speed ranges, 50^{th} percentile speed, and comparison of the 85^{th} percentile speed with the posted speed limit.

7.2.1 Speed Ranges, Mid-values and Frequencies

The first step in a frequency distribution is to select the number of bins (i.e. number of speed ranges) into which the data are fitted. The most common method, as given in Section 2.7.5, is to determine the speed ranges for several bin sizes. This is done by taking the difference between the maximum and minimum speeds of the data and dividing them by bin sizes ranging from 8 to 20, and choosing a convenient bin size.

For this project four bin sizes were used as to determine the appropriate speed ranges for the observation data. The bin sizes used were 8, 12, 16 and 20. This was done for all three observation points on the six mountain passes, resulting in 18 speed ranges to be determined, each observation point with its own speed range. Using Equation (12), the speed ranges were calculated for the four chosen bin sizes. Note Equation (12) has been adjusted for simpler implementation into the database by making use of the Excel functions MAX (number1; number2;…)

and MIN (number1; number2; …) allowing the maximum and minimum speeds to be determined by Excel and automatically substituted and used in the equation. The calculated speed ranges are contained in Table 19.

TABLE 19: SPEED RANGES FOR OBSERVATION POINTS

Mountain Pass	Obs. Point	Min. Speed [km/h]	Max. Speed [km/h]	Total Range [km/h]	Speed Range per Number of Bins [km/h]			
					8	12	16	20
Dutoitskloof Pass	Entry	31.9	102.7	70.8	9	6	5	4
	Apex	40.7	70.5	29.8	4	3	2	2
	Exit	36.4	117.2	80.8	11	7	6	5
Hex River Pass	Entry	20.3	88.1	67.8	9	6	5	4
	Apex	17.5	82.7	65.2	9	6	5	4
	Exit	16.9	73.7	56.8	8	5	7	3
Houwhoek Pass	Entry	5.6	109.8	104.2	14	9	7	6
	Apex	8.2	111.6	103.5	13	9	7	6
	Exit	18.4	101.8	83.4	11	7	6	5
Huguenot Tunnel	Entry	24.8	76.2	51.4	7	5	4	3
	Apex	26.1	86.3	60.2	8	6	4	4
	Exit	19.6	63	43.4	9	4	3	3
Piekenierskloof Pass	Entry	14.2	113.8	99.6	13	9	7	5
	Apex	22.5	102.9	80.4	11	7	6	5
	Exit	21.4	126.8	105.4	14	9	7	6
Sir Lowry's Pass	Entry	17.1	99.2	82.1	11	7	6	5
	Apex	10	114	104	11	7	6	5
	Exit	15.4	116.4	101	9	6	5	4

The convenient bin size for each of the 18 observation points was chosen as 20, since this yields the smallest speed ranges, which allows for more distinct (i.e. finer) sorting of the data. With the bin sizes known and the subsequent speed ranges determined, the observation point data were sorted into the correct speed ranges through rounding them to the corresponding mid-value of a given speed range (e.g. for the speed range 30 to 34 km/h data entries are rounded to the mid-value of 32 km/h). The rounding is done through using the following equation:

$$v_{mid} = ROUND(v/R_s\,;0) \times R_s \qquad (13)$$

where:

v_{mid} = mid-value speed

v = speed of data entry

R_s = speed range

Note that ROUND (number; num_digits) is an Excel function that rounds off the given value (i.e. number) to the specified decimal (i.e. num_digits). The mid-values are the representative value for the corresponding speed range, which is used when plotting the frequency graphs. Furthermore, the frequency of the speed range is the number of data entries per given speed range (e.g. for the speed range 30 to 34 km/h, if there are six values within this

range, the frequency of this range is six). Refer to Appendix H for the Excel spreadsheets containing the calculations for the speed ranges, mid-values and frequencies.

7.2.2 Central Tendency (50th Percentile)

Central tendency is the statistical measure or single value that attempts to describe a given set of data. For the purpose of this project, the central tendency is representative of the 50th percentile. The central tendency is derived through comparing statistical measures that describe this value, but it is ultimately described by a single measure. The most commonly used measures are the mean, median and mode. Multiple measures may be used to describe the central tendency, if the data allows for it. The mean, median and mode are calculated for both the observed speeds and mid-value speeds (i.e. adjusted speed) of each observation point. Table 20 contains the mean, median and mode for the mid-value speeds obtained in the Section 7.2.1.

TABLE 20: MEAN, MEDIAN AND MODES OF EACH OBSERVATION POINT

Mountain Pass	Entry			Apex			Exit		
	Mean	Median	Mode	Mean	Median	Mode	Mean	Median	Mode
Dutoitskloof	59.3	56	56	55.9	58	68	64.9	65	65
Hex River	52.4	52	52	47.3	48	48	47.4	45	36
Houwhoek	63.4	66	78	61.2	60	54	64.4	65	65
Huguenot Tunnel	53.0	54	60	55.3	56	60	41.6	42	45
Piekenierskloof	56.3	55	55	61.2	65	70	57.1	57	54
Sir Lowry's	57.6	60	45	67.8	72	48	73.9	78	78

Determining the central tendency from the above values is done through comparison. The primary comparison is made between the mean and median, with the mode being used if there is insufficient comparison between the mean and median. In comparing the mean and median, the skewness of the data sets was calculated. This was done using the SKEW (*number1*; *number2* ;…) function in Excel on the mid-values calculated in the previous section. The mid-values were used instead of the observed values, since they were the representative values to be used in the frequency plots in the following section. Table 21 shows the skewness factors of all the observation point data.

TABLE 21: CENTRAL TENDENCY VALUES FOR EACH OBSERVATION POINT

Mountain Pass	Entry		Apex		Exit	
	Skewness	C. Tendency	Skewness	C. Tendency	Skewness	C. Tendency
Du Toitskloof	0.887	56	-0.101	58	0.986	65
Hex River	0.000	52.4	0.198	48	0.148	36
Houwhoek	-0.255	66	-0.277	60	-0.153	65
Huguenot Tunnel	-0.199	54	0.082	55.3	0.244	45
Piekenierskloof	0.178	56.3	-0.234	65	0.496	54
Sir Lowry's	0.059	60	0.111	70	0.237	76

From the above table it can be seen that most of the factors represent either significantly positively or negatively skewed data sets. Therefore, in keeping with general practice, the median was used as the descriptive value for the central tendency. There are three exceptions, namely Hex River Entry, Huguenot Tunnel Apex and Sir Lowry's Entry. These three data sets, for all practical purposes, have the data symmetrically distributed around the mean. Therefore, these central tendency values were represented by the respective means. The central tendencies described were confirmed using visual inspection, through plotting the relevant histogram (representing numerical spread of data) and the normalised distribution graph. Figure 54 illustrates one such graph. Note the data had been normalised to create the normal distribution plot, since without doing so the graph would have been a non-descriptive jagged line, as can be seen in Figure 54.

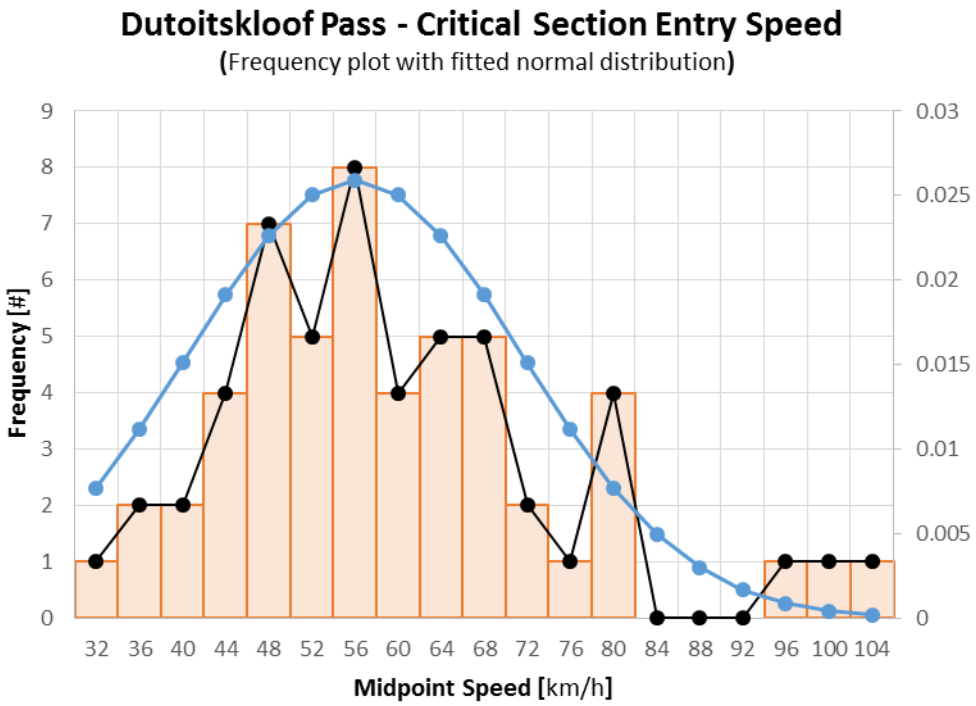

FIGURE 54: VISUAL INSPECTION OF THE CENTRAL TENDENCY
(Orange Bars: Histogram based on the mid-value speeds; **Black Line:** Non-descriptive jagged line; **Blue Line:** Normal distribution plot**)**

7.2.3 85th Percentile

The 85th percentile speed is a good indicator of what the posted speed limit for a given section of road should be. The reason is that this speed represents the speed at or below which 85 percent of drivers travel. The 85th percentile speed is determined by means of a cumulative frequency distribution, as stated in Section 4.4.2. This entails summating frequency percentages up to and including a given speed range (column Cumul% in **Figure 56**). **Figure 56** illustrates the cumulative frequency table, with the calculated mid-value speed, frequency and relevant percentages. The cumulative frequency distribution has been done for each of the observation points and can be found in Appendix H.

The cumulative frequency data illustrated in **Figure 56** were then used to plot a cumulative frequency graph, with the cumulative percentage against the upper limit of the relative speed range. Afterwards, an s-curve was drawn that best fits the resultant cumulative frequency graph. To do this, the data were normalised using the NORM.DIST(*x*; *mean*; *standard_dev*; 1) function in Excel, with *x* the mid-value speed, *mean* as the central tendency value and *standard_dev* as the relevant deviation. Figure 55 illustrates the resultant cumulative frequency graph and the line of best fit.

Du Toitskloof Pass - Critical Section Entry Speed						
Ranges	Midpoint	Frequncy	Oserv. %	Cumul.%	Norm O%	Norm C%
30 to 34	32	1	0.0188679	0.0188679	0.0076904	0.0595501
34 to 38	36	2	0.0377358	0.0566038	0.011146	0.0970061
38 to 42	40	2	0.0377358	0.0943396	0.0151004	0.1493929
42 to 46	44	4	0.0754717	0.1698113	0.0191229	0.2179072
46 to 50	48	7	0.1320755	0.3018868	0.0226368	0.3016989
50 to 54	52	5	0.0943396	0.3962264	0.0250479	0.3975244
54 to 58	56	8	0.1509434	0.5471698	0.0259073	0.5
58 to 62	60	4	0.0754717	0.6226415	0.0250479	0.6024756
⋮	⋮	⋮	⋮	⋮	⋮	⋮
90 to 94	92	0	0	0.9433962	0.001685	0.9903023
94 to 98	96	1	0.0188679	0.9622642	0.0008876	0.9953061
98 to 102	100	1	0.0188679	0.9811321	0.000437	0.9978641
102 to 106	104	1	0.0188679	1	0.0002012	0.9990869

FIGURE 56: ILLUSTRATION OF THE CUMULATIVE FREQUENCY TABLE
(Note that ranges have been condensed to save space)

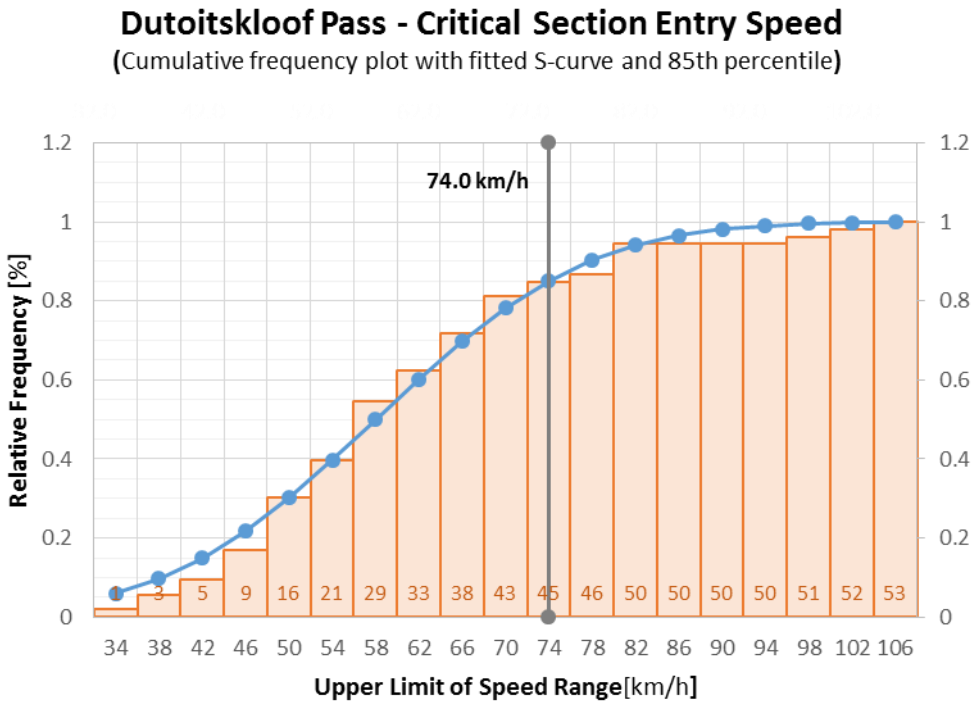

FIGURE 55: ILLUSTRATION OF CUMULATIVE FREQUENCY GRAPH AND LINE OF BEST FIT

After drawing all the relevant s-curves, the 85th percentile speeds for the three observation points per mountain pass were determined. This was done through interpolation, using the follow equation:

$$S_{85} = \frac{S_{max} - S_{min}}{P_{max} - P_{min}} \times (0.85 - P_{min}) + S_{min} \quad (14)$$

where:

S_{85} = 85th percentile speed [km/h]

S_{max} = corresponding mid-value speed for P_{max} [km/h]

S_{min} = corresponding mid-value speed for P_{min} [km/h]

P_{max} = cumulative percentage immediately greater than 85% [%]

P_{min} = cumulative percentage immediately lesser than 85% [%]

Table 22 shows the calculated 85th percentile speeds for the observation points using equation (14), as given above. For the complete calculations refer to Appendix H.

TABLE 22: 85TH PERCENTILE SPEEDS

Mountain Pass	**Entry** [km/h]	**Apex** [km/h]	**Exit** [km/h]
	Interpolation	Interpolation	Interpolation
Dutoitskloof	72.0	64.8	81.5
Hex River	67.3	61.6	58.1
Houwhoek	88.6	79.0	84.3
Huguenot Tunnel	65.5	67.2	50.6
Piekenierskloof	73.9	83.5	74.7
Sir Lowry's	79.9	90.8	94.8

7.2.4 Discussion

The two most commonly used statistics to described vehicular speeds are the 50th and 85th percentiles. The 50th percentile represents the mean traveling speed, or that speed at or below which 50 percent of the observed vehicles travel, and the 85th percentile is commonly used as a guideline for setting the posted speed limit, since this speed represents the speed at or below which 85 percent of the vehicles travel.

For the purpose of this project the 50th percentile was calculated using the central tendency approach, instead of calculating the arithmetic mean, since the arithmetic mean is only representative of the 50th percentile for a true (i.e. symmetrical) normal distribution of the data, which is seldom the case for observational data. Therefore, the skewness of each data set was calculated and used to determine which of the mean, median or mode values best represent the 50th percentile.

TABLE 23: COMPARISON OF 50TH AND 85TH PERCENTILE SPEEDS WITH THE POSTED SPEED LIMIT

Mountain Pass	**Speed Limit** [km/h]	**50th** [km/h]			**85th** [km/h]		
		Entry	Apex	Exit	Entry	Apex	Exit
Dutoitskloof	100	56	58	65	73.9	65.8	84.0
Hex River	60 (50)	52.4	48	36	69.3	63.6	59.6
Houwhoek	80	66	60	65	91.6	82.0	86.8

Huguenot Tunnel	80 (40)	54	55.3	45	67.0	69.2	52.4
Piekenierskloof	80	56.3	65	54	76.4	86.0	77.7
Sir Lowry's	80	60	70	76	82.4	93.3	96.8

Dutoitskloof Pass

The 50th percentile speeds for the Dutoitskloof Pass critical section were slower than the posted speed limit, which was expected. However, this difference is significant, with the 50th percentile being nearly half of the posted speed limit. This difference is attributed to the abnormally high posted speed limit for the pass. The 85th percentile is higher, but still a lot slower than the posted speed limit. This indicates that the posted speed limit is too high for the critical section. Furthermore, if the guidelines in the TRH17 are applied to the calculated curve radius of 200 metres, it is found that the recommended design speed for such a curve radius is 80 km/h. Thus the posted speed limit on Dutoitskloof Pass is too high. One possible reason for this high limit is to accommodate passenger vehicles that are capable of travelling at 100 km/h over the pass. Therefore, it is recommended that either a distinction is made between the operating speeds of passenger vehicles and heavy vehicles, or the speed limit for the pass should be lowered to 80 km/h for all drivers.

Hex River Pass

Based on the 50th percentile speeds, half of the heavy vehicles adhered to the recommended speed of 50 km/h to safely traverse the last reverse curve on the Hex River Pass. This speed recommendation was made due to the fatal accident history of the pass. As for the 85th percentile speed, it corresponds closely with the posted speed limit of 60 km/h, indicating that the speed limit is appropriate for the mountain pass. It was also found that for both the 50th and 85th percentile speeds, the drivers decelerate from the entry point to the exit. This can serve as an indication that the drivers still find the critical section more severe than indicated by the relevant signage on the pass and feel the need to reduce speed more than expected.

Houwhoek Pass

The 50th percentile indicates that half the drivers traverse the critical section at approximately 60 km/h, whereas the 85th percentile slightly exceeds the 80 km/h posted speed limit, but is still sufficiently close to the limit. It is evident that drivers reduce speed slightly from the entry to apex and accelerate again towards the exit, as is generally expected, for both the 50th and 85th percentile speeds.

Piekenierskloof Pass

For both speeds it was found that the apex speed is the fastest observed speed through the critical section, which is unexpected since the apex speed is generally the slowest in a curve. This can be attributed to the geometry present at the entry and exit points, which might cause drivers to reduce operating speed since the road alignment preceding the entry point and beyond the exit point are such that the drivers' sight distance is obstructed by the mountain, because of a counter-clockwise curve. This, in comparison with a critical section that has a clear sight distance of the whole section, might explain why drivers tend to increase speed in this section.

Sir Lowry's Pass

It is seen that for Sir Lowry's pass the 50th percentile speeds increase from the entry to the exit observation points. This can be attributed to the geometry of the pass. The section from the summit to the entry observation point has

many changes in horizontal alignment, which necessitates more driver control and slower descending speeds to safely navigate it, resulting in the slow entry speed. However, the foot of the pass is a straight section that leads up to a signalised intersection. Here drivers might feel that it is safe to increase their operating speed by letting the heavy vehicle increase speed under its own weight. This trend is also found in the 85th percentile speeds, which exceed the posted speed limit significantly – by as much as 18.5 percent. This necessitates more stringent speed enforcement, since it is unsafe and not plausible to propose a speed limit increase here, because of the signalised intersection at the base of the pass were vehicles may be required to stop.

Huguenot Tunnel

For both percentiles the maximum observed speed was at the apex of the critical section. This was expected, since the heavy vehicles start reducing speed here for the compulsory stop at the toll plaza. Furthermore, there is approximately only a ten kilometre per hour difference between the 50th and 85th percentile speeds. A possible reason for this is that the pass applies stringent speed enforcement and also has a dedicated descending lane. This means that the downgrade has two speed limits, an 80 km/h speed limit for the normal section and a 40 km/h speed limit for the dedicated descending lane. With both percentiles being approximately halfway between the two different speed limits, this can be evidence of the benefit of having a descending lane for heavy vehicles, since the empty heavy vehicles can travel unhindered at speeds near the speed limit, and the laden heavy vehicles can travel at a safe and slower descending rate while not affecting traffic flow that much.

7.3 Multivariable Regression Model

The multivariable regression that was done here was the same method used for the subsequent sections. The main difference between the sections was the types of variables used. Therefore the procedure will be discussed here and only the variable changes of the subsections will be given, before the results are shown.

Regression is defined as the process of estimating the relationship among variables. Therefore a multivariable regression only determines how a combination of independent variables affects the outcome of the dependent variable. For this project the dependent variable is the operating speed, with the other variables (i.e. gradient, mass, curve radius etc.) being independent. Excel has built-in data analysis functionality that allows for quick and easy analysis of data by simply selecting the relevant analysis and indicating the data to be used. Using the regression analysis function, the dependent variable (Y in Excel) is requested, with the subsequent independent variables (X in Excel). Refer to Figure 57 for an illustration of Excel's built-in regression functionality.

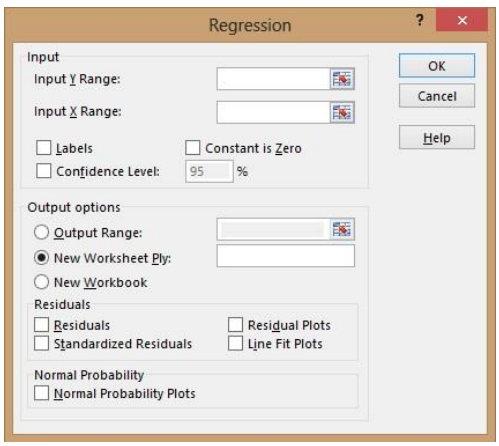

FIGURE 57: EXCEL REGRESSION FUNCTION INTERFACE

Key values that were obtained and discussed when the regression analysis was executed are outlined below.

- R^2 coefficient is a statistical indicator of how well the regression line fits and approximates the actual data points. An R^2 of 1 represents a perfect fit to the actual data points.

- The significance of the independent variables. The t-stat value is used to indicate the significance of the given independent variable. If the absolute t-stat value is approximately two or greater than two, the variable is considered as significant. The reason is that for an unscaled data set with a confidence interval of 95 percent the corresponding z-score is 1.96. Any independent variable with t-stat less than two (i.e. 1.96) was removed from the regression and the regression executed again.

- Coefficients of the significant variables. With these coefficients a mathematical model can be constructed that will estimate the operating speed with regard to the significant independent variables.

The fit (i.e. estimation accuracy) of the regression model will be better with more data used in the regression. As stated in Section 6.10, 420 heavy vehicles have been observed with only 238 have a corresponding data entry for the mass. Therefore, it is thought that a correlation should be done for the mass and number of axles, since the number of axles directly influences the GVM of the heavy vehicle as stated in Section 7.3.1. Thus, if a strong correlation is found, the whole population of observed heavy vehicles can be used in the regression.

7.3.1 Correlation: Number of Axles and GVM

The definition of correlation is finding the representability of one variable by another. Therefore, it is logical to think that the number of axles strongly relates to the mass of a heavy vehicle, since the more axles there are, the greater the mass of the potential load. The correlation was done on the whole six-month weighbridge data set, since the data include both the GVM and number of axles. However, the number of axles was not numerically expressed (e.g. 6 axles or 7 axles), but instead was indicative of the configuration of the heavy vehicle (e.g. 122 – meaning 1 steering axle, 2 tractor driving axles and a tandem axle on the trailer). Therefore, a macro was programmed to scan and convert the configuration into a numerical value that can be plotted. Refer to Appendix B for the code of the macro. The resultant plot of the GVM against the number of axles yielded the following graph (Figure 58).

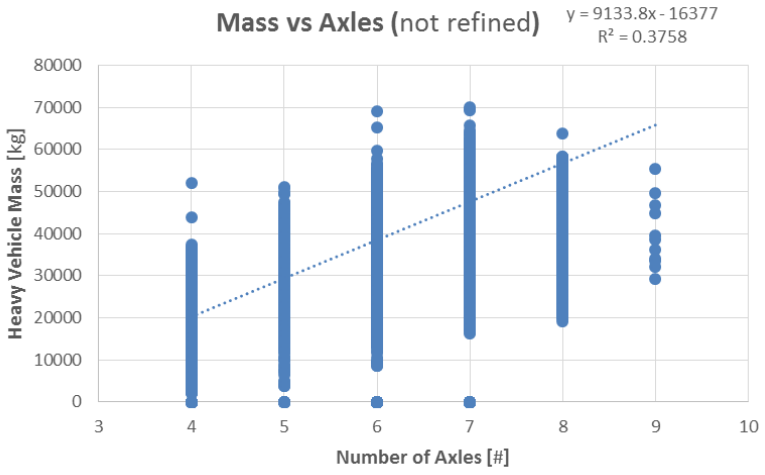

FIGURE 58: CORRELATION OF MASS AND NUMBER OF AXLES - NOT FILTERED

Figure 58 indicates the spread of the non-filtered mass data with regard to the number of axles. The trend line fitted to the data has a R^2 value of 0.3758, which indicates that the variables have a moderate correlation with a factor of 0.613.

This moderate correlation could be attributed to two reasons. Firstly, there are incorrect mass values within the database. This is evident by the points Figure 58 that have a mass of zero kilograms (i.e. 0 kg), which is not possible. Removing these data entries from the database resulted in a slight increase in the correlation factor from 0.613 to 0.616. The second reason for the moderate correlation factor is the representative or recorded mass of a given heavy vehicle relative to its axle class. For example, an empty seven-axle (i.e. 7-axle) heavy vehicle can have a recorded mass that is less than that of a loaded four-axle (i.e. 4-axle) heavy vehicle. Therefore, the mass that is used in the correlation should at least, to some degree, represent the normal or average mass transported per axle class. Thus, two means have been used to this end, namely the 10-85 method and averaging the mass. Refer to the Figure 59 for an illustration of the 10-85 method of filtering:

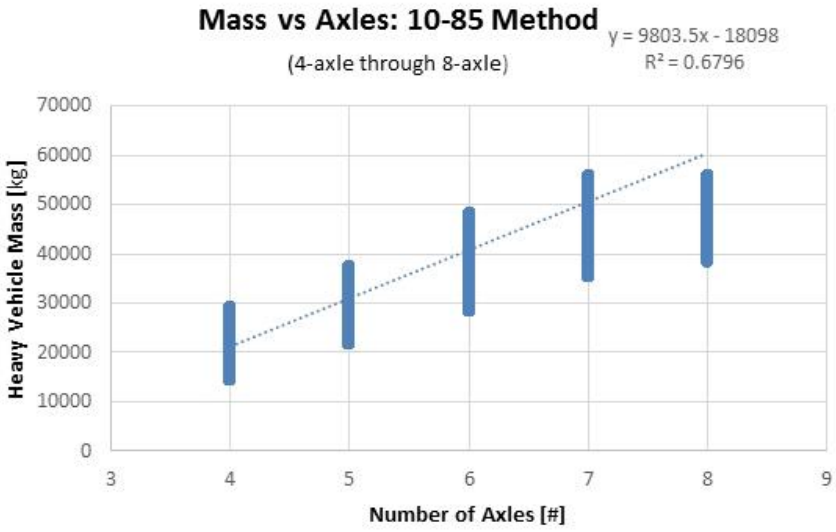

FIGURE 59: CORRELATION OF MASS AND NUMBER OF AXLES - 10-85 METHOD

Note that the nine-axle (i.e. 9-axle) heavy vehicles have been removed from the correlation, since these heavy vehicles are seldom encountered on the road, with none being observed during this research project. The 10-85 method is assumed to sufficiently remove any outlier values, which are often situated within the lower 10 percent and upper 15 percent of a data set. The trend line fitted in Figure 59 has a R^2 value of 0.680, which translates into a correlation factor of 0.824. Therefore, a good correlation was found between the mass and the number of axles after removing any outliers. This correlation was taken one step further, though. The average mass for each axle class was calculated and these were then plotted. This resulted in a strong correlation with a correlation factor of 0.975. Refer to Figure 60 for an illustration:

This correlation procedure was done for the heavy vehicles that were observed in the mountain passes as well. Using the weighbridge data and the observed number of axles, for the 420 heavy vehicles that were observed, a moderate correlation factor of 0.638 was found. It was noted that there were some instances where the axle count was different for the weighbridge and observed data. This was corrected by assigning the weighbridge axle counts

to the observed heavy vehicles, since the GVM data were obtained from the weighbridge data set itself. The correlation was done again, resulting in a small increase in the correlation factor to 0.71. Lastly, the average mass for the observed heavy vehicles was plotted against the number of axles, and a strong correlation of 0.987 was found. Table 24 provides the summary of the correlation factors for both the six-month weighbridge data set and the observed heavy vehicles.

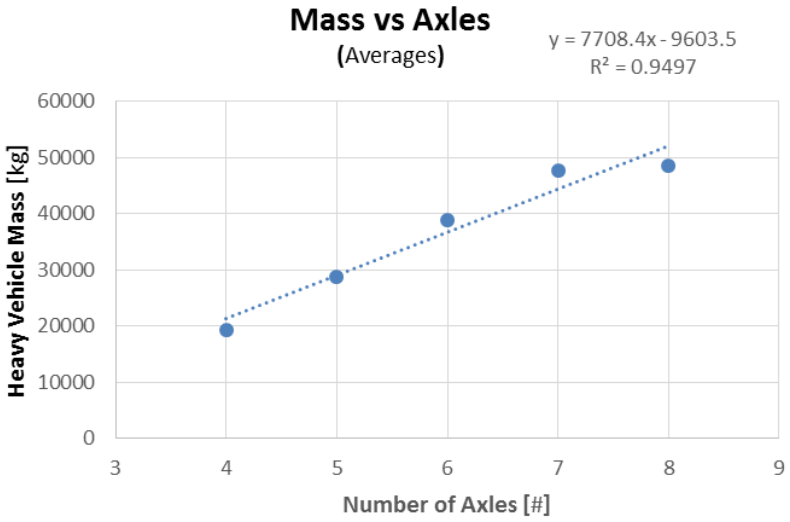

FIGURE 60: CORRELATION OF MASS AND NUMBER OF AXLES - AVERAGE MASS

TABLE 24: SUMMARY OF MASS VERSUS NUMBER OF AXLES CORRELATION

Data Set	Mass vs Axles Graph	Corr. Factor	Correlation	Trend line equation
Weighbridge	Unfiltered	0.613	Moderate	$y = 9133.8x - 16377$
	Filtered: 10-85 Method	0.824	Good	$y = 9803.5x - 18098$
	Filtered: Averaged mass	0.975	Strong	$y = 7708.4x - 9603.5$
Observed	Observed Axle Count	0.638	Moderate	$y = 6919.6x - 2292.5$
	Corrected Axle Count	0.710	Moderate	$y = 8365.8x - 11492$
	Averaged Mass	0.987	Strong	$y = 7281.9x - 5967.9$

Therefore there is a very strong correlation between the number of axles and average mass. It should be noted that because of this correlation, including both these variables as independent variables during the multivariable regression will result in an error. The reason is that the number of axles is representative of the GVM and vice versa.

7.3.2 Operating Speed vs Gradient

The section focus on downgrades in general, regardless of the primary influencing factors such as curve radius and stopping distance. Therefore, the focus of the section is to determine what effect the gradient has on the operating speed of a heavy vehicle. The gradient values that were used are as stated in Section 6.1, with the operating speed taken as the apex speed of the relevant critical sections. It is also important note, that if the data of all six mountain passes were to be used, the results would be inconclusive and counter-intuitive. The reason for this is that four of the mountain passes have critical sections with a minimum observed operating speed (speed subject to curve radius) and the remaining two mountain passes have critical sections with a maximum observed

operating speed (speed subject to stopping distance). Therefore, it was decided that the data for the four mountain passes with the minimum observed operating speed would be used. Thus plotting the relevant operating speeds against the radius resulted in the following graph to be obtained:

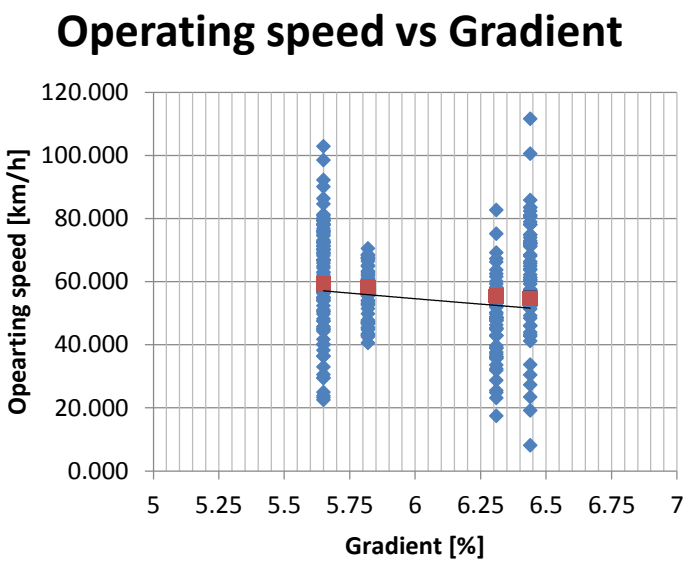

FIGURE 61: OPERATING SPEED VS GRADIENT

With the graph plotted two trend lines have been fitted, namely linear and exponential. The linear trend line had a R^2 value of 0.0144, whereas the exponential trend line have a R^2 value of 0.0173. Note, that the low R^2 values are as a result of the wide spread operating speeds.

Thus the exponential trend line had a better fit and the following exponential equation had been derived:

$$v_{est} = 117.56 \times e^{-0.128G} \tag{15}$$

where:

v_{est}	=	estimated operating speed	[km/h]
G	=	gradient of the downgrade	[%]

Note that the notation of the gradient is taken as positive in the downgrade direction. Equation (15) was then compared results obtained from St John's (1978) equation, which is as follows:

$$v_{est} = \frac{0.9}{G} \quad for\ G > 0.04 \tag{16}$$

where:

v_{est}	=	estimated operating speed	[m/s]
G	=	gradient of the downgrade	[%]

Note that Equation (16) yields and estimated operating speed in meters per second. Therefore, when comparing the two equations results, it is important to convert both estimated operating speeds to the same unit of speed.

The results for the comparison are as follows:

TABLE 25: COMPARISON RESULTS FOR OPERATING SPEED VS GRADIENT

Gradient [%]	V_est [km/h]	V_StJohn [km/h]	Diff.
4	70.45	81	-10.54
5	61.98	64.8	-2.81
6	54.54	54	0.540
7	47.98	46.28	1.70
8	42.22	40.5	1.72
9	37.14	36	1.14
10	32.68	32.4	0.28

From Table 25 it can be seen that the difference in estimated operating speed is very small for downgrade gradients greater than five percent. However, for gradients ranging from four to five percent the difference between the equations is significant, and this result can be attributed to the lack of data obtained in this research project for mountain passes with gradients ranging from four to five percent.

7.3.3 Speed Subject to curve Radius

This section focus on the decrease in heavy vehicle speeds as a result of a severe curve (i.e. small curve radius). Therefore, more specific variables were included in the regression analysis, namely the curve radius and the relevant superelevation. The first regression was done the same as for the general regression, using the average speed through the critical section and the mass of the heavy vehicle. This yielded only one statistically significant variable, namely the curve radius with a t-stat value of 3.60. As for all of the other variables, they had no significance, and therefore have been removed for the second iteration. However, in removing the other variables, the objective of the project would have been defeated. Therefore, the dependent speed should rather be represented by a single observation point (i.e. entry, apex or exit) and not the average of all the observation point speeds. Thus, the observation point speed that was used is the observation point average that is the lowest. This can be done, since the observation points were situated in the same place, relatively speaking, along each critical section, namely the entry, apex and exit. The slowest observation point average indicated the observation point speeds that were used in the regression. The reason is that this indicated the point along the curve where the influence on the operating speed was generally the greatest. The averages of the entry, apex and exit points were respectively 57.5km/h, 57.1 km/h and 58.2km/h. The speed at the apex found to be the slowest, therefore the dependent variable was taken as the observed apex speeds and the independent variables included the gradient, length of gradient, mass, curve radius and superelevation.

The second regression outcome, as shown above, found that all of the variables were statistically significant, except for the mass of the heavy vehicle and the superelevation. Even though the results were better, the objective of the project was still defeated, since the mass of the heavy vehicle does influence the operating speed of the heavy vehicle on downgrades. Note that the superelevation resulted in an abnormally high t-stat, which is an

indication that the data were in conflict with another data set. Furthermore, there was also not enough variation in the superelevation data to show any significance in the regression, since they were all approximately ten percent. Therefore, the superelevation was removed from any further regressions.

The third regression was done using the apex speed as the dependent variable, and instead of the mass the number of axles was used in the regression. **Table 26** shows the results.

TABLE 26: CURVE RADIUS REGRESSION FINAL RESULTS

Regression Statistics		**Independent Variable**	**Coefficients**	**Standard Error**	**t-Stat**
Multiple R	0.380359748	Intercept	122.6103462	20.33373504	6.029897898
R Square	0.144673538	Axles	-2.632063696	0.973199846	-2.704545944
Adjusted R Square	0.13166477	Curve Radius	0.172969891	0.033390354	5.180235271
Standard Error	15.21521947	Downgrade Length	-1.275591864	0.311688495	-4.092521486
		Gradient	-11.86922205	3.144215681	-3.764443427

As can be seen from the above table, all of the variables were statistically significant at that point, and therefore there was no need to further refine the data. From the t-stat values it is seen that the curve radius is the most significant variable, which is to be expected, since the smaller the radius the greater the effect on the operating speed. The coefficients of the variables were used to construct a mathematical model that can be used to calculate the estimated operating speed for heavy vehicles on a curve, descending a steep downgrade. The resultant equation is as follows:

$$v_{est} = 122.61 - 2.63N + 0.173R - 1.28L - 11.70G \quad (17)$$

where:

v_{est}	=	estimated operating speed	[km/h]
N	=	number of axles, including steering axles	[#]
R	=	the curve radius of the critical section	[m]
L	=	length of the downgrade, from summit to base	[km]
G	=	gradient of the downgrade	[%]

Note that the notation of the gradient is taken as positive in the downgrade direction.

7.3.4 Speed Subject to Stopping Distance

This section focuses on the drivers' perceived maximum speed on the downgrade leading to a compulsory stop or signalised intersection (i.e. chance of stopping on the red phase). Therefore, more specific variables will be used in the subsequent regression, including the stopping distance and gradient. The first regression for this section was done in the same way as the general regression in Section 7.3.2, starting with the mass of the observed heavy vehicles and refining the data input as needed. The dependent variable was taken as the average of the speeds throughout the critical section for each heavy vehicle, with the stopping distance as the average distance from the relevant observation points to the compulsory stop or intersection.

The first iteration of this regression yielded only one statistically significant variable, namely the stopping distance with a t-Stat value of 4.25. As for the gradient and the length of downgrade, these variables failed to regress. The heavy vehicle mass was replaced by the axle count of the relevant heavy vehicles, and the data size increased since the number of axles was known for all of the observed heavy vehicles. The second regression was therefore done with the average speed through the critical section as dependent variable, and the independent variables now, axle count, average stopping distance, gradient and length of downgrade.

The second iteration of regression found the axle count to have a greater significance than the mass, having a t-stat value of 1.39. However this variable was still not statistically significant. The stopping distance had a greater t-stat value than in the first iteration, with a value of 6.72. This was also greater than in the first regression, but the gradient and downgrade length variables still failed to regress. Therefore a third regression was done with further refining of the data. The dependent variable was taken as the maximum operating speed of the three observation points and the stopping distance was the actual distance from the observation point to the compulsory stop. The results for the third iteration are shown in Table 27.

TABLE 27: STOPPING DISTANCE REGRESSION FINAL RESULTS

Regression Statistics		**Independent Variable**	**Coefficients**	**Standard Error**	**t-Stat**
Multiple R	0.565090362	Intercept	-29.26741391	25.93882359	-1.128324645
R Square	0.319327117	Axles	-2.025564972	1.39222068	-1.454916596
Adjusted R Square	0.298910884	Stopping Dist.	0.017255501	0.015131163	1.14039489
Standard Error	14.01015944	Downgrade Length	17.97611564	2.909787647	6.177810141
		Gradient	0	0	65535

The results for the third regression were generally better than those in the second regression. The axle count variable had a higher t-stat value, even though it still was not statistically significant. However, the stopping distance variable lost its significance, whereas the length of downgrade variable became the most significant variable. This inconsistency and failure to have significant variables can be attributed to the lack of survey locations used in compiling the regression data set. Since only two survey locations were used, there was very little variation among some of the variables that could alter or induce statistical significance. Thus, for this section of the research project, not enough data were available to conduct a successful regression.

7.3.5 Speed Profiles

The observed operating speeds were thus sorted based on the relation of the three relevant operating speeds to each other, results can be seen in Table 28.

As can be seen from Table 28, heavy vehicles that are subjected to a stopping distance have three distinct profiles for passing through the critical section. These include skew-right down at 44 percent, decreasing at 25 percent and increasing at 14 percent. These profile show that there might be a lack in conveying information or speed enforcement, since nearly half the observations had a speed above the posted speed limit, whereas a quarter of the drivers had adhered to the speed limit and reduced speed on approach of the compulsory stop.

TABLE 28: SPEED PROFILES THROUGH CRITICAL SECTIONS

Speed Profile	Speed Subject to Curve Radius [%]	Speed Subject to Stopping Distance [%]
Linear +	18	14
Linear -	21	25
Sym. Parabola +	4	2
Sym. Parabola -	8	3
Skew left +	11	2
Skew Right +	11	4
Skew Left -	13	5
Skew Right -	14	44

As for heavy vehicles subjected to curve radius, the results are more evenly spread out as can be seen in Table 28. The three speed profiles encountered most through the critical section include decreasing, increasing and skew right down. Based on the profile definitions given in Section 6.11, the decreasing profile conforms to what is expected, that a vehicle will reduce operating speed upon approach of a curve. However, the other two profiles (increasing and skew right down) are of some concern, since it is not expected to increase operating speed through the whole curve, and to have the apex operating speed as the highest observed speed. Therefore, these findings can be indicative of a lack of information ahead of the critical section.

8 Conclusions and Recommendations

8.1 Conclusions

The focus of this section is to provide and discuss the conclusions with regard to the research questions. The conclusions are given below.

8.1.1 Critical Sections

In order to answer the research questions posed in Section 1.3, the critical sections of each downgrade had to be identified. This was done by following heavy vehicles down the whole length of the downgrade, while logging the coordinates at a fixed time interval via GPS. Subsequently, these data were used to plot the relevant speed profiles to identify the critical sections. With each individual speed profile plotted, the plots were analysed to identify any points of interest (i.e. extreme values). The relevant plots, with points of interests, were then combined to identify any areas of interest for each mountain pass. The areas of interest were then visually inspected and discussed based on the researcher's experience of the downgrade and on aerial imagery.

It was found that speed reductions on mountain passes occur near the entry or ahead of the relevant curve, with the greatest reductions in speed in the vicinity of the curve with the most severe (i.e. smallest) curve radius. This result is expected, since smaller curve radii require slower operating speeds to safely navigate the curve, so to not run off the road or roll over.

8.1.2 85^{th} Percentile Speed vs Posted Speed Limit

The typical speed limit for mountain passes or severe downgrades (in mountainous terrain) is 80 km/h. In some instances, where a descending lane is present, there may be dual speed limits (e.g. Hex River Pass and Huguenot Tunnel). However it is important to note that the speed limit for all heavy vehicles, regardless of the road class, is limited to 80 km/h.

It was found that the 85^{th} percentile speed is in general slightly higher than the posted speed limit. Two mountain passes are worth noting, namely Dutoitskloof Pass and Sir Lowry's Pass. Dutoitskloof Pass have an 85^{th} percentile speed that is significantly lower than the posted speed limit of 100km/h, however the 85^{th} percentile speed closely adheres to the general speed limit of 80km/h for mountainous rural roads and the legal limit set for South African heavy vehicles. As for Sir Lowry's Pass, the increase in the 85^{th} percentile speed through the critical section can be attributed to the intersection situated at the foot of the pass. The reason is that the heavy vehicles do not need to stop every time, since they might cross the intersection during a green phase, resulting in no need for the heavy vehicle to reduce speed.

Therefore, the general speed limit of 80 km/h is well suited for heavy vehicles, since most of the 85^{th} percentile speeds closely match the speed limit. Further motivation for the 80 km/h speed limit is derived from Dutoitskloof Pass, which has an abnormally high speed limit of 100 km/h, yet the 85^{th} percentile speeds adhere to the general speed adopted of approximately 80km/h.

8.1.3 Heavy vehicle operating speeds on downgrades

In determining what geometrical and heavy vehicle characteristics significantly influence the operating speed of heavy vehicles on mountain passes or downgrades, several variables were identified and data collected for this

purpose. The variables include the operating speed at three observations points throughout the critical section, heavy vehicle mass, number of axles, gradient of the mountain pass, downgrade length, curve radius, superelevation and stopping distance. It was also found that there was a strong correlation between the number of axles and the heavy vehicles mass, which is expected. This relationship enabled the use of the number of axles in the instances where the heavy vehicle mass data did not yield significant results. The collected data were then used to conduct multivariable regressions to find out which variables and to what extent they affect the operating speed. Therefore, three regressions were conducted in total and are outlined below.

Operating Speed vs Gradient

The correlation done between the operating speed and gradient found that the steeper the downgrade the slower the operating speed, which is expected. The following equation was derived:

$$v_{est} = 117.56 \times e^{-0.128G}$$

where:

v_{est}	=	estimated operating speed	[km/h]
G	=	gradient of the downgrade	[%]

Note that the notation of the gradient is taken as positive in the downgrade direction. This equation was compared to St John's equation, Equation (16), and it was found that the two equations yielded similar results for chosen gradients, with the result not varying more than ± 2km/h for gradient greater than 5 percent.

Operating speed subject to changes in horizontal alignment

This regression was done to determine the effect that curve radius has on downgrade operating speed. The variables that were used in the regression include the apex speed of the relevant heavy vehicles, number of axles, gradient, downgrade length, curve radius and superelevation. The number of axles was used for this regression. The following equation was found, with an R^2 of 0.145, to estimate the apex speed of heavy vehicles navigating a curve on a downgrade:

$$v_{est} = 122.61 - 2.63N + 0.173R - 1.28L - 11.70G \quad (18)$$

where:

v_{est}	=	estimated operating speed	[km/h]
N	=	number of axles, including steering axles	[#]
R	=	the curve radius of the critical section	[m]
L	=	length of the downgrade, from summit to base	[km]
G	=	gradient of the downgrade	[%]

Note that the above equation does not include the superelevation, since the mountain passes that were surveyed all had the maximum superelevation of ten percent. Therefore, this resulted in a lack of variance between the

regressed data. Furthermore, it should be noted that the above equation has poor predictive value, since the variance among the gradient data is limited, from approximately five percent to six-and-a-half percent. However the predictive value for the aforementioned gradient range is good.

Operating speed subject to stopping distance

The regression was done to determine how stopping distance in combination with downgrade length and gradient affects heavy vehicle operating speeds. The variables that were included in the regression are the average speed through critical section, the mass of heavy vehicle, the average stopping distance, and the gradient and length of the downgrade. The first iteration yielded only one statistically significant variable, namely stopping distance. The data set was refined by substituting the average speed as the maximum speed observed in the critical section, and the average stopping distance with the relevant stopping distance to where the maximum operating speed was observed. Further refinement included making use of the strong relationship between a heavy vehicles' mass and the number of axles, by replacing the mass variable with that of the number of axles.

These refinements failed to yield more than one statistically significant variable, with stopping distance losing significance and downgrade length becoming the statistically significant variable. Furthermore, the gradient failed to regress, rendering these results inconclusive. This failure to regress is attributed to the low number of survey locations (i.e. only two locations) that were used to populate the regression data set, creating a lack in variation.

8.1.4 Speed Profiles

The speed profiles for speeds subject to curve radius were fairly evenly spread across the defined speed profiles categories. However, some of the results were unexpected, such as a heavy vehicle increasing operating speed through a curve, or having its maximum observed speed at the apex of the curve.

As for heavy vehicle operating speeds subject to stopping distance, there were three distinct speed profiles obtained, namely skew right down (44%), decreasing (25%) and increasing (14%). Here to some of the results are unexpected, since it is thought that a heavy vehicle will have near constant deceleration in approach of a compulsory stop. However it is found that only a quarter of the speed profiles adhere to this expectancy.

Therefore, with these high percentages of unexpected speed profiles, it is concluded there might exist a need for improved signage ahead of critical sections on downgrades.

8.2 Recommendations

This section focusses on the recommendations, based on the experiences from this project. Therefore, recommendations will be made on the basis of the outcome of the project and for future research.

8.2.1 Based on conclusions

In addressing the research objective regarding the need for improved signage that conveys more information to heavy vehicle drivers, it was found that there is a need for better signage on downgrades. Therefore, it is recommended that signs ahead of mountain passes or steep downgrades should be updated and improved to convey better quality information to heavy vehicle drivers, such as weight-specific signs or informational signage regarding length of downgrade and gradient. The motivation for this recommendation is as follows:

- There are currently very few, if any, weight-specific signs deployed ahead of mountain passes or steep downgrades in South Africa, and the few informational signs portraying downgrade length and gradient to drivers are often observed out of context (e.g. near speed limit signs or situated on the downgrade and not ahead of the summit);

- This lack of information can have an impact on driver unfamiliarity with the given downgrade, since the driver has no guidelines on how to approach the downgrade or what to expect. This was confirmed through the logical exercise conducted on the speed profiles through the critical sections, which found that nearly half the drivers were to some extent unfamiliar with the pass for the given observation.

Therefore, based on the above stated motivations, it is argued that more information needs to be conveyed to heavy vehicle drivers who descend steep or mountainous downgrades. The equations that were derived in this project can be used for that purpose to calculate the safe descending speed regarding a given downgrade.

8.2.2 Future studies

The following set of recommendations is made to assist future research on similar issues to those addressed in this research.

Similar Studies

- Make use of datum discs, since they are easy to set up in the field and it is cheap to make.

- If laser-light boxes are used again as the chosen datum markers, it is recommended that some changes be made to the devices. The foremost is to find a means of stabilising the device, so that it is not susceptible to the wind gusts of passing vehicles or weather conditions.

- Roadworks ahead of mountainous or steep downgrades can make the collection of data more difficult, since traffic flow is interrupted and they can cause multiple heavy vehicles to queue up, as was experienced on the Hex River Pass. Therefore, it is recommended that the researcher should be informed about any active or planned road works near the selected downgrade.

- In this study it was found that the curve radius had a significant influence on the operating speed, whereas the influence from the gradient was not as significant. This can be attributed to the lack of variation in the gradient variable. Therefore it is recommended that more mountain passes with different gradients are selected.

- Two variables failed to show statistical significance, namely the superelevation and stopping distance. Therefore, more survey locations with differing values for the superelevation and stopping distance should be included, which will create greater variation amongst the data sets.

- It is recommended that freight-moving agencies are contacted and worked with to gather more information regarding the observed heavy vehicles, possibly obtaining the GPS data that can then be used to determine specific speed profiles for all observed heavy vehicles.

Other Studies

- Conducting more accurate analysis of the relationship between heavy vehicle mass and the number of axles, with a larger data set that spans several years' worth of data.
- Interview heavy-vehicle drivers who have experienced runaways or accidents, and ascertain what led to that incident to occur, since there is not a lot of readily available data on heavy vehicle accidents. To gain more insight into and information on heavy vehicle accidents, contact the relevant police or traffic departments, since all accidents are logged by them.
- Predict driver familiarity based on the speed profile of the observed vehicle. This can be augmented by interviews that can provide additional information regarding the driver and his experiences with the select downgrade, and the relevant heavy vehicle and characteristics.

9 References

Albatlan, S. 2013. Study Effect of Pads Shapes on Temperature Distribution for Disc Brake Contact Surface. International Journal of Engineering Research and Development, 8(9). :62-67.

Artus, S., Cocquempot, V., Hayat, S., Staroswiecki, M., De Larminat, P. & Covo, C. 2005. CHV's Brake Discs Temperature Estimation: Results in Open Road Tests. Paper presented at 8th International IEEE Conference on Intelligent Transportation Systems, September 13, 2005 - September 16. 2005.

Barber, S.A. & Tuten, J.M. 1986. Measurement of Interlace Temperatures during Braking. Paper presented at Truck and Bus Meeting and Exposition, November 10, 1986 - November 13. 1986.

Booi, M. 2015. Man arrested in hospital for Hex River bus crash. [Online]. Available: http://ewn.co.za/2010/05/06/Man-arrested-in-hospital-for-Hex-River-bus-crash [22 March 2015]

Bornes, V. & Vaa, T. 2011. Speed Levels of Heavy Vehicles on Norwegian Mountain Pass. Transportation Research Record, (2258). :119-130.

Bowman, B.L. & Coleman, J.A. 1990. Grade Severity Rating System. ITE Journal (Institute of Transportation Engineers), 60(7). :19-24.

Briney, A. 2007, Geography of South Africa – The World Fact book [Online]. Available: https://www.cia.gov/library/publications/the-world-factbook/geos/sf.html [21 November 2014].

Carrier, R.E. & Pachuta, J.A. 1981. Runaway Trucks in Pennsylvania. Paper presented at Truck Meeting, November 9, 1981 - November 12. 1981.

Council for Scientific and Industrial Research. 2013. 10th state of logistics survey for South Africa. Pretoria: Creative Vision.

Council for Scientific and Industrial Research. 1988. TRH17: Geometric design of rural roads. Pretoria, South Africa: Department of Transport.

Cronin, J. 2011. The Future of Rail. Johannesburg. 6 April 2011.

Eksteen, E. Operations of Huguenot tunnel, personal communication with author, Tuncor Offices, Paarl.

Emery, A.F. 2003. Measured and Predicted Temperatures of Automotive Brakes Under Heavy Or Continuous Braking. Paper presented at 2003 SAE International Truck and Bus Meeting and Exhibition, November 10, 2003 - November 12. 2003.

eNCA. 2015. Fatal accident as school bus rolls on Franschhoek pass. [Online]. Available: http://www.enca.com/south-africa/bus-goes-franschhoek [22 March 2015].

eNCA. 2015. Children dead in horror bus crash. [Online]. Available: http://www.enca.com/south-africa/children-dead-horror-bus-crash [22 March 2015].

Fancher, P.S. & Flick, M.A. 1992. Evaluation of Braking Strategies on Downgrades. Paper presented at International Truck and Bus Meeting and Exposition, November 16, 1992 - November 19. 1992.

Garber, N.J. & Hoel, L.A. 2010. Traffic and Highway Engineering. United States of America: Cengage Learning.

George, Z. & Van Zilla, L. 2015. Carnage as truck overturns on pass. [Online]. Available: http://www.iol.co.za/news/south-africa/carnage-as-truck-overturns-on-pass-1.39116#.VTjDfSGqqkp [22 March 2015].

Gordon, J. 2014. Too little, too late. District Mail, 4 December 2014.

Jacko, M.G., Spurgeon, W.M., Rusnak, R.M. & Catalano, S.B. 1968. Thermal Stability and Fade Characteristics of Friction Materials.

Kharrazi, S. & Thomson, R. 2004. Study of Heavy Truck Accidents with Focus on Manoeuvres Causing Loss of Control. International Journal of Vehicle Safety, 3(1). :32-44.

Koyana, X. & Hartley, A. 2015. Two die in mountain truck crash. [Online]. Available: http://www.iol.co.za/capetimes/two-die-in-mountain-truck-crash-1.1564940#.Vaod8fmqqkp [22 March 2015].

Li, W. 2009. Cointegration Analysis on the Relationship between China's Highway Transportation Industry and National Economic Development. Paper presented at 2009 IEEE/INFORMS International Conference on Service Operations, Logistics and Informatics, SOLI 2009, July 22, 2009 - July 24. 2009.

Mahanty, S. & Subramanian, S.C. 2009. Model Based Analysis of a Heavy Commercial Vehicle with an Electropneumatic Brake Towards Antilock Braking Systems. Paper presented at 2009 IEEE International Conference on Vehicular Electronics and Safety, ICVES 2009, November 11, 2009 - November 12. 2009.

Mat Daud, M.S., Endut, I.R. & Jaafar, H.S. 2012. Analysis of Factors Threatening the Success of Freight Movement in Malaysia. Paper presented at 2012 IEEE Business, Engineering and IndustrialApplications Colloquium, BEIAC 2012, April 7, 2012 - April 8. 2012.

Metro Count. 2011. Speed Analysis 1 – The 85th Percentile Speed. [Online]. Available: http://www.metrocount.com/downloads/flyers/Speed_analysis_1.pdf [20 March 2015].

Mohammed, N.Z., Ghazi, A. & Mustafa, H.E. 2013 Positional Accuracy Testing of Google Earth. International Journal of Multidisciplinary Sciences and Engineering, 4(6). :6-9.

Montgomery, D.C. & Runger, G.C. 2007. Applied Statistics and Probability for Engineers. United States of America: John Wiley and Sons.

National Department of Transport (DoT). 2013. Department of transport annual report 2012-2013. Pretoria: Sisters in Printing.

Papacostas, C.S. & Prevedouros, P.D. 2005. Transportation engineering and planning. Jurong, Singapore: Prentice Hall.

Reader's Digest Association of South Africa. 1984. Reader's Digest Atlas of Southern Africa. Cape Town.

Roberts, T. Mountain Passes of South Africa. [Online] Available: www.mountainpasssouthafrica.co.za [7 July 2013].

Samodien, L. 2015. Bus driver guilty of 23 deaths. [Online]. Available: http://www.iol.co.za/capetimes/bus-driver-guilty-of-23-deaths-1.1413923#.VaoeCvmqqkp [22 March 2015].

SAPA. 2015. 22 killed in De Doorns bus crash. [Online]. Available: http://mg.co.za/article/2013-03-15-22-killed-in-de-doorns-bus-crash [22 March 2015].

SAPA. 2015. Truck driver killed near Citrusdal. [Online]. Available: http://www.iol.co.za/news/south-africa/truck-driver-killed-near-citrusdal-1.378952#.Vao4EPmqqko [18 July 2015].

Sarvi, M. & Kuwahara, M. 2008. Using ITS to Improve the Capacity of Freeway Merging Sections by Transferring Freight Vehicles. IEEE Transactions on Intelligent Transportation Systems, 9(4). :580-588.

Scott, J., Fay, R., Hoover, N., Robinette, R. & Deering, D. 2003. Brake Performance Testing and Truck Runaway Analysis. Paper presented at 2003 SAE International Truck and Bus Meeting and Exhibition, November 10, 2003 - November 12. 2003.

Sesant, S. 2015. Franschhoek pass bus crash: More than two dozen recovering. [Online]. Available: http://ewn.co.za/2015/03/07/Franschhoek-Pass-bus-crash-More-than-two-dozen-recovering [22 March 2015].

St. John, A.D., & Kobett, D. R. NCHRP Report 185: Grade Effects on Traffic Flow Stability and Capacity. TRB, National Research Council, Washington D.C., 1978.

Trimble. 2015. GeoExplorer 6000 series GeoXT handheld. [Online]. Available: http://www.ascscientific.com/022501-255_GeoXT6000_DS_0211_MGIS_lr.pdf [22 February 2015].

Wikipedia. 2014. Air brake (road vehicle). [Online]. Available: https://en.wikipedia.org/wiki/Air_brake_(road_vehicle) [15 October 2014].

Appendix A

The laser light box (LLB) flashes a light when the laser beam is broken. This is done by a simple electrical circuit that uses a transistor and resistors to control the path of the electrical current. The LLB schematic is depicted below:

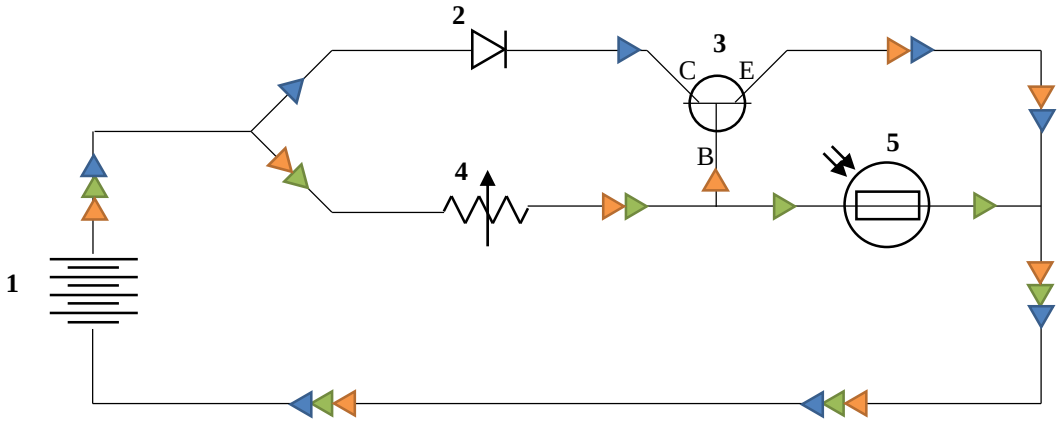

Components:

1. Supply
2. Light emitting diode (LED)
3. PNP transistor
4. Adjustable resistor
5. Light dependant resistor (LDR)

Explanation:

The LDR (5) acts as the switch for this circuit, by controlling the resistance of the circuit. When the laser beam is shined on the LDR, the resistance of the LDR decreases, allowing more current to pass through it, since the current will follow the path of least resistance (green arrows). Therefore the LED (2) will not be activated since no current will pass through it, portraying the device as being switched off.

However when the laser beam is broken, the LDR's resistance will increase, which subsequently increases the current flowing through the base of the transistor (3-B; orange arrows). With current flowing through the base of the transistor, current is also allowed to flow from the collector (3-C) to the emitter (3-E), allowing current now to pass through the LED (blue arrows). Thus, effectively turning the LED on when the laser beam is broken.

Appendix B

Clipper.lua

The *clipper.lua* program used in conjunction with VLC media player, is published under a General Public License, and is freely available for download at http://addons.videolan.org/content/show.php/Clipper?content=163792.

Logger.lua

The code for the *logger.lua* extension programmed to log the times in VLC media player, when the heavy vehicles passed over the transverse lines that delineates the control area, and save the times to a text file (.txt) is given below.

```
--"NewLogger.lua"
--"VLC Extension Script

function descriptor()
	return{
		title = "New Logger",
		version = "v1.0",
		author = "Slayer da Hell",
		description = "Extracts, log and save time intervals"
	}
end

function activate()
	dw = vlc.dialog("Logger")                                   -- Dialogue window
	dwL = dw:add_label("Enter File Name:", 1, 1, 6, 1)
	dwT = dw:add_text_input("Default", 1, 2, 3, 1)
	dwCB = dw:add_button("Create", createButton, 4, 2, 3, 1)
	dwLE = dw:add_label("Extracted Times", 1, 3, 6, 1)          -- Heading label
	dwHT = dw:add_html("", 1, 4, 6, 20)                         -- Extracted data
	dwEB = dw:add_button("Extract", extractButton, 1, 24, 2, 1)
	dwSB = dw:add_button("Save", saveButton, 3, 24, 2, 1)
	dwCB = dw:add_button("Close", closeButton, 5, 24, 2, 1)
end

function createButton()
	datafile = vlc.misc.homedir().."/"..dwT:get_text()..".txt"
	io.output(datafile)
end

counter = 1
	-- Global variable
function extractButton()
	local input = vlc.object.input()
	local item = vlc.input.item()

	if (counter == 1) then
		filename = item:name()
		curtime1 = vlc.var.get(input, "time")
		outStr = dwHT:get_text()..filename..", "..curtime1..", "
		dwHT:set_text(outStr)
		io.write(filename..", "..curtime1..", ")
		counter = 2
	elseif (counter == 2) then
		curtime2 = vlc.var.get(input, "time")
		outStr = dwHT:get_text()..curtime2.."<br/>"
		dwHT:set_text(outStr)
		io.write(curtime2, "\n")
```

```
                counter = 1
        end
end

function saveButton()
        io.close()
end

function closeButton()
        vlc.deactivate()
end

function deactivate()
        saveButton()
end

function close()
        vlc.deactivate()
end
```

Extracting Relevant Mass Data

The following section contains the code for the VBA program that was used to scan and extract any data for the observed heavy vehicles.

```
Sub extract_data()
   Dim dataRange As Range
   Dim regRange As Range
   Dim occuranceVal As Integer
   Dim regRangeSize As Integer
   Dim massSpeed() As Variant

   Set dataRange = Range("C2:C276055")
   Set regRange = Range("K2:K422")
   ReDim massSpeed(0 To 5, 0 To 0) As Variant
  For i = 2 To Application.WorksheetFunction.CountA(regRange) + 1
     If Not IsError(Application.Match(Cells(i, 11), dataRange, 0)) Then

        ReDim Preserve massSpeed(0 To 5, 0 To UBound(massSpeed, 2) + 1) As Variant

        With Range(Cells(Selection.Row, Selection.Column), Cells(Selection.Row, Selection.Column + 4)).Borders(xlEdgeBottom)
           .LineStyle = xlContinuous
           .Weight = xlThin
        End With
        Selection.Value = "Truck ID:"
        Selection.Font.Bold = True
        Selection.Offset(0, 1).FormulaR1C1 = "=R" & i & "C10"
        massSpeed(0, UBound(massSpeed, 2) - 1) = Selection.Offset(0, 1).Value
        massSpeed(3, UBound(massSpeed, 2) - 1) = Cells(i, 13).Value
        massSpeed(4, UBound(massSpeed, 2) - 1) = Cells(i, 14).Value
        massSpeed(5, UBound(massSpeed, 2) - 1) = Cells(i, 15).Value
        Selection.Offset(0, 2).Value = " Make:"
        Selection.Offset(0, 2).Font.Bold = True
        Selection.Offset(0, 3).FormulaR1C1 = "=INDEX(R2C1:R276055C8,MATCH(R" & i & "C11,R2C3:R276055C3,0),1)"
        Selection.Offset(1, 0).Select
        occuranceVal = 0
        For j = 0 To Application.WorksheetFunction.CountIf(dataRange, Cells(i, 11).Value) - 1
           ActiveCell.Offset(0, 1).FormulaR1C1 = "=INDEX(R2C1:R276055C8,MATCH(R" & i & "C11,R2C3:R276055C3,0)+" & j & ",8)"
           ActiveCell.FormulaR1C1 = "=TEXT(INDEX(R2C1:R276055C8,MATCH(R" & i & "C11,R2C3:R276055C3,0)+" & j & ",6),""dd/mm/yyyy"")"
           ActiveCell.Offset(0, 2).FormulaR1C1 = "=INDEX(R2C1:R276055C8,MATCH(R" & i & "C11,R2C3:R276055C3,0)+" & j & ",2)"
```

```
            ActiveCell.Offset(0, 3).FormulaR1C1 = "=INDEX(R2C1:R276055C8,MATCH(R" & i & "C11,R2C3:R276055C3,0)+" & j & ",5)"
            ActiveCell.Offset(0, 4).FormulaR1C1 = "=INDEX(R2C1:R276055C8,MATCH(R" & i & "C11,R2C3:R276055C3,0)+" & j & ",4)"
            Selection.Offset(1, 0).Select
            occuranceVal = occuranceVal + 1
        Next j
        Selection.Value = "Average:"
        Selection.Font.Bold = True
        Selection.Offset(0, 1).FormulaR1C1 = "=Roundup(Average(R" & Selection.Row - occuranceVal & "C" & Selection.Column + 1 &
":R" & Selection.Row - 1 & "C" & Selection.Column + 1 & "),0)"
        massSpeed(1, UBound(massSpeed, 2) - 1) = Selection.Offset(0, 1).Value
        Selection.Offset(0, 2).Value = "StDev:"
        Selection.Offset(0, 2).Font.Bold = True
        Selection.Offset(0, 3).FormulaR1C1 = "=Stdev.p(R" & Selection.Row - occuranceVal & "C" & Selection.Column + 1 & ":R" &
Selection.Row - 1 & "C" & Selection.Column + 1 & ")"
        massSpeed(2, UBound(massSpeed, 2) - 1) = Selection.Offset(0, 3).Value
         With Range(Cells(Selection.Row, Selection.Column), Cells(Selection.Row, Selection.Column + 4)).Borders(xlEdgeBottom)
            .LineStyle = xlContinuous
            .Weight = xlThick
        End With
        Selection.Offset(2, 0).Select
      End If
   Next i

   For l = 0 To 5
      For k = 0 To UBound(massSpeed, 2)
         Cells(2 + k, 24 + l).Value = massSpeed(l, k)
        ' Cells(2+k , 24 + k).Value = massSpeed(l, k)
      Next k
   Next l

   Range(Columns(Selection.Column), Columns(Selection.Column + 3)).Font.Size = 8

End Sub
```

Appendix C

The following tables contain the data that were used in determining the gradients.

Dutoitskloof Pass				
Observation	Ave. Distance [ΔX m]	Ave. Elevation [ΔY m]	Gradient [%] ΔY/ΔX	FEM
R01216A	35.414	1.817	**5.13%**	**5.12%**
R02216B	18.428	1.251	**6.79%**	**6.90%**
R012217A	31.337	1.767	**5.64%**	**5.90%**
R012217B	29.802	1.746	**5.86%**	**5.76%**
R012218A	35.421	1.973	**5.57%**	**5.56%**
Average:	30.080	1.711	**5.80%**	**5.85%**
Average Gradient:		**5.69%**		

Hex River Pass				
Observation	Ave. Distance [ΔX m]	Ave. Elevation [ΔY m]	Gradient [%] ΔY/ΔX	FEM
R012211B	24.782	1.627	**6.57%**	**6.68%**
R012212A	23.168	1.426	**6.15%**	**6.15%**
R012212B	26.893	1.647	**6.12%**	**6.05%**
R012213B	34.343	2.241	**6.53%**	**6.4%**
R021412C	16.015	0.986	**6.16%**	**6.09%**
Average:	25.040	1.585	**6.31%**	**6.28%**
Average Gradient:		**6.33%**		

Houwhoek Pass				
Observation	Ave. Distance [ΔX m]	Ave. Elevation [ΔY m]	Gradient [%] ΔY/ΔX	FEM
R012116A	29.856	1.859	**6.23%**	**6.27%**
R012116D	31.882	2.228	**6.99%**	**6.99%**
R012116E	39.988	2.439	**6.10%**	**6.00%**
R012117A	40.634	2.658	**6.54%**	**6.61%**
R012117B	36.245	2.291	**6.32%**	**6.42%**
Average:	35.721	2.295	6.44%	6.46%
Average Gradient:		**6.42%**		

Piekenierskloof Pass				
Observation	Ave. Distance [ΔX m]	Ave. Elevation [ΔY m]	Gradient [%] ΔY/ΔX	FEM
R012914B	37.476	2.175	**5.80%**	**5.79%**
R012914C	23.843	1.355	**5.68%**	**5.67%**
R012915A	39.752	2.198	**5.53%**	**5.48%**
R012915B	37.163	2.095	**5.64%**	**5.61%**
R012915C	45.036	2.552	**5.67%**	**5.62%**
Average:	36.654	2.075	**5.66%**	**5.63%**
Average Gradient:		**5.66%**		

Huguenot Tunnel				
Observation	Ave. Distance [ΔX m]	Ave. Elevation [ΔY m]	Gradient [%] ΔY/ΔX	FEM
R022612A	39.230	2.224	**5.67%**	**5.75%**
R022612B	20.648	1.288	**6.24%**	**6.34%**
R022612C	32.040	1.726	**5.39%**	**7.30%**
R022612D	43.086	2.065	**4.79%**	**4.84%**
R022613A	30.643	1.747	**5.70%**	**5.82%**
R022613B	35.281	1.819	**5.16%**	**5.31%**
Average:	33.488	1.811	**5.49%**	**5.89%**
Average Gradient:		**5.41%**		

Sir Lowry's Pass				
Observation	Ave. Distance [ΔX m]	Ave. Elevation [ΔY m]	Gradient [%] ΔY/ΔX	FEM
R012111B	24.622	1.592	**6.47%**	**6.53%**
R012112A	12.322	0.698	**5.66%**	**5.76%**
R012112B	36.530	1.960	**5.36%**	**5.39%**
R012112C	37.261	2.185	**5.87%**	**5.90%**
R012113A	26.040	1.552	**5.96%**	**6.03%**
R012113B	15.597	1.026	**6.58%**	**6.29%**
Average:	25.395	1.502	**5.98%**	**5.98%**
Average Gradient:		**5.92%**		

Appendix D

This section contains the data that were used in calculating the curve radii for Dutoitskloof Pass, Hex River Pass, Houwhoek Pass and Piekenierskloof Pass

Dutoitskloof Pass

DTKP - R012218A		Linear Calculations					Intersection		Radians				
Long	Lat	Gradient	Mid_Long	Mid_Lat	Perp	Intercept	Long_2	Lat_2	Long	Lat	Long_2	Lat_2	Radius
19.0691	-33.7539	1.3006	19.0690	-33.7540	-0.7689	-19.0921							
19.0689	-33.7541	1.3006	19.0688	-33.7542	-0.7689	-19.0924	19.0681	-33.7536	0.3328	-0.5891	0.3328	-0.5891	106.1333
19.0687	-33.7543	0.6644	19.0686	-33.7544	-1.5052	-5.0528	19.0669	-33.7519	0.3328	-0.5891	0.3328	-0.5891	325.3124
19.0684	-33.7545	0.5078	19.0683	-33.7546	-1.9694	3.7991	19.0678	-33.7537	0.3328	-0.5891	0.3328	-0.5891	115.2240
19.0681	-33.7547	0.1315	19.0679	-33.7547	-7.6043	111.2442	19.0676	-33.7523	0.3328	-0.5891	0.3328	-0.5891	252.4969
19.0678	-33.7547	-0.0199	19.0676	-33.7547	50.1866	-990.6919	19.0676	-33.7521	0.3328	-0.5891	0.3328	-0.5891	281.5994
19.0674	-33.7547	-0.1508	19.0672	-33.7547	6.6311	-160.1913	19.0675	-33.7527	0.3328	-0.5891	0.3328	-0.5891	215.3062
19.0671	-33.7547	-0.3278	19.0669	-33.7546	3.0506	-91.9210	19.0675	-33.7528	0.3328	-0.5891	0.3328	-0.5891	203.2056
19.0667	-33.7546	-0.5345	19.0666	-33.7545	1.8708	-69.4235	19.0673	-33.7532	0.3328	-0.5891	0.3328	-0.5891	155.7414
19.0665	-33.7544	-0.8619	19.0663	-33.7543	1.1602	-55.8748	19.0674	-33.7531	0.3328	-0.5891	0.3328	-0.5891	173.6637
19.0662	-33.7542	-1.2938	19.0661	-33.7541	0.7729	-48.4910							
19.0660	-33.7539												
												Average	203.1870
												Radius	205

DTKP - R012217B		Linear Calculations					Intersection		Radians				
Long	Lat	Gradient	Mid_Long	Mid_Lat	Perp	Intercept	Long_2	Lat_2	Long	Lat	Long_2	Lat_2	Radius
19.0691	-33.7538	1.9929	19.0690	-33.7539	-0.5018	-24.1854							
19.0690	-33.7540	1.1845	19.0689	-33.7541	-0.8442	-17.6557	19.0677	-33.7531	0.3328	-0.5891	0.3328	-0.5891	173.9123
19.0688	-33.7543	0.8139	19.0687	-33.7544	-1.2287	-10.3249	19.0677	-33.7532	0.3328	-0.5891	0.3328	-0.5891	160.5956
19.0686	-33.7545	0.5129	19.0684	-33.7545	-1.9495	3.4198	19.0675	-33.7527	0.3328	-0.5891	0.3328	-0.5891	221.9887
19.0683	-33.7546	0.3312	19.0681	-33.7546	-3.0194	23.8201	19.0676	-33.7531	0.3328	-0.5891	0.3328	-0.5891	174.1786
19.0680	-33.7547	0.1246	19.0678	-33.7547	-8.0277	119.3162	19.0674	-33.7517	0.3328	-0.5891	0.3328	-0.5891	318.2632
19.0677	-33.7547	0.0183	19.0675	-33.7547	-54.6779	1008.8160	19.0675	-33.7534	0.3328	-0.5891	0.3328	-0.5891	143.3161
19.0673	-33.7547	-0.2250	19.0672	-33.7547	4.4443	-118.4950	19.0677	-33.7523	0.3328	-0.5891	0.3328	-0.5891	264.3190
19.0670	-33.7547	-0.3657	19.0669	-33.7546	2.7347	-85.8971	19.0674	-33.7532	0.3328	-0.5891	0.3328	-0.5891	157.9189
19.0667	-33.7546	-0.6287	19.0666	-33.7545	1.5906	-64.0820	19.0679	-33.7524	0.3328	-0.5891	0.3328	-0.5891	263.4248
19.0665	-33.7544	-0.8146	19.0663	-33.7543	1.2275	-57.1587	19.0674	-33.7530	0.3328	-0.5891	0.3328	-0.5891	173.5055
19.0662	-33.7542	-1.1699	19.0661	-33.7541	0.8548	-50.0515							
19.0660	-33.7540												
												Average	205.1423
												Radius	205

DTKP - R012216B		Linear Calculations					Intersection		Radians				
Long	Lat	Gradient	Mid_Long	Mid_Lat	Perp	Intercept	Long_2	Lat_2	Long	Lat	Long_2	Lat_2	Radius
19.0691	-33.7538	2.4329	19.0690	-33.7539	-0.4110	-25.9160							
19.0690	-33.7540	1.2597	19.0689	-33.7541	-0.7938	-18.6168	19.0678	-33.7533	0.3328	-0.5891	0.3328	-0.5891	150.3507
19.0688	-33.7542	0.8763	19.0687	-33.7543	-1.1412	-11.9926	19.0678	-33.7532	0.3328	-0.5891	0.3328	-0.5891	152.4318
19.0687	-33.7544	0.5924	19.0685	-33.7544	-1.6881	-1.5648	19.0661	-33.7503	0.3328	-0.5891	0.3328	-0.5891	516.4548
19.0684	-33.7545	0.5202	19.0683	-33.7546	-1.9223	2.8996	19.0677	-33.7533	0.3328	-0.5891	0.3328	-0.5891	152.0077
19.0682	-33.7546	0.3071	19.0681	-33.7547	-3.2561	28.3337	19.0675	-33.7530	0.3328	-0.5891	0.3328	-0.5891	189.3396
19.0679	-33.7547	0.1616	19.0678	-33.7547	-6.1872	84.2216	19.0675	-33.7530	0.3328	-0.5891	0.3328	-0.5891	187.4710
19.0677	-33.7547	0.0247	19.0676	-33.7547	-40.4083	736.7340	19.0675	-33.7531	0.3328	-0.5891	0.3328	-0.5891	173.2892
19.0675	-33.7547	-0.1201	19.0674	-33.7547	8.3255	-192.4996	19.0678	-33.7514	0.3328	-0.5891	0.3328	-0.5891	355.1180
19.0672	-33.7547	-0.1941	19.0671	-33.7547	5.1508	-131.9655	19.0674	-33.7530	0.3328	-0.5891	0.3328	-0.5891	185.9693
19.0670	-33.7547	-0.3434	19.0669	-33.7546	2.9121	-89.2798	19.0674	-33.7530	0.3328	-0.5891	0.3328	-0.5891	180.8046
19.0668	-33.7546	-0.5030	19.0667	-33.7545	1.9880	-71.6581							
19.0666	-33.7545												
												Average	203.4285
												Radius	205

DTKP - R012216A		Linear Calculations					Intersection		Radians				
Long	Lat	Gradient	Mid_Long	Mid_Lat	Perp	Intercept	Long_2	Lat_2	Long	Lat	Long_2	Lat_2	Radius
19.0690	-33.7539	2.3342	19.0689	-33.7540	-0.4284	-25.5848							
19.0689	-33.7541	1.1351	19.0688	-33.7542	-0.8810	-16.9548	19.0679	-33.7535	0.3328	-0.5891	0.3328	-0.5891	124.3112
19.0686	-33.7544	0.6115	19.0685	-33.7545	-1.6353	-2.5712	19.0674	-33.7527	0.3328	-0.5891	0.3328	-0.5891	222.1231
19.0683	-33.7546	0.3957	19.0682	-33.7546	-2.5271	14.4324	19.0676	-33.7531	0.3328	-0.5891	0.3328	-0.5891	173.9177
19.0680	-33.7547	0.1540	19.0678	-33.7547	-6.4946	90.0839	19.0675	-33.7529	0.3328	-0.5891	0.3328	-0.5891	195.4007
19.0676	-33.7547	-0.0477	19.0675	-33.7547	20.9495	-433.2084	19.0676	-33.7525	0.3328	-0.5891	0.3328	-0.5891	230.4975
19.0673	-33.7547	-0.2211	19.0671	-33.7547	4.5227	-119.9891	19.0675	-33.7530	0.3328	-0.5891	0.3328	-0.5891	185.4086
19.0669	-33.7546	-0.4538	19.0667	-33.7546	2.2038	-75.7744	19.0675	-33.7528	0.3328	-0.5891	0.3328	-0.5891	205.2977
19.0666	-33.7545	-0.7032	19.0664	-33.7544	1.4221	-60.8685	19.0673	-33.7532	0.3328	-0.5891	0.3328	-0.5891	160.6427
19.0663	-33.7543	-1.1187	19.0662	-33.7542	0.8939	-50.7971							
19.0661	-33.7540												
												Average	187.1999
												Radius	185

Hex River Pass

HRP - R012211A		Linear Calculations					Intersection		Radians				
Long	Lat	Gradient	Mid_Long	Mid_Lat	Perp	Intercept	Long_2	Lat_2	Long	Lat	Long_2	Lat_2	Radius
19.7569	-33.4054	-21.4927	19.7569	-33.4054	0.0465	-34.3247							
19.7569	-33.4055	-4.4653	19.7569	-33.4055	0.2240	-37.8301	19.7600	-33.4048	0.3448	-0.5830	0.3449	-0.5830	0.0000
19.7569	-33.4055	-4.0222	19.7570	-33.4056	0.2486	-38.3176	19.7576	-33.4054	0.3448	-0.5830	0.3448	-0.5830	68.4267
19.7570	-33.4056	-2.5971	19.7570	-33.4056	0.3850	-41.0131	19.7579	-33.4053	0.3448	-0.5830	0.3448	-0.5830	112.5413
19.7570	-33.4057	-2.0829	19.7570	-33.4057	0.4801	-42.8912	19.7665	-33.4012	0.3448	-0.5830	0.3450	-0.5830	0.0000
19.7570	-33.4058	-2.0431	19.7570	-33.4058	0.4895	-43.0761	19.7576	-33.4055	0.3448	-0.5830	0.3448	-0.5830	62.5405
19.7571	-33.4058	-1.4681	19.7571	-33.4059	0.6812	-46.8636	19.7580	-33.4053	0.3448	-0.5830	0.3448	-0.5830	117.3554
19.7571	-33.4059	-1.2463	19.7571	-33.4059	0.8024	-49.2586	19.7578	-33.4054	0.3448	-0.5830	0.3448	-0.5830	98.9150
19.7572	-33.4060	-1.0306	19.7572	-33.4060	0.9703	-52.5764	19.7578	-33.4054	0.3448	-0.5830	0.3448	-0.5830	97.2736
19.7572	-33.4060	-0.8521	19.7573	-33.4060	1.1735	-56.5917	19.7588	-33.4043	0.3448	-0.5830	0.3449	-0.5830	250.8828
19.7573	-33.4061	-0.7874	19.7573	-33.4061	1.2701	-58.4990	19.7580	-33.4052	0.3448	-0.5830	0.3448	-0.5830	118.4369
19.7574	-33.4061	-0.6563	19.7574	-33.4062	1.5238	-63.5123	19.7582	-33.4050	0.3448	-0.5830	0.3448	-0.5830	152.0281
19.7574	-33.4062	-0.5704	19.7575	-33.4062	1.7532	-68.0441	19.7584	-33.4046	0.3448	-0.5830	0.3448	-0.5830	193.9937
19.7575	-33.4062	-0.5098	19.7576	-33.4062	1.9615	-72.1617	19.7582	-33.4050	0.3448	-0.5830	0.3448	-0.5830	147.1434
19.7576	-33.4063	-0.4313	19.7576	-33.4063	2.3188	-79.2211	19.7583	-33.4048	0.3448	-0.5830	0.3448	-0.5830	171.4401
19.7577	-33.4063	-0.3657	19.7577	-33.4063	2.7342	-87.4272	19.7582	-33.4049	0.3448	-0.5830	0.3448	-0.5830	163.3366
19.7578	-33.4063	-0.2994	19.7578	-33.4063	3.3401	-99.3990							
19.7578	-33.4064												
												Average	116.9543
												Radius	115

HRP - R012212B		Linear Calculations					Intersection		Radians				
Long	Lat	Gradient	Mid_Long	Mid_Lat	Perp	Intercept	Long_2	Lat_2	Long	Lat	Long_2	Lat_2	Radius
19.7569	-33.4053	-31.3337	19.7569	-33.4054	0.0319	-34.0359							
19.7569	-33.4055	-3.9293	19.7569	-33.4056	0.2545	-38.4337	19.7579	-33.4053	0.3448	-0.5830	0.3448	-0.5830	109.8261
19.7570	-33.4056	-2.1218	19.7570	-33.4057	0.4713	-42.7174	19.7579	-33.4053	0.3448	-0.5830	0.3448	-0.5830	105.1182
19.7571	-33.4058	-1.3102	19.7571	-33.4059	0.7632	-48.4854	19.7580	-33.4053	0.3448	-0.5830	0.3448	-0.5830	118.0361
19.7572	-33.4060	-0.8794	19.7573	-33.4061	1.1371	-55.8723	19.7581	-33.4051	0.3448	-0.5830	0.3448	-0.5830	135.6102
19.7573	-33.4061	-0.6046	19.7574	-33.4062	1.6540	-66.0846	19.7582	-33.4050	0.3448	-0.5830	0.3448	-0.5830	153.5875
19.7575	-33.4063	-0.3992	19.7577	-33.4063	2.5049	-82.8973							
19.7578	-33.4063												
												Average	124.4356
												Radius	125

HRP - R012212C		Linear Calculations					Intersection		Radians				
Long	Lat	Gradient	Mid_Long	Mid_Lat	Perp	Intercept	Long_2	Lat_2	Long	Lat	Long_2	Lat_2	Radius
19.7569	-33.4050	3.8811	19.7569	-33.4051	-0.2577	-28.3146							
19.7569	-33.4052	5.8538	19.7569	-33.4052	-0.1708	-30.0302	19.7575	-33.4053	0.3448	-0.5830	0.3448	-0.5830	70.0983
19.7569	-33.4053	-141.9544	19.7569	-33.4053	0.0070	-33.5445	19.7575	-33.4053	0.3448	-0.5830	0.3448	-0.5830	71.9046
19.7569	-33.4054	-5.4912	19.7569	-33.4054	0.1821	-37.0034	19.7697	-33.4031	0.3448	-0.5830	0.3450	-0.5830	0.0000
19.7569	-33.4055	-5.2404	19.7569	-33.4055	0.1908	-37.1757	19.7581	-33.4053	0.3448	-0.5830	0.3448	-0.5830	132.0474
19.7569	-33.4056	-3.4953	19.7570	-33.4056	0.2861	-39.0580	19.7574	-33.4055	0.3448	-0.5830	0.3448	-0.5830	48.2590
19.7570	-33.4057	-1.6609	19.7570	-33.4057	0.6021	-45.3013	19.7575	-33.4054	0.3448	-0.5830	0.3448	-0.5830	71.0124
19.7570	-33.4058	-1.1327	19.7571	-33.4058	0.8829	-50.8484	19.7586	-33.4045	0.3448	-0.5830	0.3449	-0.5830	225.7675
19.7571	-33.4059	-1.0163	19.7571	-33.4059	0.9839	-52.8459	19.7488	-33.4141	0.3448	-0.5830	0.3447	-0.5832	0.0000
19.7572	-33.4060	-1.0351	19.7572	-33.4060	0.9661	-52.4939	19.7580	-33.4052	0.3448	-0.5830	0.3448	-0.5830	117.8242
19.7573	-33.4060	-0.8486	19.7573	-33.4061	1.1784	-56.6890	19.7580	-33.4052	0.3448	-0.5830	0.3448	-0.5830	123.4565
19.7573	-33.4061	-0.6868	19.7574	-33.4061	1.4561	-62.1746	19.7582	-33.4050	0.3448	-0.5830	0.3448	-0.5830	144.4372
19.7574	-33.4062	-0.5614	19.7575	-33.4062	1.7814	-68.6020	19.7582	-33.4050	0.3448	-0.5830	0.3448	-0.5830	148.9881
19.7575	-33.4062	-0.4554	19.7576	-33.4063	2.1960	-76.7940	19.7582	-33.4049	0.3448	-0.5830	0.3448	-0.5830	158.3022
19.7576	-33.4063	-0.3727	19.7577	-33.4063	2.6829	-86.4144	19.7584	-33.4043	0.3448	-0.5830	0.3448	-0.5830	220.8328
19.7577	-33.4063	-0.3191	19.7578	-33.4063	3.1333	-95.3142							
19.7578	-33.4064												
												Average	109.4950
												Radius	110

HRP - R012213A		Linear Calculations					Intersection		Radians				
Long	Lat	Gradient	Mid_Long	Mid_Lat	Perp	Intercept	Long_2	Lat_2	Long	Lat	Long_2	Lat_2	Radius
19.7569	-33.4053	-5.8842	19.7569	-33.4054	0.1699	-36.7630							
19.7569	-33.4054	-6.2232	19.7569	-33.4055	0.1607	-36.5802	19.7575	-33.4054	0.3448	-0.5830	0.3448	-0.5830	66.3646
19.7570	-33.4056	-2.6745	19.7570	-33.4056	0.3739	-40.7927	19.7580	-33.4052	0.3448	-0.5830	0.3448	-0.5830	123.2384
19.7570	-33.4057	-2.0100	19.7570	-33.4057	0.4975	-43.2352	19.7580	-33.4052	0.3448	-0.5830	0.3448	-0.5830	122.8902
19.7570	-33.4058	-1.5525	19.7571	-33.4058	0.6441	-46.1317	19.7579	-33.4053	0.3448	-0.5830	0.3448	-0.5830	109.1449
19.7571	-33.4059	-1.1866	19.7572	-33.4059	0.8428	-50.0563	19.7580	-33.4052	0.3448	-0.5830	0.3448	-0.5830	123.4849
19.7572	-33.4060	-0.9410	19.7572	-33.4060	1.0627	-54.4021	19.7580	-33.4052	0.3448	-0.5830	0.3448	-0.5830	127.5161
19.7573	-33.4061	-0.7459	19.7573	-33.4061	1.3406	-59.8935	19.7581	-33.4051	0.3448	-0.5830	0.3448	-0.5830	141.0352
19.7574	-33.4062	-0.5938	19.7575	-33.4062	1.6842	-66.6819	19.7581	-33.4051	0.3448	-0.5830	0.3448	-0.5830	140.0024
19.7575	-33.4062	-0.4558	19.7576	-33.4063	2.1941	-76.7564	19.7583	-33.4048	0.3448	-0.5830	0.3448	-0.5830	172.2191
19.7577	-33.4063	-0.3519	19.7577	-33.4063	2.8414	-89.5469							
19.7578	-33.4063												
												Average	125.0995
												Radius	125

HRP - R012213B		Linear Calculations					Intersection		Radians				
Long	Lat	Gradient	Mid_Long	Mid_Lat	Perp	Intercept	Long_2	Lat_2	Long	Lat	Long_2	Lat_2	Radius
19.7569	-33.4052	-32.8235	19.7569	-33.4054	0.0305	-34.0073							
19.7569	-33.4055	-3.1189	19.7570	-33.4056	0.3206	-39.7401	19.7578	-33.4053	0.3448	-0.5830	0.3448	-0.5830	103.0113
19.7570	-33.4057	-1.4318	19.7571	-33.4059	0.6984	-47.2044	19.7580	-33.4052	0.3448	-0.5830	0.3448	-0.5830	126.6291
19.7572	-33.4060	-0.8461	19.7573	-33.4061	1.1820	-56.7582	19.7582	-33.4051	0.3448	-0.5830	0.3448	-0.5830	145.6377
19.7574	-33.4062	-0.5002	19.7576	-33.4063	1.9993	-72.9081							
19.7577	-33.4063												
												Average	125.0927
												Radius	125

Houwhoek Pass

HHP - R012116A		Linear Calculations					Intersection		Radians				
Long	Lat	Gradient	Mid_Long	Mid_Lat	Perp	Intercept	Long_2	Lat_2	Long	Lat	Long_2	Lat_2	Radius
19.1873	-34.2178	0.3539	19.1874	-34.2177	-2.8260	20.0051							
19.1876	-34.2177	0.1869	19.1877	-34.2176	-5.3498	68.4336	19.1881	-34.2197	0.3349	-0.5972	0.3349	-0.5972	220.8881
19.1879	-34.2176	0.0270	19.1881	-34.2176	-37.0039	675.8156	19.1881	-34.2196	0.3349	-0.5972	0.3349	-0.5972	214.8129
19.1882	-34.2176	-0.1346	19.1884	-34.2176	7.4291	-176.7703	19.1880	-34.2201	0.3349	-0.5972	0.3349	-0.5973	263.1525
19.1885	-34.2176	-0.2693	19.1887	-34.2177	3.7131	-105.4666	19.1882	-34.2196	0.3349	-0.5972	0.3349	-0.5972	213.3214
19.1889	-34.2177	-0.4478	19.1890	-34.2178	2.2330	-77.0661	19.1883	-34.2193	0.3349	-0.5972	0.3349	-0.5972	180.3767
19.1891	-34.2178	-0.6954	19.1893	-34.2179	1.4381	-61.8134	19.1884	-34.2192	0.3349	-0.5972	0.3349	-0.5972	170.1537
19.1894	-34.2180	-1.0285	19.1895	-34.2181	0.9723	-52.8767	19.1881	-34.2195	0.3349	-0.5972	0.3349	-0.5972	210.6325
19.1896	-34.2182	-1.3914	19.1897	-34.2184	0.7187	-48.0098	19.1886	-34.2192	0.3349	-0.5972	0.3349	-0.5972	151.2195
19.1898	-34.2185	-2.2255	19.1898	-34.2186	0.4493	-42.8414	19.1886	-34.2191	0.3349	-0.5972	0.3349	-0.5972	144.5168
19.1899	-34.2187	-4.6762	19.1899	-34.2189	0.2138	-38.3226							
19.1899	-34.2190												
												Average	196.5638
												Radius	195

HHP - R012116D		Linear Calculations					Intersection		Radians				
Long	Lat	Gradient	Mid_Long	Mid_Lat	Perp	Intercept	Long_2	Lat_2	Long	Lat	Long_2	Lat_2	Radius
19.1874	-34.2177	0.2747	19.1875	-34.2177	-3.6402	35.6296							
19.1877	-34.2176	0.0974	19.1879	-34.2176	-10.2696	162.8345	19.1881	-34.2201	0.3349	-0.5972	0.3349	-0.5973	261.8934
19.1881	-34.2176	-0.0488	19.1882	-34.2176	20.4877	-427.3414	19.1881	-34.2197	0.3349	-0.5972	0.3349	-0.5972	216.2504
19.1884	-34.2176	-0.2299	19.1886	-34.2177	4.3507	-117.7006	19.1882	-34.2196	0.3349	-0.5972	0.3349	-0.5972	209.4632
19.1888	-34.2177	-0.4293	19.1889	-34.2178	2.3295	-78.9181	19.1882	-34.2195	0.3349	-0.5972	0.3349	-0.5972	200.5443
19.1891	-34.2178	-0.6682	19.1892	-34.2179	1.4966	-62.9374	19.1882	-34.2195	0.3349	-0.5972	0.3349	-0.5972	204.0284
19.1894	-34.2180	-0.9637	19.1895	-34.2181	1.0377	-54.1313	19.1885	-34.2192	0.3349	-0.5972	0.3349	-0.5972	160.4743
19.1896	-34.2183	-1.5176	19.1897	-34.2184	0.6589	-46.8630	19.1886	-34.2192	0.3349	-0.5972	0.3349	-0.5972	151.4965
19.1898	-34.2185	-2.7138	19.1899	-34.2187	0.3685	-41.2898							
19.1899	-34.2188												
												Average	200.5929
												Radius	200

HHP - R012116E		Linear Calculations					Intersection		Radians				
Long	Lat	Gradient	Mid_Long	Mid_Lat	Perp	Intercept	Long_2	Lat_2	Long	Lat	Long_2	Lat_2	Radius
19.1872	-34.2178	0.3713	19.1874	-34.2177	-2.6929	17.4515							
19.1876	-34.2177	0.1494	19.1878	-34.2176	-6.6923	94.1930	19.1881	-34.2198	0.3349	-0.5972	0.3349	-0.5972	236.5188
19.1880	-34.2176	-0.0448	19.1882	-34.2176	22.3225	-462.5456	19.1881	-34.2201	0.3349	-0.5972	0.3349	-0.5973	261.1832
19.1884	-34.2176	-0.2262	19.1886	-34.2177	4.4212	-119.0550	19.1883	-34.2193	0.3349	-0.5972	0.3349	-0.5972	182.1004
19.1889	-34.2177	-0.5112	19.1890	-34.2178	1.9563	-71.7579	19.1881	-34.2197	0.3349	-0.5972	0.3349	-0.5972	221.3935
19.1892	-34.2179	-0.7923	19.1894	-34.2180	1.2622	-58.4389	19.1884	-34.2193	0.3349	-0.5972	0.3349	-0.5972	176.3419
19.1895	-34.2182	-1.2931	19.1897	-34.2183	0.7734	-49.0587	19.1886	-34.2191	0.3349	-0.5972	0.3349	-0.5972	149.5441
19.1898	-34.2185	-2.5221	19.1899	-34.2186	0.3965	-41.8273							
19.1899	-34.2188												
												Average	182.4265
												Radius	180

HHP - R012117A		Linear Calculations					Intersection		Radians				
Long	Lat	Gradient	Mid_Long	Mid_Lat	Perp	Intercept	Long_2	Lat_2	Long	Lat	Long_2	Lat_2	Radius
19.1872	-34.2178	0.3405	19.1874	-34.2177	-2.9367	22.1291							
19.1876	-34.2177	0.1544	19.1877	-34.2176	-6.4769	90.0591	19.1881	-34.2200	0.3349	-0.5972	0.3349	-0.5973	257.1806
19.1879	-34.2176	-0.0004	19.1881	-34.2176	265.3830	-509.2665	19.1881	-34.2197	0.3349	-0.5972	0.3349	-0.5972	225.0814
19.1883	-34.2176	-0.1773	19.1885	-34.2176	5.6404	-142.4475	19.1881	-34.2196	0.3349	-0.5972	0.3349	-0.5972	209.9012
19.1887	-34.2177	-0.3794	19.1888	-34.2177	2.6357	-84.7947	19.1882	-34.2196	0.3349	-0.5972	0.3349	-0.5972	206.6990
19.1890	-34.2178	-0.6164	19.1892	-34.2179	1.6224	-65.3495	19.1882	-34.2195	0.3349	-0.5972	0.3349	-0.5972	206.6690
19.1893	-34.2180	-0.9123	19.1895	-34.2181	1.0962	-55.2533	19.1884	-34.2192	0.3349	-0.5972	0.3349	-0.5972	163.7688
19.1896	-34.2182	-1.4579	19.1897	-34.2184	0.6859	-47.3810	19.1886	-34.2192	0.3349	-0.5972	0.3349	-0.5972	151.1141
19.1898	-34.2185	-2.6931	19.1899	-34.2187	0.3713	-41.3443							
19.1899	-34.2188												
												Average	202.9163
												Radius	205

HHP - R012117B		Linear Calculations					Intersection		Radians				
Long	Lat	Gradient	Mid_Long	Mid_Lat	Perp	Intercept	Long_2	Lat_2	Long	Lat	Long_2	Lat_2	Radius
19.1874	-34.2177	0.2560	19.1876	-34.2177	-3.9070	40.7481							
19.1877	-34.2176	0.1088	19.1879	-34.2176	-9.1907	142.1327	19.1881	-34.2194	0.3349	-0.5972	0.3349	-0.5972	190.7342
19.1881	-34.2176	-0.0878	19.1883	-34.2176	11.3891	-252.7537	19.1881	-34.2195	0.3349	-0.5972	0.3349	-0.5972	198.3077
19.1884	-34.2176	-0.2791	19.1886	-34.2177	3.5825	-102.9606	19.1878	-34.2205	0.3349	-0.5972	0.3349	-0.5973	313.5634
19.1888	-34.2177	-0.4060	19.1889	-34.2178	2.4628	-81.4755	19.1881	-34.2197	0.3349	-0.5972	0.3349	-0.5972	220.2278
19.1891	-34.2178	-0.6078	19.1892	-34.2179	1.6453	-65.7896	19.1884	-34.2193	0.3349	-0.5972	0.3349	-0.5972	166.5141
19.1894	-34.2180	-0.9382	19.1895	-34.2181	1.0659	-54.6725	19.1883	-34.2194	0.3349	-0.5972	0.3349	-0.5972	190.0370
19.1896	-34.2182	-1.3410	19.1897	-34.2184	0.7457	-48.5284	19.1886	-34.2192	0.3349	-0.5972	0.3349	-0.5972	151.6937
19.1898	-34.2185	-2.2161	19.1898	-34.2186	0.4512	-42.8779							
19.1899	-34.2187												
												Average	204.4397
												Radius	205

Piekenierskloof Pass

PKNKP - R012015A		Linear Calculations					Intersection		Radians				
Long	Lat	Gradient	Mid_Long	Mid_Lat	Perp	Intercept	Long_2	Lat_2	Long	Lat	Long_2	Lat_2	Radius
18.9547	-32.6517	-0.3629	18.9548	-32.6517	2.7558	-84.8871							
18.9549	-32.6518	-0.4705	18.9550	-32.6518	2.1255	-72.9398	18.9541	-32.6537	0.3308	-0.5699	0.3308	-0.5699	218.7712
18.9551	-32.6518	-0.5812	18.9551	-32.6519	1.7207	-65.2675	18.9543	-32.6534	0.3308	-0.5699	0.3308	-0.5699	185.2432
18.9552	-32.6519	-0.7270	18.9553	-32.6520	1.3756	-58.7270	18.9548	-32.6527	0.3308	-0.5699	0.3308	-0.5699	90.9611
18.9554	-32.6520	-1.0622	18.9554	-32.6521	0.9415	-50.4978	18.9531	-32.6542	0.3308	-0.5699	0.3308	-0.5699	341.8763
18.9555	-32.6521	-1.1673	18.9555	-32.6522	0.8567	-48.8907	18.9546	-32.6530	0.3308	-0.5699	0.3308	-0.5699	130.3135
18.9556	-32.6522	-1.5375	18.9556	-32.6523	0.6504	-44.9815	18.9545	-32.6530	0.3308	-0.5699	0.3308	-0.5699	139.8452
18.9556	-32.6524	-2.0596	18.9557	-32.6524	0.4855	-41.8561	18.9533	-32.6536	0.3308	-0.5699	0.3308	-0.5699	295.0827
18.9557	-32.6525	-2.4156	18.9557	-32.6526	0.4140	-40.4997	18.9551	-32.6529	0.3308	-0.5699	0.3308	-0.5699	80.8203
18.9558	-32.6527	-5.5885	18.9558	-32.6527	0.1789	-36.0447	18.9528	-32.6533	0.3308	-0.5699	0.3308	-0.5699	337.4018
18.9558	-32.6528	-7.6942	18.9558	-32.6529	0.1300	-35.1165	18.9551	-32.6530	0.3308	-0.5699	0.3308	-0.5699	82.4382
18.9558	-32.6530	15.2097	18.9558	-32.6530	-0.0657	-31.4067	18.9541	-32.6529	0.3308	-0.5699	0.3308	-0.5699	186.0832
18.9558	-32.6531	6.3090	18.9558	-32.6532	-0.1585	-29.6486	18.9544	-32.6530	0.3308	-0.5699	0.3308	-0.5699	159.3782
18.9558	-32.6533	3.6294	18.9558	-32.6533	-0.2755	-27.4305	18.9541	-32.6529	0.3308	-0.5699	0.3308	-0.5699	186.5511
18.9557	-32.6534	2.5647	18.9557	-32.6535	-0.3899	-25.2624							
18.9557	-32.6536												
												Average	187.2897
												Radius	185

PKNKP - R012015C		Linear Calculations					Intersection		Radians				
Long	Lat	Gradient	Mid_Long	Mid_Lat	Perp	Intercept	Long_2	Lat_2	Long	Lat	Long_2	Lat_2	Radius
18.9546	-32.6516	-0.4009	18.9548	-32.6517	2.4945	-79.9344							
18.9551	-32.6518	-0.6775	18.9552	-32.6519	1.4761	-60.6310	18.9545	-32.6530	0.3308	-0.5699	0.3308	-0.5699	135.9327
18.9554	-32.6521	-1.3473	18.9555	-32.6522	0.7422	-46.7215	18.9545	-32.6530	0.3308	-0.5699	0.3308	-0.5699	136.4985
18.9557	-32.6524	-2.8066	18.9557	-32.6525	0.3563	-39.4066	18.9546	-32.6529	0.3308	-0.5699	0.3308	-0.5699	130.2600
18.9558	-32.6527	-15.0486	18.9558	-32.6529	0.0665	-33.9125	18.9545	-32.6530	0.3308	-0.5699	0.3308	-0.5699	148.8707
18.9558	-32.6530	5.8042	18.9558	-32.6532	-0.1723	-29.3873	18.9545	-32.6530	0.3308	-0.5699	0.3308	-0.5699	149.8870
18.9557	-32.6533	2.2975	18.9557	-32.6535	-0.4352	-24.4031							
18.9556	-32.6536												
												Average	140.2898
												Radius	140

PKNKP - R0120215D		Linear Calculations					Intersection		Radians				
Long	Lat	Gradient	Mid_Long	Mid_Lat	Perp	Intercept	Long_2	Lat_2	Long	Lat	Long_2	Lat_2	Radius
18.9549	-32.6517	-0.5208	18.9551	-32.6518	1.9201	-69.0482							
18.9553	-32.6519	-1.0015	18.9554	-32.6521	0.9985	-51.5790	18.9545	-32.6530	0.3308	-0.5699	0.3308	-0.5699	138.2069
18.9556	-32.6522	-1.9585	18.9557	-32.6524	0.5106	-42.3310	18.9546	-32.6530	0.3308	-0.5699	0.3308	-0.5699	134.6563
18.9557	-32.6526	-5.8197	18.9558	-32.6528	0.1718	-35.9099	18.9546	-32.6530	0.3308	-0.5699	0.3308	-0.5699	130.7723
18.9558	-32.6529	7.9595	18.9558	-32.6531	-0.1256	-30.2716	18.9542	-32.6529	0.3308	-0.5699	0.3308	-0.5699	174.7298
18.9558	-32.6533	2.7617	18.9557	-32.6534	-0.3621	-25.7897							
18.9556	-32.6536												
												Average	144.5913
												Radius	145

PKNKP - R01216C		Linear Calculations					Intersection		Radians				
Long	Lat	Gradient	Mid_Long	Mid_Lat	Perp	Intercept	Long_2	Lat_2	Long	Lat	Long_2	Lat_2	Radius
18.9545	-32.6516	-0.3226	18.9547	-32.6517	3.1002	-91.4147							
18.9549	-32.6517	-0.5396	18.9551	-32.6518	1.8531	-67.7771	18.9543	-32.6533	0.3308	-0.5699	0.3308	-0.5699	180.2589
18.9552	-32.6519	-0.8717	18.9554	-32.6520	1.1472	-54.3982	18.9545	-32.6530	0.3308	-0.5699	0.3308	-0.5699	135.6820
18.9555	-32.6522	-1.5376	18.9556	-32.6523	0.6504	-44.9805	18.9545	-32.6530	0.3308	-0.5699	0.3308	-0.5699	144.8616
18.9557	-32.6524	-2.9209	18.9557	-32.6526	0.3424	-39.1423	18.9546	-32.6530	0.3308	-0.5699	0.3308	-0.5699	128.2314
18.9558	-32.6527	-19.1867	18.9558	-32.6529	0.0521	-33.6409	18.9546	-32.6530	0.3308	-0.5699	0.3308	-0.5699	138.6895
18.9558	-32.6531	4.6172	18.9558	-32.6532	-0.2166	-28.5477	18.9544	-32.6529	0.3308	-0.5699	0.3308	-0.5699	155.5358
18.9557	-32.6534	2.0060	18.9557	-32.6536	-0.4985	-23.2040							
18.9556	-32.6537												
												Average	147.2099
												Radius	145

PKNKP - R01217A		Linear Calculations					Intersection		Radians				
Long	Lat	Gradient	Mid_Long	Mid_Lat	Perp	Intercept	Long_2	Lat_2	Long	Lat	Long_2	Lat_2	Radius
18.9548	-32.6517	-0.3380	18.9548	-32.6517	2.9582	-88.7240							
18.9549	-32.6517	-0.4547	18.9550	-32.6518	2.1992	-74.3377	18.9544	-32.6532	0.3308	-0.5699	0.3308	-0.5699	163.6010
18.9551	-32.6518	-0.6037	18.9552	-32.6519	1.6565	-64.0513	18.9543	-32.6533	0.3308	-0.5699	0.3308	-0.5699	177.0053
18.9552	-32.6519	-0.7578	18.9553	-32.6520	1.3196	-57.6650	18.9544	-32.6532	0.3308	-0.5699	0.3308	-0.5699	166.9448
18.9554	-32.6520	-0.9503	18.9554	-32.6521	1.0523	-52.5985	18.9548	-32.6527	0.3308	-0.5699	0.3308	-0.5699	99.5171
18.9555	-32.6521	-1.3647	18.9556	-32.6522	0.7328	-46.5421	18.9539	-32.6534	0.3308	-0.5699	0.3308	-0.5699	219.9239
18.9556	-32.6523	-1.6130	18.9556	-32.6523	0.6200	-44.4042	18.9544	-32.6531	0.3308	-0.5699	0.3308	-0.5699	160.8979
18.9557	-32.6524	-2.0715	18.9557	-32.6525	0.4827	-41.8030	18.9551	-32.6528	0.3308	-0.5699	0.3308	-0.5699	76.9226
18.9557	-32.6525	-4.2935	18.9558	-32.6526	0.2329	-37.0676	18.9544	-32.6529	0.3308	-0.5699	0.3308	-0.5699	157.3467
18.9558	-32.6527	-8.2183	18.9558	-32.6528	0.1217	-34.9593	18.9521	-32.6532	0.3308	-0.5699	0.3308	-0.5699	412.0213
18.9558	-32.6528	-12.4891	18.9558	-32.6529	0.0801	-34.1707	18.9550	-32.6530	0.3308	-0.5699	0.3308	-0.5699	86.8051
18.9558	-32.6530	8.0423	18.9558	-32.6531	-0.1243	-30.2961	18.9533	-32.6528	0.3308	-0.5699	0.3308	-0.5699	277.5472
18.9558	-32.6531	5.2349	18.9558	-32.6532	-0.1910	-29.0322	18.9546	-32.6530	0.3308	-0.5699	0.3308	-0.5699	138.2091
18.9558	-32.6533	3.0358	18.9557	-32.6534	-0.3294	-26.4092	18.9547	-32.6531	0.3308	-0.5699	0.3308	-0.5699	116.2726
18.9557	-32.6535	1.9667	18.9557	-32.6535	-0.5085	-23.0154							
18.9556	-32.6536												
												Average	173.3088
												Radius	175

Appendix E

The following data below were collected and processed to determine the superelevation of the critical sections that subjected heavy vehicles to curve radius.

Dutoitskloof Pass

Stake	Hor. Angle			Vert. Angle			Sight Distance	Calculations							
	Degree	Min	Sec	Degree	Min	Sec		H_DEG	V_DEG	H_DIST	V_DIST	ΔVert	ΔHor	α	*e*
1-1	0	0	0	88	34	12	37.197	0.00	88.57	37.185	0.9283	0.6644	6.573	5.77	0.101
1-2	349	54	53	89	35	49	37.509	349.91	89.60	37.508	0.2639				
2-1	358	42	18	88	56	53	48.423	358.71	88.95	48.415	0.8890	0.6504	6.629	5.60	0.098
2-2	350	50	25	89	42	59	48.205	350.84	89.72	48.204	0.2386				
3-1	356	49	38	89	6	0	60.412	356.83	89.10	60.405	0.9489	0.6499	6.659	5.57	0.098
3-2	350	30	35	89	42	46	59.639	350.51	89.71	59.638	0.2990				
4-1	355	13	40	89	9	9	69.985	355.23	89.15	69.977	1.0352	0.6618	6.623	5.71	0.100
4-2	349	50	6	89	41	22	68.888	349.84	89.69	68.887	0.3734				
5-1	353	1	10	89	11	58	83.045	353.02	89.20	83.037	1.1603	0.6751	6.661	5.79	0.101
5-2	348	31	25	89	39	30	81.366	348.52	89.66	81.365	0.4852				
											Average	0.6603	6.6291	5.6886	**0.0996**

Houwhoek Pass

Stake	Hor. Angle			Vert. Angle			Sight Distance	Calculations							
	Degree	Min	Sec	Degree	Min	Sec		H_DEG	V_DEG	H_DIST	V_DIST	ΔVert	ΔHor	α	*e*
1-1	0	0	0	87	34	34	24.149	0.00	87.58	24.127	1.0213	0.9023	7.475	6.88	0.121
1-2	17	11	40	89	40	20	20.811	17.19	89.67	20.811	0.1191				
2-1	12	19	51	89	46	1	34.975	12.33	89.77	34.975	0.1423	0.9314	7.456	7.12	0.125
2-2	24	22	32	91	23	0	32.690	24.38	91.38	32.680	-0.7892				
3-1	19	42	53	90	51	59	46.220	19.71	90.87	46.215	-0.6989	0.8513	7.426	6.54	0.115
3-2	28	35	53	92	2	9	43.636	28.60	92.04	43.608	-1.5501				
4-1	25	1	43	91	32	23	57.774	25.03	91.54	57.753	-1.5524	0.8778	7.391	6.77	0.119
4-2	32	9	42	92	30	23	55.571	32.16	92.51	55.518	-2.4302				
5-1	28	55	38	91	59	6	68.651	28.93	91.99	68.610	-2.3779	0.8293	7.324	6.46	0.113
5-2	34	46	43	92	46	43	66.160	34.78	92.78	66.082	-3.2072				
											Average	0.8784	7.4143	6.7552	**0.1185**

Hex River Pass

Stake	Hor. Angle			Vert. Angle			Sight Distance	Calculations							
	Degree	Min	Sec	Degree	Min	Sec		H_DEG	V_DEG	H_DIST	V_DIST	ΔVert	ΔHor	α	*e*
1-1	0	0	0	92	27	46	12.946	0.00	92.46	12.934	-0.5563	0.7393	7.381	5.72	0.100
1-2	329	14	9	95	8	46	14.444	329.24	95.15	14.386	-1.2956				
2-1	355	39	48	92	50	8	26.729	355.66	92.84	26.696	-1.3223	0.7612	7.403	5.87	0.103
2-2	339	58	19	94	21	29	27.418	339.97	94.36	27.339	-2.0835				
3-1	351	44	56	92	58	42	42.023	351.75	92.98	41.966	-2.1834	0.7345	7.399	5.67	0.099
3-2	341	36	38	94	4	52	41	341.61	94.08	40.896	-2.9179				
4-1	347	54	48	93	2	45	57.059	347.91	93.05	56.978	-3.0318	0.7808	7.390	6.03	0.106
4-2	340	29	19	93	54	13	56.003	340.49	93.90	55.873	-3.8126				
5-1	344	37	35	93	5	28	70.456	344.63	93.09	70.353	-3.7993	0.7794	7.382	6.03	0.106
5-2	338	40	10	93	48	10	69.037	338.67	93.80	68.885	-4.5787				
											Average	0.7590	7.3909	5.8636	**0.1027**

Piekenierskloof Pass

Stake	Hor. Angle			Vert. Angle			Sight Distance	Calculations							
	Degree	Min	Sec	Degree	Min	Sec		H_DEG	V_DEG	H_DIST	V_DIST	ΔVert	ΔHor	α	*e*
1-1	0	0	0	88	36	46	69.854	0.00	88.61	69.834	1.6911	1.0657	10.676	5.70	0.100
1-2	351	33	9	89	27	29	66.125	351.55	89.46	66.122	0.6254				
2-1	356	3	12	88	48	33	80.788	356.05	88.81	80.771	1.6790	1.0841	10.616	5.83	0.102
2-2	349	7	12	89	33	5	75.982	349.12	89.55	75.980	0.5949				
3-1	352	31	17	88	55	53	92.185	352.52	88.93	92.169	1.7192	1.0935	10.799	5.78	0.101
3-2	346	15	35	89	35	28	87.676	346.26	89.59	87.674	0.6257				
4-1	349	5	1	89	2	16	103.532	349.08	89.04	103.517	1.7386	1.0545	10.798	5.58	0.098
4-2	343	38	40	89	36	8	98.546	343.64	89.60	98.544	0.6842				
											Average	1.0744	10.7223	5.7226	**0.1002**

Appendix F

Appendix F1

Heavy Vehicle Summary								
Truck ID	Axels	Ave Axels	Avg_Mass	StDev	Entry	Apex	Exit	Profile
DTKP_10	7	7	33040	3754.2	55.8	64.9	57.1	Downward Parabola
DTKP_13	6	6	37675	7859.2	62.3	67.7	61.7	Downward Parabola
DTKP_15	6	6	42858	1629.8	54.3	62.4	65.7	Increasing
DTKP_16	5	5	27945	6609.8	36.8	47.3	44.7	Skew Left Down
DTKP_18	6	6	39849	5712.6	39.0	53.3	40.8	Downward Parabola
DTKP_19	6	6	47657	775.7	76.6	59.5	95.2	Skew Right Up
DTKP_20	7	7	50706	4188.5	54.8	44.8	52.7	Upward Parabola
DTKP_21	7	7	51378	9644.1	58.0	67.3	67.9	Increasing
DTKP_22	7	7	45910	5490.0	69.9	58.2	57.9	Decreasing
DTKP_23	7	7	49244	9136.0	46.7	47.0	62.6	Increasing
DTKP_24	5	5	36524	1735.5	94.8	66.5	103.5	Skew Right Up
DTKP_25	6	6	45840	2032.5	55.4	63.1	59.2	Skew Left Down
DTKP_27	5	5	40928	650.7	60.9	43.0	50.0	Skew Left Up
DTKP_28	5	5	37350	490.0	45.0	52.6	47.8	Skew Left Down
DTKP_29	5	5	37350	490.0	81.4	47.1	57.5	Skew Left Up
DTKP_30	6	6	36037	13446.2	41.6	45.3	62.9	Increasing
DTKP_31	7	7	50287	11934.7	54.0	57.8	36.4	Skew Right Down
DTKP_32	7	7	34448	5399.7	53.3	65.2	69.8	Increasing
DTKP_33	5	5	24980	7175.2	43.5	58.8	57.3	Skew Left Down
DTKP_34	6	6	35978	9090.4	47.9	56.8	53.5	Skew Left Down
DTKP_37	7	7	52543	2027.3	49.7	57.9	53.6	Skew Left Down
DTKP_39	5	5	23433	3535.0	56.1	52.9	56.1	Upward Parabola
DTKP_41	6	6	44234	7606.6	62.6	43.1	59.4	Skew Left Up
DTKP_42	7	7	30869	5567.7	58.0	60.7	66.8	Increasing
DTKP_5	4	4	18937	3454.1	56.6	68.4	62.2	Skew Left Down
DTKP_53	6	6	24622	5179.4	50.6	57.3	67.9	Increasing
DTKP_6	7	7	39809	12972.2	53.5	68.6	63.5	Skew Left Down
DTKP_7	6	6	34436	10137.2	43.4	55.5	62.8	Increasing
DTKP_8	6	6	34436	10137.2	71.9	57.8	79.3	Skew Right Up
HGNTT_101	7	7	52655	1886.9	57.0	57.7	45.8	Skew Right Down
HGNTT_102	7	7	53140	1753.7	47.3	57.7	46.5	Downward Parabola
HGNTT_110	6	6	33240	13288.2	46.9	49.2	36.0	Skew Right Down
HGNTT_111	7	6	32380	3945.3	52.5	62.4	46.2	Skew Right Down
HGNTT_14	6	6	37952	9462.0	33.1	39.0	33.9	Downward Parabola
HGNTT_15	7	7	48192	6941.1	60.0	52.8	41.7	Decreasing
HGNTT_16	7	7	50250	11473.0	54.9	42.3	28.7	Decreasing
HGNTT_18	7	7	37653	5441.2	52.8	58.9	48.0	Skew Right Down
HGNTT_19	7	7	37455	10215.8	47.1	60.1	41.5	Skew Right Down
HGNTT_20	5	5	25065	3866.0	58.5	61.1	40.0	Skew Right Down
HGNTT_24	4	4	27446	7740.4	56.4	61.7	44.0	Skew Right Down
HGNTT_25	6	6	28394	4748.7	33.2	35.1	25.7	Skew Right Down
HGNTT_26	7	7	47680	10364.6	66.9	62.2	52.9	Decreasing
HGNTT_31	4	5	26976	12426.2	66.0	77.9	46.1	Skew Right Down
HGNTT_32	6	6	32508	5539.2	46.6	44.2	35.5	Decreasing
HGNTT_34	7	7	47658	8429.3	51.1	58.3	38.8	Skew Right Down
HGNTT_35	6	6	38530	10156.4	57.5	59.5	40.4	Skew Right Down
HGNTT_36	7	7	51690	7119.9	36.2	40.4	33.4	Skew Right Down
HGNTT_37	6	6	43387	6674.3	60.1	55.9	42.1	Decreasing
HGNTT_39	6	6	27088	4616.5	33.2	43.3	35.8	Skew Left Down
HGNTT_48	6	6	24957	4911.7	52.8	57.3	47.6	Skew Right Down
HGNTT_49	6	6	35457	7254.3	60.3	56.6	63.0	Upward Parabola
HGNTT_53	7	7	51588	5795.1	36.9	41.0	34.4	Skew Right Down
HGNTT_55	7	7	42288	6469.9	43.7	41.6	33.2	Decreasing
HGNTT_56	6	6	39012	7220.8	34.0	38.9	35.8	Skew Left Down
HGNTT_57	5	5	24080	0.0	56.5	53.3	43.1	Decreasing
HGNTT_60	6	6	31556	4322.6	45.7	41.8	32.7	Decreasing
HGNTT_61	7	7	45689	8834.8	49.3	61.5	45.6	Skew Right Down
HGNTT_62	7	7	54148	7711.1	60.7	59.4	44.8	Decreasing
HGNTT_63	7	7	50229	13133.0	57.7	63.6	36.0	Skew Right Down
HGNTT_64	6	6	17007	1686.7	41.6	51.6	32.9	Skew Right Down
HGNTT_65	7	7	45005	8594.5	24.8	26.1	19.6	Skew Right Down
HGNTT_66	7	7	35269	5497.2	42.5	49.9	35.9	Skew Right Down
HGNTT_67	5	5	27383	5460.1	64.2	73.7	55.4	Skew Right Down

HGNTT_68	6	6	31911	5668.5	55.2	57.7	32.5	Skew Right Down
HGNTT_69	6	6	29170	5723.0	50.3	62.4	45.1	Skew Right Down
HGNTT_70	4	4	20473	5596.6	59.8	54.9	43.2	Decreasing
HGNTT_73	7	7	36563	6035.3	64.0	62.5	39.8	Decreasing
HGNTT_74	7	7	48757	12627.0	51.5	55.0	37.3	Skew Right Down
HGNTT_75	7	7	51304	5394.5	38.4	41.5	30.7	Skew Right Down
HGNTT_77	5	5	28596	6541.9	43.4	45.4	36.6	Skew Right Down
HGNTT_83	6	6	32326	7378.4	49.5	59.3	41.0	Skew Right Down
HGNTT_86	6	6	46936	303.2	47.1	53.8	42.3	Skew Right Down
HGNTT_90	5	7	45115	10391.0	37.8	39.0	28.6	Skew Right Down
HGNTT_91	7	7	40040	5673.4	59.9	62.3	50.5	Skew Right Down
HGNTT_95	7	7	44392	8215.8	48.4	54.1	39.0	Skew Right Down
HGNTT_96	7	7	55810	565.6	44.2	42.7	33.9	Decreasing
HGNTT_97	5	5	26628	5910.6	65.0	60.4	40.5	Decreasing
HHP_11	5	5	31239	11675.3	41.8	55.7	62.8	Increasing
HHP_12	5	5	32874	10653.4	42.6	60.3	64.9	Increasing
HHP_15	6	6	46494	207.6	27.2	33.7	51.1	Increasing
HHP_17	6	5	40701	12213.0	61.8	72.4	98.2	Increasing
HHP_18	6	6	47134	66.0	78.9	61.3	58.3	Decreasing
HHP_19	6	6	32440	9815.7	69.8	71.2	75.7	Increasing
HHP_2	7	7	56099	1930.3	69.6	56.1	56.2	Skew Left Up
HHP_21	6	6	47019	1455.0	53.3	72.0	76.7	Increasing
HHP_22	6	6	33276	6714.7	73.7	48.5	46.9	Decreasing
HHP_23	6	6	39302	6526.5	105.2	59.3	68.1	Skew Left Up
HHP_24	6	6	39525	7171.4	56.6	60.7	64.7	Increasing
HHP_25	7	7	46711	11258.0	70.9	83.6	69.0	Downward Parabola
HHP_27	4	4	30000	311.1	77.6	41.2	45.3	Skew Left Up
HHP_28	7	7	55788	258.4	34.0	46.1	51.6	Increasing
HHP_29	7	7	55788	258.4	56.7	60.7	43.4	Skew Right Down
HHP_3	7	7	55272	1844.7	71.6	78.1	101.8	Increasing
HHP_30	8	6	21060	0.0	59.3	65.8	80.6	Increasing
HHP_31	8	6	20427	197.5	100.2	79.0	87.6	Skew Left Up
HHP_34	6	6	44598	7158.7	75.1	78.1	89.6	Increasing
HHP_35	6	6	45338	1125.2	22.2	23.5	18.4	Skew Right Down
HHP_36	6	6	38654	14003.8	18.2	19.2	18.9	Downward Parabola
HHP_37	7	7	53815	2935.7	52.1	42.7	42.1	Decreasing
HHP_38	6	6	38113	5227.1	67.3	74.0	49.8	Skew Right Down
HHP_39	7	6	31435	13416.7	5.6	8.2	21.2	Increasing
HHP_4	4	5	34605	1120.6	72.4	72.5	62.9	Skew Right Down
HHP_40	6	6	47240	0.0	41.8	57.2	68.2	Increasing
HHP_41	6	6	41587	2300.9	84.4	83.5	72.8	Decreasing
HHP_43	6	6	41354	1570.9	75.1	81.1	101.0	Increasing
HHP_44	4	4	21688	1777.8	47.2	61.4	66.8	Increasing
HHP_45	6	6	33400	1920.0	80.6	56.9	60.7	Skew Left Up
HHP_46	7	7	53415	1111.6	55.0	54.7	59.8	Skew Right Up
HHP_48	8	8	50719	9831.4	61.5	57.5	55.4	Decreasing
HHP_49	8	8	51344	8246.8	73.0	55.2	57.6	Skew Left Up
HHP_5	6	6	33968	3392.5	63.6	68.2	77.8	Increasing
HHP_50	7	7	41194	13298.1	20.4	27.3	58.5	Increasing
HHP_51	4	4	21372	3665.3	79.0	80.9	70.1	Skew Right Down
HHP_52	7	7	43583	10535.5	47.3	44.0	38.6	Decreasing
HHP_53	5	5	18144	3248.6	76.8	74.8	67.2	Decreasing
HHP_54	7	7	50120	120.0	44.0	51.4	64.7	Increasing
HHP_55	6	6	41196	8259.8	46.2	52.2	66.5	Increasing
HHP_56	6	6	39107	11785.1	36.3	43.3	30.4	Skew Right Down
HHP_57	7	7	55295	1055.2	80.3	82.5	70.0	Skew Right Down
HHP_58	6	6	40530	12086.7	76.4	46.0	57.8	Skew Left Up
HHP_6	7	6	49777	3013.1	75.7	63.7	56.8	Decreasing
HHP_60	7	7	41425	8648.5	88.8	65.0	79.3	Skew Left Up
HHP_61	7	7	51474	6999.5	57.3	49.3	52.7	Skew Left Up
HHP_62	7	7	44153	10435.2	34.6	30.5	51.5	Skew Right Up
HHP_64	6	6	37595	12801.4	51.4	57.6	47.1	Skew Right Down
HHP_65	4	4	14487	2476.4	82.1	72.1	66.1	Decreasing
HHP_7	7	7	52940	2017.3	61.1	66.4	89.1	Increasing
HHP_8	7	7	52940	2017.3	71.4	57.0	57.0	Decreasing
HHP_9	6	6	31023	2680.9	90.8	62.3	57.3	Decreasing
HRP_11	7	7	46654	9837.9	20.3	17.5	16.9	Decreasing
HRP_16	4	4	15946	3716.5	69.5	57.7	59.0	Skew Left Up
HRP_17	6	6	37973	9463.7	66.7	54.4	57.8	Skew Left Up
HRP_22	7	7	48334	9471.6	43.6	39.7	37.2	Decreasing

HRP_23	7	7	48067	3531.2	51.8	45.3	55.2	Skew Right Up
HRP_24	6	6	36790	6863.2	26.2	24.9	28.6	Skew Right Up
HRP_26	7	7	52689	2051.0	50.9	57.9	45.9	Skew Right Down
HRP_28	7	7	49474	8230.1	53.9	60.2	45.0	Skew Right Down
HRP_29	5	5	34024	3603.1	56.9	45.3	52.0	Skew Left Up
HRP_30	6	7	47717	8286.5	38.6	33.7	28.7	Decreasing
HRP_31	7	7	54200	0.0	33.2	32.4	36.2	Skew Right Up
HRP_32	7	7	49341	10076.6	47.5	43.0	39.6	Decreasing
HRP_35	7	7	45289	11669.3	47.2	47.8	42.2	Skew Right Down
HRP_37	7	7	36485	5281.1	43.0	47.7	41.9	Downward Parabola
HRP_44	5	5	32726	1101.3	65.1	69.2	45.5	Skew Right Down
HRP_47	7	7	46036	9228.1	42.8	45.1	38.4	Skew Right Down
HRP_48	7	7	51567	6202.7	36.5	31.9	41.7	Skew Right Up
HRP_52	5	5	34720	2219.8	54.8	48.8	48.1	Decreasing
HRP_53	7	7	50804	4471.2	49.6	49.8	58.9	Increasing
HRP_54	7	7	44392	8215.8	53.3	43.0	53.9	Upward Parabola
HRP_56	7	7	33969	3128.9	80.7	75.2	64.2	Decreasing
HRP_7	7	7	38939	14758.5	42.2	38.9	36.3	Decreasing
PKNKP_1	7	7	47800	10853.0	38.9	45.0	32.1	Skew Right Down
PKNKP_10	6	7	41189	12402.1	67.2	102.9	83.4	Skew Left Down
PKNKP_11	4	6	16260	0.0	54.3	92.3	74.0	Skew Left Down
PKNKP_12	5	7	34440	8807.4	52.9	79.6	66.1	Skew Left Down
PKNKP_14	6	6	47449	1976.8	60.9	61.5	56.6	Skew Right Down
PKNKP_16	8	7	44980	11685.6	42.5	54.1	48.1	Skew Left Down
PKNKP_17	7	7	52793	1221.7	51.3	70.0	55.7	Skew Left Down
PKNKP_18	6	6	44898	4570.0	61.5	73.2	69.4	Skew Left Down
PKNKP_19	5	6	49581	2387.6	52.6	67.0	60.5	Skew Left Down
PKNKP_2	7	7	42127	10875.6	36.6	58.3	48.2	Skew Left Down
PKNKP_22	7	7	51520	1681.8	52.5	64.3	52.4	Downward Parabola
PKNKP_23	7	7	47146	10006.6	42.2	47.5	39.4	Skew Right Down
PKNKP_26	6	6	45382	9126.9	67.7	70.4	60.8	Skew Right Down
PKNKP_27	7	7	55698	601.4	57.7	72.6	67.9	Skew Left Down
PKNKP_29	7	7	54238	4346.0	74.1	72.5	62.7	Decreasing
PKNKP_3	6	6	30485	5608.7	42.3	36.5	39.1	Skew Left Up
PKNKP_30	6	6	42780	4148.9	53.3	54.1	40.8	Skew Right Down
PKNKP_31	7	7	44503	6928.6	50.7	40.1	37.1	Decreasing
PKNKP_32	6	6	40945	7094.2	53.7	56.4	59.9	Increasing
PKNKP_33	8	7	50326	11463.3	25.3	23.9	21.4	Decreasing
PKNKP_34	6	6	41744	4564.3	55.0	55.1	54.5	Downward Parabola
PKNKP_35	4	4	22995	3326.6	49.6	40.3	46.3	Skew Left Up
PKNKP_36	7	7	38894	4405.3	35.4	29.5	44.8	Skew Right Up
PKNKP_37	6	6	47657	775.7	42.1	44.3	33.9	Skew Right Down
PKNKP_38	6	6	47657	775.7	41.7	45.8	43.1	Downward Parabola
PKNKP_39	7	6	46996	1008.9	67.1	59.8	72.5	Skew Right Up
PKNKP_4	6	5	36393	2762.6	61.3	72.8	63.8	Downward Parabola
PKNKP_40	7	7	55280	1596.6	71.1	69.2	51.2	Decreasing
PKNKP_41	7	7	55280	1596.6	74.8	75.0	57.4	Skew Right Down
PKNKP_42	6	6	44732	2980.6	45.5	50.5	38.7	Skew Right Down
PKNKP_43	7	7	54629	1782.5	47.0	53.9	51.2	Skew Left Down
PKNKP_44	7	7	54629	1782.5	65.2	66.9	57.3	Skew Right Down
PKNKP_45	7	6	34975	13404.1	49.4	50.6	52.9	Increasing
PKNKP_46	6	6	38685	14375.6	40.8	54.7	63.8	Increasing
PKNKP_48	7	7	48458	10539.9	74.3	71.4	71.1	Decreasing
PKNKP_49	5	7	27105	6375.3	54.9	63.0	56.3	Downward Parabola
PKNKP_5	7	7	32003	3388.5	61.5	67.0	63.9	Downward Parabola
PKNKP_50	7	7	51886	2770.1	65.7	68.3	66.0	Downward Parabola
PKNKP_51	6	6	35262	6310.9	16.5	23.3	22.4	Skew Left Down
PKNKP_52	7	7	52536	4936.4	77.6	52.4	76.6	Upward Parabola
PKNKP_55	7	7	48307	7995.3	44.4	38.3	35.4	Decreasing
PKNKP_56	6	6	42373	7346.9	38.7	51.1	39.6	Downward Parabola
PKNKP_57	7	7	49596	8082.2	47.0	58.1	47.0	Downward Parabola
PKNKP_58	4	4	17939	1532.7	32.9	30.6	37.9	Skew Right Up
PKNKP_59	8	8	47864	13895.0	70.1	68.9	68.8	Decreasing
PKNKP_6	6	6	48372	852.5	56.8	76.9	62.4	Skew Left Down
PKNKP_60	7	7	54737	892.1	43.3	58.6	62.7	Increasing
PKNKP_61	6	6	44745	5815.8	23.4	33.0	30.9	Skew Left Down
PKNKP_62	6	6	39645	9516.8	79.4	75.9	69.5	Decreasing
PKNKP_63	7	7	54845	2028.2	43.2	36.4	34.4	Decreasing
PKNKP_64	7	7	51638	7565.7	55.6	55.2	53.3	Decreasing
PKNKP_65	7	7	50287	11934.7	25.0	22.5	23.5	Skew Left Up

PKNKP_66	6	6	39076	10628.3	39.4	41.7	39.3	Downward Parabola
PKNKP_67	7	7	37893	7540.8	45.0	65.9	51.2	Skew Left Down
PKNKP_68	6	7	47986	8601.0	77.8	75.5	63.8	Decreasing
PKNKP_69	6	6	40694	12321.2	52.2	74.6	64.7	Skew Left Down
PKNKP_7	7	7	47212	9756.0	14.2	25.0	23.3	Skew Left Down
PKNKP_70	7	7	51787	6885.6	68.5	65.0	51.5	Decreasing
PKNKP_71	6	6	39800	13577.8	79.9	78.4	65.3	Decreasing
PKNKP_72	6	6	39116	11567.2	69.7	84.6	75.5	Skew Left Down
PKNKP_73	7	7	48741	8436.7	38.1	47.5	39.3	Downward Parabola
PKNKP_74	5	6	45785	8252.8	81.3	80.9	74.2	Decreasing
PKNKP_75	5	6	47314	7025.6	66.0	78.2	76.9	Skew Left Down
PKNKP_76	6	6	46334	3795.4	87.6	86.4	76.5	Decreasing
PKNKP_77	7	7	55209	626.0	46.6	56.9	52.5	Skew Left Down
PKNKP_78	6	6	43831	5471.6	89.6	81.4	76.8	Decreasing
PKNKP_79	5	5	25656	2881.2	64.9	27.9	126.8	Skew Right Up
PKNKP_8	7	7	47212	9756.0	19.8	29.6	40.7	Increasing
PKNKP_80	6	6	26323	1772.3	66.6	69.0	62.1	Skew Right Down
PKNKP_81	6	6	26323	1772.3	72.8	76.0	80.1	Increasing
PKNKP_84	6	6	40836	10384.9	86.6	79.2	69.2	Decreasing
PKNKP_85	6	6	32450	10710.0	48.4	62.1	50.5	Downward Parabola
PKNKP_9	5	6	48089	937.4	68.2	90.1	72.8	Skew Left Down
PKNKP_90	5	6	46954	5515.4	73.6	79.5	76.8	Downward Parabola
SLP_11	6	5	38454	9262.2	63.5	60.6	98.6	Skew Right Up
SLP_13	6	6	44868	2366.7	39.8	57.0	61.3	Increasing
SLP_17	6	6	38031	7576.7	82.7	93.2	64.8	Skew Right Down
SLP_18	6	6	40245	12503.5	42.8	72.4	91.7	Increasing
SLP_19	6	6	44239	5598.1	78.9	93.5	107.9	Increasing
SLP_2	6	6	25430	9875.0	24.6	45.2	73.8	Increasing
SLP_22	6	6	28016	4556.8	62.0	88.6	111.9	Increasing
SLP_23	6	6	43278	7083.9	44.7	49.8	77.7	Increasing
SLP_24	4	4	28228	6000.3	46.3	52.8	57.8	Increasing
SLP_3	6	7	47489	5503.0	18.5	38.4	52.8	Increasing
SLP_4	7	7	52940	2017.3	43.6	54.5	58.1	Increasing
SLP_6	6	6	27388	9140.6	30.2	41.2	44.4	Increasing
SLP_9	6	6	38858	7627.3	99.2	63.9	56.8	Decreasing

Appendix F2

Dutoitskloof Pass		**Entry Time [s]**			**Apex Time [s]**			**Exit Time [s]**			**Speed [km/h]**			**Shape**
ID	**Axels**	**T1**	**T2**	**ΔT**	**T1**	**T2**	**ΔT**	**T1**	**T2**	**ΔT**	**Entry**	**Apex**	**Exit**	**0.05**
DTKP_1	6	2.67	4.32	**1.65**	2.93	4.30	**1.37**	2.71	4.05	**1.34**	54.7	61.9	68.2	Increasing
DTKP_2	6	4.04	5.93	**1.89**	4.08	5.79	**1.70**	3.12	5.18	**2.05**	47.8	49.9	44.5	Skew Right Down
DTKP_3	7	5.43	7.22	**1.80**	3.53	5.52	**2.00**	4.34	6.06	**1.72**	50.3	42.5	53.2	Skew Right Up
DTKP_4	5	4.90	6.35	**1.45**	3.75	5.32	**1.58**	3.44	4.44	**1.00**	62.3	53.9	91.4	Skew Right Up
DTKP_5	4	3.93	5.52	**1.60**	3.24	4.48	**1.24**	1.98	3.45	**1.47**	56.6	68.4	62.2	Skew Left Down
DTKP_6	7	5.28	6.97	**1.69**	2.26	3.50	**1.24**	1.65	3.09	**1.44**	53.5	68.6	63.5	Skew Left Down
DTKP_7	6	1.62	3.71	**2.08**	3.33	4.86	**1.53**	3.46	4.92	**1.46**	43.4	55.5	62.8	Increasing
DTKP_8	6	4.68	5.93	**1.26**	3.69	5.16	**1.47**	2.25	3.41	**1.15**	71.9	57.8	79.3	Skew Right Up
DTKP_9	4	1.79	3.19	**1.40**	2.78	4.43	**1.65**	2.49	3.88	**1.39**	64.5	51.5	65.9	Upward Parabola
DTKP_10	7	1.93	3.55	**1.62**	2.51	3.82	**1.31**	2.20	3.80	**1.60**	55.8	64.9	57.1	Downward Parabola
DTKP_11	5	2.02	3.39	**1.37**	2.28	3.48	**1.20**	2.34	3.80	**1.47**	65.8	70.5	62.3	Skew Right Down
DTKP_12	7	3.16	4.31	**1.15**	2.12	3.51	**1.39**	2.43	3.80	**1.37**	78.6	61.1	66.7	Skew Left Up
DTKP_13	6	2.66	4.11	**1.45**	2.09	3.35	**1.25**	2.28	3.76	**1.48**	62.3	67.7	61.7	Downward Parabola
DTKP_14	4	4.12	5.25	**1.13**	2.99	4.41	**1.43**	2.79	4.15	**1.36**	80.0	59.5	67.2	Skew Left Up
DTKP_15	6	5.16	6.83	**1.66**	3.45	4.81	**1.36**	3.03	4.42	**1.39**	54.3	62.4	65.7	Increasing
DTKP_16	5	6.60	9.05	**2.46**	3.55	5.34	**1.80**	3.74	5.78	**2.05**	36.8	47.3	44.7	Skew Left Down
DTKP_17	7	4.46	7.29	**2.84**	4.65	6.60	**1.95**	2.78	4.45	**1.67**	31.9	43.6	54.7	Increasing
DTKP_18	6	4.64	6.95	**2.32**	3.78	5.38	**1.60**	4.52	6.76	**2.24**	39.0	53.3	40.8	Downward Parabola
DTKP_19	6	3.96	5.14	**1.18**	3.07	4.49	**1.43**	3.08	4.04	**0.96**	76.6	59.5	95.2	Skew Right Up
DTKP_20	7	4.31	5.96	**1.65**	2.84	4.73	**1.90**	2.48	4.21	**1.74**	54.8	44.8	52.7	Upward Parabola
DTKP_21	7	3.45	5.00	**1.56**	3.33	4.60	**1.26**	2.74	4.08	**1.35**	58.0	67.3	67.9	Increasing
DTKP_22	7	3.77	5.07	**1.29**	2.55	4.01	**1.46**	2.99	4.57	**1.58**	69.9	58.2	57.9	Decreasing
DTKP_23	7	3.41	5.35	**1.93**	3.87	5.68	**1.81**	3.22	4.68	**1.46**	46.7	47.0	62.6	Increasing
DTKP_24	5	5.25	6.21	**0.95**	1.89	3.16	**1.28**	2.35	3.23	**0.88**	94.8	66.5	103.5	Skew Right Up
DTKP_25	6	3.58	5.21	**1.63**	3.04	4.38	**1.35**	3.25	4.80	**1.54**	55.4	63.1	59.2	Skew Left Down
DTKP_26	6	2.28	3.16	**0.88**	2.34	3.59	**1.26**	2.18	3.17	**0.99**	102.7	67.6	92.4	Skew Left Up
DTKP_27	5	7.48	8.97	**1.48**	3.97	5.95	**1.98**	3.77	5.60	**1.83**	60.9	43.0	50.0	Skew Left Up
DTKP_28	5	2.72	4.72	**2.01**	2.50	4.12	**1.62**	3.74	5.65	**1.91**	45.0	52.6	47.8	Skew Left Down

DTKP_29	5	2.90	4.01	**1.11**	3.26	5.07	**1.80**	4.84	6.43	**1.59**	81.4	47.1	57.5	Skew Left Up
DTKP_30	6	5.76	7.93	**2.17**	4.83	6.71	**1.88**	3.54	4.99	**1.45**	41.6	45.3	62.9	Increasing
DTKP_31	7	1.17	2.85	**1.67**	3.08	4.55	**1.47**	5.62	8.13	**2.51**	54.0	57.8	36.4	Skew Right Down
DTKP_32	7	2.22	3.91	**1.70**	2.55	3.85	**1.30**	2.13	3.44	**1.31**	53.3	65.2	69.8	Increasing
DTKP_33	5	4.15	6.22	**2.08**	3.68	5.12	**1.45**	2.97	4.56	**1.60**	43.5	58.8	57.3	Skew Left Down
DTKP_34	6	1.89	3.78	**1.88**	2.39	3.89	**1.50**	2.60	4.31	**1.71**	47.9	56.8	53.5	Skew Left Down
DTKP_35	6	1.25	2.17	**0.92**	1.92	3.16	**1.24**	2.54	3.32	**0.78**	98.7	68.5	117.2	Skew Right Up
DTKP_36	7	5.62	6.92	**1.30**	4.66	6.53	**1.86**	4.13	5.89	**1.76**	69.5	45.6	52.0	Skew Left Up
DTKP_37	7	3.22	5.04	**1.82**	3.79	5.25	**1.47**	3.11	4.82	**1.71**	49.7	57.9	53.6	Skew Left Down
DTKP_38	6	4.35	6.36	**2.01**	2.88	4.45	**1.57**	2.35	3.93	**1.58**	45.1	54.2	57.8	Increasing
DTKP_39	5	6.64	8.25	**1.61**	4.12	5.72	**1.61**	4.11	5.74	**1.63**	56.1	52.9	56.1	Upward Parabola
DTKP_40	6	4.51	6.21	**1.70**	4.38	5.91	**1.53**	5.27	7.29	**2.01**	53.3	55.5	45.4	Skew Right Down
DTKP_41	6	3.70	5.15	**1.44**	3.95	5.92	**1.97**	4.34	5.88	**1.54**	62.6	43.1	59.4	Skew Left Up
DTKP_42	7	2.20	3.75	**1.56**	2.53	3.93	**1.40**	2.28	3.65	**1.37**	58.0	60.7	66.8	Increasing
DTKP_43	6	4.95	6.32	**1.36**	3.15	4.96	**1.81**	3.92	5.86	**1.94**	66.3	46.9	47.1	Skew Left Up
DTKP_44	7	4.91	6.82	**1.91**	3.15	5.11	**1.97**	3.79	5.27	**1.48**	47.2	43.2	61.7	Skew Right Up
DTKP_45	6	4.99	6.26	**1.27**	0.41	1.67	**1.26**	2.22	3.26	**1.04**	71.2	67.4	88.1	Skew Right Up
DTKP_46	7	5.01	6.85	**1.84**	3.22	5.00	**1.78**	2.27	3.59	**1.32**	49.1	47.8	69.3	Skew Right Up
DTKP_47	6	4.12	5.45	**1.34**	2.68	4.02	**1.34**	2.71	3.84	**1.13**	67.6	63.4	80.7	Skew Right Up
DTKP_48	7	1.44	2.58	**1.15**	3.32	4.76	**1.43**	3.13	4.35	**1.22**	78.8	59.2	74.8	Skew Left Up
DTKP_49	4	5.27	7.09	**1.83**	1.55	3.34	**1.79**	3.91	5.12	**1.21**	49.5	47.5	75.5	Skew Right Up
DTKP_50	7	5.15	6.69	**1.54**	3.10	4.92	**1.82**	3.82	5.11	**1.28**	58.7	46.6	71.3	Skew Right Up
DTKP_51	6	4.26	5.61	**1.36**	2.64	4.05	**1.41**	3.39	4.39	**1.00**	66.6	60.2	91.5	Skew Right Up
DTKP_52	7	6.28	8.73	**2.45**	7.02	9.11	**2.09**	3.37	4.74	**1.37**	36.8	40.7	66.8	Increasing
DTKP_53	6	3.33	5.11	**1.79**	3.40	4.89	**1.48**	2.57	3.91	**1.35**	50.6	57.3	67.9	Increasing

Hex River Pass		**Entry Time [s]**			**Apex Time [s]**			**Exit Time [s]**			**Speed [km/h]**			**Shape**
ID	**Axels**	**T1**	**T2**	**ΔT**	**T1**	**T2**	**ΔT**	**T1**	**T2**	**ΔT**	**EN**	**M**	**EX**	**0.05**
HRP_1	7	6.45	11.01	**4.56**	7.79	8.74	**0.95**	4.52	6.55	**2.03**	36.7	35.7	37.4	Upward Parabola
HRP_2	6	3.47	6.15	**2.68**	3.64	4.29	**0.65**	4.02	5.30	**1.28**	62.6	51.9	59.4	Skew Left Up
HRP_3	7	5.02	8.54	**3.52**	6.75	7.65	**0.90**	7.27	9.28	**2.01**	47.5	37.7	37.8	Skew Left Up
HRP_4	6	6.62	9.33	**2.71**	4.63	5.34	**0.71**	5.02	6.13	**1.11**	61.7	47.7	68.5	Skew Right Up
HRP_5	6	9.23	14.90	**5.67**	11.04	12.37	**1.32**	10.58	13.15	**2.57**	29.5	25.5	29.5	Upward Parabola
HRP_6	7	3.05	5.85	**2.80**	6.31	6.86	**0.55**	5.63	7.17	**1.54**	59.7	61.7	49.3	Skew Right Down
HRP_7	7	5.58	9.56	**3.97**	6.79	7.66	**0.87**	5.79	7.89	**2.09**	42.2	38.9	36.3	Decreasing
HRP_8	6	4.88	8.86	**3.98**	4.49	5.19	**0.69**	4.58	6.23	**1.65**	42.1	48.7	46.1	Skew Left Down
HRP_9	7	7.08	10.41	**3.33**	5.57	6.48	**0.91**	5.57	7.44	**1.87**	50.2	37.1	40.7	Skew Left Up
HRP_10	6	7.69	10.95	**3.26**	4.34	5.03	**0.70**	4.72	5.79	**1.07**	51.3	48.5	70.9	Skew Right Up
HRP_11	7	12.96	21.19	**8.23**	13.35	15.28	**1.93**	13.02	17.51	**4.49**	20.3	17.5	16.9	Decreasing
HRP_12	6	3.58	5.80	**2.22**	3.52	4.03	**0.50**	3.72	4.94	**1.23**	75.4	67.3	62.0	Decreasing
HRP_13	6	5.23	8.40	**3.17**	3.95	4.66	**0.71**	3.05	4.40	**1.35**	52.9	47.6	56.3	Skew Right Up
HRP_14	7	7.23	9.74	**2.50**	4.02	4.61	**0.59**	3.30	4.68	**1.37**	66.8	57.4	55.3	Decreasing
HRP_15	6	5.85	9.46	**3.61**	3.65	4.33	**0.67**	4.22	6.09	**1.87**	46.4	50.3	40.6	Skew Right Down
HRP_16	4	4.36	6.77	**2.41**	3.84	4.42	**0.59**	3.18	4.47	**1.29**	69.5	57.7	59.0	Skew Left Up
HRP_17	6	4.73	7.24	**2.51**	4.54	5.16	**0.62**	3.81	5.12	**1.32**	66.7	54.4	57.8	Skew Left Up
HRP_18	7	8.52	13.05	**4.53**	8.16	9.10	**0.93**	7.78	9.87	**2.09**	37.0	36.2	36.4	Upward Parabola
HRP_19	7	5.36	7.91	**2.56**	3.81	4.51	**0.69**	5.09	6.47	**1.38**	65.4	48.8	55.2	Skew Left Up
HRP_20	6	12.33	18.74	**6.41**	9.84	11.02	**1.18**	7.42	9.78	**2.37**	26.1	28.7	32.1	Increasing
HRP_21	4	8.64	11.83	**3.20**	4.84	5.49	**0.65**	4.84	6.34	**1.51**	52.4	52.3	50.4	Decreasing
HRP_22	7	6.58	10.42	**3.84**	6.82	7.68	**0.85**	6.17	8.21	**2.04**	43.6	39.7	37.2	Decreasing
HRP_23	7	6.01	9.25	**3.23**	4.45	5.19	**0.75**	4.98	6.36	**1.38**	51.8	45.3	55.2	Skew Right Up
HRP_24	6	10.28	16.66	**6.39**	7.92	9.28	**1.36**	12.20	14.85	**2.65**	26.2	24.9	28.6	Skew Right Up
HRP_25	7	2.57	4.87	**2.30**	3.66	4.23	**0.57**	3.68	4.79	**1.11**	72.7	59.3	68.3	Skew Left Up
HRP_26	7	5.83	9.12	**3.29**	4.91	5.50	**0.58**	5.28	6.94	**1.65**	50.9	57.9	45.9	Skew Right Down
HRP_27	6	7.67	11.12	**3.45**	6.19	6.89	**0.70**	5.76	7.51	**1.75**	48.5	48.2	43.4	Decreasing
HRP_28	7	4.85	7.95	**3.10**	5.58	6.15	**0.56**	5.11	6.80	**1.69**	53.9	60.2	45.0	Skew Right Down
HRP_29	5	7.81	10.75	**2.94**	4.94	5.68	**0.75**	5.10	6.56	**1.46**	56.9	45.3	52.0	Skew Left Up
HRP_30	6	11.83	16.16	**4.33**	6.12	7.13	**1.01**	6.96	9.61	**2.65**	38.6	33.7	28.7	Decreasing
HRP_31	7	4.00	9.05	**5.05**	8.28	9.32	**1.04**	7.27	9.37	**2.10**	33.2	32.4	36.2	Skew Right Up
HRP_32	7	5.03	8.55	**3.52**	2.16	2.94	**0.79**	7.35	9.27	**1.92**	47.5	43.0	39.6	Decreasing
HRP_33	7	6.92	11.16	**4.24**	7.22	8.15	**0.93**	7.47	9.84	**2.37**	39.5	36.4	32.0	Decreasing
HRP_34	7	5.58	8.40	**2.82**	4.44	5.09	**0.64**	4.25	5.57	**1.32**	59.3	52.6	57.5	Upward Parabola
HRP_35	7	5.31	8.86	**3.55**	5.63	6.34	**0.71**	5.95	7.75	**1.80**	47.2	47.8	42.2	Skew Right Down
HRP_36	7	2.87	5.28	**2.41**	3.23	3.74	**0.51**	3.95	5.18	**1.24**	69.5	66.4	61.4	Decreasing
HRP_37	7	7.66	11.55	**3.90**	6.42	7.13	**0.71**	6.12	7.94	**1.81**	43.0	47.7	41.9	Downward Parabola
HRP_38	7	1.14	3.04	**1.90**	2.63	3.04	**0.41**	1.71	2.74	**1.03**	88.1	82.7	73.7	Decreasing
HRP_39	5	2.85	5.83	**2.98**	4.42	5.29	**0.87**	3.50	4.88	**1.38**	56.3	39.1	55.0	Upward Parabola
HRP_40	5	7.00	10.32	**3.32**	4.63	5.56	**0.93**	2.81	5.29	**2.48**	50.4	36.2	30.6	Decreasing
HRP_41	7	3.35	6.01	**2.67**	3.31	3.85	**0.54**	2.95	4.04	**1.09**	62.7	62.6	69.6	Skew Right Up
HRP_42	7	5.44	7.91	**2.47**	4.50	5.08	**0.58**	3.51	4.97	**1.46**	67.9	58.2	52.0	Decreasing

HRP_43	4	0.19	2.76	**2.57**	2.94	3.56	**0.62**	1.27	2.90	**1.64**	65.2	54.6	46.4	Decreasing
HRP_44	5	5.72	8.29	**2.57**	3.43	3.92	**0.49**	4.25	5.92	**1.67**	65.1	69.2	45.5	Skew Right Down
HRP_45	7	5.48	9.20	**3.71**	5.94	6.64	**0.70**	4.28	6.35	**2.07**	45.1	48.6	36.7	Skew Right Down
HRP_46	7	10.69	17.76	**7.07**	10.93	12.39	**1.46**	12.30	15.29	**2.99**	23.7	23.2	25.4	Skew Right Up
HRP_47	7	8.52	12.43	**3.91**	5.73	6.48	**0.75**	6.42	8.40	**1.98**	42.8	45.1	38.4	Skew Right Down
HRP_48	7	5.97	10.56	**4.59**	6.82	7.88	**1.06**	4.39	6.21	**1.82**	36.5	31.9	41.7	Skew Right Up
HRP_49	7	4.61	7.14	**2.53**	3.79	4.32	**0.53**	3.38	4.61	**1.22**	66.2	63.8	62.0	Decreasing
HRP_50	7	7.44	10.63	**3.20**	7.15	7.94	**0.79**	5.90	8.08	**2.17**	52.4	42.9	35.0	Decreasing
HRP_51	5	10.36	14.80	**4.44**	7.09	7.95	**0.87**	7.78	9.77	**1.99**	37.7	39.0	38.1	Downward Parabola
HRP_52	5	5.20	8.26	**3.06**	4.19	4.89	**0.69**	4.21	5.79	**1.58**	54.8	48.8	48.1	Decreasing
HRP_53	7	1.49	4.86	**3.38**	6.74	7.42	**0.68**	4.46	5.75	**1.29**	49.6	49.8	58.9	Increasing
HRP_54	7	6.91	10.04	**3.14**	4.94	5.72	**0.79**	4.14	5.55	**1.41**	53.3	43.0	53.9	Upward Parabola
HRP_55	7	9.27	12.76	**3.49**	7.73	8.68	**0.95**	4.01	5.62	**1.61**	48.0	35.8	47.2	Upward Parabola
HRP_56	7	4.60	6.67	**2.07**	3.25	3.70	**0.45**	3.12	4.31	**1.18**	80.7	75.2	64.2	Decreasing
HRP_57	7	4.89	8.78	**3.89**	5.51	6.24	**0.73**	2.70	4.30	**1.60**	43.0	46.4	47.5	Increasing
HRP_58	4	3.58	5.84	**2.25**	4.48	5.06	**0.58**	4.90	6.27	**1.37**	74.3	58.2	55.5	Decreasing
HRP_59	6	6.09	8.67	**2.58**	5.31	6.06	**0.75**	4.42	6.28	**1.86**	64.9	44.9	40.8	Decreasing
HRP_60	7	3.25	5.90	**2.65**	4.58	5.28	**0.70**	3.53	4.66	**1.13**	63.3	48.4	67.3	Skew Right Up

Houwhoek Pass		**Entry Time [s]**			**Apex Time [s]**			**Exit Time [s]**			**Speed [km/h]**			**Shape**
ID	**Axels**	**T1**	**T2**	**ΔT**	**T1**	**T2**	**ΔT**	**T1**	**T2**	**ΔT**	**EN**	**M**	**EX**	**0.05**
HHP_1	6	1.92	6.70	**4.78**	4.51	5.88	**1.38**	1.62	2.78	**1.16**	47.7	64.1	80.6	Increasing
HHP_2	7	0.45	3.73	**3.28**	2.27	3.85	**1.57**	3.71	5.38	**1.67**	69.6	56.1	56.2	Skew Left Up
HHP_3	7	0.19	3.38	**3.19**	3.85	4.98	**1.13**	2.82	3.74	**0.92**	71.6	78.1	101.8	Increasing
HHP_4	4	2.19	5.34	**3.15**	4.18	5.39	**1.22**	3.38	4.87	**1.49**	72.4	72.5	62.9	Skew Right Down
HHP_5	6	0.93	4.52	**3.59**	3.40	4.69	**1.29**	2.87	4.07	**1.20**	63.6	68.2	77.8	Increasing
HHP_6	7	1.89	4.90	**3.02**	4.13	5.51	**1.38**	2.83	4.48	**1.65**	75.7	63.7	56.8	Decreasing
HHP_7	7	1.60	5.34	**3.74**	3.46	4.79	**1.33**	3.10	4.15	**1.05**	61.1	66.4	89.1	Increasing
HHP_8	7	3.04	6.24	**3.20**	3.03	4.57	**1.55**	3.51	5.15	**1.64**	71.4	57.0	57.0	Decreasing
HHP_9	6	0.54	3.05	**2.51**	1.48	2.90	**1.42**	3.20	4.83	**1.63**	90.8	62.3	57.3	Decreasing
HHP_10	6	0.34	2.42	**2.08**	2.47	3.26	**0.79**	1.64	2.56	**0.93**	109.8	111.6	101.1	Skew Right Down
HHP_11	5	1.76	7.22	**5.46**	5.56	7.15	**1.58**	3.86	5.34	**1.49**	41.8	55.7	62.8	Increasing
HHP_12	5	0.42	5.78	**5.35**	3.02	4.48	**1.46**	5.04	6.49	**1.44**	42.6	60.3	64.9	Increasing
HHP_13	5	0.69	3.66	**2.97**	4.00	5.60	**1.59**	3.45	4.82	**1.37**	76.9	55.4	68.3	Skew Left Up
HHP_14	4	0.60	2.75	**2.16**	3.15	4.37	**1.22**	2.03	3.40	**1.37**	105.8	72.1	68.4	Decreasing
HHP_15	6	0.95	9.34	**8.39**	11.17	13.79	**2.61**	6.03	7.86	**1.83**	27.2	33.7	51.1	Increasing
HHP_16	4	2.05	7.36	**5.31**	1.91	3.58	**1.67**	4.38	5.86	**1.48**	43.0	52.8	63.3	Increasing
HHP_17	6	1.88	5.57	**3.69**	4.54	5.76	**1.22**	2.81	3.76	**0.95**	61.8	72.4	98.2	Increasing
HHP_18	6	2.62	5.51	**2.89**	4.09	5.52	**1.44**	3.16	4.76	**1.60**	78.9	61.3	58.3	Decreasing
HHP_19	6	4.55	7.82	**3.27**	2.51	3.75	**1.24**	1.98	3.22	**1.24**	69.8	71.2	75.7	Increasing
HHP_20	5	0.68	3.39	**2.72**	3.32	4.20	**0.88**	1.81	3.04	**1.23**	84.0	100.6	76.2	Skew Right Down
HHP_21	6	2.85	7.13	**4.28**	4.28	5.50	**1.23**	4.05	5.27	**1.22**	53.3	72.0	76.7	Increasing
HHP_22	6	0.96	4.06	**3.10**	4.04	5.86	**1.82**	2.94	4.94	**2.00**	73.7	48.5	46.9	Decreasing
HHP_23	6	0.83	3.00	**2.17**	3.62	5.10	**1.49**	2.91	4.28	**1.38**	105.2	59.3	68.1	Skew Left Up
HHP_24	6	0.91	4.95	**4.03**	2.71	4.17	**1.45**	2.83	4.28	**1.45**	56.6	60.7	64.7	Increasing
HHP_25	7	2.51	5.73	**3.22**	4.26	5.31	**1.06**	1.60	2.96	**1.36**	70.9	83.6	69.0	Downward Parabola
HHP_26	7	0.84	4.34	**3.50**	2.80	3.98	**1.18**	2.69	4.34	**1.65**	65.3	74.9	56.8	Skew Right Down
HHP_27	4	4.95	7.89	**2.94**	4.54	6.68	**2.14**	3.54	5.61	**2.07**	77.6	41.2	45.3	Skew Left Up
HHP_28	7	2.59	9.31	**6.71**	6.16	8.08	**1.91**	4.27	6.08	**1.82**	34.0	46.1	51.6	Increasing
HHP_29	7	3.25	7.27	**4.02**	5.97	7.42	**1.45**	3.65	5.81	**2.15**	56.7	60.7	43.4	Skew Right Down
HHP_30	8	1.71	5.56	**3.85**	4.61	5.95	**1.34**	2.99	4.15	**1.16**	59.3	65.8	80.6	Increasing
HHP_31	8	0.98	3.25	**2.28**	2.03	3.14	**1.12**	0.88	1.94	**1.07**	100.2	79.0	87.6	Skew Left Up
HHP_32	7	2.61	6.24	**3.63**	4.18	5.47	**1.29**	2.70	3.77	**1.06**	62.9	68.5	88.0	Increasing
HHP_33	5	1.32	3.92	**2.59**	1.91	3.01	**1.09**	2.20	3.38	**1.18**	88.0	80.6	79.3	Decreasing
HHP_34	6	0.51	3.54	**3.04**	3.03	4.16	**1.13**	1.73	2.77	**1.04**	75.1	78.1	89.6	Increasing
HHP_35	6	3.43	13.71	**10.28**	6.94	10.69	**3.75**	6.40	11.50	**5.09**	22.2	23.5	18.4	Skew Right Down
HHP_36	6	6.50	19.03	**12.53**	4.82	9.41	**4.58**	15.22	20.18	**4.96**	18.2	19.2	18.9	Downward Parabola
HHP_37	7	4.68	9.06	**4.38**	7.75	9.81	**2.06**	5.14	7.36	**2.22**	52.1	42.7	42.1	Decreasing
HHP_38	6	0.93	4.32	**3.39**	2.11	3.31	**1.19**	3.95	5.83	**1.88**	67.3	74.0	49.8	Skew Right Down
HHP_39	7	19.60	60.54	**40.94**	47.25	58.05	**10.80**	44.14	48.56	**4.41**	5.6	8.2	21.2	Increasing
HHP_40	6	0.85	6.32	**5.47**	4.48	6.02	**1.54**	3.55	4.93	**1.37**	41.8	57.2	68.2	Increasing
HHP_41	6	0.95	3.65	**2.70**	3.44	4.50	**1.06**	2.09	3.38	**1.29**	84.4	83.5	72.8	Decreasing
HHP_42	6	3.13	7.10	**3.97**	4.45	5.69	**1.24**	3.25	4.18	**0.93**	57.5	71.4	101.0	Increasing
HHP_43	6	1.03	4.08	**3.04**	3.72	4.80	**1.09**	2.48	3.41	**0.93**	75.1	81.1	101.0	Increasing
HHP_44	4	0.81	5.65	**4.84**	4.41	5.85	**1.44**	4.62	6.02	**1.40**	47.2	61.4	66.8	Increasing
HHP_45	6	2.30	5.13	**2.83**	2.92	4.47	**1.55**	2.94	4.48	**1.54**	80.6	56.9	60.7	Skew Left Up
HHP_46	7	1.51	5.65	**4.15**	6.42	8.03	**1.61**	3.64	5.21	**1.57**	55.0	54.7	59.8	Skew Right Up
HHP_47	5	0.64	3.78	**3.14**	4.41	5.43	**1.03**	2.84	4.15	**1.31**	72.6	85.9	71.6	Downward Parabola
HHP_48	8	4.19	7.90	**3.71**	3.34	4.88	**1.53**	3.44	5.13	**1.69**	61.5	57.5	55.4	Decreasing
HHP_49	8	1.81	4.93	**3.13**	3.84	5.44	**1.60**	3.52	5.15	**1.62**	73.0	55.2	57.6	Skew Left Up

HHP_50	7	4.91	16.08	**11.16**	3.78	7.01	**3.23**	4.10	5.70	**1.60**	20.4	27.3	58.5	Increasing
HHP_51	4	3.20	6.09	**2.89**	4.61	5.70	**1.09**	2.90	4.24	**1.34**	79.0	80.9	70.1	Skew Right Down
HHP_52	7	4.00	8.83	**4.82**	6.52	8.52	**2.00**	4.12	6.55	**2.43**	47.3	44.0	38.6	Decreasing
HHP_53	5	0.65	3.62	**2.97**	3.34	4.52	**1.18**	2.57	3.96	**1.39**	76.8	74.8	67.2	Decreasing
HHP_54	7	2.69	7.87	**5.18**	5.90	7.61	**1.72**	4.93	6.37	**1.45**	44.0	51.4	64.7	Increasing
HHP_55	6	1.58	6.53	**4.95**	7.20	8.89	**1.69**	3.91	5.31	**1.41**	46.2	52.2	66.5	Increasing
HHP_56	6	3.93	10.22	**6.29**	6.37	8.41	**2.04**	6.25	9.33	**3.08**	36.3	43.3	30.4	Skew Right Down
HHP_57	7	2.02	4.87	**2.84**	2.26	3.33	**1.07**	2.84	4.17	**1.34**	80.3	82.5	70.0	Skew Right Down
HHP_58	6	0.19	3.18	**2.99**	2.83	4.75	**1.92**	2.90	4.52	**1.62**	76.4	46.0	57.8	Skew Left Up
HHP_59	7	1.01	5.96	**4.95**	3.82	5.42	**1.60**	3.35	4.75	**1.40**	46.1	55.3	66.9	Increasing
HHP_60	7	1.74	4.32	**2.57**	2.69	4.04	**1.36**	3.42	4.60	**1.18**	88.8	65.0	79.3	Skew Left Up
HHP_61	7	1.19	5.17	**3.98**	4.32	6.11	**1.79**	2.91	4.68	**1.78**	57.3	49.3	52.7	Skew Left Up
HHP_62	7	1.28	7.87	**6.59**	7.82	10.72	**2.89**	3.61	5.43	**1.82**	34.6	30.5	51.5	Skew Right Up
HHP_63	6	2.21	5.45	**3.24**	5.33	6.54	**1.21**	3.22	4.91	**1.69**	70.4	73.0	55.5	Skew Right Down
HHP_64	6	4.41	8.84	**4.44**	3.10	4.63	**1.53**	3.55	5.54	**1.99**	51.4	57.6	47.1	Skew Right Down
HHP_65	4	2.53	5.31	**2.78**	3.18	4.40	**1.22**	2.92	4.34	**1.42**	82.1	72.1	66.1	Decreasing

Huguenot Tunnel		**Entry Time [s]**			**Apex Time [s]**			**Exit Time [s]**			**Speed [km/h]**			**Shape**
ID	**Axels**	**T1**	**T2**	**ΔT**	**T1**	**T2**	**ΔT**	**T1**	**T2**	**ΔT**	**EN**	**M**	**EX**	**0.05**
HGNTT_1	7	3.51	5.17	**1.66**	2.52	4.67	**2.15**	7.37	9.73	**2.36**	65.69	60.24	46.93	Decreasing
HGNTT_2	7	2.90	4.98	**2.09**	2.74	5.32	**2.58**	9.12	12.30	**3.17**	52.11	50.11	34.93	Decreasing
HGNTT_3	7	1.87	3.82	**1.96**	3.87	6.19	**2.32**	6.01	8.77	**2.76**	55.53	55.67	40.12	Skew Right Down
HGNTT_4	7	6.06	8.90	**2.84**	3.89	7.69	**3.80**	7.72	11.22	**3.51**	38.35	34.02	31.61	Decreasing
HGNTT_5	7	1.90	4.63	**2.72**	2.70	6.16	**3.47**	6.89	11.16	**4.27**	39.94	37.26	25.96	Decreasing
HGNTT_6	5	1.56	4.43	**2.87**	3.82	7.43	**3.61**	1.17	3.74	**2.57**	37.89	35.80	43.10	Skew Right Up
HGNTT_7	6	1.49	3.28	**1.78**	2.23	4.12	**1.89**	7.31	9.52	**2.21**	60.96	68.39	50.22	Skew Right Down
HGNTT_8	7	1.76	3.90	**2.14**	0.60	2.57	**1.97**	7.55	10.14	**2.59**	50.79	65.50	42.86	Skew Right Down
HGNTT_9	7	1.66	3.85	**2.19**	1.90	4.38	**2.48**	4.83	7.23	**2.40**	49.72	52.15	46.28	Skew Right Down
HGNTT_10	6	5.09	7.10	**2.02**	4.60	6.87	**2.26**	3.77	6.30	**2.53**	53.92	57.16	43.85	Skew Right Down
HGNTT_11	6	2.16	3.72	**1.56**	2.06	3.92	**1.85**	3.70	6.05	**2.36**	69.87	69.73	47.08	Decreasing
HGNTT_12	6	1.58	3.47	**1.89**	1.50	3.50	**2.00**	4.73	7.08	**2.35**	57.53	64.57	47.17	Skew Right Down
HGNTT_13	7	2.97	4.88	**1.91**	2.19	4.60	**2.41**	6.81	10.33	**3.52**	57.05	53.61	31.51	Decreasing
HGNTT_14	6	9.45	12.74	**3.29**	6.84	10.15	**3.32**	7.30	10.57	**3.28**	33.09	38.96	33.86	Downward Parabola
HGNTT_15	7	1.89	3.70	**1.81**	1.80	4.25	**2.45**	5.83	8.48	**2.66**	59.95	52.80	41.73	Decreasing
HGNTT_16	7	1.45	3.43	**1.98**	2.96	6.01	**3.05**	10.63	14.50	**3.87**	54.94	42.34	28.68	Decreasing
HGNTT_17	6	2.78	7.10	**4.32**	4.42	8.42	**4.01**	6.34	11.09	**4.74**	25.14	32.25	23.38	Skew Right Down
HGNTT_18	7	6.05	8.11	**2.06**	3.56	5.75	**2.19**	7.61	9.92	**2.31**	52.81	58.94	47.98	Skew Right Down
HGNTT_19	7	2.40	4.71	**2.31**	4.17	6.32	**2.15**	6.06	8.73	**2.67**	47.15	60.05	41.50	Skew Right Down
HGNTT_20	5	4.29	6.15	**1.86**	4.21	6.33	**2.11**	3.12	5.89	**2.77**	58.49	61.13	40.02	Skew Right Down
HGNTT_21	6	1.84	3.82	**1.98**	0.50	2.69	**2.20**	3.86	6.38	**2.52**	54.89	58.82	44.01	Skew Right Down
HGNTT_22	7	1.98	3.61	**1.63**	1.80	3.82	**2.02**	1.00	3.35	**2.34**	66.56	64.00	47.32	Decreasing
HGNTT_23	4	3.95	5.59	**1.64**	2.93	5.55	**2.63**	2.93	5.64	**2.71**	66.24	49.16	40.90	Decreasing
HGNTT_24	4	0.82	2.74	**1.93**	2.37	4.46	**2.09**	5.34	7.87	**2.52**	56.43	61.74	43.96	Skew Right Down
HGNTT_25	6	3.48	6.75	**3.27**	6.55	10.23	**3.68**	10.09	14.40	**4.31**	33.23	35.11	25.73	Skew Right Down
HGNTT_26	7	1.24	2.86	**1.62**	2.12	4.19	**2.08**	1.32	3.42	**2.10**	66.93	62.19	52.87	Decreasing
HGNTT_27	7	3.29	5.15	**1.87**	1.40	3.91	**2.51**	3.39	6.14	**2.74**	58.28	51.55	40.43	Decreasing
HGNTT_28	6	2.77	4.96	**2.19**	1.73	4.25	**2.53**	8.14	11.04	**2.90**	49.76	51.13	38.22	Skew Right Down
HGNTT_29	4	3.67	5.28	**1.62**	1.86	4.04	**2.18**	6.41	9.13	**2.72**	67.22	59.28	40.76	Decreasing
HGNTT_30	6	0.92	2.86	**1.94**	1.60	3.31	**1.71**	5.39	7.60	**2.21**	56.04	75.58	50.23	Skew Right Down
HGNTT_31	4	0.23	1.87	**1.65**	1.80	3.45	**1.66**	6.07	8.47	**2.40**	66.02	77.94	46.11	Skew Right Down
HGNTT_32	6	2.52	4.85	**2.33**	2.23	5.15	**2.92**	6.06	9.18	**3.12**	46.64	44.21	35.52	Decreasing
HGNTT_33	7	2.64	4.87	**2.23**	2.17	4.25	**2.08**	8.68	11.18	**2.50**	48.75	62.20	44.41	Skew Right Down
HGNTT_34	7	1.98	4.11	**2.13**	2.65	4.87	**2.22**	5.66	8.52	**2.86**	51.08	58.25	38.77	Skew Right Down
HGNTT_35	6	3.29	5.18	**1.89**	4.64	6.82	**2.17**	1.74	4.49	**2.75**	57.52	59.52	40.37	Skew Right Down
HGNTT_36	7	5.96	8.96	**3.01**	3.67	6.87	**3.20**	3.02	6.34	**3.32**	36.16	40.41	33.39	Skew Right Down
HGNTT_37	6	1.88	3.68	**1.81**	2.93	5.24	**2.31**	2.70	5.34	**2.63**	60.15	55.95	42.09	Decreasing
HGNTT_38	7	3.85	5.88	**2.02**	2.65	4.97	**2.31**	0.72	3.19	**2.47**	53.75	55.85	44.93	Skew Right Down
HGNTT_39	6	6.46	9.73	**3.27**	5.51	8.49	**2.98**	3.09	6.18	**3.10**	33.20	43.33	35.81	Skew Left Down
HGNTT_40	7	0.65	2.12	**1.47**	1.61	3.42	**1.81**	6.49	8.70	**2.22**	73.89	71.43	50.04	Decreasing
HGNTT_41	7	0.89	2.31	**1.43**	1.55	3.05	**1.50**	3.10	5.08	**1.98**	76.24	86.28	56.12	Skew Right Down
HGNTT_42	6	1.54	3.39	**1.84**	1.59	3.72	**2.14**	3.36	5.75	**2.39**	59.07	60.48	46.40	Skew Right Down
HGNTT_43	7	1.90	3.46	**1.56**	1.67	3.46	**1.78**	2.97	4.97	**2.00**	69.78	72.47	55.55	Skew Right Down
HGNTT_44	7	0.91	2.68	**1.77**	2.57	4.74	**2.17**	5.35	7.70	**2.35**	61.33	59.54	47.18	Decreasing
HGNTT_45	7	2.93	4.77	**1.84**	2.35	4.88	**2.53**	8.62	3.63	**4.99**	59.10	51.12	22.22	Decreasing
HGNTT_46	6	4.48	6.69	**2.21**	3.63	5.85	**2.22**	5.79	3.99	**1.80**	49.28	58.11	61.64	Increasing
HGNTT_47	7	1.41	3.75	**2.34**	2.75	5.01	**2.26**	4.95	7.88	**2.92**	46.47	57.09	37.95	Skew Right Down
HGNTT_48	6	4.07	6.13	**2.06**	2.34	4.60	**2.25**	6.09	3.76	**2.33**	52.81	57.32	47.58	Skew Right Down
HGNTT_49	6	3.84	5.65	**1.80**	2.17	4.45	**2.28**	5.73	7.50	**1.76**	60.30	56.61	62.95	Upward Parabola
HGNTT_50	6	2.20	5.04	**2.83**	4.66	7.46	**2.80**	5.36	8.31	**2.95**	38.39	46.15	37.60	Downward Parabola
HGNTT_51	6	2.46	4.69	**2.24**	2.73	5.37	**2.64**	6.93	9.61	**2.68**	48.61	48.93	41.33	Skew Right Down

HGNTT_52	7	2.72	4.25	**1.53**	1.29	3.00	**1.71**	3.60	5.42	**1.83**	70.90	75.62	60.66	Skew Right Down
HGNTT_53	7	3.14	6.09	**2.95**	3.86	7.00	**3.15**	6.60	9.82	**3.22**	36.90	41.05	34.43	Skew Right Down
HGNTT_54	6	1.38	3.04	**1.66**	1.50	3.59	**2.08**	5.31	7.77	**2.46**	65.49	62.03	45.02	Decreasing
HGNTT_55	7	1.46	3.95	**2.49**	2.95	6.06	**3.11**	4.39	7.73	**3.34**	43.74	41.58	33.24	Decreasing
HGNTT_56	6	2.23	5.43	**3.20**	5.77	9.09	**3.32**	9.77	12.86	**3.09**	33.99	38.88	35.84	Skew Left Down
HGNTT_57	5	3.78	5.71	**1.93**	2.91	5.33	**2.42**	4.50	7.08	**2.57**	56.46	53.31	43.08	Decreasing
HGNTT_58	7	5.96	8.34	**2.38**	3.25	5.80	**2.55**	3.66	6.49	**2.83**	45.77	50.68	39.22	Skew Right Down
HGNTT_59	6	5.11	7.99	**2.88**	5.02	8.00	**2.99**	2.75	5.67	**2.93**	37.81	43.26	37.89	Downward Parabola
HGNTT_60	6	2.56	4.94	**2.38**	5.62	8.71	**3.09**	6.93	10.32	**3.40**	45.66	41.77	32.65	Decreasing
HGNTT_61	7	2.24	4.44	**2.20**	2.94	5.04	**2.10**	4.21	6.64	**2.43**	49.31	61.50	45.64	Skew Right Down
HGNTT_62	7	1.65	3.44	**1.79**	2.84	5.01	**2.18**	4.28	6.76	**2.48**	60.72	59.37	44.75	Decreasing
HGNTT_63	7	1.62	3.50	**1.88**	0.57	2.60	**2.03**	4.82	7.90	**3.08**	57.69	63.57	36.01	Skew Right Down
HGNTT_64	6	2.25	4.87	**2.61**	4.03	6.53	**2.50**	9.41	12.77	**3.37**	41.63	51.60	32.94	Skew Right Down
HGNTT_65	7	9.05	13.42	**4.38**	6.17	11.13	**4.96**	4.86	10.53	**5.66**	24.85	26.07	19.59	Skew Right Down
HGNTT_66	7	5.16	7.72	**2.56**	4.25	6.84	**2.59**	3.44	6.53	**3.09**	42.50	49.86	35.92	Skew Right Down
HGNTT_67	5	1.67	3.37	**1.69**	1.67	3.43	**1.75**	4.31	6.31	**2.00**	64.16	73.71	55.39	Skew Right Down
HGNTT_68	6	3.18	5.15	**1.97**	1.99	4.23	**2.24**	3.85	7.26	**3.41**	55.15	57.71	32.53	Skew Right Down
HGNTT_69	6	0.58	2.74	**2.16**	3.77	5.85	**2.07**	4.64	7.09	**2.46**	50.33	62.36	45.09	Skew Right Down
HGNTT_70	4	1.23	3.05	**1.82**	3.55	5.90	**2.35**	5.92	8.48	**2.57**	59.79	54.89	43.17	Decreasing
HGNTT_71	7	3.81	6.76	**2.95**	5.46	8.76	**3.29**	6.61	10.24	**3.63**	36.82	39.26	30.52	Skew Right Down
HGNTT_72	6	1.34	3.10	**1.75**	1.44	3.64	**2.20**	4.48	6.84	**2.36**	62.04	58.62	47.03	Decreasing
HGNTT_73	7	1.42	3.11	**1.70**	1.46	3.52	**2.07**	4.81	7.59	**2.79**	64.01	62.49	39.81	Decreasing
HGNTT_74	7	2.64	4.75	**2.11**	2.73	5.08	**2.35**	6.51	9.48	**2.97**	51.52	55.01	37.35	Skew Right Down
HGNTT_75	7	4.12	6.94	**2.83**	3.72	6.83	**3.11**	5.87	9.47	**3.61**	38.44	41.53	30.73	Skew Right Down
HGNTT_76	5	1.16	2.78	**1.63**	2.26	4.18	**1.91**	4.60	6.92	**2.32**	66.83	67.59	47.81	Skew Right Down
HGNTT_77	5	4.01	6.52	**2.50**	5.64	8.49	**2.85**	5.14	8.17	**3.03**	43.43	45.42	36.62	Skew Right Down
HGNTT_78	6	1.96	4.35	**2.39**	3.85	6.62	**2.77**	5.99	9.36	**3.37**	45.56	46.68	32.94	Skew Right Down
HGNTT_79	7	1.86	3.62	**1.76**	5.20	8.24	**3.03**	7.75	11.32	**3.58**	61.80	42.63	30.98	Decreasing
HGNTT_80	7	2.46	5.06	**2.60**	3.23	5.69	**2.46**	4.10	7.99	**3.88**	41.83	52.58	28.55	Skew Right Down
HGNTT_81	7	3.59	5.23	**1.63**	2.71	4.71	**1.99**	2.67	4.58	**1.91**	66.64	64.84	57.92	Decreasing
HGNTT_82	6	0.19	2.01	**1.82**	2.66	4.82	**2.16**	5.47	7.79	**2.32**	59.85	59.91	47.70	Skew Right Down
HGNTT_83	6	1.68	3.88	**2.20**	2.84	5.02	**2.18**	3.62	6.33	**2.71**	49.47	59.29	40.96	Skew Right Down
HGNTT_84	7	4.06	6.04	**1.98**	2.73	4.73	**2.00**	8.42	10.97	**2.55**	55.05	64.65	43.47	Skew Right Down
HGNTT_85	7	3.16	5.71	**2.55**	3.35	6.49	**3.14**	6.61	9.76	**3.15**	42.69	41.15	35.17	Decreasing
HGNTT_86	6	2.36	4.67	**2.31**	3.85	6.25	**2.40**	5.70	8.32	**2.62**	47.09	53.75	42.33	Skew Right Down
HGNTT_87	7	1.68	3.45	**1.77**	2.05	4.14	**2.09**	1.36	3.61	**2.26**	61.49	61.86	49.13	Skew Right Down
HGNTT_88	7	2.03	4.05	**2.03**	1.93	4.34	**2.41**	4.09	6.48	**2.39**	53.61	53.61	46.43	Skew Right Down
HGNTT_89	7	3.29	5.44	**2.15**	2.15	4.78	**2.63**	7.73	10.73	**3.01**	50.47	49.18	36.85	Decreasing
HGNTT_90	5	1.39	4.27	**2.88**	4.67	7.99	**3.32**	2.15	6.04	**3.88**	37.77	38.96	28.55	Skew Right Down
HGNTT_91	7	2.17	3.99	**1.81**	2.79	4.87	**2.07**	5.44	7.64	**2.20**	59.92	62.34	50.48	Skew Right Down
HGNTT_92	6	2.08	3.87	**1.78**	2.17	4.10	**1.93**	5.82	8.13	**2.31**	60.96	67.08	47.99	Skew Right Down
HGNTT_93	7	6.35	8.65	**2.30**	4.68	7.48	**2.80**	5.20	8.02	**2.82**	47.25	46.21	39.25	Decreasing
HGNTT_94	7	3.15	5.53	**2.39**	3.35	6.74	**3.39**	8.39	11.94	**3.55**	45.54	38.13	31.21	Decreasing
HGNTT_95	7	4.34	6.58	**2.24**	3.18	5.57	**2.39**	9.46	12.31	**2.85**	48.45	54.07	38.96	Skew Right Down
HGNTT_96	7	0.89	3.35	**2.46**	3.92	6.95	**3.02**	10.10	13.37	**3.27**	44.23	42.75	33.87	Decreasing
HGNTT_97	5	2.80	4.47	**1.67**	2.79	4.93	**2.14**	5.85	8.59	**2.73**	64.97	60.36	40.54	Decreasing
HGNTT_98	6	0.83	3.42	**2.59**	1.96	4.36	**2.40**	5.09	8.25	**3.16**	42.00	53.91	35.08	Skew Right Down
HGNTT_99	7	1.18	2.61	**1.43**	1.98	3.77	**1.79**	4.93	6.91	**1.98**	76.19	72.39	55.90	Decreasing
HGNTT_100	7	1.28	3.08	**1.80**	1.71	3.65	**1.94**	8.83	11.37	**2.54**	60.49	66.59	43.61	Skew Right Down
HGNTT_101	7	1.59	3.50	**1.91**	3.13	5.37	**2.24**	5.01	7.43	**2.42**	57.01	57.68	45.76	Skew Right Down
HGNTT_102	7	4.17	6.47	**2.30**	3.61	5.85	**2.24**	2.02	4.41	**2.39**	47.27	57.72	46.48	Downward Parabola
HGNTT_103	7	1.66	3.52	**1.87**	1.84	3.85	**2.01**	2.80	5.15	**2.35**	58.29	64.38	47.22	Skew Right Down
HGNTT_104	6	1.29	2.82	**1.53**	1.26	2.86	**1.60**	5.64	7.46	**1.82**	71.15	80.81	60.86	Skew Right Down
HGNTT_105	7	0.69	2.13	**1.44**	1.49	3.14	**1.65**	2.79	4.57	**1.78**	75.54	78.35	62.28	Skew Right Down
HGNTT_106	7	1.90	4.55	**2.65**	2.55	5.60	**3.04**	6.18	9.45	**3.27**	41.02	42.49	33.95	Skew Right Down
HGNTT_107	7	0.95	2.49	**1.55**	1.73	3.65	**1.92**	8.96	11.51	**2.55**	70.29	67.46	43.47	Decreasing
HGNTT_108	6	1.36	3.05	**1.69**	1.44	3.56	**2.12**	5.64	7.96	**2.32**	64.21	61.00	47.76	Decreasing
HGNTT_109	6	3.52	5.72	**2.20**	2.14	4.70	**2.55**	3.55	6.14	**2.59**	49.35	50.58	42.79	Skew Right Down
HGNTT_110	6	2.53	4.85	**2.32**	2.44	5.07	**2.63**	5.26	8.33	**3.08**	46.90	49.17	36.02	Skew Right Down
HGNTT_111	7	1.54	3.61	**2.07**	3.29	5.36	**2.07**	4.39	6.79	**2.40**	52.49	62.37	46.19	Skew Right Down
HGNTT_112	7	8.47	10.56	**2.10**	3.23	6.44	**3.21**	10.62	13.52	**2.90**	51.84	40.28	38.22	Decreasing

Piekenierskloof Pass		**Entry Time [s]**			**Apex Time [s]**			**Exit Time [s]**			**Speed [km/h]**			**Shape**
ID	**Axels**	**T1**	**T2**	**ΔT**	**T1**	**T2**	**ΔT**	**T1**	**T2**	**ΔT**	**EN**	**M**	**EX**	**0.05**
PKNKP_1	7	2.28	4.64	**2.36**	1.55	3.56	**2.02**	2.52	8.98	**6.46**	38.9	45.0	32.1	Skew Right Down
PKNKP_2	7	1.74	4.24	**2.51**	2.18	3.73	**1.56**	2.24	6.54	**4.30**	36.6	58.3	48.2	Skew Left Down
PKNKP_3	6	3.09	5.26	**2.17**	2.30	4.78	**2.48**	6.06	11.36	**5.30**	42.3	36.5	39.1	Skew Left Up
PKNKP_4	6	1.81	3.31	**1.50**	1.48	2.72	**1.25**	0.94	4.19	**3.25**	61.3	72.8	63.8	Downward Parabola
PKNKP_5	7	2.09	3.58	**1.49**	1.70	3.05	**1.35**	0.68	3.92	**3.24**	61.5	67.0	63.9	Downward Parabola
PKNKP_6	6	1.12	2.74	**1.61**	1.41	2.59	**1.18**	1.94	5.27	**3.33**	56.8	76.9	62.4	Skew Left Down

PKNKP_7	7	8.65	15.12	**6.46**	10.41	14.04	**3.63**	4.88	13.77	**8.89**	14.2	25.0	23.3	Skew Left Down
PKNKP_8	7	4.92	9.56	**4.64**	2.52	5.59	**3.07**	0.84	5.93	**5.10**	19.8	29.6	40.7	Increasing
PKNKP_9	5	0.85	2.20	**1.35**	1.25	2.26	**1.01**	1.72	4.57	**2.85**	68.2	90.1	72.8	Skew Left Down
PKNKP_10	6	0.37	1.73	**1.37**	0.78	1.66	**0.88**	0.56	3.04	**2.49**	67.2	102.9	83.4	Skew Left Down
PKNKP_11	4	1.22	2.91	**1.69**	1.40	2.38	**0.98**	1.16	3.96	**2.80**	54.3	92.3	74.0	Skew Left Down
PKNKP_12	5	0.85	2.59	**1.73**	1.39	2.53	**1.14**	2.16	5.29	**3.14**	52.9	79.6	66.1	Skew Left Down
PKNKP_13	6	1.17	2.77	**1.60**	1.11	2.38	**1.27**	2.07	5.43	**3.36**	57.4	71.5	61.7	Skew Left Down
PKNKP_14	6	0.85	2.35	**1.51**	1.95	3.43	**1.48**	3.60	7.27	**3.67**	60.9	61.5	56.6	Skew Right Down
PKNKP_15	4	2.30	4.22	**1.91**	1.48	3.36	**1.88**	2.17	7.22	**5.05**	48.1	48.3	41.1	Skew Right Down
PKNKP_16	8	0.62	2.78	**2.16**	2.38	4.05	**1.68**	3.69	8.00	**4.31**	42.5	54.1	48.1	Skew Left Down
PKNKP_17	7	3.46	5.25	**1.79**	2.01	3.30	**1.30**	1.42	5.14	**3.72**	51.3	70.0	55.7	Skew Left Down
PKNKP_18	6	1.73	3.23	**1.49**	1.43	2.67	**1.24**	0.28	3.27	**2.99**	61.5	73.2	69.4	Skew Left Down
PKNKP_19	5	1.58	3.33	**1.75**	2.08	3.43	**1.35**	1.91	5.33	**3.43**	52.6	67.0	60.5	Skew Left Down
PKNKP_20	6	0.19	1.00	**0.81**	1.24	2.53	**1.29**	2.77	6.43	**3.66**	113.8	70.3	56.6	Decreasing
PKNKP_21	4	0.38	1.98	**1.60**	0.30	1.91	**1.61**	1.39	5.18	**3.80**	57.3	56.4	54.6	Decreasing
PKNKP_22	7	1.37	3.12	**1.75**	2.13	3.54	**1.41**	2.65	6.61	**3.96**	52.5	64.3	52.4	Downward Parabola
PKNKP_23	7	3.01	5.19	**2.18**	1.30	3.21	**1.91**	3.25	8.51	**5.26**	42.2	47.5	39.4	Skew Right Down
PKNKP_24	5	1.65	2.99	**1.34**	0.19	1.35	**1.16**	1.82	4.99	**3.17**	68.5	78.2	65.5	Downward Parabola
PKNKP_25	6	1.04	2.53	**1.50**	1.24	2.84	**1.60**	2.52	6.40	**3.88**	61.3	56.5	53.4	Decreasing
PKNKP_26	6	1.90	3.26	**1.36**	1.80	3.09	**1.29**	1.67	5.08	**3.41**	67.7	70.4	60.8	Skew Right Down
PKNKP_27	7	0.46	2.05	**1.59**	2.05	3.30	**1.25**	1.26	4.31	**3.05**	57.7	72.6	67.9	Skew Left Down
PKNKP_28	5	2.19	4.29	**2.10**	2.13	3.39	**1.26**	1.65	5.94	**4.30**	43.6	72.2	48.3	Skew Left Down
PKNKP_29	7	1.28	2.52	**1.24**	1.17	2.43	**1.25**	0.88	4.18	**3.31**	74.1	72.5	62.7	Decreasing
PKNKP_30	6	1.96	3.68	**1.72**	2.01	3.69	**1.68**	2.34	7.42	**5.08**	53.3	54.1	40.8	Skew Right Down
PKNKP_31	7	3.59	5.40	**1.81**	0.70	2.97	**2.26**	2.14	7.73	**5.59**	50.7	40.1	37.1	Decreasing
PKNKP_32	6	0.36	2.07	**1.71**	0.19	1.80	**1.61**	0.27	3.73	**3.46**	53.7	56.4	59.9	Increasing
PKNKP_33	8	2.22	5.85	**3.63**	2.85	6.64	**3.79**	4.88	14.57	**9.68**	25.3	23.9	21.4	Decreasing
PKNKP_34	6	2.35	4.01	**1.67**	0.68	2.32	**1.65**	1.56	5.36	**3.80**	55.0	55.1	54.5	Downward Parabola
PKNKP_35	4	0.46	2.31	**1.85**	1.56	3.81	**2.25**	2.45	6.92	**4.48**	49.6	40.3	46.3	Skew Left Up
PKNKP_36	7	2.56	5.15	**2.59**	4.04	7.11	**3.08**	1.78	6.41	**4.63**	35.4	29.5	44.8	Skew Right Up
PKNKP_37	6	3.59	5.77	**2.18**	2.63	4.68	**2.05**	2.63	8.75	**6.12**	42.1	44.3	33.9	Skew Right Down
PKNKP_38	6	1.73	3.94	**2.20**	0.82	2.80	**1.98**	2.38	7.20	**4.81**	41.7	45.8	43.1	Downward Parabola
PKNKP_39	7	0.61	1.98	**1.37**	1.09	2.61	**1.52**	1.86	4.72	**2.86**	67.1	59.8	72.5	Skew Right Up
PKNKP_40	7	1.88	3.17	**1.29**	1.86	3.17	**1.31**	1.33	5.38	**4.05**	71.1	69.2	51.2	Decreasing
PKNKP_41	7	0.75	1.97	**1.23**	1.32	2.53	**1.21**	0.71	4.32	**3.62**	74.8	75.0	57.4	Skew Right Down
PKNKP_42	6	2.09	4.11	**2.02**	3.16	4.95	**1.80**	4.13	9.49	**5.36**	45.5	50.5	38.7	Skew Right Down
PKNKP_43	7	1.99	3.95	**1.95**	1.18	2.87	**1.68**	3.44	7.50	**4.05**	47.0	53.9	51.2	Skew Left Down
PKNKP_44	7	1.47	2.88	**1.41**	1.20	2.55	**1.36**	1.96	5.58	**3.62**	65.2	66.9	57.3	Skew Right Down
PKNKP_45	7	1.51	3.37	**1.86**	0.73	2.52	**1.79**	3.39	7.31	**3.92**	49.4	50.6	52.9	Increasing
PKNKP_46	6	3.14	5.39	**2.25**	1.93	3.58	**1.66**	0.19	3.44	**3.25**	40.8	54.7	63.8	Increasing
PKNKP_47	7	1.85	4.85	**3.00**	2.96	4.99	**2.02**	2.94	7.38	**4.44**	30.6	44.8	46.7	Increasing
PKNKP_48	7	1.95	3.19	**1.24**	1.50	2.77	**1.27**	2.22	5.13	**2.92**	74.3	71.4	71.1	Decreasing
PKNKP_49	5	0.19	1.86	**1.67**	1.61	3.05	**1.44**	1.29	4.98	**3.68**	54.9	63.0	56.3	Downward Parabola
PKNKP_50	7	1.72	3.12	**1.40**	0.96	2.29	**1.33**	1.34	4.48	**3.14**	65.7	68.3	66.0	Downward Parabola
PKNKP_51	6	8.64	14.21	**5.57**	7.24	11.14	**3.89**	6.49	15.75	**9.25**	16.5	23.3	22.4	Skew Left Down
PKNKP_52	7	1.41	2.59	**1.18**	2.94	4.67	**1.73**	2.16	4.87	**2.71**	77.6	52.4	76.6	Upward Parabola
PKNKP_53	5	2.24	3.95	**1.71**	1.65	3.09	**1.44**	2.13	4.72	**2.60**	53.7	63.0	79.9	Increasing
PKNKP_54	5	0.51	2.25	**1.73**	1.35	2.63	**1.27**	2.14	5.71	**3.57**	53.0	71.2	58.1	Skew Left Down
PKNKP_55	7	1.94	4.01	**2.07**	1.66	4.03	**2.37**	3.92	9.78	**5.86**	44.4	38.3	35.4	Decreasing
PKNKP_56	6	1.57	3.95	**2.37**	2.32	4.09	**1.78**	3.66	8.90	**5.24**	38.7	51.1	39.6	Downward Parabola
PKNKP_57	7	0.59	2.54	**1.95**	1.39	2.95	**1.56**	2.82	7.24	**4.42**	47.0	58.1	47.0	Downward Parabola
PKNKP_58	4	2.55	5.35	**2.79**	2.52	5.48	**2.96**	4.14	9.62	**5.47**	32.9	30.6	37.9	Skew Right Up
PKNKP_59	8	0.97	2.28	**1.31**	0.19	1.51	**1.32**	3.15	6.16	**3.01**	70.1	68.9	68.8	Decreasing
PKNKP_60	7	1.68	3.80	**2.12**	1.84	3.39	**1.55**	2.31	5.61	**3.31**	43.3	58.6	62.7	Increasing
PKNKP_61	6	2.69	6.62	**3.93**	1.85	4.60	**2.75**	2.08	8.78	**6.70**	23.4	33.0	30.9	Skew Left Down
PKNKP_62	6	1.76	2.92	**1.16**	0.19	1.38	**1.19**	1.15	4.14	**2.98**	79.4	75.9	69.5	Decreasing
PKNKP_63	7	2.09	4.21	**2.12**	2.76	5.25	**2.49**	6.97	13.00	**6.02**	43.2	36.4	34.4	Decreasing
PKNKP_64	7	2.79	4.44	**1.65**	1.10	2.74	**1.64**	1.93	5.82	**3.89**	55.6	55.2	53.3	Decreasing
PKNKP_65	7	5.37	9.04	**3.67**	6.09	10.12	**4.03**	6.70	15.51	**8.81**	25.0	22.5	23.5	Skew Left Up
PKNKP_66	6	1.91	4.24	**2.33**	1.09	3.26	**2.17**	3.34	8.62	**5.28**	39.4	41.7	39.3	Downward Parabola
PKNKP_67	7	1.16	3.20	**2.04**	1.22	2.59	**1.38**	2.79	6.84	**4.05**	45.0	65.9	51.2	Skew Left Down
PKNKP_68	6	0.52	1.70	**1.18**	0.63	1.83	**1.20**	0.90	4.15	**3.25**	77.8	75.5	63.8	Decreasing
PKNKP_69	6	1.01	2.77	**1.76**	1.04	2.25	**1.22**	1.99	5.19	**3.20**	52.2	74.6	64.7	Skew Left Down
PKNKP_70	7	2.29	3.63	**1.34**	1.48	2.87	**1.40**	2.17	6.20	**4.03**	68.5	65.0	51.5	Decreasing
PKNKP_71	6	1.81	2.95	**1.15**	1.63	2.79	**1.16**	0.62	3.79	**3.17**	79.9	78.4	65.3	Decreasing
PKNKP_72	6	1.51	2.83	**1.32**	1.41	2.48	**1.07**	1.88	4.63	**2.75**	69.7	84.6	75.5	Skew Left Down
PKNKP_73	7	1.61	4.01	**2.41**	1.90	3.81	**1.91**	2.23	7.51	**5.27**	38.1	47.5	39.3	Downward Parabola
PKNKP_74	5	1.36	2.49	**1.13**	1.21	2.33	**1.12**	1.87	4.66	**2.79**	81.3	80.9	74.2	Decreasing
PKNKP_75	5	1.10	2.49	**1.39**	0.45	1.61	**1.16**	0.82	3.51	**2.70**	66.0	78.2	76.9	Skew Left Down
PKNKP_76	6	0.99	2.04	**1.05**	1.23	2.28	**1.05**	2.35	5.06	**2.71**	87.6	86.4	76.5	Decreasing

PKNKP_77	7	3.10	5.07	**1.97**	2.45	4.05	**1.59**	1.87	5.83	**3.95**	46.6	56.9	52.5	Skew Left Down
PKNKP_78	6	0.90	1.93	**1.02**	1.20	2.31	**1.12**	1.09	3.79	**2.70**	89.6	81.4	76.8	Decreasing
PKNKP_79	5	1.86	3.27	**1.41**	2.32	5.57	**3.25**	1.85	3.49	**1.64**	64.9	27.9	126.8	Skew Right Up
PKNKP_80	6	1.25	2.63	**1.38**	1.02	2.34	**1.32**	1.93	5.28	**3.34**	66.6	69.0	62.1	Skew Right Down
PKNKP_81	6	0.83	2.09	**1.26**	0.19	1.38	**1.19**	0.81	3.40	**2.59**	72.8	76.0	80.1	Increasing
PKNKP_82	7	1.29	2.48	**1.19**	1.08	2.24	**1.16**	0.79	3.64	**2.85**	76.9	77.9	72.6	Skew Right Down
PKNKP_83	7	0.69	2.20	**1.51**	1.17	2.53	**1.36**	3.86	7.00	**3.14**	60.8	66.6	66.1	Skew Left Down
PKNKP_84	6	0.84	1.90	**1.06**	0.85	1.99	**1.14**	0.63	3.62	**3.00**	86.6	79.2	69.2	Decreasing
PKNKP_85	6	1.38	3.28	**1.90**	2.03	3.49	**1.46**	2.69	6.80	**4.10**	48.4	62.1	50.5	Downward Parabola
PKNKP_86	7	2.01	4.33	**2.32**	3.59	5.42	**1.82**	3.12	9.04	**5.92**	39.5	49.8	35.0	Skew Right Down
PKNKP_87	6	1.89	3.03	**1.14**	3.32	4.24	**0.92**	1.03	3.28	**2.25**	80.7	98.6	92.3	Skew Left Down
PKNKP_88	5	1.11	2.19	**1.08**	0.56	1.69	**1.13**	1.31	3.91	**2.60**	85.3	80.2	79.8	Decreasing
PKNKP_89	8	1.18	2.36	**1.18**	1.52	2.71	**1.19**	1.26	4.31	**3.05**	78.0	76.2	68.0	Decreasing
PKNKP_90	5	0.63	1.87	**1.25**	0.75	1.90	**1.14**	0.74	3.44	**2.70**	73.6	79.5	76.8	Downward Parabola

Sir Lowrys Pass		**Entry Time [s]**			**Apex Time [s]**			**Exit Time [s]**			**Speed [km/h]**			**Shape**
ID	**Axels**	**T1**	**T2**	**ΔT**	**T1**	**T2**	**ΔT**	**T1**	**T2**	**ΔT**	**EN**	**M**	**EX**	**0.05**
SLP_1	6	2.33	3.52	**1.20**	7.24	9.07	**1.83**	0.83	2.33	**1.51**	30.42	39.27	61.60	Increasing
SLP_2	6	3.21	4.68	**1.48**	4.30	5.89	**1.59**	1.07	2.33	**1.26**	24.60	45.22	73.80	Increasing
SLP_3	6	2.16	4.12	**1.96**	3.47	5.35	**1.88**	2.08	3.83	**1.76**	18.54	38.39	52.85	Increasing
SLP_4	7	1.15	1.99	**0.83**	4.76	6.08	**1.32**	1.90	3.50	**1.60**	43.64	54.52	58.06	Increasing
SLP_5	6	2.75	3.21	**0.47**	2.78	3.60	**0.81**	0.64	1.70	**1.07**	77.73	88.39	86.96	Skew Left Down
SLP_6	6	7.46	8.67	**1.20**	5.36	7.10	**1.75**	1.97	4.06	**2.09**	30.19	41.23	44.41	Increasing
SLP_7	6	1.41	1.79	**0.38**	4.24	5.06	**0.81**	0.66	1.68	**1.03**	96.71	88.39	90.56	Skew Left Up
SLP_8	6	3.16	5.29	**2.13**	5.20	12.40	**7.20**	7.92	13.95	**6.03**	17.07	10.00	15.41	Skew Left Up
SLP_9	6	2.17	2.54	**0.37**	3.29	4.42	**1.13**	1.9	3.5	**1.64**	99.22	63.92	56.80	Decreasing
SLP_10	7	1.04	2.25	**1.20**	4.51	6.14	**1.62**	0.91	2.12	**1.21**	30.24	44.40	76.45	Increasing
SLP_11	6	1.80	2.37	**0.57**	3.64	4.83	**1.19**	0.37	1.31	**0.94**	63.49	60.64	98.55	Skew Right Up
SLP_12	4	1.29	1.79	**0.50**	2.14	2.77	**0.63**	0.19	1.26	**1.07**	72.48	114.03	86.56	Skew Left Down
SLP_13	6	1.56	2.47	**0.91**	3.62	4.88	**1.26**	0.62	2.14	**1.52**	39.82	56.98	61.26	Increasing
SLP_14	5	3.52	4.13	**0.61**	5.85	6.73	**0.88**	0.91	2.08	**1.18**	59.64	81.79	78.99	Skew Left Down
SLP_15	6	2.58	3.44	**0.86**	4.98	6.39	**1.41**	2.03	3.70	**1.67**	42.52	50.91	55.71	Increasing
SLP_16	7	1.84	2.37	**0.53**	2.47	3.26	**0.79**	0.19	1.59	**1.40**	68.64	90.72	66.28	Downward Parabola
SLP_17	6	1.51	1.94	**0.44**	2.17	2.94	**0.77**	0.19	1.62	**1.43**	82.70	93.17	64.81	Skew Right Down
SLP_18	6	1.44	2.29	**0.85**	3.05	4.04	**0.99**	0.48	1.49	**1.01**	42.76	72.44	91.66	Increasing
SLP_19	6	2.47	2.93	**0.46**	3.29	4.06	**0.77**	0.50	1.36	**0.86**	78.89	93.49	107.87	Increasing
SLP_20	7	2.59	3.59	**1.00**	5.43	6.87	**1.44**	1.24	3.01	**1.78**	36.42	49.86	52.23	Increasing
SLP_21	7	1.13	1.70	**0.57**	1.45	2.53	**1.08**	0.79	1.95	**1.17**	63.48	66.66	79.55	Increasing
SLP_22	6	0.79	1.38	**0.59**	2.35	3.17	**0.81**	1.04	1.87	**0.83**	62.03	88.63	111.90	Increasing
SLP_23	6	1.52	2.34	**0.81**	1.83	3.27	**1.45**	0.83	2.03	**1.20**	44.74	49.78	77.65	Increasing
SLP_24	4	2.15	2.94	**0.79**	1.46	2.82	**1.36**	0.19	1.80	**1.61**	46.27	52.81	57.84	Increasing
SLP_25	7	2.33	3.15	**0.83**	2.97	3.86	**0.89**	1.20	2.60	**1.40**	43.98	80.64	66.40	Skew Left Down
SLP_26	7	2.13	2.71	**0.58**	3.46	4.42	**0.96**	1.15	2.38	**1.23**	62.72	75.12	75.57	Increasing
SLP_27	4	2.10	2.55	**0.44**	2.43	3.37	**0.93**	0.35	1.34	**0.99**	81.74	77.23	93.78	Skew Right Up
SLP_28	4	1.53	1.98	**0.46**	2.63	3.31	**0.67**	0.35	1.14	**0.80**	79.61	107.06	116.37	Increasing
SLP_29	7	1.41	2.44	**1.03**	3.95	4.81	**0.86**	0.47	1.44	**0.97**	35.41	83.75	95.56	Increasing
SLP_30	6	1.19	1.61	**0.43**	3.00	4.15	**1.15**	0.96	2.42	**1.47**	85.49	62.43	63.26	Skew Left Up
SLP_31	7	1.69	2.17	**0.48**	3.35	4.53	**1.18**	1.16	2.28	**1.13**	75.15	60.79	82.31	Skew Right Up
SLP_32	6	2.47	2.97	**0.50**	4.04	5.06	**1.01**	0.66	1.81	**1.15**	72.54	71.19	80.53	Skew Right Up
SLP_33	6	1.19	1.88	**0.69**	2.80	3.78	**0.98**	0.56	1.77	**1.21**	52.48	73.42	76.46	Increasing
SLP_34	7	1.49	1.90	**0.41**	3.38	4.25	**0.87**	0.74	1.73	**0.99**	89.33	82.51	93.76	Upward Parabola
SLP_35	7	2.42	3.03	**0.62**	2.43	3.24	**0.81**	1.02	2.11	**1.08**	58.90	88.89	85.66	Skew Left Down
SLP_36	6	2.52	3.00	**0.49**	1.77	2.69	**0.92**	0.89	2.43	**1.55**	74.49	78.11	60.01	Skew Right Down
SLP_37	6	2.26	3.14	**0.87**	1.34	2.88	**1.54**	1.06	2.95	**1.88**	41.68	46.77	49.32	Increasing
SLP_38	6	3.29	3.81	**0.52**	2.57	3.81	**1.24**	1.02	2.16	**1.14**	70.29	58.20	81.45	Skew Right Up
SLP_39	7	2.05	2.81	**0.76**	3.18	4.06	**0.88**	1.00	2.18	**1.18**	47.61	82.03	78.78	Skew Left Down
SLP_40	6	0.19	0.78	**0.59**	2.42	3.39	**0.97**	0.69	1.86	**1.17**	62.01	74.23	79.22	Increasing
SLP_41	6	5.21	6.03	**0.82**	7.63	9.88	**2.25**	1.99	4.05	**2.06**	44.27	31.97	45.17	Upward Parabola

Appendix G

This section contains the individual speed profiles for each followed heavy vehicle.

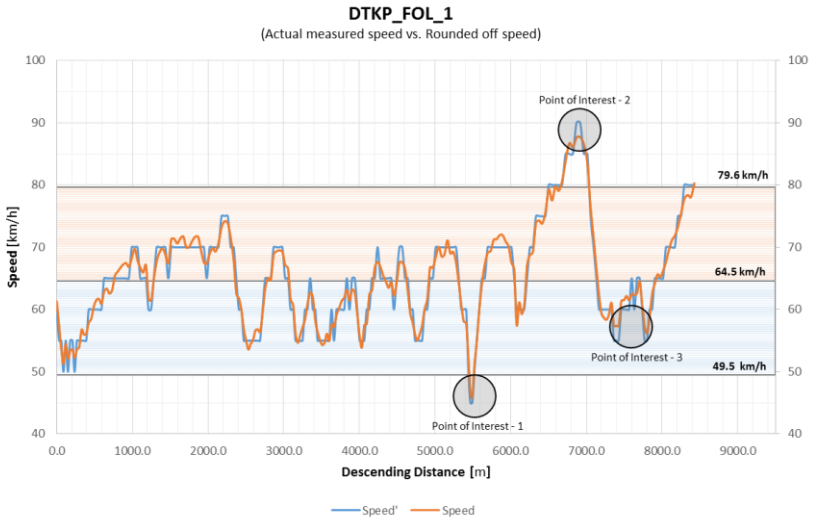

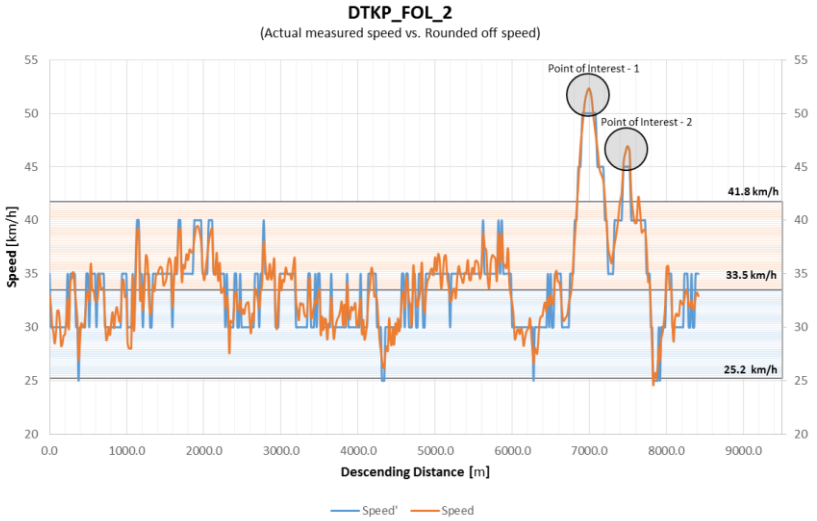

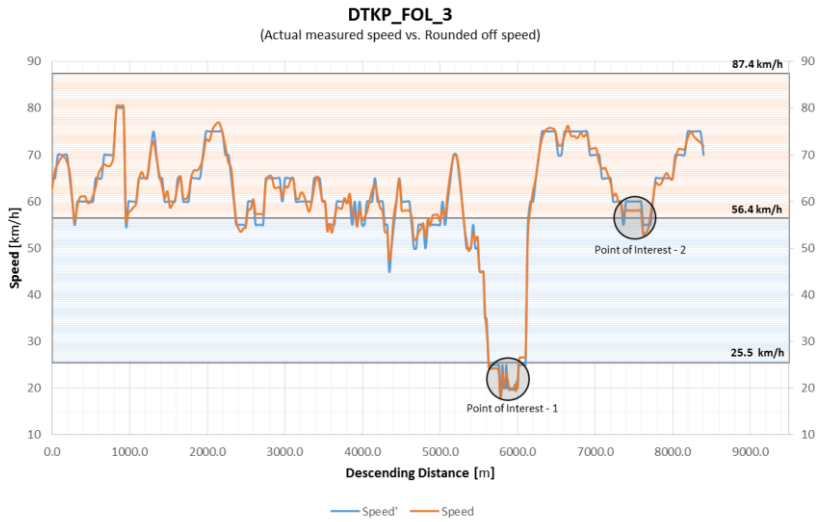

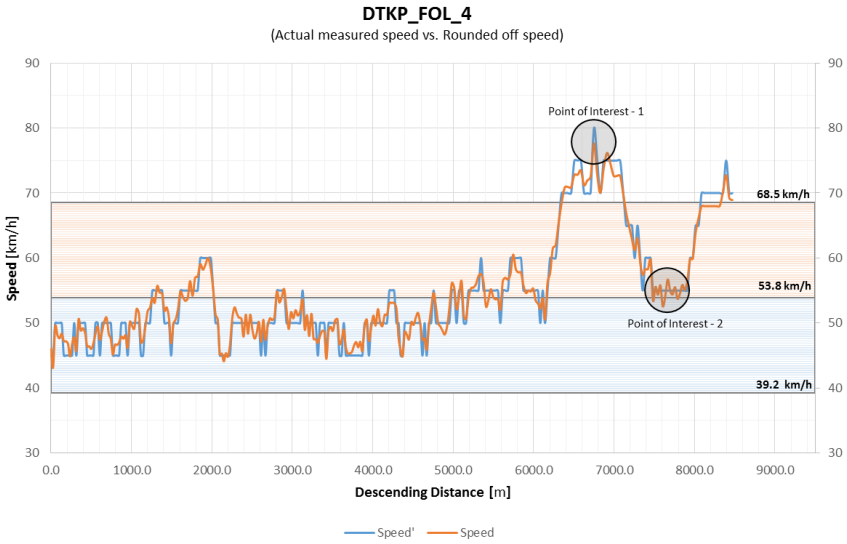

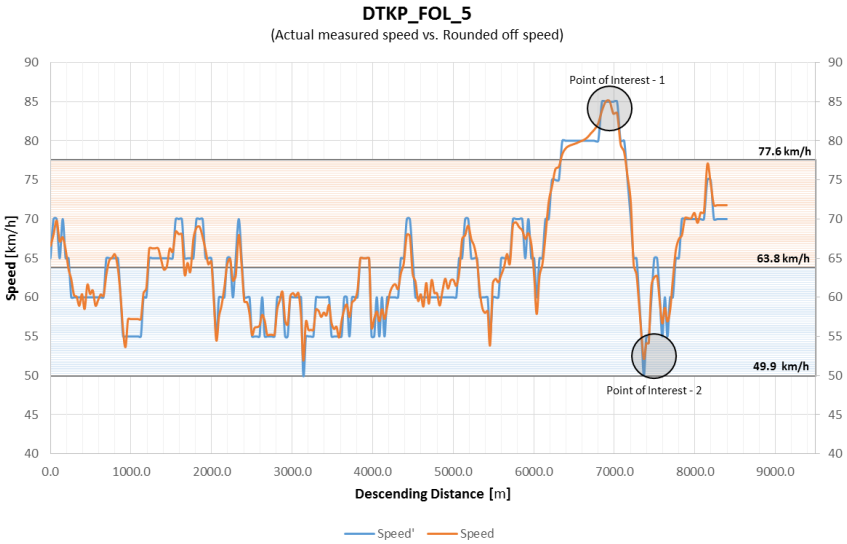

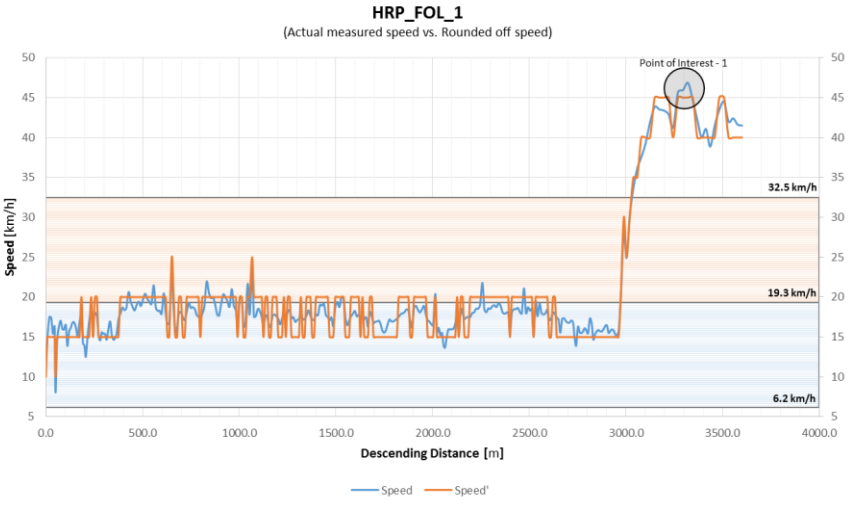

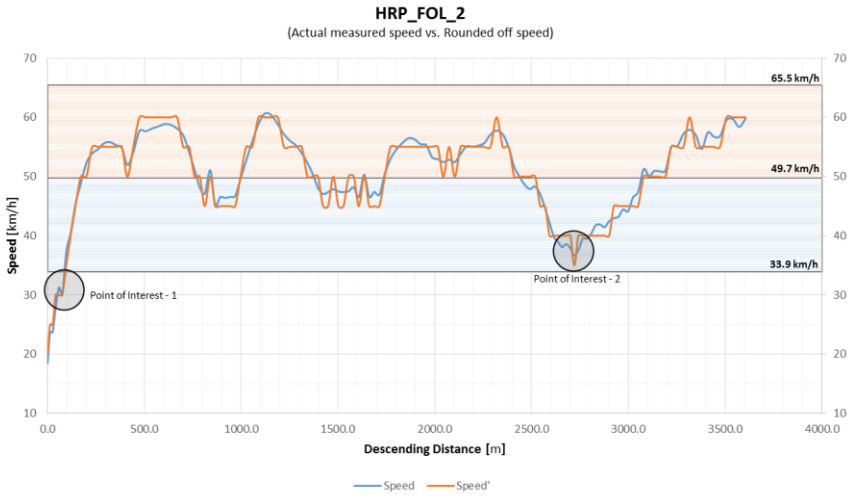

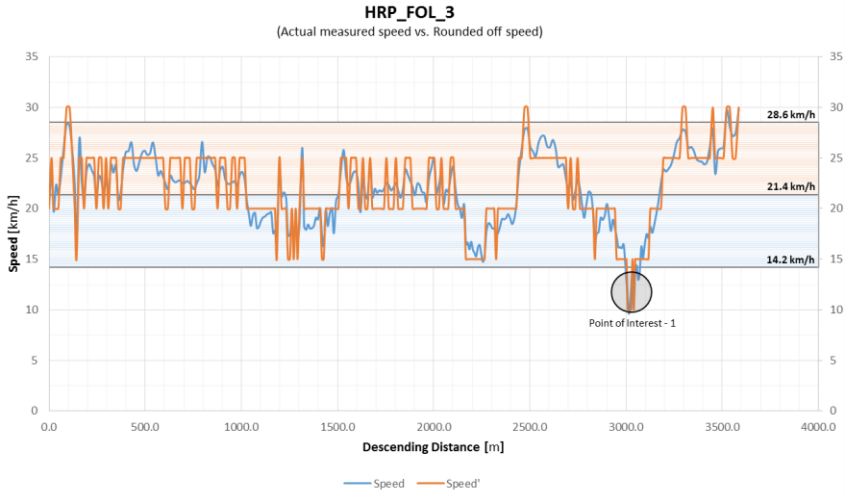

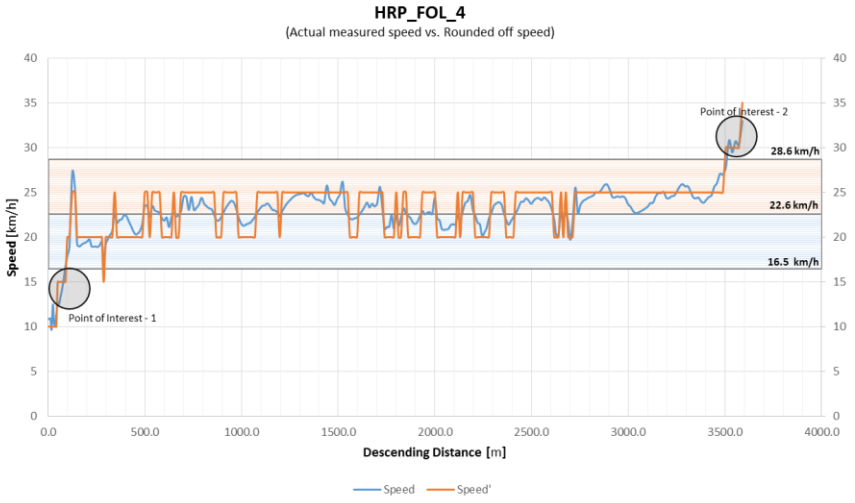

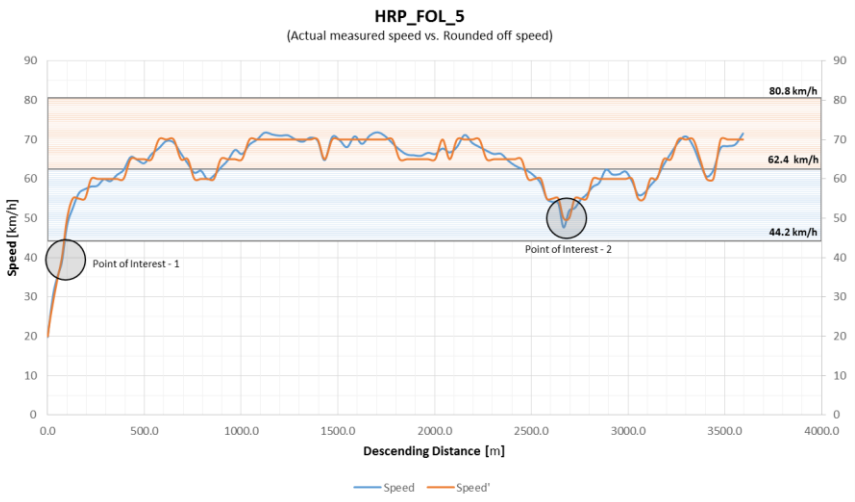

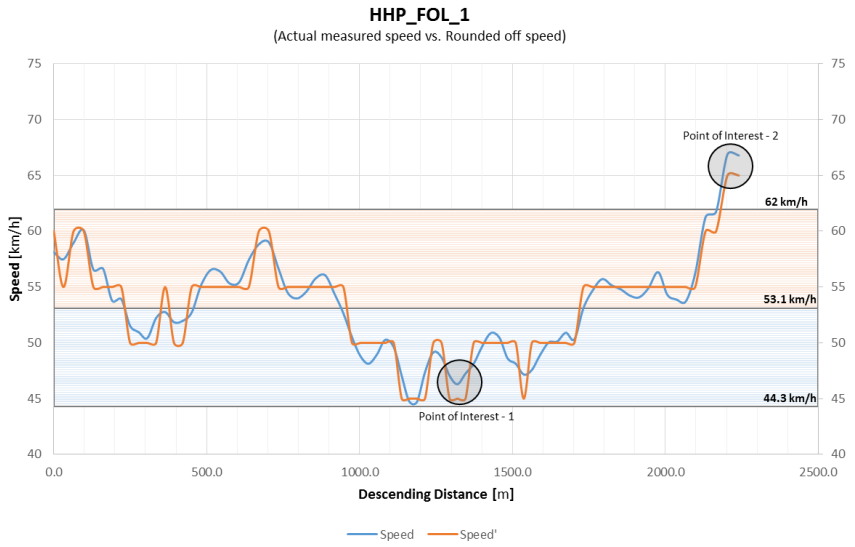

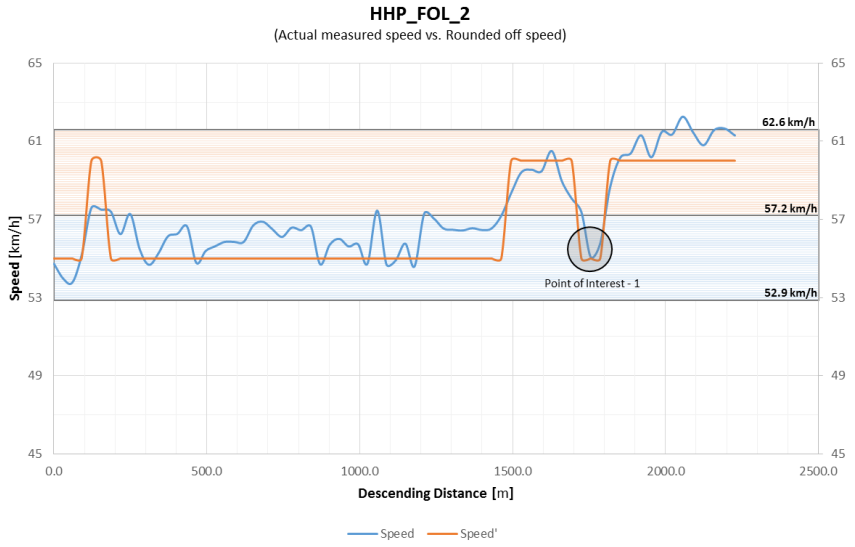

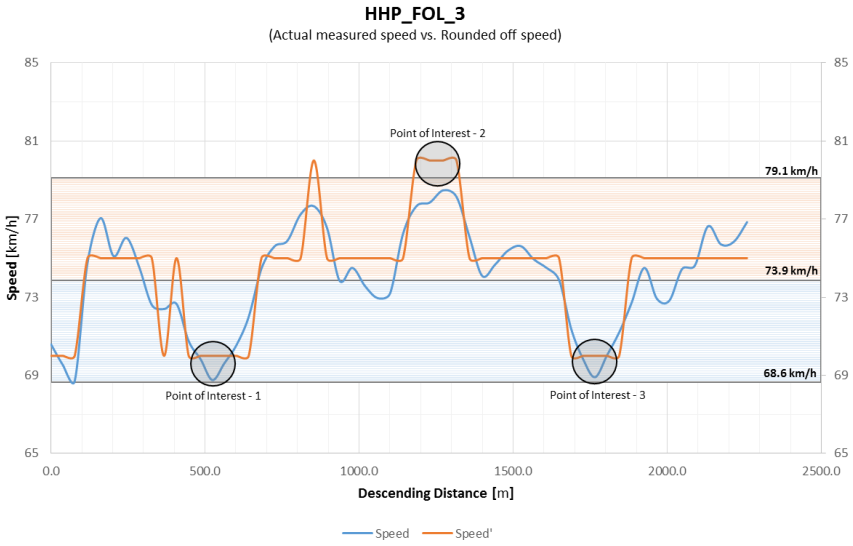

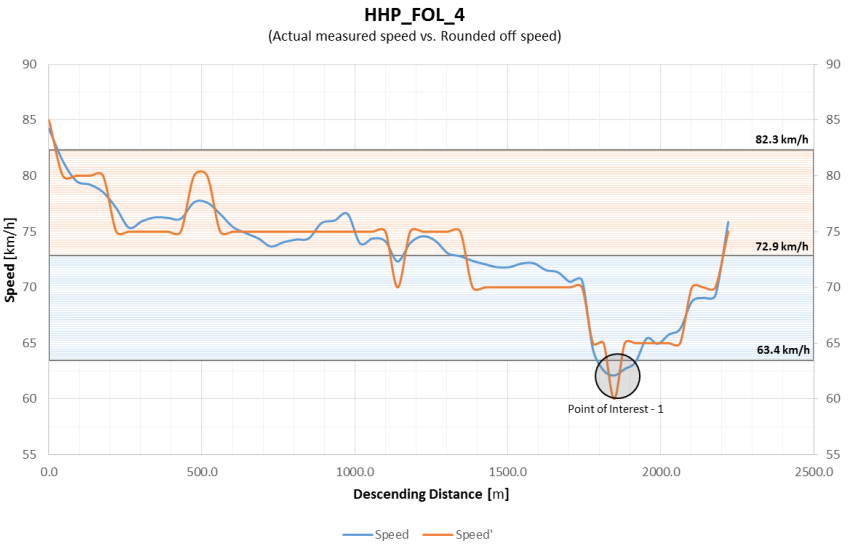

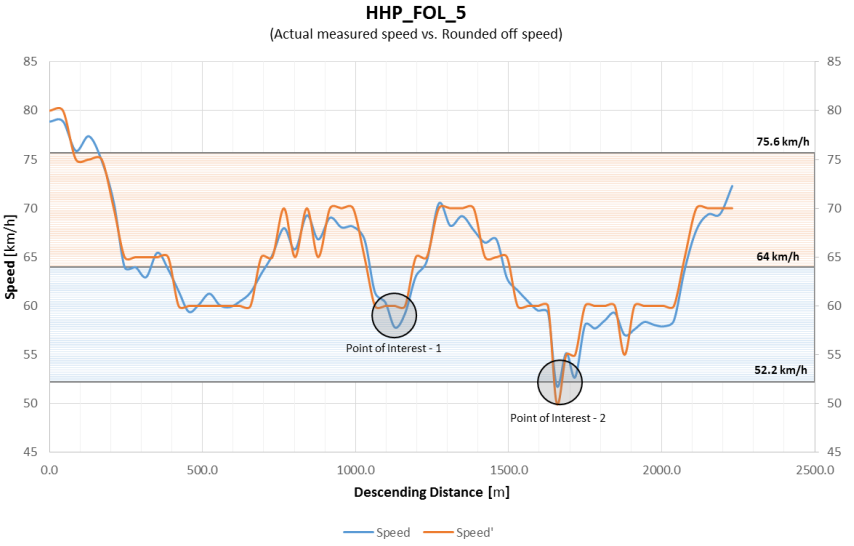

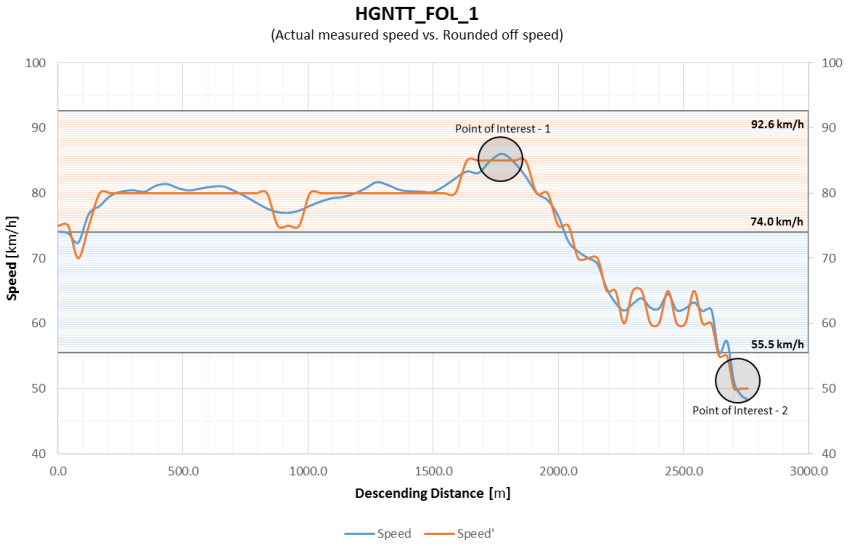

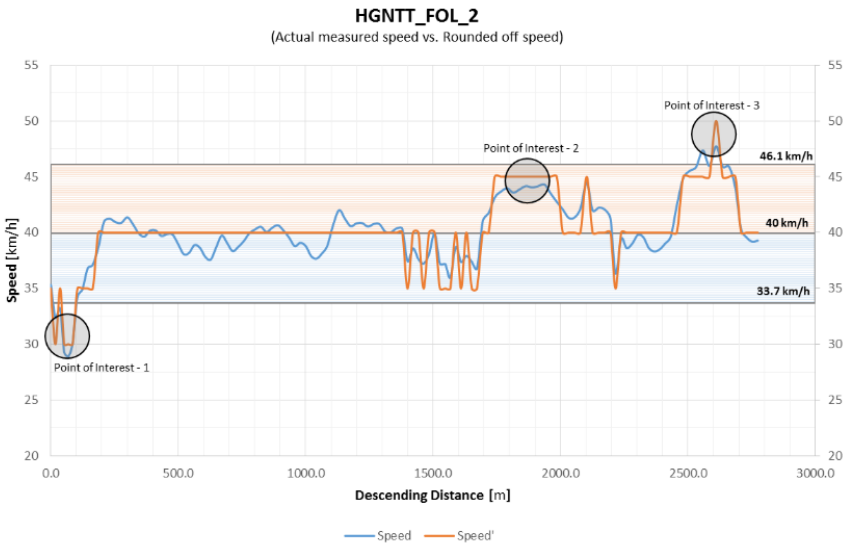

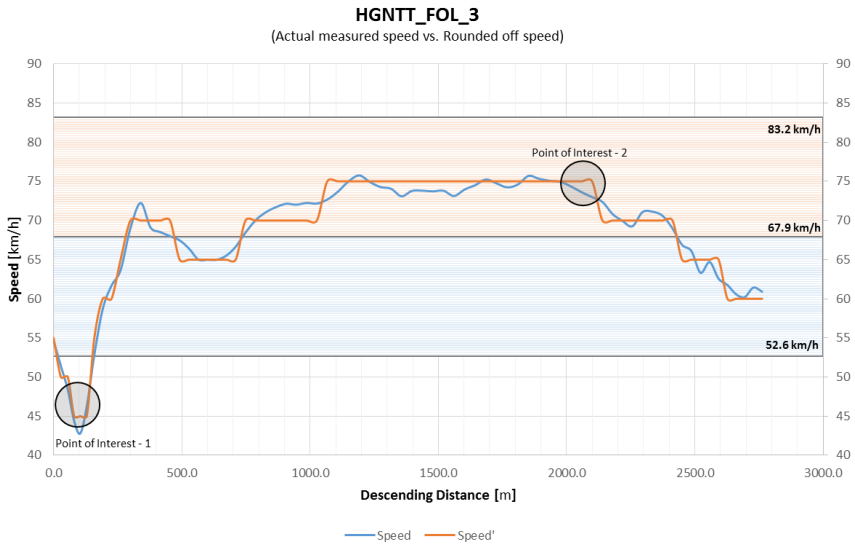

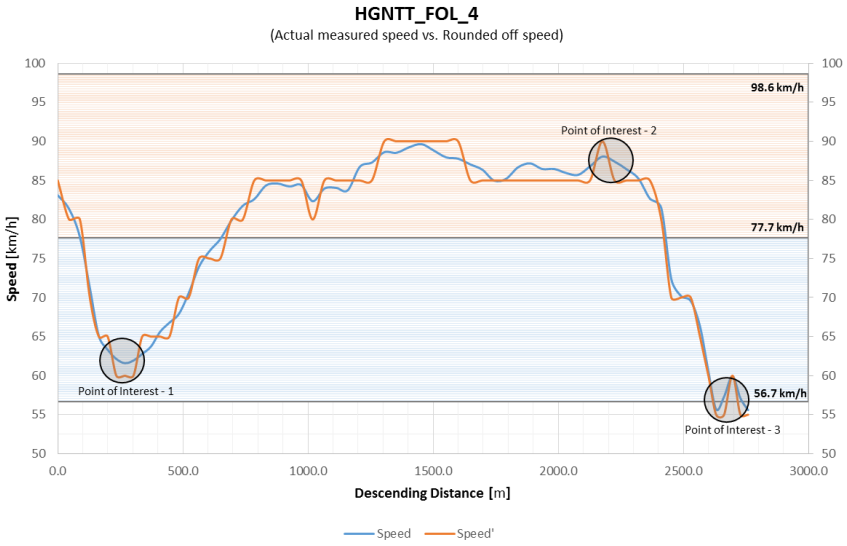

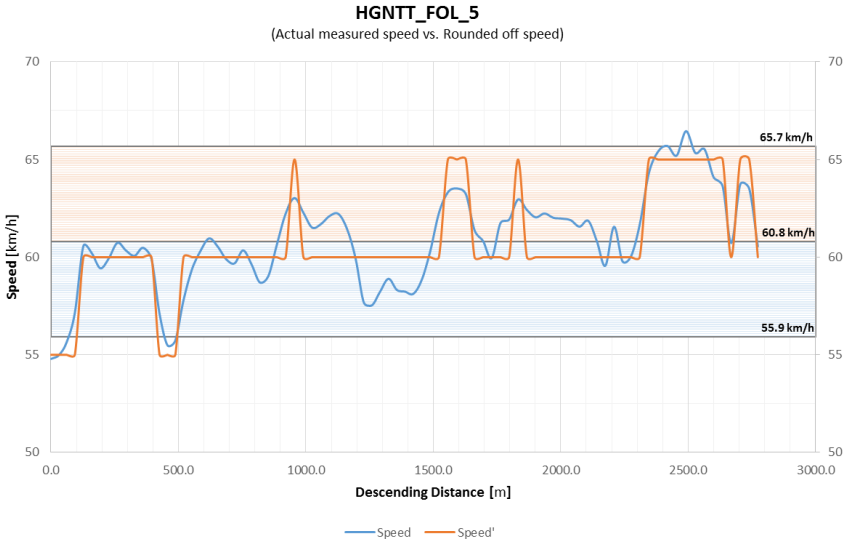

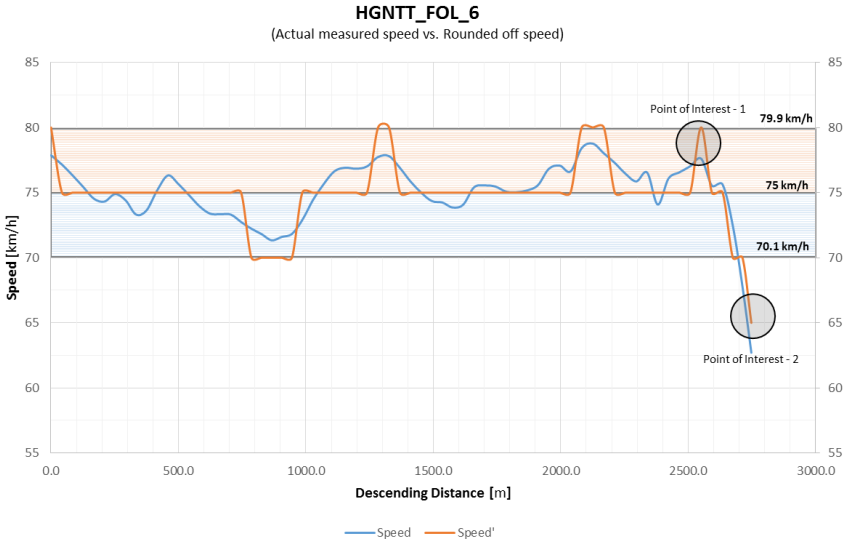

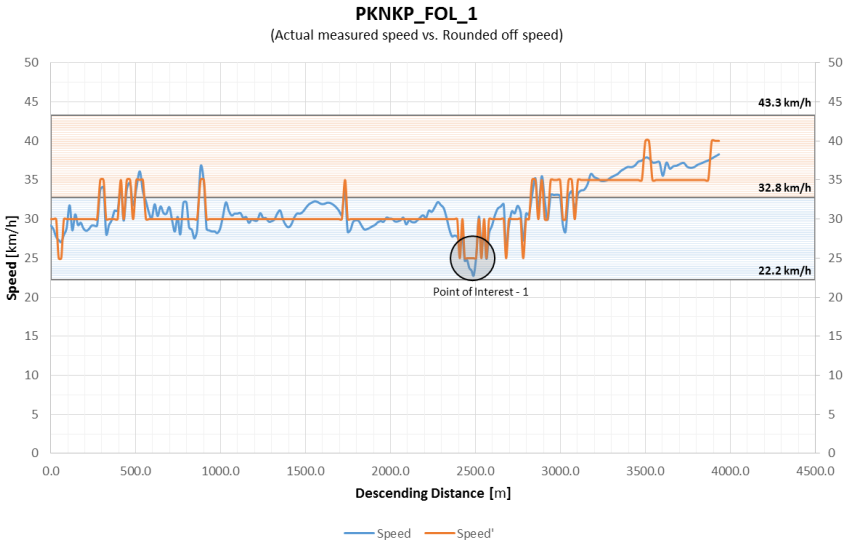

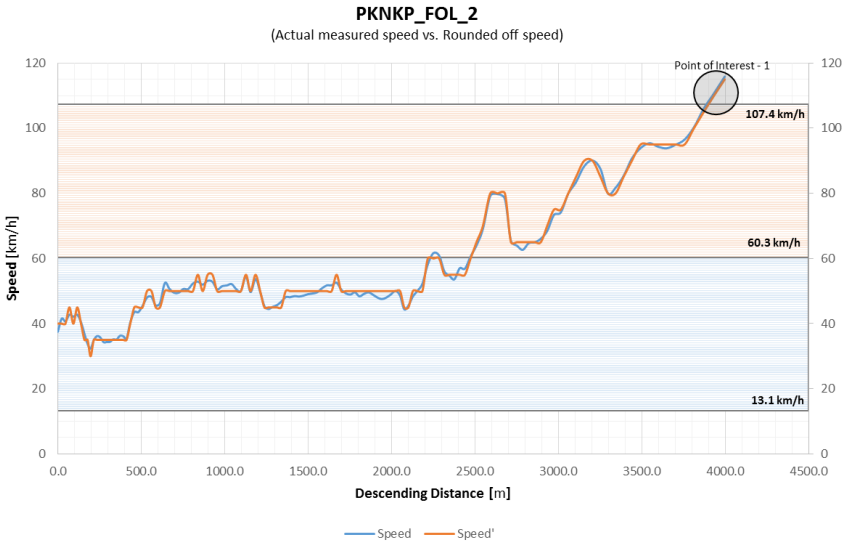

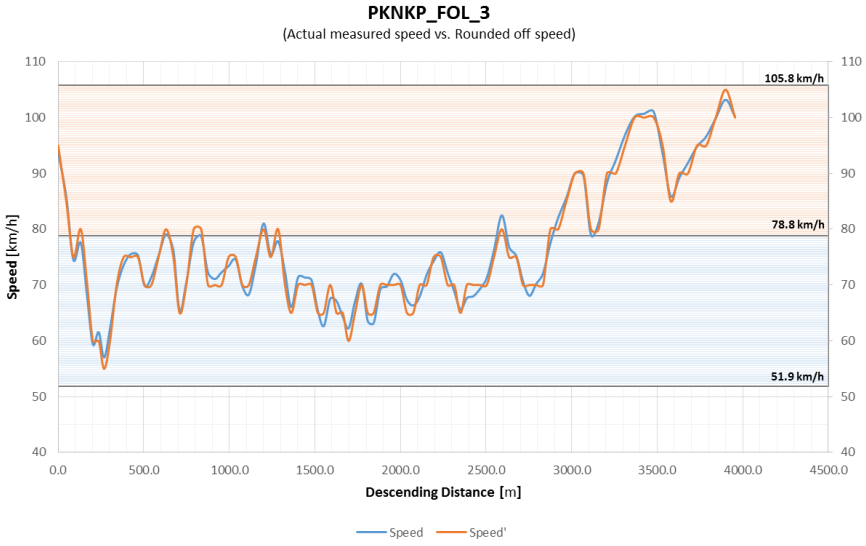

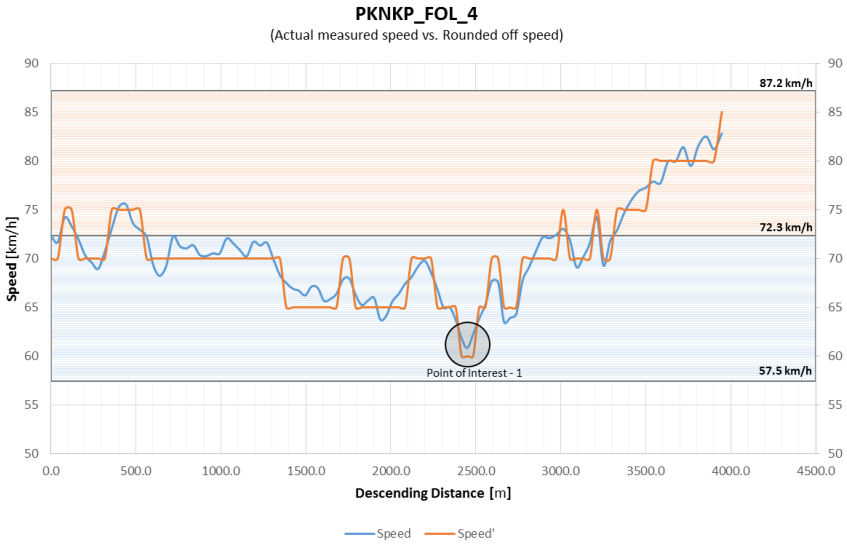

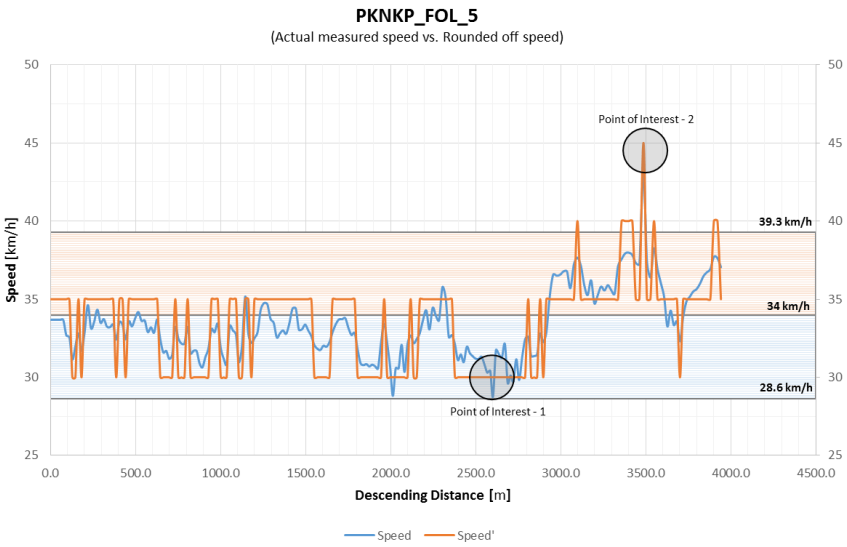

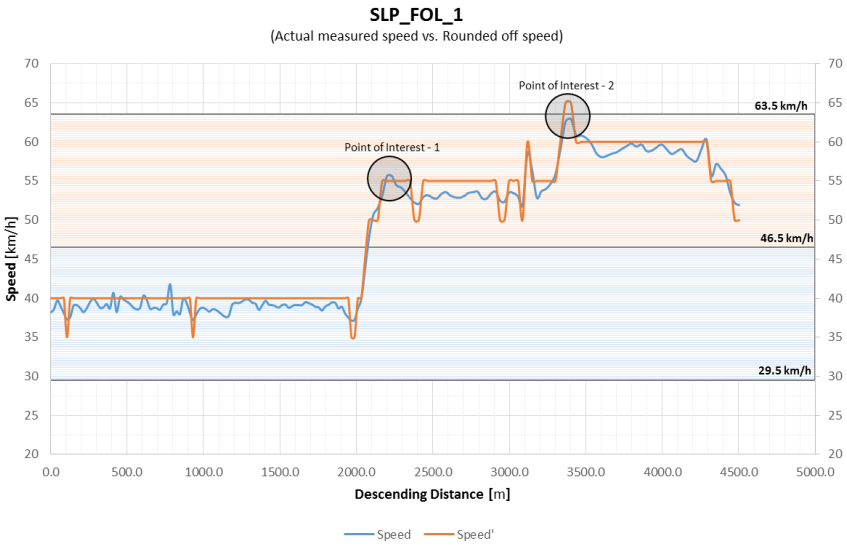

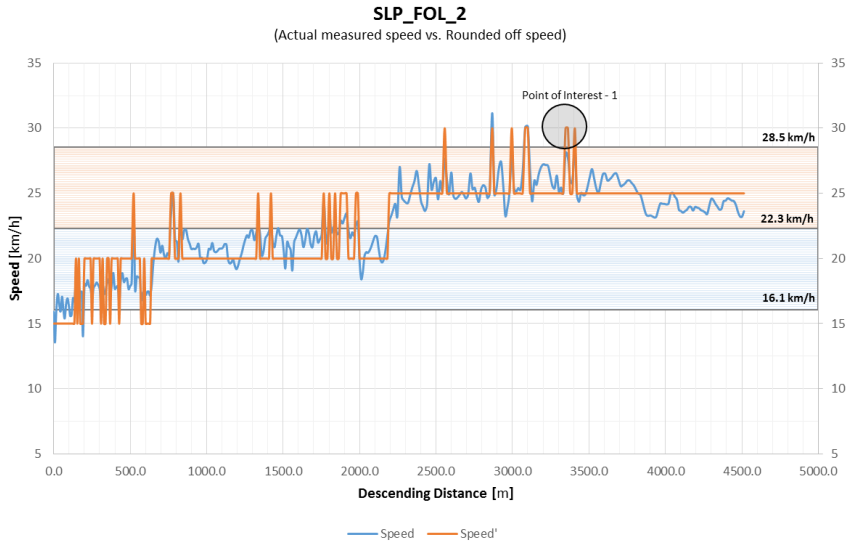

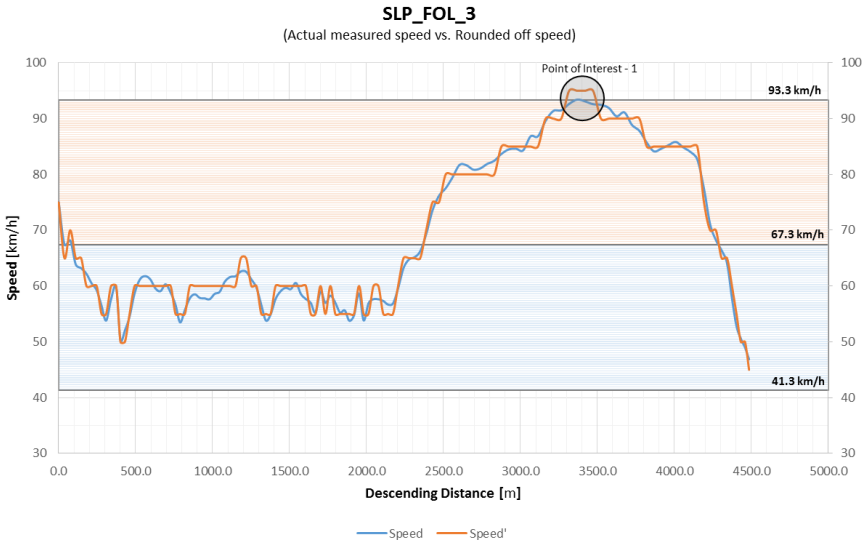

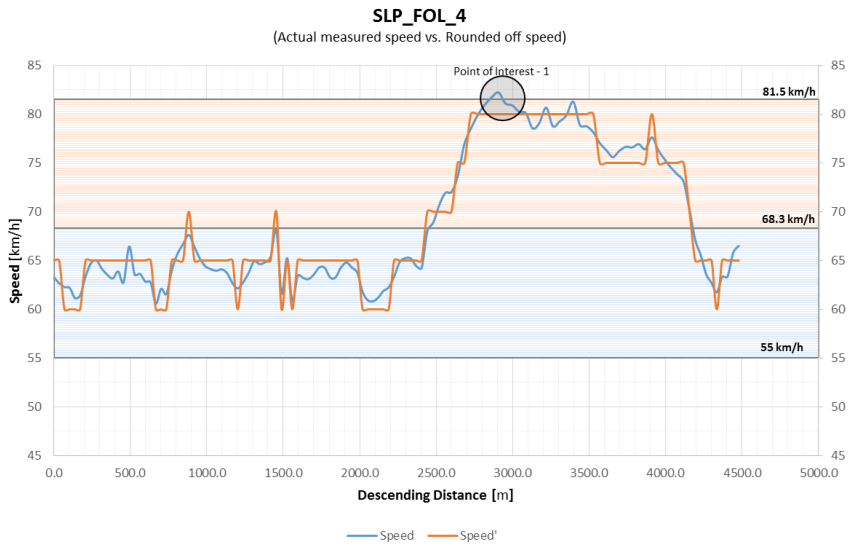

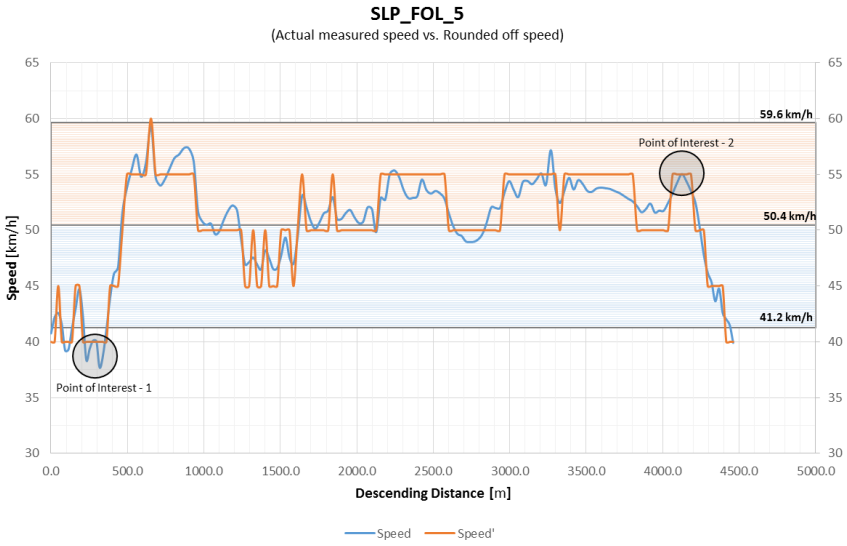

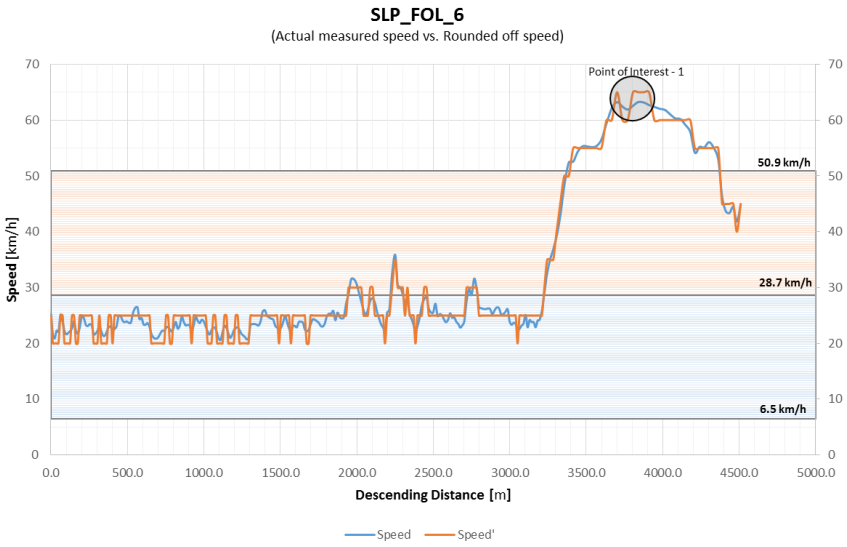

Appendix H

Appendix H1

This section contains the calculated speed ranges, mid-values and frequencies of the calculated operating speeds for the heavy vehicles.

Dutoitskloof - Speed Range Intervals			
	Entry	Apex	Exit
Min	31.9	40.7	36.4
Max	102.7	70.5	117.2
Range	70.8	29.8	80.8
8	9	4	11
12	6	3	7
16	5	2	6
20	4	2	5
Bin Size	**4**	**2**	**5**

Dutoitskloof - Speed Statistics			
Actual	**Entry**	**Apex**	**Exit**
Stdev	15.115	8.520	15.876
Mean	59.1	55.8	64.9
Median	55.8	57.3	62.6
Mode	#N/A	#N/A	#N/A
Skewness	0.895	-0.069	1.067
C. Tendency	55.78	55.84	62.63
Adjusted	**Entry**	**Apex**	**Exit**
Stdev	15.399	8.560	15.736
Mean	59.3	55.9	64.9
Median	56.0	58.0	65.0
Mode	56.0	68.0	65.0
Skewness	0.887	-0.101	0.986
C. Tendency	56.00	55.89	65.00

Dutoitskloof Pass - Entry Speed						
Ranges	**Midpoint**	**Freq.**	**Oserv. %**	**Cumul.%**	**Norm O%**	**Norm C%**
30 to 34	32	1	0.0188679	0.0188679	0.0076904	0.0595501
34 to 38	36	2	0.0377358	0.0566038	0.011146	0.0970061
38 to 42	40	2	0.0377358	0.0943396	0.0151004	0.1493929
42 to 46	44	4	0.0754717	0.1698113	0.0191229	0.2179072
46 to 50	48	7	0.1320755	0.3018868	0.0226368	0.3016989
50 to 54	52	5	0.0943396	0.3962264	0.0250479	0.3975244
54 to 58	56	8	0.1509434	0.5471698	0.0259073	0.5
58 to 62	60	4	0.0754717	0.6226415	0.0250479	0.6024756
62 to 66	64	5	0.0943396	0.7169811	0.0226368	0.6983011
66 to 70	68	5	0.0943396	0.8113208	0.0191229	0.7820928
70 to 74	72	2	0.0377358	0.8490566	0.0151004	0.8506071
74 to 78	76	1	0.0188679	0.8679245	0.011146	0.9029939
78 to 82	80	4	0.0754717	0.9433962	0.0076904	0.9404499
82 to 86	84	0	0	0.9433962	0.0049599	0.9654925
86 to 90	88	0	0	0.9433962	0.0029901	0.9811491
90 to 94	92	0	0	0.9433962	0.001685	0.9903023
94 to 98	96	1	0.0188679	0.9622642	0.0008876	0.9953061
98 to 102	100	1	0.0188679	0.9811321	0.000437	0.9978641
102 to 106	104	1	0.0188679	1	0.0002012	0.9990869

Dutoitskloof Pass - Apex Speed						
Ranges	**Midpoint**	**Freq.**	**Oserv. %**	**Cumul.%**	**Norm O%**	**Norm C%**
39 to 41	40	1	0.0188679	0.0188679	0.0083263	0.0317284
41 to 43	42	2	0.0377358	0.0566038	0.0125005	0.0523667
43 to 45	44	4	0.0754717	0.1320755	0.0177703	0.0824656
45 to 47	46	5	0.0943396	0.2264151	0.0239196	0.1240399
47 to 49	48	4	0.0754717	0.3018868	0.0304862	0.1784272
49 to 51	50	1	0.0188679	0.3207547	0.0367911	0.2458129
51 to 53	52	3	0.0566038	0.3773585	0.0420411	0.3248874
53 to 55	54	3	0.0566038	0.4339623	0.0454879	0.4127702
55 to 57	56	3	0.0566038	0.490566	0.0466024	0.5052761
57 to 59	58	6	0.1132075	0.6037736	0.0452076	0.5974978
59 to 61	60	5	0.0943396	0.6981132	0.0415246	0.6845733
61 to 63	62	3	0.0566038	0.754717	0.0361153	0.7624409
63 to 65	64	3	0.0566038	0.8113208	0.0297418	0.8283911
65 to 67	66	2	0.0377358	0.8490566	0.0231917	0.8812933
67 to 69	68	7	0.1320755	0.9811321	0.0171234	0.9214844
69 to 71	70	1	0.0188679	1	0.0119712	0.9504034

Dutoitskloof Pass - Exit Speed						
Ranges	**Midpoint**	**Freq.**	**Oserv. %**	**Cumul.%**	**Norm O%**	**Norm C%**
32.5 to 37.5	35	1	0.0188679	0.0188679	0.0041191	0.0282982
37.5 to 42.5	40	1	0.0188679	0.0377358	0.0071771	0.0560665
42.5 to 47.5	45	4	0.0754717	0.1132075	0.0113044	0.1018745
47.5 to 52.5	50	3	0.0566038	0.1698113	0.0160955	0.1702425
52.5 to 57.5	55	8	0.1509434	0.3207547	0.0207165	0.2625605
57.5 to 62.5	60	9	0.1698113	0.490566	0.0241037	0.3753427
62.5 to 67.5	65	10	0.1886792	0.6792453	0.0253516	0.5
67.5 to 72.5	70	6	0.1132075	0.7924528	0.0241037	0.6246573
72.5 to 77.5	75	2	0.0377358	0.8301887	0.0207165	0.7374395
77.5 to 82.5	80	2	0.0377358	0.8679245	0.0160955	0.8297575
82.5 to 87.5	85	0	0	0.8679245	0.0113044	0.8981255
87.5 to 92.5	90	4	0.0754717	0.9433962	0.0071771	0.9439335
92.5 to 97.5	95	1	0.0188679	0.9622642	0.0041191	0.9717018
97.5 to 102.5	100	0	0	0.9622642	0.002137	0.9869308
102.5 to 107.5	105	1	0.0188679	0.9811321	0.0010023	0.9944872
107.5 to 112.5	110	0	0	0.9811321	0.0004249	0.9978793
112.5 to 117.5	115	1	0.0188679	1	0.0001628	0.9992569

Hex River - Speed Range Intervals			
	Entry	Apex	Exit
Min	20.3	17.5	16.9
Max	88.1	82.7	73.7
Range	67.8	65.2	56.8
8	9	9	8
12	6	6	5
16	5	5	4
20	4	4	3
Bin Size	**4**	**4**	**3**

Hex River - Speed Statistics			
Actual	**Entry**	**Apex**	**Exit**
Stdev	14.341	12.694	12.669
Mean	52.3	47.3	47.4
Median	51.5	47.8	46.2
Mode	#N/A	#N/A	#N/A
Skewness	0.009	0.197	0.067
C. Tendency	52.28	47.77	47.44
Adjusted	**Entry**	**Apex**	**Exit**
Stdev	14.268	13.013	12.595
Mean	52.4	47.3	47.4
Median	52.0	48.0	45.0
Mode	52.0	48.0	36.0
Skewness	0.000	0.198	0.148
C. Tendency	52.40	48.00	45.00

Hex River Pass - Entry Speed								
Ranges	**Midpoint**	**Freq.**	**Oserv. %**	**Cumul.%**	**Norm O%**	**Norm C%**	**Actual O%**	**Actual C%**
18 to 22	20	1	0.01667	0.01667	0.00212	0.01158	0.00221	0.01221
22 to 26	24	1	0.01667	0.03333	0.00386	0.02327	0.00398	0.02433
26 to 30	28	3	0.05000	0.08333	0.00648	0.04362	0.00664	0.04526
30 to 34	32	1	0.01667	0.10000	0.01006	0.07639	0.01024	0.07871
34 to 38	36	4	0.06667	0.16667	0.01444	0.12519	0.01461	0.12821
38 to 42	40	2	0.03333	0.20000	0.01917	0.19240	0.01929	0.19601
42 to 46	44	7	0.11667	0.31667	0.02351	0.27802	0.02355	0.28195
46 to 50	48	7	0.11667	0.43333	0.02666	0.37889	0.02661	0.38280
50 to 54	52	10	0.16667	0.60000	0.02795	0.48882	0.02781	0.49233
54 to 58	56	3	0.05000	0.65000	0.02708	0.59960	0.02690	0.60245
58 to 62	60	3	0.05000	0.70000	0.02426	0.70287	0.02406	0.70492
62 to 66	64	7	0.11667	0.81667	0.02009	0.79189	0.01992	0.79318
66 to 70	68	6	0.10000	0.91667	0.01538	0.86288	0.01525	0.86356
70 to 74	72	1	0.01667	0.93333	0.01088	0.91523	0.01080	0.91549
74 to 78	76	2	0.03333	0.96667	0.00712	0.95094	0.00708	0.95096
78 to 82	80	1	0.01667	0.98333	0.00431	0.97347	0.00429	0.97339
82 to 86	84	0	0.00000	0.98333	0.00241	0.98661	0.00241	0.98652
86 to 90	88	1	0.01667	1.00000	0.00124	0.99370	0.00125	0.99363

Hex River Pass - Apex Speed								
Ranges	**Midpoint**	**Freq.**	**Oserv. %**	**Cumul.%**	**Norm O%**	**Norm C%**	**Actual O%**	**Actual C%**
14 to 18	16	1	0.01667	0.01667	0.00149	0.00696	0.00137	0.00616
18 to 22	20	0	0.00000	0.01667	0.00303	0.01571	0.00287	0.01434
22 to 26	24	3	0.05000	0.06667	0.00560	0.03257	0.00544	0.03055
26 to 30	28	1	0.01667	0.08333	0.00941	0.06215	0.00934	0.05965
30 to 34	32	3	0.05000	0.13333	0.01440	0.10943	0.01452	0.10701
34 to 38	36	7	0.11667	0.25000	0.02004	0.17822	0.02044	0.17685
38 to 42	40	4	0.06667	0.31667	0.02538	0.26935	0.02606	0.27016
42 to 46	44	7	0.11667	0.43333	0.02924	0.37927	0.03007	0.38315
46 to 50	48	13	0.21667	0.65000	0.03066	0.50000	0.03142	0.50715
50 to 54	52	4	0.06667	0.71667	0.02924	0.62073	0.02973	0.63044
54 to 58	56	5	0.08333	0.80000	0.02538	0.73065	0.02547	0.74156
58 to 62	60	5	0.08333	0.88333	0.02004	0.82178	0.01976	0.83229
62 to 66	64	2	0.03333	0.91667	0.01440	0.89057	0.01388	0.89944
66 to 70	68	3	0.05000	0.96667	0.00941	0.93785	0.00883	0.94448
70 to 74	72	0	0.00000	0.96667	0.00560	0.96743	0.00509	0.97184
74 to 78	76	1	0.01667	0.98333	0.00303	0.98429	0.00265	0.98692
78 to 82	80	0	0.00000	0.98333	0.00149	0.99304	0.00125	0.99444
82 to 86	84	1	0.01667	1.00000	0.00067	0.99717	0.00054	0.99784

Hex River Pass - Exit Speed								
Ranges	**Midpoint**	**Freq.**	**Oserv. %**	**Cumul.%**	**Norm O%**	**Norm C%**	**Actual O%**	**Actual C%**
16.5 to 19.5	18	1	0.01667	0.01667	0.00318	0.01603	0.00212	0.01006
19.5 to 22.5	21	0	0.00000	0.01667	0.00516	0.02836	0.00357	0.01844
22.5 to 25.5	24	1	0.01667	0.03333	0.00789	0.04773	0.00568	0.03213
25.5 to 28.5	27	0	0.00000	0.03333	0.01141	0.07649	0.00857	0.05331
28.5 to 31.5	30	4	0.06667	0.10000	0.01559	0.11684	0.01220	0.08428
31.5 to 34.5	33	2	0.03333	0.13333	0.02012	0.17036	0.01644	0.12713
34.5 to 37.5	36	7	0.11667	0.25000	0.02454	0.23744	0.02094	0.18320
37.5 to 40.5	39	4	0.06667	0.31667	0.02828	0.31691	0.02522	0.25256
40.5 to 43.5	42	7	0.11667	0.43333	0.03079	0.40587	0.02871	0.33372
43.5 to 46.5	45	5	0.08333	0.51667	0.03167	0.50000	0.03091	0.42353
46.5 to 49.5	48	4	0.06667	0.58333	0.03079	0.59413	0.03146	0.51751
49.5 to 52.5	51	3	0.05000	0.63333	0.02828	0.68309	0.03027	0.61053
52.5 to 55.5	54	6	0.10000	0.73333	0.02454	0.76256	0.02754	0.69759
55.5 to 58.5	57	3	0.05000	0.78333	0.02012	0.82964	0.02369	0.77466
58.5 to 61.5	60	4	0.06667	0.85000	0.01559	0.88316	0.01927	0.83917
61.5 to 64.5	63	3	0.05000	0.90000	0.01141	0.92351	0.01482	0.89025
64.5 to 67.5	66	1	0.01667	0.91667	0.00789	0.95227	0.01077	0.92849
67.5 to 70.5	69	3	0.05000	0.96667	0.00516	0.97164	0.00741	0.95557
70.5 to 73.5	72	1	0.01667	0.98333	0.00318	0.98397	0.00481	0.97370
73.5 to 76.5	75	1	0.01667	1.00000	0.00186	0.99139	0.00296	0.98519

Houwhoek - Speed Range Intervals			
	Entry	Apex	Exit
Min	5.6	8.2	18.4
Max	109.8	111.6	101.8
Range	104.2	103.5	83.4
8	14	13	11
12	9	9	7
16	7	7	6
20	6	6	5
Bin Size	**6**	**6**	**5**

Houwhoek - Speed Statistics			
Actual	**Entry**	**Apex**	**Exit**
Stdev	21.481	18.130	18.425
Mean	63.0	61.4	64.4
Median	65.3	61.3	64.7
Mode	#N/A	#N/A	#N/A
Skewness	-0.280	-0.330	-0.155
C. Tendency	65.27	61.32	64.74
Adjusted	**Entry**	**Apex**	**Exit**
Stdev	21.620	18.205	18.533
Mean	63.4	61.2	64.4
Median	66.0	60.0	65.0
Mode	78.0	54.0	65.0
Skewness	-0.255	-0.277	-0.153
C. Tendency	66.00	60.00	65.00

Houwhoek Pass - Entry Speed

Ranges	Midpoint	Freq.	Oserv. %	Cumul.%	Norm O%	Norm C%	Actual O%	Actual C%
3 to 9	6	1	0.0154	0.0154	0.0004	0.0028	0.0004	0.0029
9 to 15	12	0	0.0000	0.0154	0.0008	0.0062	0.0009	0.0066
15 to 21	18	2	0.0308	0.0462	0.0016	0.0132	0.0016	0.0139
21 to 27	24	1	0.0154	0.0615	0.0028	0.0260	0.0029	0.0274
27 to 33	30	1	0.0154	0.0769	0.0046	0.0479	0.0048	0.0503
33 to 39	36	3	0.0462	0.1231	0.0070	0.0826	0.0073	0.0865
39 to 45	42	5	0.0769	0.2000	0.0100	0.1335	0.0103	0.1394
45 to 51	48	5	0.0769	0.2769	0.0130	0.2025	0.0134	0.2107
51 to 57	54	6	0.0923	0.3692	0.0158	0.2894	0.0162	0.2999
57 to 63	60	7	0.1077	0.4769	0.0178	0.3907	0.0180	0.4031
63 to 69	66	3	0.0462	0.5231	0.0185	0.5000	0.0186	0.5136
69 to 75	72	10	0.1538	0.6769	0.0178	0.6093	0.0177	0.6230
75 to 81	78	11	0.1692	0.8462	0.0158	0.7106	0.0156	0.7233
81 to 87	84	3	0.0462	0.8923	0.0130	0.7975	0.0127	0.8084
87 to 93	90	3	0.0462	0.9385	0.0100	0.8665	0.0096	0.8752
93 to 99	96	0	0.0000	0.9385	0.0070	0.9174	0.0067	0.9237
99 to 105	102	1	0.0154	0.9538	0.0046	0.9521	0.0043	0.9564
105 to 111	108	3	0.0462	1.0000	0.0028	0.9740	0.0026	0.9767

Houwhoek Pass - Apex Speed

Ranges	Midpoint	Freq.	Oserv. %	Cumul.%	Norm O%	Norm C%	Actual O%	Actual C%
3 to 9	6	1	0.0154	0.0154	0.0003	0.0015	0.0002	0.0011
9 to 15	12	0	0.0000	0.0154	0.0007	0.0042	0.0005	0.0033
15 to 21	18	1	0.0154	0.0308	0.0015	0.0105	0.0013	0.0084
21 to 27	24	1	0.0154	0.0462	0.0031	0.0240	0.0026	0.0198
27 to 33	30	2	0.0308	0.0769	0.0056	0.0497	0.0049	0.0420
33 to 39	36	1	0.0154	0.0923	0.0092	0.0937	0.0083	0.0812
39 to 45	42	4	0.0615	0.1538	0.0134	0.1614	0.0125	0.1433
45 to 51	48	4	0.0615	0.2154	0.0176	0.2549	0.0168	0.2312
51 to 57	54	11	0.1692	0.3846	0.0208	0.3709	0.0203	0.3431
57 to 63	60	10	0.1538	0.5385	0.0219	0.5000	0.0219	0.4709
63 to 69	66	7	0.1077	0.6462	0.0208	0.6291	0.0213	0.6018
69 to 75	72	11	0.1692	0.8154	0.0176	0.7451	0.0185	0.7220
75 to 81	78	5	0.0769	0.8923	0.0134	0.8386	0.0144	0.8212
81 to 87	84	5	0.0769	0.9692	0.0092	0.9063	0.0101	0.8945
87 to 93	90	0	0.0000	0.9692	0.0056	0.9503	0.0063	0.9431
93 to 99	96	0	0.0000	0.9692	0.0031	0.9760	0.0035	0.9721
99 to 105	102	1	0.0154	0.9846	0.0015	0.9895	0.0018	0.9876
105 to 111	108	0	0.0000	0.9846	0.0007	0.9958	0.0008	0.9950
111 to 117	114	1	0.0154	1.0000	0.0003	0.9985	0.0003	0.9982

Houwhoek Pass - Exit Speed

Ranges	Midpoint	Freq.	Oserv. %	Cumul.%	Norm O%	Norm C%	Actual O%	Actual C%
17.5 to 22.5	20	3	0.0462	0.0462	0.0011	0.0076	0.0011	0.0076
22.5 to 27.5	25	0	0.0000	0.0462	0.0021	0.0155	0.0021	0.0155
27.5 to 32.5	30	1	0.0154	0.0615	0.0036	0.0295	0.0037	0.0297
32.5 to 37.5	35	0	0.0000	0.0615	0.0058	0.0528	0.0059	0.0533
37.5 to 42.5	40	2	0.0308	0.0923	0.0087	0.0887	0.0088	0.0897
42.5 to 47.5	45	4	0.0615	0.1538	0.0120	0.1403	0.0122	0.1420
47.5 to 52.5	50	4	0.0615	0.2154	0.0155	0.2092	0.0157	0.2119
52.5 to 57.5	55	8	0.1231	0.3385	0.0186	0.2947	0.0188	0.2986
57.5 to 62.5	60	6	0.0923	0.4308	0.0208	0.3937	0.0209	0.3985
62.5 to 67.5	65	11	0.1692	0.6000	0.0215	0.5000	0.0217	0.5057
67.5 to 72.5	70	8	0.1231	0.7231	0.0208	0.6063	0.0208	0.6124
72.5 to 77.5	75	4	0.0615	0.7846	0.0186	0.7053	0.0185	0.7112
77.5 to 82.5	80	5	0.0769	0.8615	0.0155	0.7908	0.0154	0.7963
82.5 to 87.5	85	0	0.0000	0.8615	0.0120	0.8597	0.0118	0.8643
87.5 to 92.5	90	4	0.0615	0.9231	0.0087	0.9113	0.0085	0.9148
92.5 to 97.5	95	0	0.0000	0.9231	0.0058	0.9472	0.0056	0.9498
97.5 to 102.5	100	5	0.0769	1.0000	0.0036	0.9705	0.0035	0.9722

Huguenot - Speed Range Intervals			
	Entry	Apex	Exit
Min	24.8	26.1	19.6
Max	76.2	86.3	63.0
Range	51.4	60.2	43.4
8	7	8	6
12	5	6	4
16	4	4	3
20	3	4	3
Bin Size	**3**	**4**	**3**

Huguenot - Speed Statistics			
Actual	**Entry**	**Apex**	**Exit**
Stdev	11.122	11.378	8.613
Mean	53.2	55.2	41.5
Median	53.7	56.8	41.6
Mode	#N/A	#N/A	#N/A
Skewness	-0.163	0.022	0.173
C. Tendency	53.68	55.24	41.61
Adjusted	**Entry**	**Apex**	**Exit**
Stdev	11.053	11.325	8.618
Mean	53.0	55.3	41.6
Median	54.0	56.0	42.0
Mode	60.0	60.0	45.0
Skewness	-0.199	0.082	0.244
C. Tendency	54.00	55.32	42.00

Huguenot Tunnel - Entry Speed								
Ranges	**Midpoint**	**Freq**	**Oserv. %**	**Cumul.%**	**Norm O%**	**Norm C%**	**Actual O%**	**Actual C%**
22.5 to 25.5	24	2	0.0179	0.0179	0.0009	0.0033	0.0010	0.0038
25.5 to 28.5	27	0	0.0000	0.0179	0.0018	0.0073	0.0020	0.0082
28.5 to 31.5	30	0	0.0000	0.0179	0.0034	0.0150	0.0037	0.0166
31.5 to 34.5	33	4	0.0357	0.0536	0.0059	0.0287	0.0064	0.0315
34.5 to 37.5	36	3	0.0268	0.0804	0.0096	0.0517	0.0101	0.0559
37.5 to 40.5	39	7	0.0625	0.1429	0.0144	0.0874	0.0150	0.0934
40.5 to 43.5	42	7	0.0625	0.2054	0.0200	0.1388	0.0207	0.1467
43.5 to 46.5	45	7	0.0625	0.2679	0.0259	0.2078	0.0264	0.2175
46.5 to 49.5	48	13	0.1161	0.3839	0.0311	0.2936	0.0315	0.3047
49.5 to 52.5	51	10	0.0893	0.4732	0.0348	0.3930	0.0348	0.4047
52.5 to 55.5	54	9	0.0804	0.5536	0.0361	0.5000	0.0359	0.5113
55.5 to 58.5	57	12	0.1071	0.6607	0.0348	0.6070	0.0343	0.6172
58.5 to 61.5	60	14	0.1250	0.7857	0.0311	0.7064	0.0305	0.7150
61.5 to 64.5	63	5	0.0446	0.8304	0.0259	0.7922	0.0253	0.7989
64.5 to 67.5	66	10	0.0893	0.9196	0.0200	0.8612	0.0194	0.8659
67.5 to 70.5	69	3	0.0268	0.9464	0.0144	0.9126	0.0139	0.9158
70.5 to 73.5	72	2	0.0179	0.9643	0.0096	0.9483	0.0092	0.9502
73.5 to 76.5	75	4	0.0357	1.0000	0.0059	0.9713	0.0057	0.9724

Huguenot Tunnel - Apex Speed								
Ranges	**Midpoint**	**Freq**	**Oserv. %**	**Cumul.%**	**Norm O%**	**Norm C%**	**Actual O%**	**Actual C%**
26 to 30	28	1	0.0089	0.0089	0.0019	0.0079	0.0020	0.0083
30 to 34	32	1	0.0089	0.0179	0.0042	0.0197	0.0044	0.0206
34 to 38	36	4	0.0357	0.0536	0.0082	0.0440	0.0084	0.0455
38 to 42	40	12	0.1071	0.1607	0.0141	0.0880	0.0143	0.0903
42 to 46	44	8	0.0714	0.2321	0.0214	0.1587	0.0215	0.1617
46 to 50	48	8	0.0714	0.3036	0.0286	0.2590	0.0286	0.2624
50 to 54	52	15	0.1339	0.4375	0.0337	0.3847	0.0337	0.3881
54 to 58	56	13	0.1161	0.5536	0.0352	0.5239	0.0350	0.5268
58 to 62	60	20	0.1786	0.7321	0.0323	0.6602	0.0321	0.6623
62 to 66	64	14	0.1250	0.8571	0.0263	0.7783	0.0261	0.7794
66 to 70	68	6	0.0536	0.9107	0.0188	0.8685	0.0187	0.8690
70 to 74	72	4	0.0357	0.9464	0.0119	0.9296	0.0118	0.9297
74 to 78	76	3	0.0268	0.9732	0.0067	0.9661	0.0066	0.9660
78 to 82	80	2	0.0179	0.9911	0.0033	0.9853	0.0033	0.9852
82 to 86	84	0	0.0000	0.9911	0.0014	0.9943	0.0014	0.9943
86 to 90	88	1	0.0089	1.0000	0.0005	0.9980	0.0006	0.9980

Huguenot Tunnel - Exit Speed								
Ranges	**Midpoint**	**Freq**	**Oserv. %**	**Cumul.%**	**Norm O%**	**Norm C%**	**Actual O%**	**Actual C%**
19.5 to 22.5	21	2	0.0179	0.0179	0.0024	0.0074	0.0026	0.0084
22.5 to 25.5	24	1	0.0089	0.0268	0.0052	0.0184	0.0057	0.0204
25.5 to 28.5	27	2	0.0179	0.0446	0.0102	0.0409	0.0110	0.0449
28.5 to 31.5	30	7	0.0625	0.1071	0.0176	0.0819	0.0187	0.0888
31.5 to 34.5	33	12	0.1071	0.2143	0.0268	0.1482	0.0281	0.1587
34.5 to 37.5	36	12	0.1071	0.3214	0.0363	0.2431	0.0375	0.2573
37.5 to 40.5	39	14	0.1250	0.4464	0.0436	0.3639	0.0442	0.3808
40.5 to 43.5	42	16	0.1429	0.5893	0.0463	0.5000	0.0463	0.5179
43.5 to 46.5	45	17	0.1518	0.7411	0.0436	0.6361	0.0429	0.6529
46.5 to 49.5	48	14	0.1250	0.8661	0.0363	0.7569	0.0352	0.7708
49.5 to 52.5	51	4	0.0357	0.9018	0.0268	0.8518	0.0256	0.8621
52.5 to 55.5	54	2	0.0179	0.9196	0.0176	0.9181	0.0165	0.9248
55.5 to 58.5	57	4	0.0357	0.9554	0.0102	0.9591	0.0094	0.9630
58.5 to 61.5	60	2	0.0179	0.9732	0.0052	0.9816	0.0047	0.9836
61.5 to 64.5	63	3	0.0268	1.0000	0.0024	0.9926	0.0021	0.9935

Piekenierskloof - Speed Range Intervals			
	Entry	Apex	Exit
Min	14.2	22.5	21.4
Max	113.8	102.9	126.8
Range	99.6	80.4	105.4
8	13	11	14
12	9	7	9
16	7	6	7
20	5	5	6
Bin Size	**5**	**5**	**6**

Piekenierskloof - Speed Statistics			
Actual	**Entry**	**Apex**	**Exit**
Stdev	17.902	17.811	17.148
Mean	56.2	61.1	56.9
Median	54.6	63.7	57.0
Mode	#N/A	#N/A	#N/A
Skewness	0.142	-0.298	0.498
C. Tendency	54.59	63.68	56.95
Adjusted	**Entry**	**Apex**	**Exit**
Stdev	18.083	17.722	16.858
Mean	56.3	61.2	57.1
Median	55.0	65.0	57.0
Mode	55.0	70.0	54.0
Skewness	0.178	-0.234	0.496
C. Tendency	55.00	65.00	57.00

Piekenierskloof Pass - Entry Speed								
Ranges	**Midpoint**	**Freq**	**Oserv. %**	**Cumul.%**	**Norm O%**	**Norm C%**	**Actual O%**	**Actual C%**
12.5 to 17.5	15	2	0.0222	0.0222	0.0019	0.0135	0.0019	0.0135
17.5 to 22.5	20	1	0.0111	0.0333	0.0034	0.0265	0.0034	0.0267
22.5 to 27.5	25	3	0.0333	0.0667	0.0056	0.0486	0.0057	0.0492
27.5 to 32.5	30	1	0.0111	0.0778	0.0085	0.0834	0.0087	0.0848
32.5 to 37.5	35	3	0.0333	0.1111	0.0120	0.1344	0.0122	0.1369
37.5 to 42.5	40	11	0.1222	0.2333	0.0156	0.2034	0.0160	0.2075
42.5 to 47.5	45	9	0.1000	0.3333	0.0189	0.2901	0.0193	0.2961
47.5 to 52.5	50	7	0.0778	0.4111	0.0212	0.3911	0.0216	0.3988
52.5 to 57.5	55	14	0.1556	0.5667	0.0221	0.5000	0.0223	0.5091
57.5 to 62.5	60	7	0.0778	0.6444	0.0212	0.6089	0.0213	0.6188
62.5 to 67.5	65	7	0.0778	0.7222	0.0189	0.7099	0.0188	0.7196
67.5 to 72.5	70	7	0.0778	0.8000	0.0156	0.7966	0.0154	0.8053
72.5 to 77.5	75	6	0.0667	0.8667	0.0120	0.8656	0.0116	0.8729
77.5 to 82.5	80	7	0.0778	0.9444	0.0085	0.9166	0.0081	0.9221
82.5 to 87.5	85	2	0.0222	0.9667	0.0056	0.9514	0.0053	0.9553
87.5 to 92.5	90	2	0.0222	0.9889	0.0034	0.9735	0.0032	0.9760
92.5 to 97.5	95	0	0.0000	0.9889	0.0019	0.9865	0.0017	0.9880
97.5 to 102.5	100	0	0.0000	0.9889	0.0010	0.9936	0.0009	0.9944
102.5 to 107.5	105	0	0.0000	0.9889	0.0005	0.9972	0.0004	0.9976
107.5 to 112.5	110	0	0.0000	0.9889	0.0002	0.9988	0.0002	0.9990
112.5 to 117.5	115	1	0.0111	1.0000	0.0001	0.9995	0.0001	0.9996

Piekenierskloof Pass - Apex Speed								
Ranges	**Midpoint**	**Freq**	**Oserv. %**	**Cumul.%**	**Norm O%**	**Norm C%**	**Actual O%**	**Actual C%**
22.5 to 27.5	25	4	0.0444	0.0444	0.0018	0.0120	0.0021	0.0150
27.5 to 32.5	30	4	0.0444	0.0889	0.0032	0.0241	0.0037	0.0293
32.5 to 37.5	35	3	0.0333	0.1222	0.0054	0.0452	0.0061	0.0537
37.5 to 42.5	40	4	0.0444	0.1667	0.0083	0.0792	0.0093	0.0919
42.5 to 47.5	45	4	0.0444	0.2111	0.0119	0.1295	0.0129	0.1472
47.5 to 52.5	50	8	0.0889	0.3000	0.0157	0.1987	0.0167	0.2213
52.5 to 57.5	55	10	0.1111	0.4111	0.0192	0.2863	0.0199	0.3131
57.5 to 62.5	60	6	0.0667	0.4778	0.0216	0.3889	0.0219	0.4183
62.5 to 67.5	65	9	0.1000	0.5778	0.0225	0.5000	0.0223	0.5296
67.5 to 72.5	70	11	0.1222	0.7000	0.0216	0.6111	0.0210	0.6387
72.5 to 77.5	75	11	0.1222	0.8222	0.0192	0.7137	0.0183	0.7375
77.5 to 82.5	80	10	0.1111	0.9333	0.0157	0.8013	0.0147	0.8203
82.5 to 87.5	85	2	0.0222	0.9556	0.0119	0.8705	0.0109	0.8844
87.5 to 92.5	90	2	0.0222	0.9778	0.0083	0.9208	0.0075	0.9303
92.5 to 97.5	95	0	0.0000	0.9778	0.0054	0.9548	0.0048	0.9607
97.5 to 102.5	100	1	0.0111	0.9889	0.0032	0.9759	0.0028	0.9793
102.5 to 107.5	105	1	0.0111	1.0000	0.0018	0.9880	0.0015	0.9898

Piekenierskloof Pass - Exit Speed								
Ranges	**Midpoint**	**Freq**	**Oserv. %**	**Cumul.%**	**Norm O%**	**Norm C%**	**Actual O%**	**Actual C%**
21 to 27	24	4	0.0444	0.0444	0.0035	0.0251	0.0037	0.0273
27 to 33	30	2	0.0222	0.0667	0.0066	0.0546	0.0068	0.0580
33 to 39	36	7	0.0778	0.1444	0.0109	0.1064	0.0110	0.1109
39 to 45	42	10	0.1111	0.2556	0.0159	0.1868	0.0159	0.1916
45 to 51	48	7	0.0778	0.3333	0.0205	0.2967	0.0203	0.3008
51 to 57	54	15	0.1667	0.5000	0.0233	0.4294	0.0229	0.4317
57 to 63	60	11	0.1222	0.6222	0.0233	0.5706	0.0229	0.5706
63 to 69	66	13	0.1444	0.7667	0.0205	0.7033	0.0202	0.7012
69 to 75	72	9	0.1000	0.8667	0.0159	0.8132	0.0158	0.8099
75 to 81	78	9	0.1000	0.9667	0.0109	0.8936	0.0110	0.8902
81 to 87	84	1	0.0111	0.9778	0.0066	0.9454	0.0067	0.9427
87 to 93	90	1	0.0111	0.9889	0.0035	0.9749	0.0036	0.9730
93 to 99	96	0	0.0000	0.9889	0.0016	0.9897	0.0017	0.9886
99 to 105	102	0	0.0000	0.9889	0.0007	0.9962	0.0007	0.9957
105 to 111	108	0	0.0000	0.9889	0.0002	0.9988	0.0003	0.9985
111 to 117	114	0	0.0000	0.9889	0.0001	0.9996	0.0001	0.9996
117 to 123	120	0	0.0000	0.9889	0.0000	0.9999	0.0000	0.9999
123 to 129	126	1	0.0111	1.0000	0.0000	1.0000	0.0000	1.0000

Sir Lowry's - Speed Range Intervals			
	Entry	Apex	Exit
Min	18.5	32.0	44.4
Max	99.2	114.0	116.4
Range	80.7	82.1	72.0
8	11	11	9
12	7	7	6
16	6	6	5
20	5	5	4
Bin Size	**5**	**5**	**4**

Sir Lowry's - Speed Statistics			
Actual	**Entry**	**Apex**	**Exit**
Stdev	20.513	19.634	17.825
Mean	58.3	69.0	75.4
Median	60.8	71.8	77.1
Mode	#N/A	#N/A	#N/A
Skewness	0.068	0.105	0.276
C. Tendency	58.32	69.00	77.05
Adjusted	**Entry**	**Apex**	**Exit**
Stdev	20.554	19.944	18.064
Mean	58.6	69.0	75.3
Median	60.0	70.0	76.0
Mode	45.0	90.0	80.0
Skewness	0.059	0.111	0.237
C. Tendency	58.63	70.00	76.00

Sir Lowry's Pass - Entry Speed								
Ranges	**Midpoint**	**Freq**	**Oserv. %**	**Cumul.%**	**Norm O%**	**Norm C%**	**Actual O%**	**Actual C%**
17.5 to 22.5	20	1	0.0250	0.0250	0.0033	0.0301	0.0026	0.0232
22.5 to 27.5	25	1	0.0250	0.0500	0.0051	0.0509	0.0040	0.0395
27.5 to 32.5	30	3	0.0750	0.1250	0.0074	0.0819	0.0059	0.0640
32.5 to 37.5	35	2	0.0500	0.1750	0.0100	0.1252	0.0082	0.0992
37.5 to 42.5	40	2	0.0500	0.2250	0.0129	0.1824	0.0108	0.1467
42.5 to 47.5	45	7	0.1750	0.4000	0.0156	0.2537	0.0135	0.2074
47.5 to 52.5	50	2	0.0500	0.4500	0.0178	0.3374	0.0159	0.2810
52.5 to 57.5	55	0	0.0000	0.4500	0.0191	0.4300	0.0177	0.3653
57.5 to 62.5	60	4	0.1000	0.5500	0.0194	0.5267	0.0187	0.4566
62.5 to 67.5	65	3	0.0750	0.6250	0.0185	0.6218	0.0186	0.5503
67.5 to 72.5	70	3	0.0750	0.7000	0.0167	0.7100	0.0176	0.6413
72.5 to 77.5	75	3	0.0750	0.7750	0.0141	0.7872	0.0157	0.7249
77.5 to 82.5	80	4	0.1000	0.8750	0.0113	0.8508	0.0133	0.7975
82.5 to 87.5	85	2	0.0500	0.9250	0.0085	0.9003	0.0106	0.8573
87.5 to 92.5	90	1	0.0250	0.9500	0.0061	0.9365	0.0080	0.9038
92.5 to 97.5	95	1	0.0250	0.9750	0.0041	0.9616	0.0057	0.9381
97.5 to 102.5	100	1	0.0250	1.0000	0.0026	0.9779	0.0039	0.9620

Sir Lowry's Pass - Apex Speed								
Ranges	**Midpoint**	**Freq**	**Oserv. %**	**Cumul.%**	**Norm O%**	**Norm C%**	**Actual O%**	**Actual C%**
27.5 to 32.5	30	1	0.0250	0.0250	0.0027	0.0224	0.0004	0.0029
32.5 to 37.5	35	0	0.0000	0.0250	0.0043	0.0396	0.0009	0.0065
37.5 to 42.5	40	3	0.0750	0.1000	0.0065	0.0663	0.0016	0.0138
42.5 to 47.5	45	3	0.0750	0.1750	0.0091	0.1050	0.0029	0.0273
47.5 to 52.5	50	3	0.0750	0.2500	0.0121	0.1580	0.0048	0.0502
52.5 to 57.5	55	3	0.0750	0.3250	0.0151	0.2260	0.0074	0.0865
57.5 to 62.5	60	4	0.1000	0.4250	0.0176	0.3080	0.0104	0.1395
62.5 to 67.5	65	2	0.0500	0.4750	0.0194	0.4010	0.0135	0.2112
67.5 to 72.5	70	2	0.0500	0.5250	0.0200	0.5000	0.0162	0.3007
72.5 to 77.5	75	4	0.1000	0.6250	0.0194	0.5990	0.0181	0.4043
77.5 to 82.5	80	4	0.1000	0.7250	0.0176	0.6920	0.0186	0.5151
82.5 to 87.5	85	2	0.0500	0.7750	0.0151	0.7740	0.0177	0.6247
87.5 to 92.5	90	5	0.1250	0.9000	0.0121	0.8420	0.0156	0.7251
92.5 to 97.5	95	2	0.0500	0.9500	0.0091	0.8950	0.0127	0.8100
97.5 to 102.5	100	0	0.0000	0.9500	0.0065	0.9337	0.0095	0.8766
102.5 to 107.5	105	1	0.0250	0.9750	0.0043	0.9604	0.0066	0.9248
107.5 to 112.5	110	0	0.0000	0.9750	0.0027	0.9776	0.0043	0.9571
112.5 to 117.5	115	1	0.0250	1.0000	0.0016	0.9880	0.0025	0.9772

Sir Lowry's Pass - Exit Speed								
Ranges	**Midpoint**	**Freq**	**Oserv. %**	**Cumul.%**	**Norm O%**	**Norm C%**	**Actual O%**	**Actual C%**
42 to 46	44	2	0.0500	0.0500	0.0046	0.0382	0.0003	0.0016
46 to 50	48	1	0.0250	0.0750	0.0066	0.0606	0.0006	0.0042
50 to 54	52	2	0.0500	0.1250	0.0091	0.0920	0.0013	0.0098
54 to 58	56	3	0.0750	0.2000	0.0120	0.1341	0.0025	0.0210
58 to 62	60	4	0.1000	0.3000	0.0149	0.1879	0.0045	0.0416
62 to 66	64	2	0.0500	0.3500	0.0177	0.2532	0.0072	0.0763
66 to 70	68	2	0.0500	0.4000	0.0200	0.3289	0.0106	0.1294
70 to 74	72	1	0.0250	0.4250	0.0216	0.4124	0.0142	0.2040
74 to 78	76	4	0.1000	0.5250	0.0221	0.5000	0.0175	0.2995
78 to 82	80	6	0.1500	0.6750	0.0216	0.5876	0.0196	0.4114
82 to 86	84	2	0.0500	0.7250	0.0200	0.6711	0.0200	0.5309
86 to 90	88	2	0.0500	0.7750	0.0177	0.7468	0.0187	0.6478
90 to 94	92	4	0.1000	0.8750	0.0149	0.8121	0.0159	0.7520
94 to 98	96	1	0.0250	0.9000	0.0120	0.8659	0.0124	0.8371
98 to 102	100	1	0.0250	0.9250	0.0091	0.9080	0.0088	0.9005
102 to 106	104	0	0.0000	0.9250	0.0066	0.9394	0.0057	0.9436
106 to 110	108	1	0.0250	0.9500	0.0046	0.9618	0.0034	0.9705
110 to 114	112	1	0.0250	0.9750	0.0030	0.9769		
114 to 118	116	1	0.0250	1.0000	0.0019	0.9866		

Appendix H2

This section contains the cumulative frequency graphs that were used to determine the 85th percentile speed.

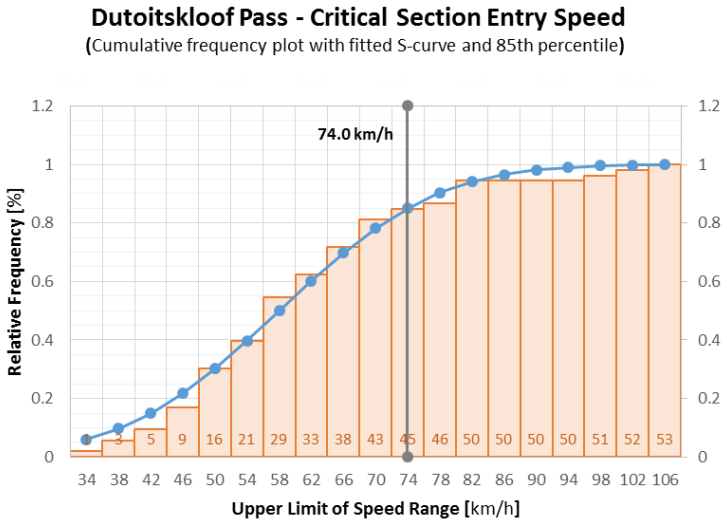

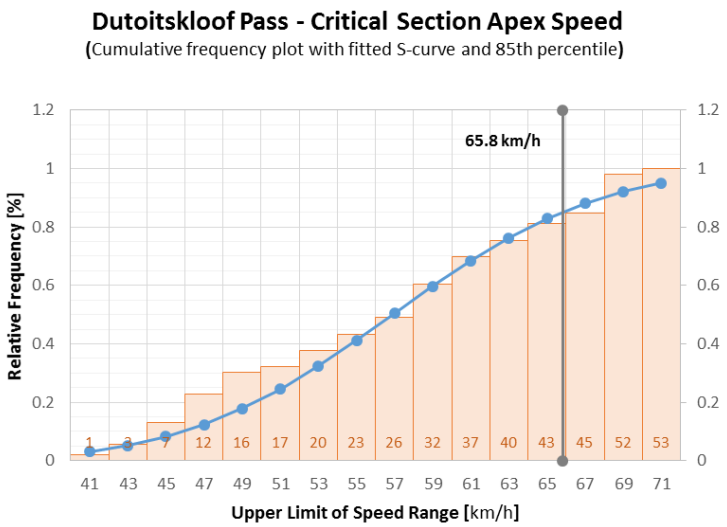

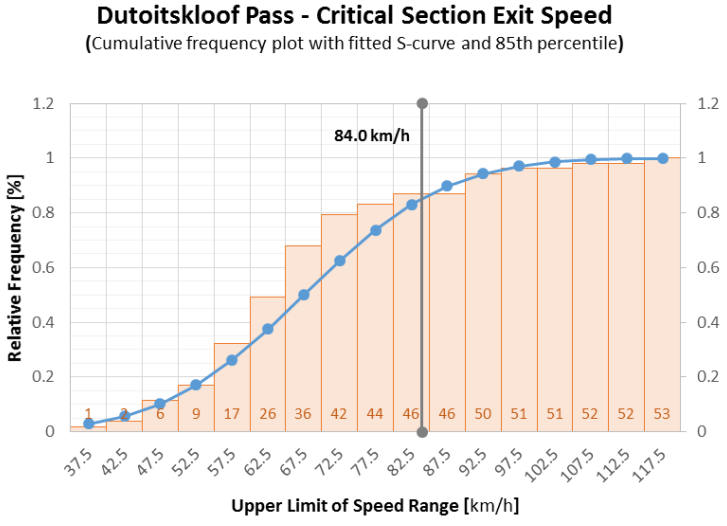

Hex River Pass - Critical Section Entry Speed
(Cumulative frequency plot with fitted S-curve and 85th percentile)

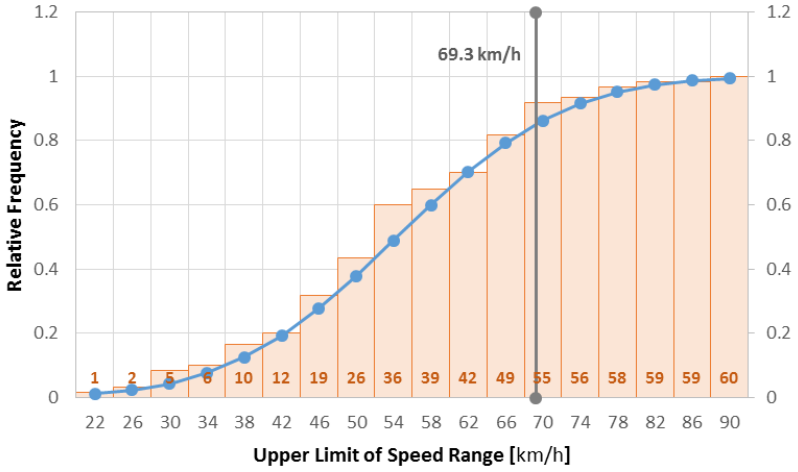

Hex River Pass - Critical Section Apex Speed
(Cumulative frequency plot with fitted S-curve and 85th percentile)

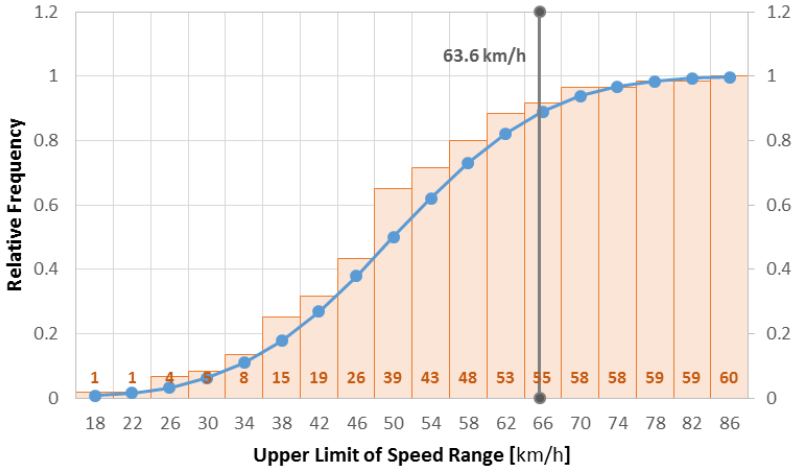

Hex River Pass - Critical Section Exit Speed
(Cumulative frequency plot with fitted S-curve and 85th percentile)

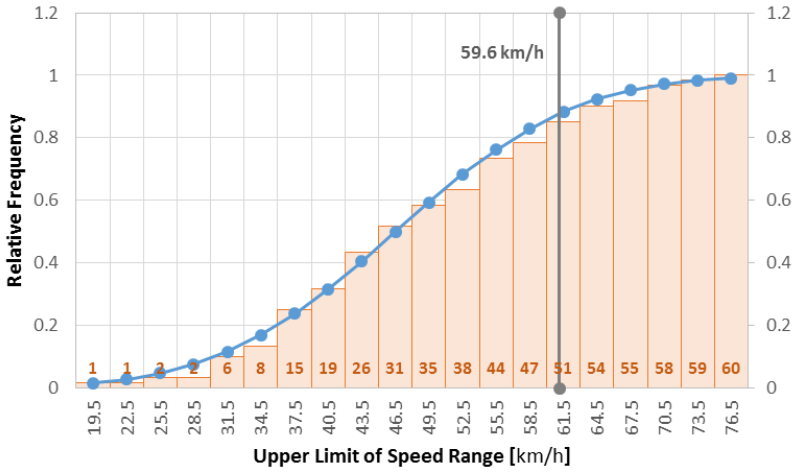

Hex River Pass - Critical Section Entry Speed
(Cumulative frequency plot with fitted S-curve and 85th percentile)

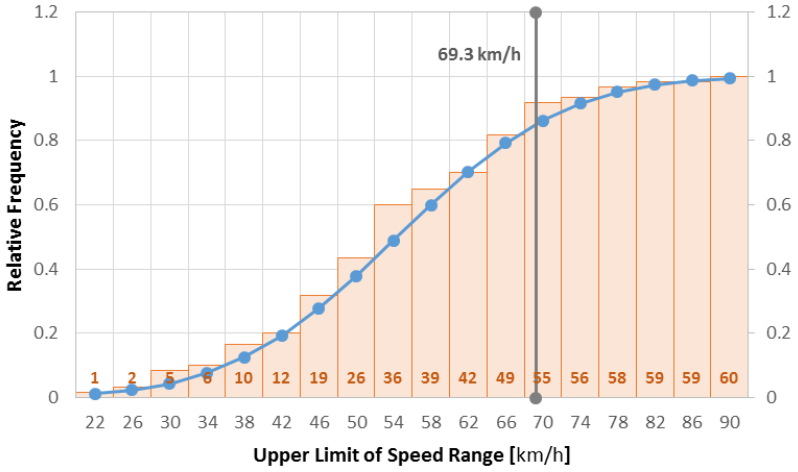

Hex River Pass - Critical Section Apex Speed
(Cumulative frequency plot with fitted S-curve and 85th percentile)

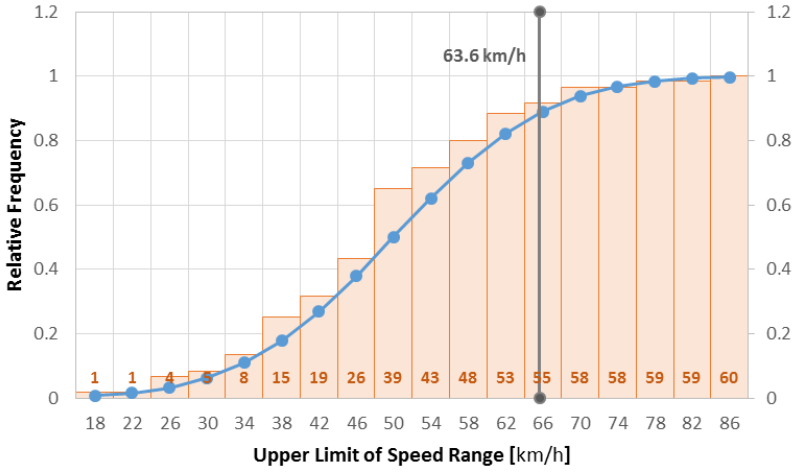

Hex River Pass - Critical Section Exit Speed
(Cumulative frequency plot with fitted S-curve and 85th percentile)

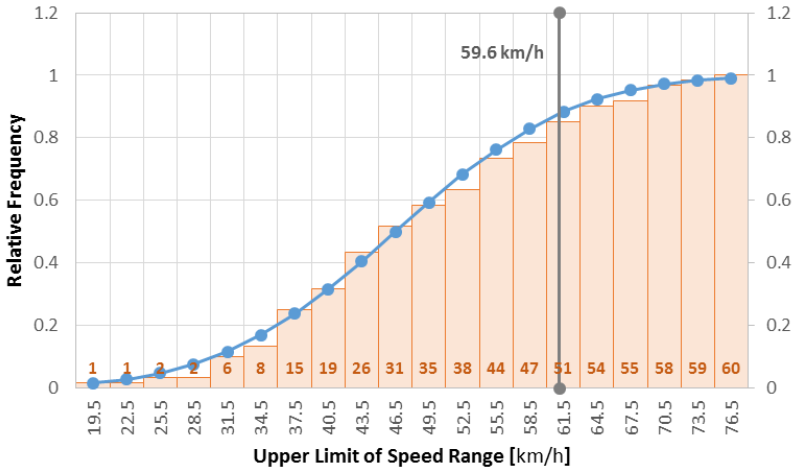

Huguenot Tunnel - Critical Section Entry Speed
(Cumulative frequency plot with fitted S-curve and 85th percentile)

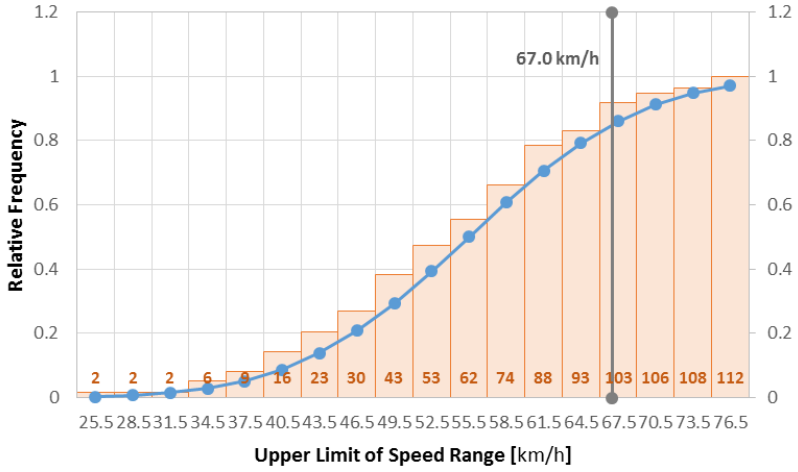

Huguenot Tunnel - Critical Section Apex Speed
(Cumulative frequency plot with fitted S-curve and 85th percentile)

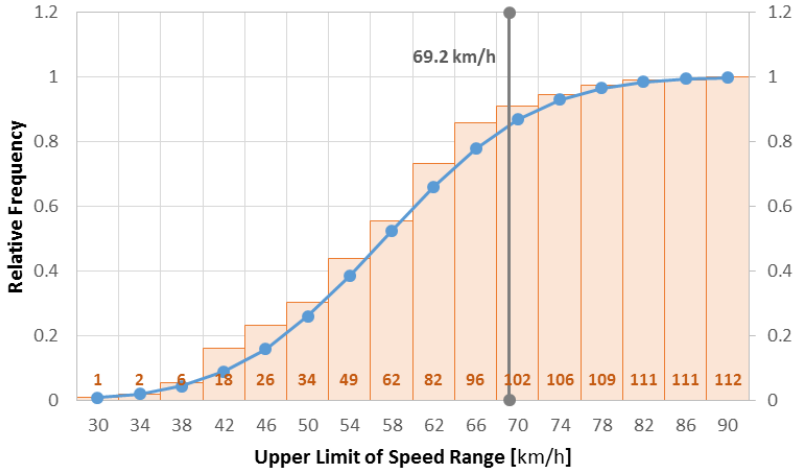

Huguenot Tunnel - Critical Section Exit Speed
(Cumulative frequency plot with fitted S-curve and 85th percentile)

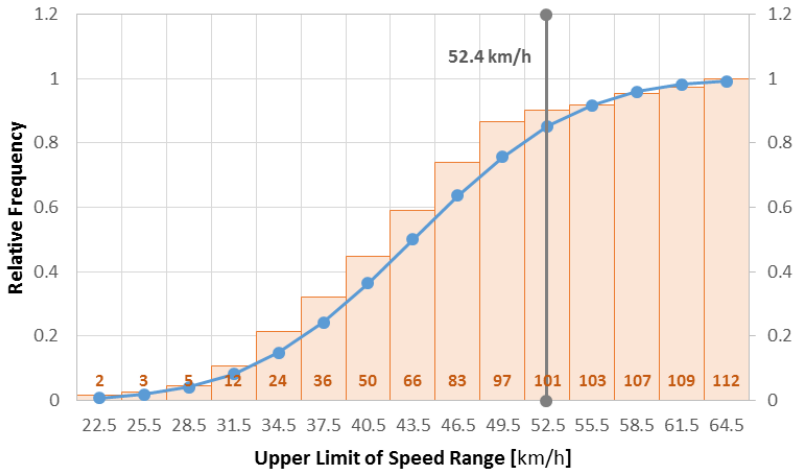

Piekenierskloof Pass - Critical Section Entry Speed
(Cumulative frequency plot with fitted S-curve and 85th percentile)

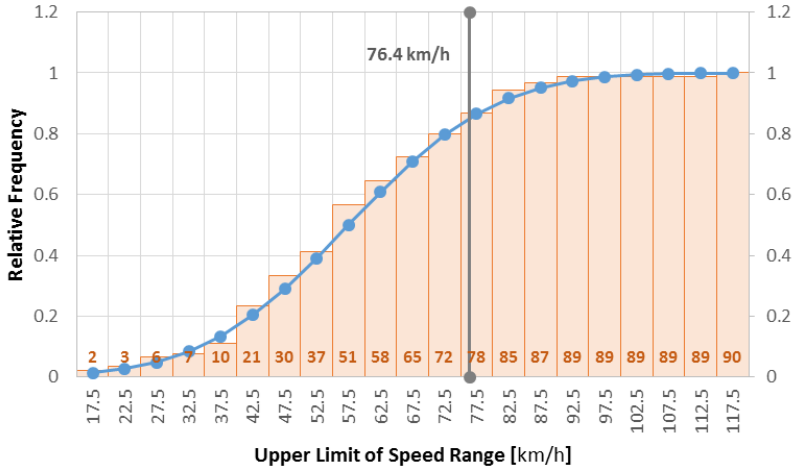

Piekenierskloof Pass - Critical Section Apex Speed
(Cumulative frequency plot with fitted S-curve and 85th percentile)

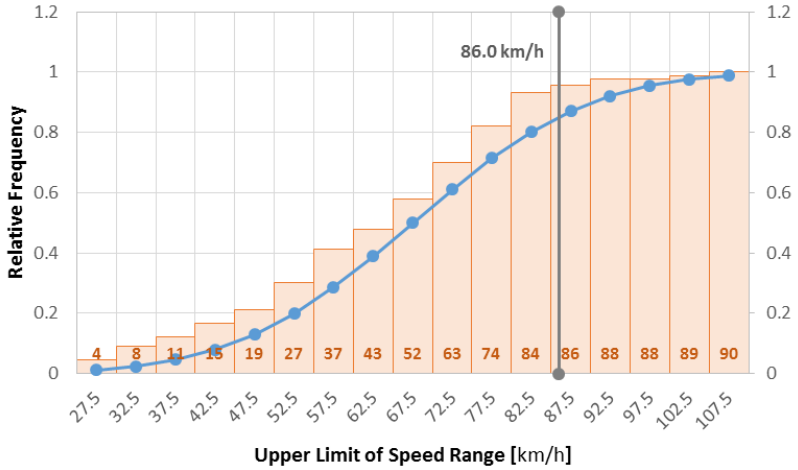

Piekenierskloof Pass - Critical Section Exit Speed
(Cumulative frequency plot with fitted S-curve and 85th percentile)

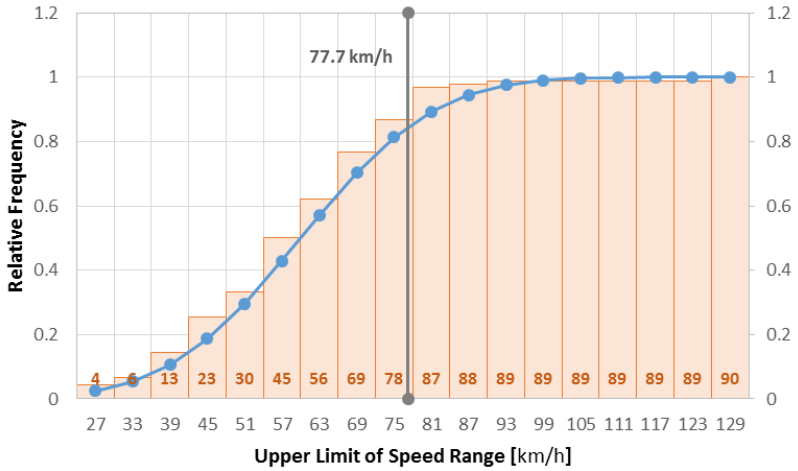

Sir Lowry's Pass - Critical Section Entry Speed
(Cumulative frequency plot with fitted S-curve and 85th percentile)

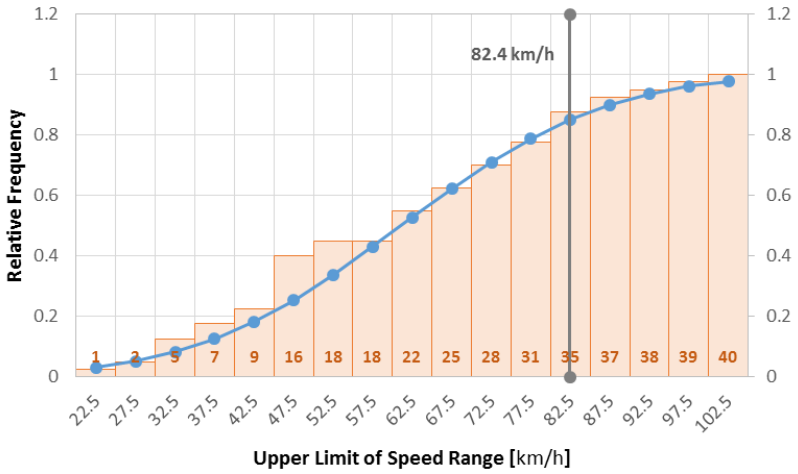

Sir Lowry's Pass - Critical Section Apex Speed
(Cumulative frequency plot with fitted S-curve and 85th percentile)

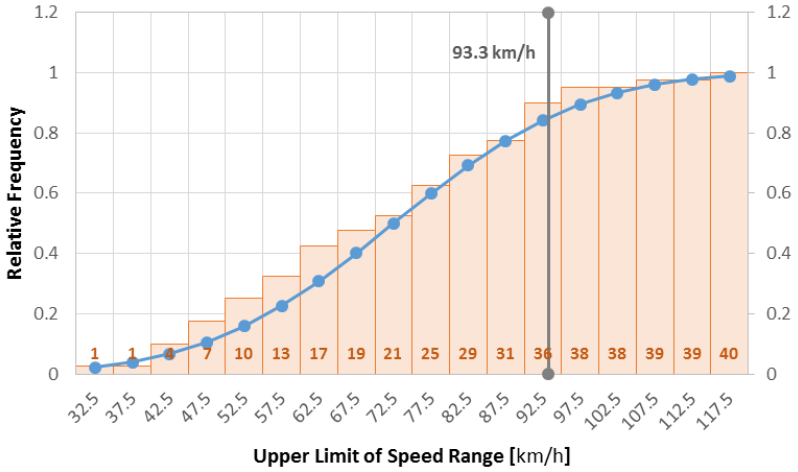

Sir Lowry's Pass - Critical Section Exit Speed
(Cumulative frequency plot with fitted S-curve and 85th percentile)